Compression Lap Splices and Compression Development of Headed and Hooked Bars in Beam-Column Joints

By
Guido Valentini
Rémy D. Lequesne
Andrés Lepage
David Darwin

A Report on Research Sponsored by

CONCRETE REINFORCING STEEL INSTITUTE
EDUCATION AND RESEARCH FOUNDATION

Structural Engineering and Engineering Materials
SM Report No. 159
July 2024

THE UNIVERSITY OF KANSAS CENTER FOR RESEARCH, INC.
2385 Irving Hill Road, Lawrence, Kansas 66045-7563

COMPRESSION LAP SPLICES AND COMPRESSION DEVELOPMENT OF HEADED AND HOOKED BARS IN BEAM-COLUMN JOINTS

By

Guido Valentini
Rémy D. Lequesne
Andrés Lepage
David Darwin

A Report on Research Sponsored by

Concrete Reinforcing Steel Institute Education and Research Foundation

Structural Engineering and Engineering Materials
SM Report No. 159
THE UNIVERSITY OF KANSAS CENTER FOR RESEARCH, INC.
LAWRENCE, KANSAS
July 2024

Abstract

ACI 318-19 Building Code provisions for compression lap splices and for headed and hooked bar development in special moment frame (SMF) joints were evaluated against databases of test results. Recommendations are made for simplifying and improving code requirements.

Compression lap splice length provisions (ACI 318-19 §25.5.5) produce calculated lengths longer than Class B tension lap splice lengths under certain design conditions. The provisions were shown to also be a poor fit to a database of 89 test results (with 72 specimens in the database violating the ACI 318-19 minimum lap splice length). Several equations exist that better fit the dataset, including several tension development length equations. Defining compression lap splice length requirements as a function of the tension development length is a more accurate alternative to §25.5.5 that eliminates the need to calculate both tension and compression development lengths and prevents design cases where calculated lengths are longer in compression than in tension.

Provisions for headed and hooked bar development were compared against databases of exterior beam-column connection tests with 35 and 27 specimens, respectively. Analyses show that satisfying the compression development length requirements of §25.4.9, as mandated by §18.8.2.2, is not necessary for preventing anchorage distress in special moment frame joints with either headed or hooked bars. None of the 59 specimens (35 with headed bars and 24 with hooked bars) with drift ratio capacities above 3% satisfied §25.4.9. The analyses also show that joints that did not satisfy the ACI 318-19 provisions for headed or hooked bar tension development length (§18.8.5.2 for headed bars and §25.4.3 for hooked bars) still exhibited satisfactory behavior, suggesting that §18.8.5.2 and §25.4.3 are considerably conservative. Other equations were evaluated and found to better fit the data, including the equation in ACI 318-19 §18.8.5.1, which analyses suggest might be applicable to both headed and hooked bars.

Acknowledgments

Support for this research was provided by the Concrete Reinforcing Steel Institute (CRSI) Education and Research Foundation.

Table of Contents

List of Figures

List of Tables

Chapter 1: Introduction

1.1 Background and Motivation

For reinforced concrete to function as a composite, concrete and steel bars must interact such that forces in one material can transfer into the other. This interaction is referred to as bond, which is understood to result from multiple mechanisms. Bond first manifests by mechanical adhesion between the two materials, but this is a relatively weak mechanism that is eliminated by small relative displacements (bar slip). Bar slip causes frictional forces to develop as a result of the roughness of the interface. Finally, in deformed bars, mechanical anchorage takes place due to bearing of bar deformations against the concrete. For bars in compression, a fourth mechanism is active: bearing of the end of the bar on concrete.

Bond research has been primarily focused on bars in tension [1]. ACI 408R-03 [1] and fib bulletin 72 [2] provide thorough reports on bond and development of straight reinforcing bars in tension. ACI 408R-03 states that bond of straight bars is primarily governed by:

- The mechanical properties of the concrete (tensile and bearing strength),
- The volume of concrete around the bars (related to concrete cover and bar spacing),
- The presence of confinement in the form of transverse reinforcement (ties, spirals), which controls crack propagation,
- The surface condition of the bar, and
- The geometry of the bar (deformation height, spacing, width, and face angle).

Comparatively little research has been conducted to investigate bond of bars in compression. In general, bond in compression is understood to be affected by the same factors as in tension, except that end bearing in compression is also important.

For design, the length required for a reinforcing bar embedded in concrete to transfer a force equal to $A_b f_y$ through bond is referred to as the *development length*. The force in question can be either tension and compression, leading to design requirements for *tension development length*, ℓ_d, and *compression development length*, ℓ_{dc}, for straight bars. The overlap length required to transfer the force ($A_b f_y$) between bars is referred to as *lap splice length*. There are design requirements for *tension lap splice length*, ℓ_{st}, which are related to ℓ_d, and *compression lap splice length*, ℓ_{sc}, which are not related to ℓ_{dc}. Due to the beneficial contribution of end bearing to bond in compression, ℓ_{dc} and ℓ_{sc} should not be longer than ℓ_d and ℓ_{st}, respectively. However, as will be described in Chapter 2, the ACI 318-19 [3] provisions for ℓ_{dc} sometimes produce required lengths that are substantially longer than ℓ_d. This problem motivates the work in Chapter 2.

Headed and hooked bars, which are common in beam-column joints and other connections, transfer tension force in a bar to the concrete through a combination of bond along the straight portion of the bar and bearing of the head or hook against concrete. The development lengths of headed and hooked bars (ℓ_{dt} and ℓ_{dh}, respectively) are based on tests under direct tension. Due in part to the lack of tests of headed and hooked bars in compression, heads and hooks are not generally considered effective for transferring compression forces to concrete. Nevertheless, there are applications, such as in beam-column joints subjected to earthquake-induced shaking, where headed and hooked bars are subjected to cyclic tension and compression forces. Very little research has been aimed at understanding the behavior of headed and hooked bars in compression, and it is unclear whether the design of headed and hooked bars in joints should consider compression force demands.

ACI 318-19 [3] governs the design of special moment frames (SMF) and prescribes that reinforcement terminating in a joint must be detailed so that both the tension and compression

development lengths are satisfied. The work in Chapters 3 and 4 will show that it is not necessary for either headed or hooked bars to satisfy the compression development length requirements to obtain acceptable beam-column joint behavior under reversed cyclic displacements. Moreover, Chapters 3 and 4 will show that the tension development requirements for headed and hooked bars in ACI 318-19 also appear considerably conservative in SMF joints.

A history of ACI Building Code provisions related to these issues is in Appendix A.

1.2 Scope

In Chapter 2, the ACI 408R-03 database of compression lap splice test results [4] was used to evaluate ACI 318-19 provisions for compression development and lap splice length. ACI 318-19 provisions are shown to be imprecise and highly conservative. Equations from other design standards and researchers were evaluated and recommendations are made for improving and simplifying ACI 318-19 provisions for compression development.

In Chapter 3, a database based on those from Kang et al. [5] and Ghimire, Darwin, and Lepage [6] is used to evaluate development length provisions for headed bars in SMF joints. The database includes test results from reinforced concrete exterior beam-column connection specimens with headed bars subjected to reversed cyclic loading. Recommendations are made for improving ACI 318-19 provisions.

In Chapter 4, a database assembled by the authors is used to evaluate development length provisions for hooked bars in SMF joints. The database includes results from tests of reinforced concrete exterior beam-column joint specimens with hooked bars that are subjected to reversed cyclic loading. Recommendations are made for improving ACI 318-19 provisions.

Chapter 5 provides a summary of major findings and recommendations from prior chapters.

Notation is defined at the end of each chapter. Chapter 6 provides references used in Chapters 1 through 5 and the appendices.

1.3 Notation

A_b	=	cross-sectional area of reinforcing bar (in.^{2})
f_y	=	specified yield stress for steel reinforcement (psi)
ℓ_d	=	tension development length (in.)
ℓ_{dc}	=	compression development length (in.)
ℓ_{sc}	=	compression lap splice length (in.)
ℓ_{st}	=	tension lap splice length (in.)
ℓ_{dt}	=	headed bar tension development length (in.)
ℓ_{dh}	=	hooked bar tension development length (in.)

Chapter 2: Development and Lap Splice Length of Straight Bars in Compression

2.1 Introduction

Section 25.5.5 of ACI 318-19 [3] requires that the compression lap splice length, ℓ_{sc}, satisfy Eq. (1), which is a function of the specified yield stress of the reinforcing steel and the bar diameter, with a minimum required length of 12 in. (300 mm).

$$\begin{aligned} &\text{(a) } \max\{0.0005 f_y d_b \text{ ; } 12 \text{ in.}\} && \text{for } f_y \le 60{,}000 \text{ psi} \\ &\text{(b) } \max\{(0.0009 f_y - 24) d_b \text{ ; } 12 \text{ in.}\} && \text{for } 60{,}000 \text{ psi} < f_y \le 80{,}000 \text{ psi} \\ &\text{(c) } \max\{(0.0009 f_y - 24) d_b \text{ ; } \ell_{st}\} && \text{for } 80{,}000 \text{ psi} < f_y \end{aligned} \qquad \text{Eq. (1)} \quad \text{(lb, in.)}$$

The provisions are applicable to No. 11 (36 mm) or smaller deformed bars in compression. The calculated splice length is to be increased by one-third when the concrete compressive strength is less than 3000 psi (21 MPa). For compression lap splices in columns, Chapter 10 of ACI 318-19 (§10.7.5.2.1) allows the calculated lap splice length to be multiplied by 0.83 or 0.75 if the splice is enclosed throughout its length by sufficient ties or spiral reinforcement. Sufficient refers, in this case, to an effective reinforcement ratio of ties greater or equal than 0.0015 in both directions throughout the splice length or spirals that meet ACI 318-19 §25.7.3 throughout the splice length, respectively. The provisions do not account for smaller quantities of transverse reinforcement in columns or for any quantity of transverse reinforcement for lap splices in members other than columns.

This contrasts with other ACI 318-19 equations related to bond, which do account for several of these variables. Consider the tension development length (§25.4.2), tension lap splice length (§25.5.2), and compression development length (§25.4.9) equations, shown in Eqs. (2) to (4), respectively. These equations not only include the steel reinforcement yield stress and bar diameter, but also the concrete compressive strength and factors accounting for lightweight concrete and transverse reinforcement. Equations (2) and (3) furthermore include modification

factors accounting for reinforcement grade, epoxy coating, bar size, reinforcement casting position, and concrete cover.

$$\ell_d = max\left\{\left(\frac{3}{40}\frac{f_y}{\lambda\sqrt{f_c'}}\frac{\psi_t\psi_e\psi_s\psi_g}{\left(\frac{c_{b,318}+K_{tr,318}}{d_b}\right)}\right)d_b \text{ ; 12 in.}\right\} \quad \text{Eq. (2) (lb, in.)}$$

$$\ell_{st} = \max\left\{\begin{pmatrix}1.0\ell_d & \text{(Class A splice)}\\ 1.3\ell_d & \text{(Class B splice)}\end{pmatrix}\text{; 12 in.}\right\} \quad \text{Eq. (3) (lb, in.)}$$

$$\ell_{dc} = \max\left\{\frac{f_y\psi_r}{50\lambda\sqrt{f_c'}}d_b \text{ ; } 0.0003f_y\psi_r d_b \text{ ; 8 in.}\right\} \quad \text{Eq. (4) (lb, in.)}$$

Since tension development, compression development, and compression lap splicing provisions represent very similar physical phenomena, it would be reasonable to expect that these provisions account for the same variables. The fact that they do not can lead to questionable (and possibly inefficient) designs. One of the issues is that in certain cases the calculated compression lap splice length can be considerably longer than the respective tension lap splice length. For instance, a compression lap splice of No. 8 (25 mm) Grade 80 (550) uncoated bars in a beam with a concrete compressive strength of 8000 psi (55 MPa) and closely spaced ties would be 48 in. (1220 mm) according to Eq. 1 (§25.5.5) if there is less than 12 in. (300 mm) of fresh concrete below it. This is 20% longer than the tension lap splice length of 40 in. (1020 mm) calculated with Eq. 3 (§25.5.2) for Class B lap splices. Even though §10.7.5.2 permits the calculated compression lap splice length to be reduced to 40 in. (1020 mm), that reduction is only permitted in columns. Furthermore, the compression lap splice length is almost three times the compression development length of 18 in. (457 mm) calculated with Eq. 4 (§25.4.9).

The fact that $\ell_{sc} > \ell_{st}$ in a reasonable design scenario is cause to question whether Section 25.5.5 (Eq. 1) can be improved. There is a need to identify equations for compression lap splice length that account for key variables (such as bar yield stress, bar diameter, concrete compressive strength, and transverse reinforcement) to consistently produce calculated lengths shorter than the tension lap splice lengths.

2.2 Database Description

This study examined the results in Group 1 of the ACI 408 compression lap splice database [4], which contains results from 91 tests of columns with lap-spliced bars subjected to monotonic compression. A summary of specimen variables is provided in Appendix B. The cross sections of columns in the database are shown in Figure 1. The distribution of important variables within the database are shown in Figures 2 through 7.

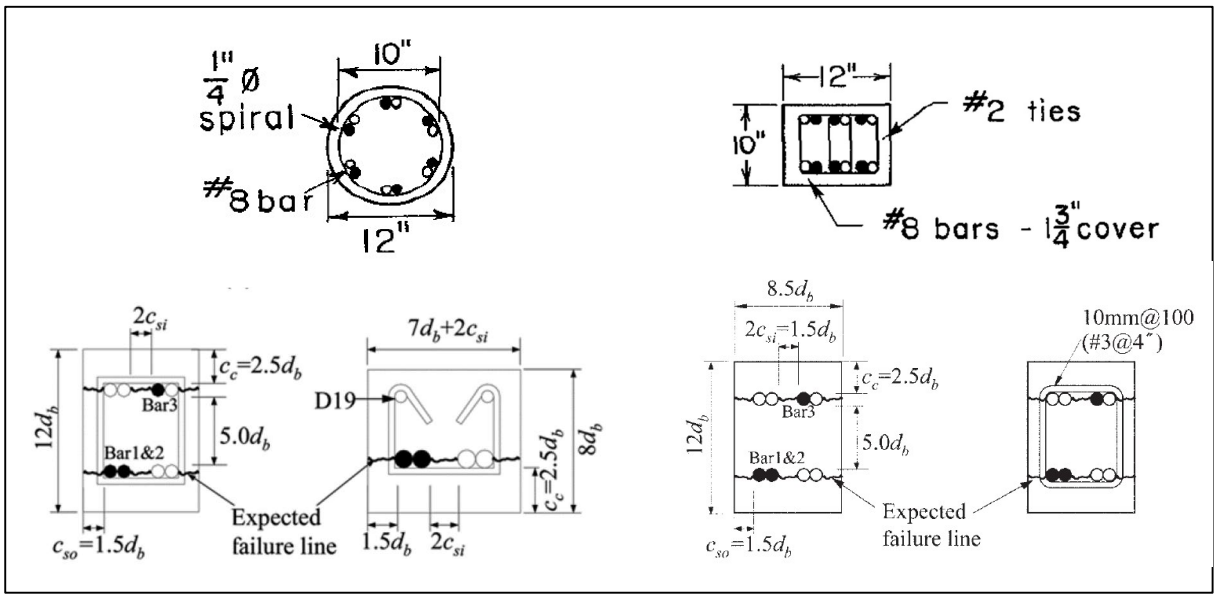

Figure 1 – Cross-sections of column specimens in database (from Refs. [7, 8, 9, 10])

(1 in. = 25.4 mm)

Most of the columns (87 out of 91) had rectangular cross-sections, and the ratio of long-to-short cross-sectional dimension was nominally between 1.0 and 1.4. Four specimens had circular cross sections. All lap-spliced bars had bond and bearing interactions with the concrete and the reported bar stress at lap splice failure did not exceed the yield stress. To limit the scope to specimens exhibiting stresses similar to those observed in practice, the two specimens that failed with steel stresses below 40 ksi (275 MPa) were removed from the dataset, resulting in a set of results from 89 tests.

The column longitudinal reinforcement, which was lap spliced, consisted of either No. 7, 8, or 9 (22, 25, or 29 mm) reinforcing bars (Figure 2). These bar sizes are reasonably representative of the bar sizes used in columns, walls, and beams where compression lap splices are common in practice. The rectangular columns in the database had either four or six longitudinal bars and the circular columns had six longitudinal bars. Either half or all of the column bars were lap spliced, and there were no columns with staggered lap splices in this dataset.

Approximately half (47%) of the columns had transverse reinforcement within the lap splice consisting of evenly spaced ties or hoops in the rectangular columns or a spiral in the circular columns. Figure 3 shows the distribution of the value obtained from $(c_{b,318} + K_{tr,318})/d_b$, which ranged from 1.25 to 4.0, and Figure 4 shows the distribution of $K_{tr,318}/d_b$, which ranged from 0 to 2. In this database, $c_{b,318}/d_b$ was greater than $K_{tr,318}/d_b$ in 89% of the specimens. In ACI 318-19, $(c_{b,318} + K_{tr,318})/d_b$ is part of the tension development length equation and does not apply for compression development, but it is used here because no analogous term is available within the building code for compression lap splices.

The distribution of concrete compressive strengths and reinforcement stresses at failure are shown in Figure 5 and Figure 6, respectively. Concrete compressive strength was measured using

either 4 by 8 in. (100 by 200 mm) or 6 by 12 in. (150 by 300 mm) cylinders. To reduce scatter in results associated with differences in cylinder size, the measured strengths were converted to an equivalent 6 by 12 in. (150 by 300 mm) cylinder using the method described by Reineck et al. [11] ($f_{1c,mod}$ was obtained by multiplying results from 4 by 8 in. (100 by 200 mm) or 6 by 12 in. (150 by 300 mm) cylinders by (0.92/0.95) and 1.00, respectively). The converted concrete compressive strengths ranged from 3.5 to 14.2 ksi (24 to 98 MPa). Specimens failed with bar stresses of 40 to 83 ksi (275 to 570 MPa), with most specimens (70%) failing at bar stresses between 50 and 70 ksi (345 to 482 MPa). Bar stresses were inferred from readings from strain gauges on the lap-spliced reinforcement, except for four specimens reported by Pfister and Mattock [7], who inferred bar stresses in these tests using a method calibrated against bar strain measurements.

The lap splices had lengths of 3.5 to 30 in. (89 to 760 mm) (Figure 7), but the majority were shorter than 14 in. (356 mm). Given this distribution, and to avoid reducing the number of tests in the database too severely, no minimum lap splice length was applied in the analyses even though ACI 318-19 requires a minimum length of 12 in. (300 mm). As stated above, the database was filtered to only include specimens exhibiting a bar stress of at least 40 ksi (275 MPa) at failure.

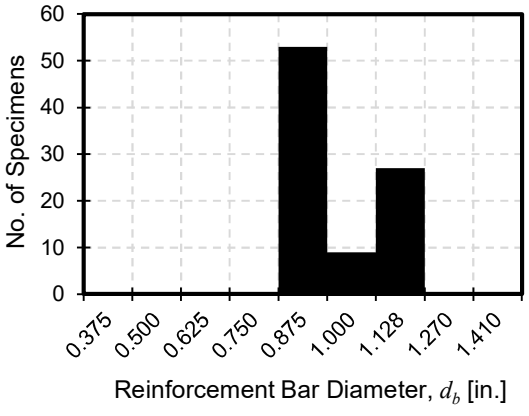

Figure 2 – Histogram of bar diameter
(1 in. = 25.4 mm)

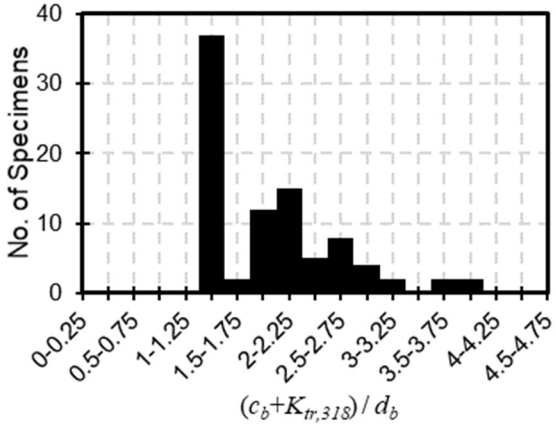

Figure 3 – Histogram of $(c_{b,318} + K_{tr,318})/d_b$ values

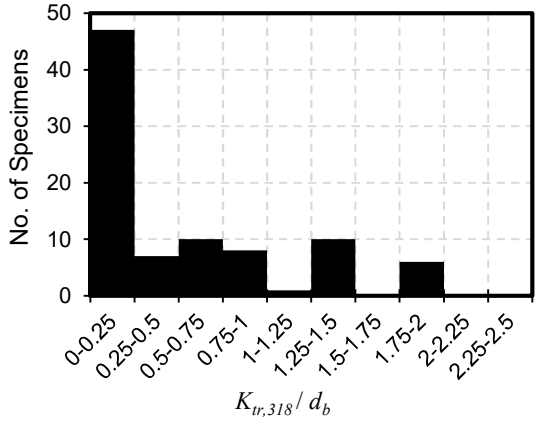

Figure 4 – Histogram of $K_{tr,318}/d_b$

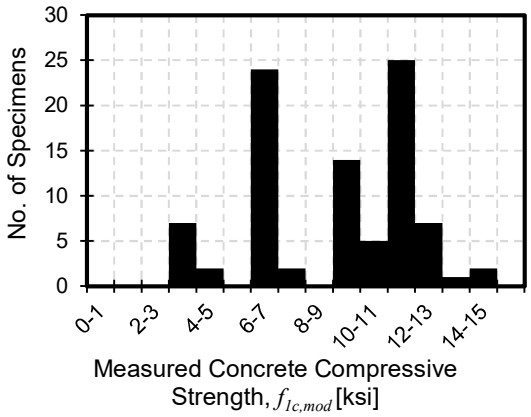

Figure 5 – Histogram of measured concrete compressive strength (1 ksi = 6.895 MPa)

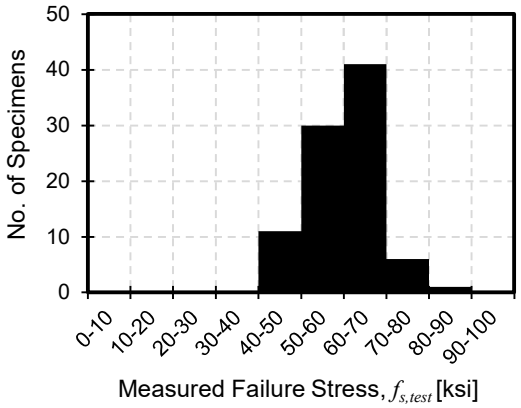

Figure 6 – Histogram of measured steel stress at failure (1 ksi = 6.895 MPa)

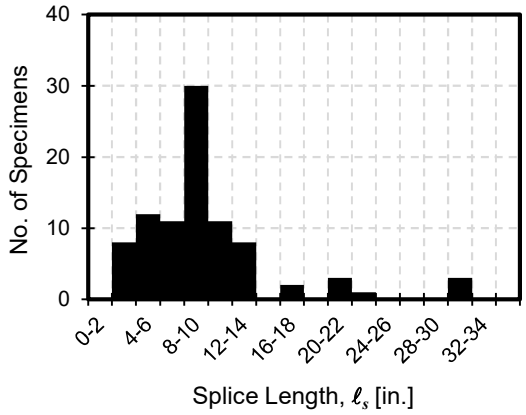

Figure 7 – Histogram of lap splice lengths (1 in. = 25.4 mm)

When assessing equations using a dataset, it is necessary to acknowledge unintended biases within the dataset. Such biases can occur because, as shown in Figures 2 through 7, the variables are not randomly distributed. Decisions made by researchers can also, inadvertently, cause independent variables to be correlated within a database. For example, it was found that concrete compressive strength and lap splice length are somewhat correlated in this database (Figure 8). All specimens with a concrete compressive strength above 10 ksi (69 MPa) also had a lap splice length of not more than 12 in. (300 mm). No other correlations were observed among the variables plotted in Figures 2 through 7. Plots similar to Figure 8 for other sets of variables are in Appendix C.

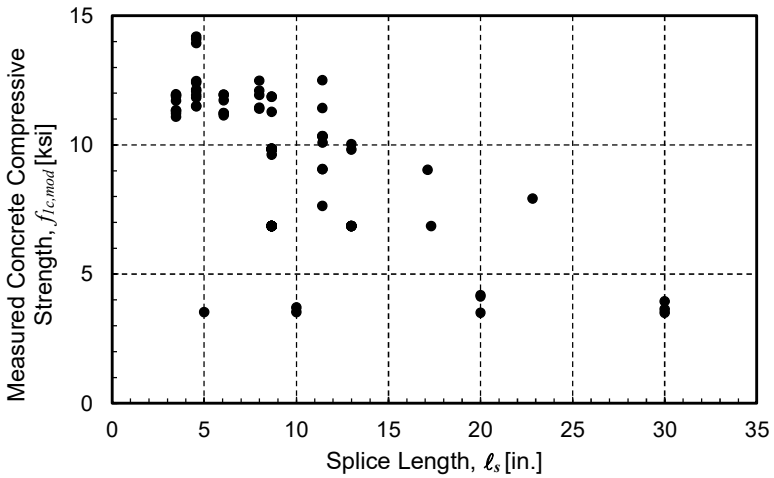

Figure 8 – Correlation between concrete compressive strength and lap splice length
(1 in. = 25.4 mm, 1 ksi = 6.895 MPa)

2.3 Comparisons with Design Equations

The database was used to evaluate the ACI 318-19 [3] compression lap splice provisions in Eq. (1) (§25.5.5). This was done by comparing the bar stress at failure, $f_{s,test}$, against $f_{s,calc}$, which was obtained by solving the design equations in Eq. (1) for bar stress and replacing f_y with $f_{s,calc}$ to obtain Eq. (5) (without applying the limits of 12 in. (300 mm) or ℓ_{st}). The stress $f_{s,calc}$ is a function of the provided lap splice length and bar diameter, with the choice of equation (a), (b), or (c) based on the measured failure stress.

$$\begin{array}{lll} \text{(a)} \ \ell_{sc}/(0.0005 d_b) & \text{for } f_{s,test} \le 60{,}000 \text{ psi} & \\ \text{(b)} \ (\ell_{sc}/d_b + 24)/0.0009 & \text{for } 60{,}000 \text{ psi} < f_{s,test} \le 80{,}000 \text{ psi} & \text{Eq. (5)} \\ \text{(c)} \ (\ell_{sc}/d_b + 24)/0.0009 & \text{for } f_{s,test} > 80{,}000 \text{ psi} & \text{(lb, in.)} \end{array}$$

A test-to-calculated stress ratio (T/C) was then calculated for each specimen as the quotient of $f_{s,test}$ and $f_{s,calc}$. The modification factor in ACI 318-19 §10.7.5.2.1 that accounts for transverse reinforcement was included where it was applicable. The mean T/C for the database for Eq. (5) was 2.58 with a coeficient of variation, CV, of 0.60, and values ranging from 0.97 to 6.50. The

high mean and *CV* indicate that the ACI provisions are imprecise and sometimes overly conservative.

To better understand the trends, *T*/*C* values are plotted in Figures 9 through 12 versus several variables known to govern bond: $(c_{b,318} + K_{tr,318})/d_b$, $f_{1c,mod}$, $f_{s,test}$, and ℓ_s. Figure 9 includes no limits on $(c_{b,318} + K_{tr,318})/d_b$ because this term does not apply to compression lap splices (the limit of 2.5 for tension bar development is omitted). The ACI 318-19 minimum lap splice length of 12 in. (300 mm) was also not applied as a limit, although these plots do distinguish between specimens with lap splice lengths of at least $\ell_{sc,min}$ = 12 in. (300 mm) and those with shorter lap splices.

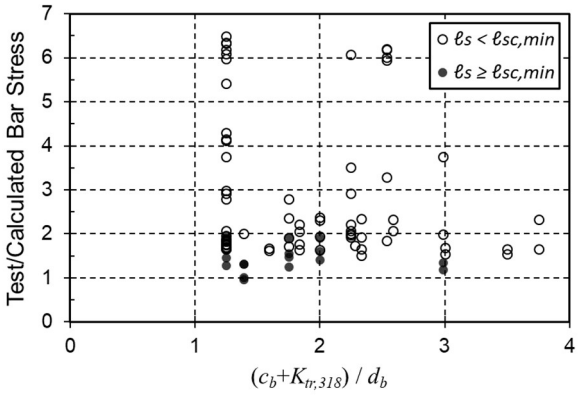

Figure 9 – ACI 318-19 compression lap splice : *T*/*C* vs. $(c_{b,318} + K_{tr,318})/d_b$

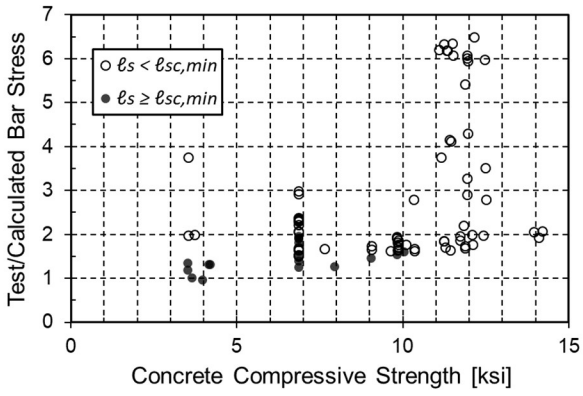

Figure 10 – ACI 318-19 compression lap splice: *T*/*C* vs. measured concrete compressive strength, $f_{1c,mod}$

(1 ksi = 6.895 MPa)

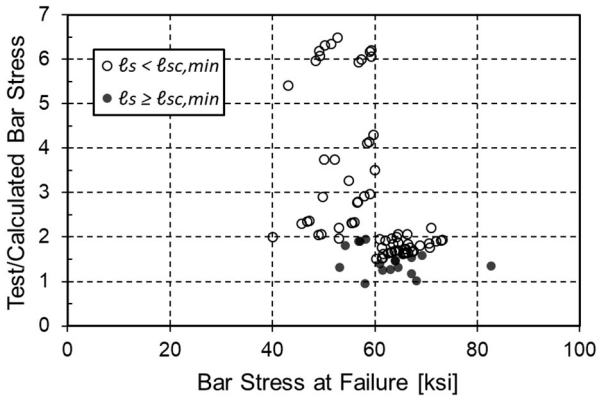

Figure 11 – ACI 318-19 compression lap splice: T/C vs. bar stress at failure, $f_{s,test}$

(1 ksi = 6.895 MPa)

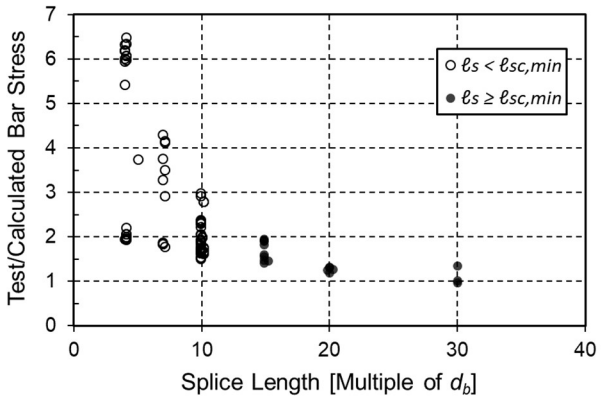

Figure 12 – ACI 318-19 compression lap splice: T/C vs. provided lap splice length, ℓ_s

(1 in. = 25.4 mm)

Figure 10 suggests that ACI 318-19 §25.5.5 tends to become more conservative as the concrete compressive strength increases, although there is considerable scatter. Figure 11 shows that Eq. 5(b) produces substantially less scatter for bar stresses greater than 60 ksi (420 MPa) than Eq. 5(a) produces for bar stresses less than 60 ksi (420 MPa). By inspection, it is also clear that Eq. 5(a) is considerably more conservative than Eq. 5(b). Figure 12 shows that the provisions become less conservative with longer lap splice lengths.

The scatter in Figures 9 through 12 increases for specimens with $f_{1c,mod} > 10{,}000$ psi (69 MPa) and $f_{s,test} \leq 60{,}000$ psi (420 MPa), which coincides with use of the equation applicable for $f_{s,test} \leq 60{,}000$ psi (420 MPa), Eq. 1(a). Many specimens with $f_{1c,mod} > 10{,}000$ psi (69 MPa) tended to have short lap splice lengths (below the ACI minimum) and, thus, also had lower bar stresses at failure. The black circles in Figures 9 through 12, representing the 17 specimens with $\ell_s > 12$ in. (300 mm), had T/C values between 0.97 and 2.0. Among these 17 specimens, the scatter is still greater for $f_{s,test} \leq 60{,}000$ psi than for $f_{s,test} > 60{,}000$ psi (420 MPa) (Figure 11). Given this scatter, and given that these equations sometimes produce calculated lap splice lengths that are longer for

compression than tension, there is a need to consider alternative expressions for design of compression lap splices.

2.4 Comparisons with other Compression Development Length Equations

2.4.1 Equations Considered

In addition to the comparisons with the ACI 318-19 [3] provisions, T/C values were calculated for another six expressions for either compression development length or compression lap splice length. These include: item (b) of the compression lap splice provisions from ACI 318-19 § 25.5.5.1, the ACI 318-19 §25.4.9 compression development length provisions, the 'complex' equation proposed by Chun, Lee, and Oh [9], the 'simplified' equation proposed by Chun, Lee, and Oh [12], the equation proposed by Cairns [13], and the fib Model Code [14] provisions.

i) Expression (b) of ACI 318-19 §25.5.5.1 compression lap splice length provisions (with §10.7.5.2.1 modifiers for confinement)

The ACI 318-19 lap splice length provisions (Eq. (1)) prescribe three different expressions (a, b, and c) for length, depending on the value of the steel reinforcement yield stress. Here only expression (b), reproduced in Eq. (6), is considered, regardless of the steel stress at failure. The minimum required lap splice length of 12 in. (300 mm) was omitted for this comparison. The confinement modifiers from §10.7.5.2.1 were used where applicable.

$$\ell_{sc} = (0.0009 f_y - 24) d_b \qquad \text{Eq. (6)}$$
$$\text{(lb, in.)}$$

ii) Development of straight bars in compression (ACI 318-19 §25.4.9)

Equation (4), repeated below, shows the ACI 318-19 [3] compression development length (§25.4.9) equations. The Code imposes a minimum compression development length of 8 in. (200 mm), which was omitted in these comparisons.

$$\ell_{dc} = \max\left\{ \frac{f_y \psi_r}{50\lambda\sqrt{f'_c}} d_b \ ; \ 0.0003 f_y \psi_r d_b \right\} \qquad \text{Eq. (7) (lb, in.)}$$

where $\sqrt{f'_c} \le 100$ psi. Factor λ was 1.0 because no specimens in this database had lightweight concrete. The confining reinforcement factor, ψ_r, was also always 1.0 except for the four circular column specimens reported in Pfister and Mattock [7].

iii) 'Complex' equation for compression lap splices from Chun, Lee, and Oh [9]

Chun et al. [8, 9, 10] report results from tests of columns with compression lap splices with and without confinement. They propose Eq. (8), referred to herein as the 'complex' equation, to distinguish it from the 'simplified' Eq. (9) proposed by the same authors.

$$\frac{l_s}{d_b} = \left(\frac{\frac{f_y}{0.82\sqrt{f'_c}} - 198 - 21\delta}{134 + 18\frac{K_{tr,318}}{d_b}} \right)^2 \qquad \text{Eq. (8) (lb, in.)}$$

$$\text{where } \frac{K_{tr,318}}{d_b} \le 1.76 \ ; \ \frac{l_s}{d_b} \le \begin{cases} 0.0005 f_y & \text{if } f_y \le 60{,}000 \text{ psi} \\ 0.0009 f_y - 24 & \text{if } f_y > 60{,}000 \text{ psi} \end{cases}$$

iv) 'Simplified' equation for compression lap splices proposed by Chun, Lee, and Oh. [12]

The simplified equation from Chun, Lee, and Oh [12], Eq. (9), is indeed much simpler than Eq. (8). Aside from simplicity, it is notable that Eq. (9) includes concrete compressive strength to the quarter power as opposed to its square root.

$$\frac{l_s}{d_b} = \frac{1.4 f_y}{\psi_{sc}\sqrt{f'_c}} - 52 \qquad \text{Eq. (9) (SI)}$$

$$\text{with } \psi_{sc} = 1 + 0.084\frac{K_{tr,318}}{d_b} \ ; \ \frac{l_s}{d_b} \le \begin{cases} 0.071 f_y & \text{if } f_y \le 420 \text{ MPa} \\ 0.13 f_y - 24 & \text{if } f_y > 420 \text{ MPa} \end{cases}$$

v) Compression lap splice equation proposed by Cairns [13]

Cairns [13] proposed Eq. (10) for compression lap splice strength based on tension splice equations using test data from different sources. The equation highlights the role of transverse reinforcement and end bearing in compression lap splices. Based on the empirical finding that compression lap splices tend to fail when transverse reinforcement yields [14], this compression splice equation uses the yield stress of the transverse reinforcing steel, f_{yt}. Within the available database, this parameter was only measured and reported by Pfister and Mattock [7]. Where no information about the transverse reinforcing steel was reported, a yield stress of 60,000 psi (420 MPa) was assumed for calculating T/C.

$$f_{sc} = \left[16.9 \frac{\ell_s}{d_b} + 354 + 0.026 \frac{A_{tr} \cdot f_{yt} \cdot \ell_s}{s \cdot d_b^{\,2}} \right] \sqrt{f_c'} \qquad \text{Eq. (10)} \text{ (lb, in.)}$$

vi) fib Model Code [15] provisions

The *fib* 2010 Model Code method is notably different from the other equations considered. First, a basic bond strength is calculated from the characteristic concrete compressive strength, f_{ck}, bar diameter, bar surface characteristics, bar position during casting, and characteristic strength of steel reinfocement. This basic bond strength is then modified to obtain a design bond strength, depending on concrete cover, bar spacing, and other factors affecting confinement. Finally, the design bond strength is used to determine a required length of lap splice in compression, l_b. These provisions are reproduced in Eq. (11) in the original SI units. A minimum lap length, $l_{b,min}$, is prescribed but has been omited in Eq. (11).

Length of lap in compression:

$$l_b = \frac{\varnothing}{4 f_{bd}}\left(f_{yd} - F_h / A_s\right); \quad f_{yd} = f_{yk}/\gamma_s; \quad F_h = 60 f_{bd} A_s;$$

$$l_b \geq l_{b,\min} = \max\left\{0.7\frac{\varnothing}{4}\frac{f_{yd}}{f_{bd}}\ ; 15\varnothing\ ; 200\text{ mm}\right\}\text{(ignored)}$$

Design bond strength:

$$f_{bd} = \left(\alpha_2 + \alpha_3\right) f_{bd,0} - 2\, p_{tr}/\gamma_c < 2.5 f_{bd,0} - 0.4\, p_{tr}/\gamma_c < 1.5\sqrt{f_{ck}}/\gamma_c\ ; \qquad \text{Eq. (11) (SI)}$$

$\alpha_2 = \left(\frac{c_{min,fib}}{\emptyset}\right)^{0.5}\left(\frac{c_{max,fib}}{c_{min,fib}}\right)^{0.15}$ for ribbed bars; $\alpha_3 = k_d\left(K_{tr,fib} - \alpha_t/50\right) \geq 0.0$

$$K_{tr,fib} = n_t A_{st}/\left(n_b \varnothing s_t\right) \leq 0.05$$

Basic bond strength:

$$f_{bd,0} = \eta_1\eta_2\eta_3\eta_4\left(f_{ck}/25\right)^{0.5}/\gamma_c$$

2.4.2 Results

Figure 13 shows the range, mean, and *CV* of the *T*/*C* for each of these compression lap splice or development length equations, and well as for the already discussed ACI 318-19 compression lap splice provisions. To examine the merits of the selected equations, a set of plots analogous to Figures 9 through 12 are in Appendix D for each of the equations considerd in Figure 13.

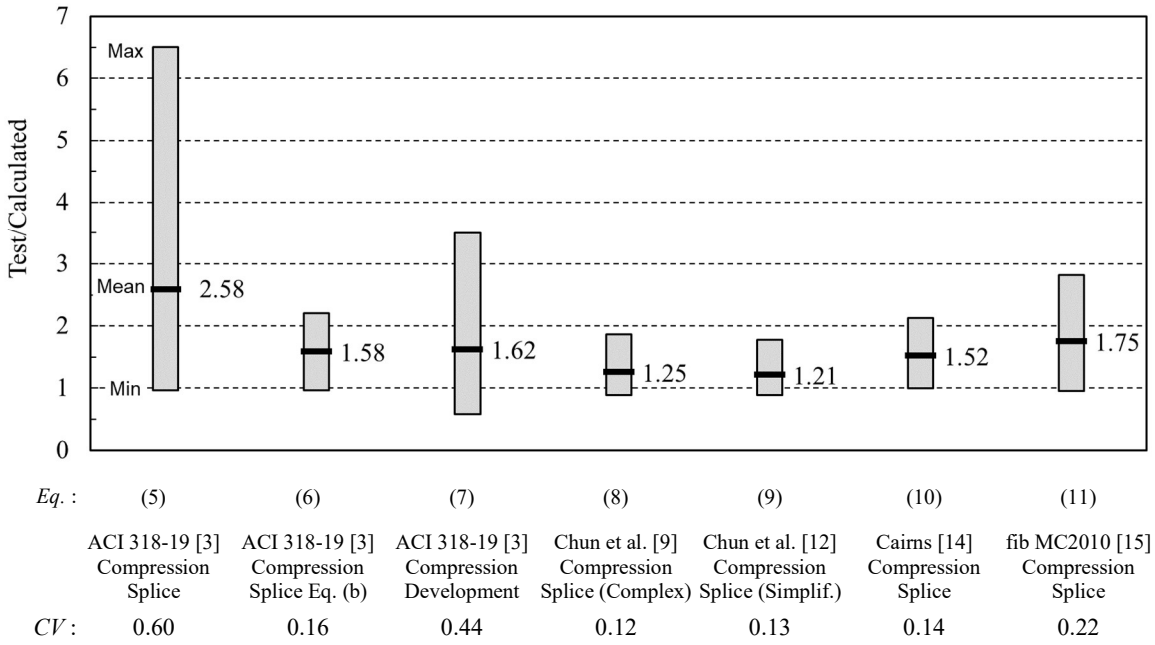

Eq. :	(5)	(6)	(7)	(8)	(9)	(10)	(11)
	ACI 318-19 [3] Compression Splice	ACI 318-19 [3] Compression Splice Eq. (b)	ACI 318-19 [3] Compression Development	Chun et al. [9] Compression Splice (Complex)	Chun et al. [12] Compression Splice (Simplif.)	Cairns [14] Compression Splice	fib MC2010 [15] Compression Splice
CV :	0.60	0.16	0.44	0.12	0.13	0.14	0.22

Figure 13 – *T*/*C* for compression lap splice and development length equations

The worst performance in terms of scatter is the ACI 318-19 compression lap splice provisions, with a *CV* of 0.60 (although it must be emphasized that all specimens with $T/C > 2.0$ violated the ACI 318-19 minimum lap splice length).

When solely applying Eq. (b) of the ACI 318-19 compression lap splice provisions (Eq. (6)) to the entire database, as opposed to discriminating by steel failure stress, the calculated stresses are much closer to the measured values than when using the entire provision (Eq. (5)), with a mean of 1.58 and *CV* of 0.16. Figure 66 in Appendix D shows that, although the scatter is relatively low, use of Eq. (6) does not appear to properly account for effects of confinment or concrete compressive strength. Furthermore, it produces relatively low *T*/*C* values for lap splices longer than $20d_b$ and for the only specimen with a bar stress greater than 80 ksi (550 MPa).

The ACI 318-19 compression development length equation, Eq. (7), exhibited more scatter than Eq. (6), with a mean of 1.62 and *CV* of 0.44. Although not shown here, removing the 100 psi

(0.69 MPa) limit on $\sqrt{f_c'}$ did not result in a substantial improvement for the ACI 318-19 development length equation and is not recommended. Figure 67 in Appendix D shows the ACI 318-19 compression development length equation does not properly account for effects of confinment or concrete compressive strength. Furthermore, they produce *T*/*C* values below 1.0 for lap splices longer than $12d_b$ and for the only specimen with a bar stress greater than 80 ksi (550 MPa). It would not be acceptable to use the ACI 318-19 §25.4.9 compression development length provisions for compression lap splice design.

The two equations proposed by Chun, Lee, and Oh [9, 12], Eqs. (8) and (9), show similar results in terms of mean and *CV*, and they are the most accurate and precise of the equations referenced in Figure 13. The simplified equation in particular, which includes only four independent variables (f_y, f_c', d_b, and $K_{tr,318}$), provides a very good fit with the data given its simplicity. Figure 68 and Figure 69 in Appendix D show that the 'complex' equation properly accounts for effects of confinement, concrete compressive strength, and lap splice length, with *T*/*C* values that are similar across the range of these variables in the database. Furthermore, the 'complex' equation becomes slightly more conservative for higher bar stresses, which is desireable since only one test result is available for bar stresses greater than 80 ksi (550 MPa). The 'simplified' equation also does a good job accounting for effects of confinement and concrete compressive strength and tends to become more conservative for longer lap splices and higher bar stresses. It appears that either equation is a candidate for use in design.

The Cairns [13] equation, Eq. (10), also produces a very good fit to the data, with a mean of 1.52 and *CV* of 0.14. This equation is the only one considered that uses the yield stress of the transverse reinforcing steel, f_{yt}. Figure 70 in Appendix D shows that this equation also does a good job accounting for effects of confinement, concrete compressive strength, and lap splice length,

with T/C values that are similar across the range of these variables in the database. Furthermore, it becomes more conservative for higher bar stresses, which is desireable since only one test result is available for bar stresses greater than 80 ksi (550 MPa). This equation is a candidate for use in design.

The fib Model Code [15] design provisions, condensed in Eq. (11), have a mean T/C of 1.75 and CV of 0.22 and are more complex than the other equations considered. They are considerably more accurate and precise than the ACI 318-19 provisions but less accurate and precise than the equations proposed by researchers. Figure 71 in Appendix D shows that fib Model Code design provisions also do a good job accounting for effects of confinement, concrete compressive strength, bar stress, and lap splice length, with T/C values that are similar across the range of these variables in the database. These provisions appear appropriate for use in design.

2.5 Comparisons with Tension Development Equations

2.5.1 Equations Considered

The prior section demonstrates that several equations exist that fit the database of compression lap splice tests relatively well and might be candidates for use in design. Nevertheless, since the mechanics of bond share some similarities for bars in tension and compression, this section explores the potential to use existing tension development length equations for design of compression lap splices. Tension development has long been studied and designers are familiar using equations for tension development length. If feasible, use of the same or similar equations for design of compression and tension lap splices would simplify design.

Six equations were considered: the ACI 318-19 [3] tension development length equation; the ACI 408R-03 [1] tension development length equation; an equation proposed by Lepage,

Yasso, and Darwin [16]; an equation proposed by Darwin, Lutz, and Zuo [17]; an equation proposed by Canbay and Frosch [18]; and an equation proposed by Frosch, Fleet, and Glucksman [19].

i) ACI 318-19 [3] tension development length for deformed bars and wires

ACI 318-19 [3] §25.4.2 prescribes that the tension development length for deformed bars and wires shall be the greater of (a) and (b) in Eq. 12:

Development length shall be the greater of (a) and (b):

$$\text{(a) } \ell_d = \left(\frac{3}{40} \frac{f_y}{\lambda \sqrt{f_c'}} \frac{\psi_t \psi_e \psi_s \psi_g}{\left(\frac{c_{b,318} + K_{tr,318}}{d_b} \right)} \right) d_b \qquad \text{(b) 12 in. (ignored)}$$

with ψ_t, ψ_e, ψ_s, and ψ_g per Table 25.4.2.5 (with linear interpolation for ψ_g depending on the bar stress). For bars with $f_y \geq 80{,}000$ psi (550 MPa) spaced ≤ 6 in. (150 mm) on center, transverse reinforcement shall be provided such that $K_{tr,318} \geq 0.5 d_b$

$$K_{tr,318} = \frac{40 A_{tr}}{sn} \; ; \; \sqrt{f_c'} \leq 100 \text{ psi} \; ; \left(\frac{c_{b,318} + K_{tr,318}}{d_b} \right) \leq 2.5 \; ; \; \psi_t \psi_e \leq 1.7$$

Eq. (12) (lb, in.)

ACI 318-19 defines $K_{tr,318}$ as a factor that represents the contribution of transverse reinforcement across potential splitting planes and whose determination involves the considereation of multiple splitting scenarios in seach of the most unfavorable case.

The values of the reinfocement grade factor ψ_g used for design are tabulated in ACI 318-19 and are a function of only bar grade. In this section, ψ_g was defined as a linear function of $f_{s,calc}$ rather than bar grade:

$$\psi_g = 0.55 + 0.3(f_{s,calc}/40{,}000) \qquad \text{Eq. (13) (lb, in.)}$$

This required an iterative solution process to solve for $f_{s,calc}$, since $f_{s,calc}$ was both an input and output.

ii) ACI 408R-03 [1] tension development length equation

The recommendations for tension development length by ACI Committee 408 account for numerous parameters, including transverse reinforcement, concrete cover, bar geometry, bar stress, and concrete strength (Eq. (14)).

$$\frac{\ell_d}{d_b} = \frac{\left(\frac{f_y}{\phi f_c'^{1/4}} - 2400\right)\alpha\beta\lambda}{76.3\left(\frac{c\omega + K_{tr,408}}{d_b}\right)} \geq 16$$

$$\text{with: } \omega = 0.1\,\frac{c_{\max,408}}{c_{\min,408}} + 0.9 \leq 1.25 \quad ; \quad t_r = 9.6\,R_r + 0.28 \leq 1.72 \; ;$$

$$t_d = 0.03\,d_b + 0.22 \quad ; \quad K_{tr,408} = \frac{0.52 t_r t_d A_{tr}}{sn} f_c'^{1/2} \; ; \quad f_c'^{1/4} \leq 11.0 \; ;$$

$$f_y \leq 80\,\text{ksi} \qquad \left(\frac{c\omega + K_{tr,408}}{d_b}\right) \leq 4.0$$

Eq. (14) (lb, in.)

iii) Lepage, Yasso, and Darwin [16] equation

The equation recommended in Lepage, Yasso, and Darwin [16], shown as Eq. (15), was derived from ACI 408R-03. It allows the use of higher-grade reinforcement and higher strength concrete than permitted by the base equations. A reinforcement yield stress modification factor, ψ_y, is introduced to account for the fact that lap splice length and bar grade are not proportional. As with the ACI 318-19 §25.4.2 tension development length equation, solving for $f_{s,calc}$ in this case

requires extra attention because the steel stress variable is present both as a proportional factor for ℓ_d and in the definition of ψ_y. An iterative solution process is required to solve for $f_{s,calc}$.

$$\ell_d = \frac{1}{90}\frac{f_y \psi_t \psi_e \psi_y}{\lambda f'^{1/4}_c \left(\frac{c_{b,318}\omega + K_{tr,318}}{d_b}\right)} d_b \geq \max(12\text{ in.}, 16 d_b)$$

$$\text{with } \psi_y = 1.5 - \frac{30{,}000}{f_y} \geq 0.75 \; ; \left(\frac{c_{b,318}\omega + K_{tr,318}}{d_b}\right) \leq 4.0$$

Eq. (15) (lb, in.)

iv) Darwin, Lutz and Zuo [17] equation

The equation recommended in Darwin, Lutz and Zuo [17] (Eq. (16)) is based on the ACI 408R-03 tension development length equations. The variable $K_{tr,408}$ is replaced with K'_{tr}, which eliminates the t_r term representing the effect of relative rib area. The upper limit for the confinement term, in this case ($c\omega$+K'_{tr}/d_b), is 4, similar to ACI 408R-03.

$$\ell_d = \frac{\left(\frac{f_y}{f'^{1/4}_c} - 2400\right)\psi_t \psi_e \lambda}{1.5\left(\frac{c\omega + K'_{tr}}{d_b}\right)} d_b \geq 16$$

$$\text{with: } \omega = 0.1\,\frac{c_{\max,408}}{c_{\min,408}} + 0.9 \leq 1.25 \quad ; \quad t_d = 0.03\, d_b + 0.22$$

$$K'_{tr} = \frac{t_d A_{tr} \sqrt{f'_c}}{2sn} \; ; \quad \left(\frac{c\omega + K'_{tr}}{d_b}\right) \leq 4.0$$

Eq. (16) (lb, in.)

v) Canbay and Frosch [18] equation

Canbay and Frosch [18] proposed a simplified design equation applicable for the design of beams and slabs. The proposed expression, which can be used to calculate either development

or lap splice lengths, depends only on the yield stress and bar diameter of the longitudinal reinforcement and the concrete compressive strength.

$$\ell_d = \frac{0.9 \cdot 10^{-6} f_y{}^2 \sqrt{d_b}}{\sqrt{f_c'}} d_b \geq 12\ in., 16 d_b \qquad \text{Eq. (17)} \text{ (psi, in.)}$$

vi) Frosch, Fleet, and Glucksman [19] equation

Frosch, Fleet, and Glucksman [19] recommend a design expression for bond strength (not development length). The first term deals with the contribution of concrete to bond strength, while the second term accounts for transverse reinforcement.

$$f_b = \left(f_c'\right)^{0.25} \left(\frac{l_s}{d_b}\right)^{0.5} \left(\frac{c_{so}}{d_b}\right)^{0.25} + \frac{30 N_s \left(N_l A_t\right)}{N_b A_b} \qquad \text{Eq. (18)} \text{ (lb, in.)}$$

2.5.2 Methods for Evaluating Tension Development Equations against Database

There is an important difference between the mechanics of bond for bars in tension and compression: bars in compression benefit from end bearing of the bar on concrete. To develop the same bar force, a shorter lap splice length should be needed in compression than in tension.

Therefore, in addition to assessing *T*/*C* values for the tension equations (Table 1). Three methods for adjusting the tension development length equations were also considered. Each of these methods was calibrated to obtain a minimum *T*/*C* value of 1.0 when compared against the database of compression lap splice tests. This minimum *T*/*C* value was selected for simplicity and consistency, and may not reflect the appropriate level of conservatism for design.

Method #1: r_l length multiplier

Method 1 for converting the calculated length in tension to a calculated length in compression is shown in Eq. (19). Each calculated tension development length, ℓ_d, was multiplied

by r_1, a constant that differs for each equation that was selected to produce a minimum T/C of 1.0 when compared with the test results in the database, that is, to achieve a 0% fractal.

$$\ell_{sc} = r_1 \ell_d \qquad \text{Eq. (19)}$$

For instance, for the ACI 408R-03 [1] equation, this results in:

$$\ell_{sc} = r_1 \cdot l_{d,408} = r_1 \frac{\left(\frac{f_y}{\phi f'^{1/4}_c} - 2400\omega\right)\alpha\beta\lambda}{76.3\left(\frac{c\omega + K_{tr,408}}{d_b}\right)} d_b \qquad \text{Eq. (20) (lb, in.)}$$

This method is simple and intuitive, but also not exactly correct: the force transferred by end bearing is unlikely proportional to development length. This approach is still considered given its simplicity.

Method #2: r_2 bar stress multiplier

If a bar developed in compression transfers force to the concrete through end bearing, then for the same target yield stress, less force must transfer through bond in compression than in tension. Method 2 assumes that the tension development length equations represent the length necessary to transfer a given force through bond. In Method 2, the calculated lap splice length in compression is obtained from the tension development length equations for a bar stress of $r_2 f_y$ (Eq. (21)). Multiplier r_2 affects f_y everywhere it may appear in the equations, including variables that are a function of f_y such as ψ_y in the Lepage, Yasso and Darwin [16] equation.

$$\ell_{sc} = \ell_d \left(r_2 f_y\right) \qquad \text{Eq. (21)}$$

The r_2 value is a constant that differs for each equation that, as with r_1, was selected to produce a minimum T/C of 1.0, which corresponds to a 0% fractal.

As with Method 1, Method 2 is simple and intuitive, but also not exactly correct: the force transferred by end bearing is unlikely to be proportional to bar stress. This approach is still considered given its simplicity.

Method #3: ψ_y modifier in Lepage, Yasso. And Darwin equation [16]

The Lepage, Yasso, and Darwin [16] equation includes a reinforcement yield stress factor, ψ_y. Their tension development length equation [Eq. (16)] is proportional to this factor, which has the form A – B / f_y, where A is 1.5 and B is 30,000 psi (210 MPa). Method 3 consists of modifying the constant B to obtain a minimum *T*/*C* of 1.0, which again corresponds to a 0% fractal. The calculated value of B is 55,600, which is rounded to 50,000 in Eq. (22).

$$\psi_y = 1.5 - \frac{50{,}000}{f_y} \geq 0.75 \qquad \text{Eq. (22)}$$
(lb, in.)

2.5.3 Results

Table 1 summarizes the *T*/*C* statistics obtained for the six considered tension development length equations and shows how their behavior changes with the derived r_1, r_2, and ψ_y factors.

Figures 14, 15, and 16 are analogous to Figure 13 and show the range, mean, and *CV* of the *T*/*C* for each tension development equation considered, including the value of r_1 and r_2 where applicable.

Table 1 – Summary of *T*/*C* statistics for original and altered tension development equations

	ACI 318-19 [3]	ACI 408R-03 [1]	Lepage et al. [16]	Darwin et al. [17]	Canbay and Frosch [18]	Frosch et al. [19]
	Original Equation					
mean	2.62	1.76	2.02	1.74	2.00	1.73
SD	1.04	0.23	0.35	0.21	0.42	0.38
CV	0.40	0.13	0.17	0.12	0.21	0.22
max	6.02	2.30	2.76	2.28	3.30	2.67
min	1.39	1.19	1.35	1.28	1.27	1.01
	Method 1: Using r_1					
r_1	0.61	0.69	0.66	0.63	0.62	0.97
mean	1.78	1.51	1.75	1.44	1.58	1.71
SD	0.66	0.24	0.36	0.23	0.33	0.38
CV	0.37	0.16	0.21	0.16	0.21	0.22
max	3.94	2.09	2.58	1.97	2.61	2.64
min	1.00	1.00	1.00	1.00	1.00	1.00
	Method 2: Using r_2					
r_2	0.72	0.84	0.74	0.78	0.79	0.99
mean	1.89	1.47	1.50	1.36	1.58	1.72
SD	0.75	0.19	0.26	0.16	0.33	0.38
CV	0.40	0.13	0.17	0.12	0.21	0.22
max	4.33	1.92	2.06	1.78	2.61	2.64
min	1.00	1.00	1.00	1.00	1.00	1.00
	Method 3 using optimized ψ_y (A=1.5, B=50,000)					
mean			1.39			
SD			0.20			
CV			0.14			
max			1.82			
min			1.00			

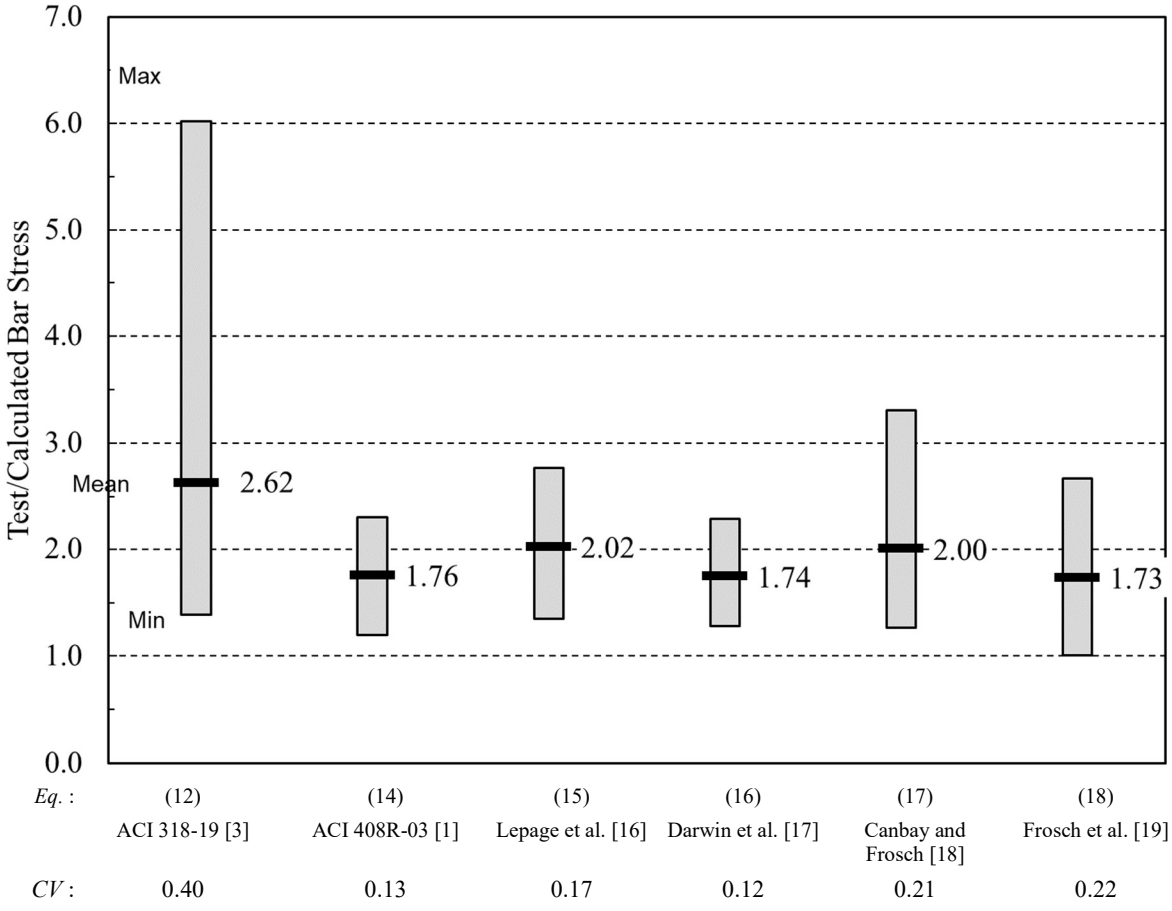

Eq. :	(12)	(14)	(15)	(16)	(17)	(18)
	ACI 318-19 [3]	ACI 408R-03 [1]	Lepage et al. [16]	Darwin et al. [17]	Canbay and Frosch [18]	Frosch et al. [19]
CV :	0.40	0.13	0.17	0.12	0.21	0.22

Figure 14 – *T*/*C* for tension development length equations with no modification

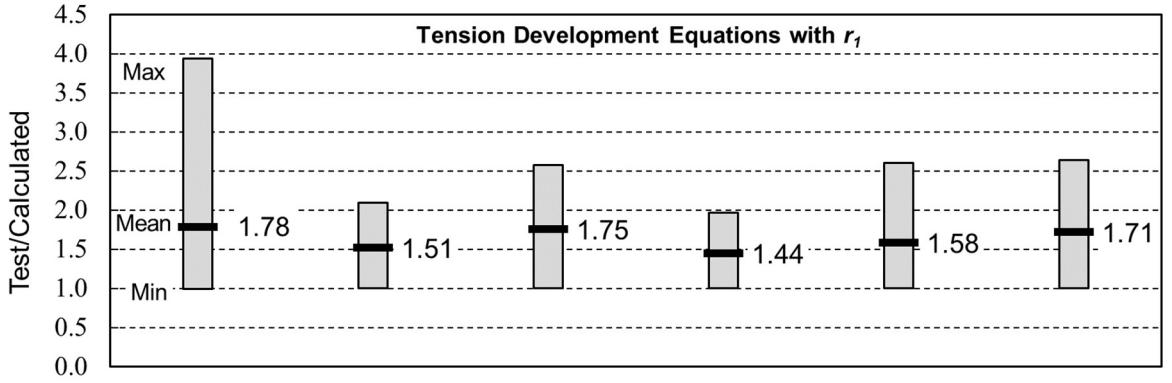

Eq. :	(12)	(14)	(15)	(16)	(17)	(18)
	ACI 318-19 [3]	ACI 408R-03 [1]	Lepage et al. [16]	Darwin et al. [17]	Canbay and Frosch [18]	Frosch et al. [19]
CV :	0.37	0.16	0.21	0.16	0.21	0.22
r_1 :	0.61	0.69	0.66	0.63	0.62	0.97

Figure 15 – *T*/*C* for tension development length equations including r_1 multiplier

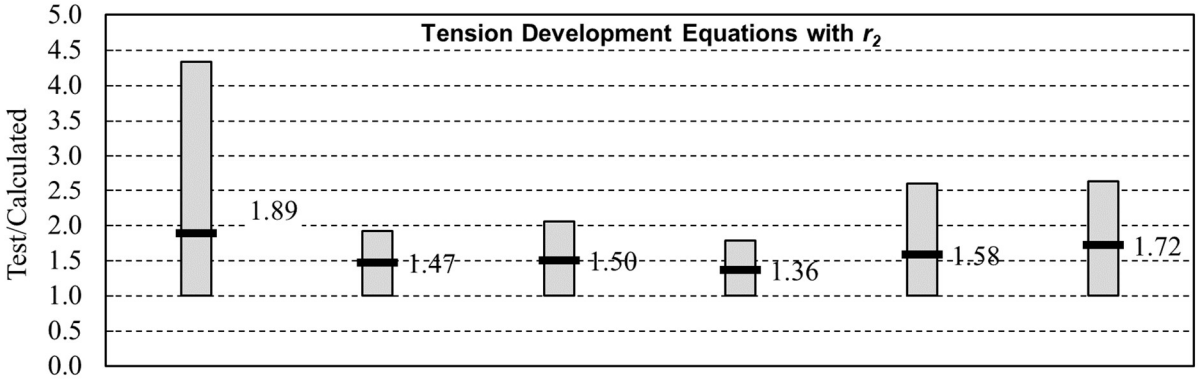

Eq. :	(12)	(14)	(15)	(16)	(17)	(18)
	ACI 318-19 [3]	ACI 408R-03 [1]	Lepage et al. [16]	Darwin et al. [17]	Canbay and Frosch [18]	Frosch et al. [19]
CV :	0.33	0.13	0.17	0.12	0.21	0.20
r_2 :	0.96	0.84	0.74	0.78	0.79	0.93

Figure 16 – T/C for tension development length equations including r_2 multiplier

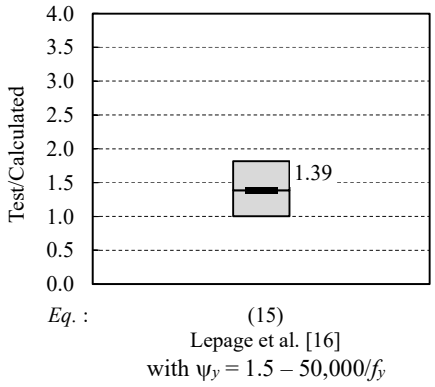

Figure 17 – *T*/*C* for Lepage et al. [16] recommended provisions with modified ψ_y

Table 1 and Figure 14 show that the unaltered tension development length equations all have lower mean and *CV* values than the current ACI 318-19 provisions for compression lap splices. The ACI 318-19 tension development length equation has the highest mean (2.62) and scatter (*CV* of 0.40) of the six tension development equations considered. The other five unmodified tension development length equations in Figure 14 have *CV* values that are similar to the most precise compression lap splice equations shown in Figure 13 (*CV* values were 0.12 to

0.21 for tension equations in Figure 14 and 0.12 to 0.22 for compression equations in Figure 13). These results strongly suggest that it may be possible to determine compression lap splice lengths as a function of tension lap splice lengths without losing precision.

Moreover, Figures 15, 16, and 17 suggest that all three methods for modifying the tension development length equations to obtain a 0% fractal have potential, with the bar stress (r_2) multiplier resulting in marginally better accuracy and precision than the bar length (r_1) multiplier for the ACI 408R-03, Lepage et al., and Darwin et al. equations. For the remaining equations, the use of either r_1 or r_2 produce similar results.

Figure 18 shows T/C for the ACI 408R-03 tension development equation versus $f_{1c,mod}$ for (a) the original equation, (b) the equation with r_1, and (c) the equation with r_2. For the original equation, Figure 18(a), the values of T/C range from 1.19 to 2.30. In Figure 18(b), when r_1 is under effect, the minimum value of T/C becomes 1.00 after targeting the 0% fractal. Figure 18(c) with r_2 also has a minimum T/C value of 1.00, but the range of values is reduced compared to Figure 18(b). The trend line is also somewhat more horizontal in Figure 18(c) than in Figure 18(b), which along with the reduced scatter, shows that using r_2 produces a marginally better fit to the data than either r_1 or the original equation.

Appendix E has a set of plots (Figures 72 through 84) analogous to those in Figures 9 through 12 that show the behavior of each equation in terms of T/C versus $(c_{b,318} + K_{tr,318})/d_b$, $f_{1c,mod}$, $f_{s,test}$, and ℓ_s.

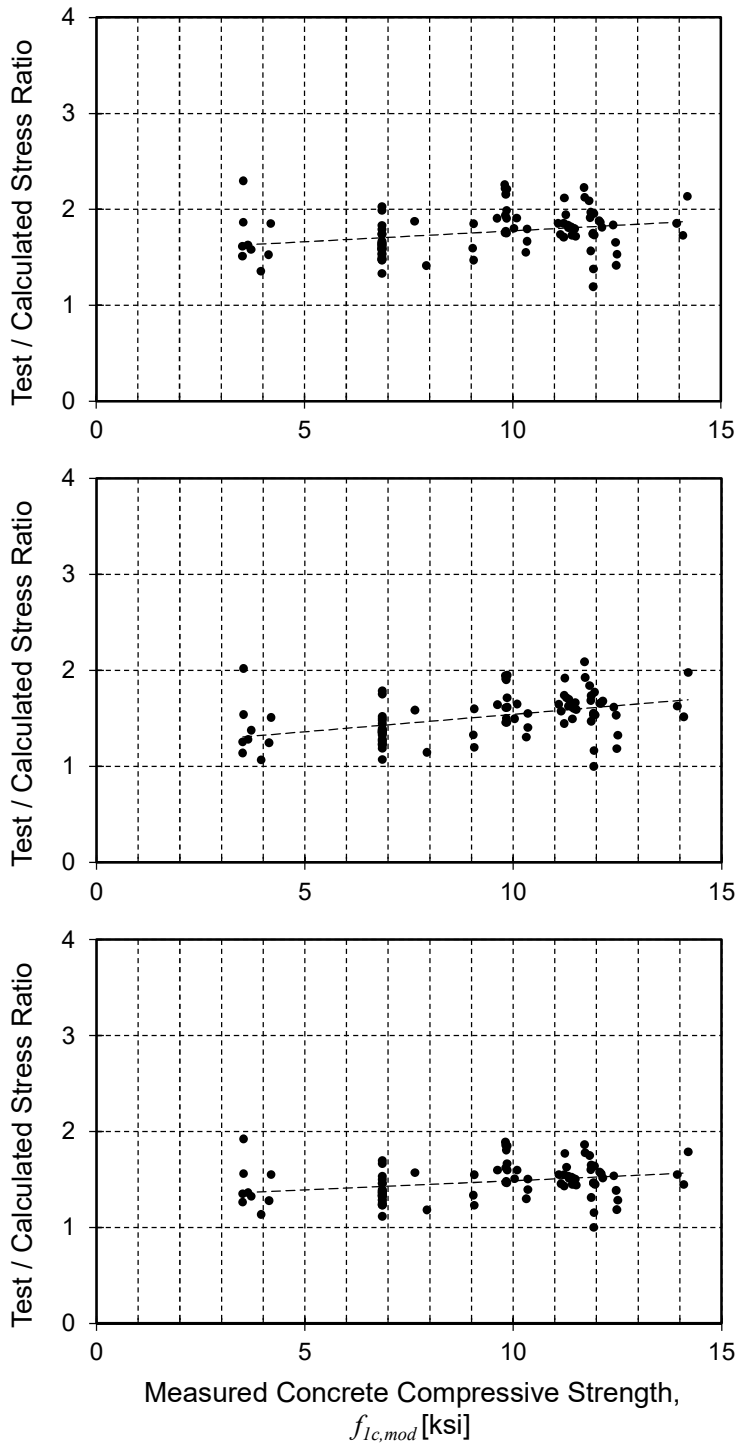

Figure 18 – Behavior of ACI 408R-03 [1] tension development length in terms of T/C against $f_{1c,mod}$: (a) original equation (b) with $r_1 = 0.69$ (c) with $r_2 = 0.84$

(1 ksi = 6.895 MPa)

Collectively, the plots in Appendix E show that all of the selected tension development equations (Eqs. (13) through (17)) more effectively account for the key variables than the ACI 318-19 compression lap splice provisions. Of the tension equations considered, the ACI 318-19 development length equation is the least effective at representing the effects of $(c_{b,318} + K_{tr,318})/d_b$, $f_{1c,mod}$, $f_{s,test}$, and ℓ_s, as evidenced by the clearly sloped trendline in the Appendix E plots.

Figure 72 shows the ACI 408R-03, Lepage et al., Darwin et al., and Frosch et al. equations all have trendlines with nearly zero slope when T/C is plotted versus $(c_{b,318} + K_{tr,318})/d_b$, suggesting these equations effectively account for cover and transverse reinforcement.

Figure 75 shows that, of the equations considered, the ACI 408R-03 and Darwin et al. equations are most effective at representing the effect of concrete compressive strength. The Lepage et al., Canbay and Frosch, and Frosch et al. equations behave similarly in terms of T/C versus $f_{1c,mod}$.

Figure 78 shows that all of the equations considered, except for the ACI 318-19 tension development length equation, exhibit a positive trend between T/C and bar stress, indicating more conservatism for higher bar stresses. This is a fortunate trend given the sparse data for bar stresses greater than 70 ksi (480 MPa).

Figure 81 shows the six equations become less conservative as the provided lap splice length increases, similar to the compression equations, with the ACI 318-19 tension development length equation exhibiting the most extreme trend.

The plots in Appendix E show that the application of r_1, r_2, or the optimized ψ_y do not alter these general trends.

Collectively, these results show that it may be possible to base compression lap splice requirements on tension development length provisions. For example, it might be feasible to set

the compression development length equal to r_1 times the tension development length. This approach simplifies the building code and ensures that calculated compression development lengths will never exceed the tension development length. Another appealing aspect of the length multiplier (r_1) method is that it avoids a separate length calculation for bar subjected to both tension and compression. As most research on bond has been focused on the behavior in tension, tension development length equations tend to account for more relevant variables and to be supported by more experimental data than compression development length equations.

The bar stress (r_2) multiplier approach produces a somewhat better fit to the data than the r_1 approach, particularly for the ACI 408R-03, Lepage et al., and Darwin et al. equations. The improvement is evident from the somewhat lower mean and *CV* values obtained with the r_2 approach. For the remaining equations, the use of r_2 produced similar results to the use of r_1. Depending on the tension development length equation, the r_2 approach might produce more accurate and precise results, but also requires that the tension development length equation to be recomputed. This is slightly less convenient than using a fraction of an already calculated length (r_1 approach).

Figures 16 and 17 show that the revised definition for ψ_y in the Lepage et al. equation led to less scatter than the r_2 approach.

2.6 Conclusions

1. ACI 318-19 [3] equations for compression lap splice length in §25.5.5 can produce calculated lengths that are substantially longer than the length of a Class B tension lap splice (§25.5.2). This is counter to expectations since compression lap splices benefit from end bearing and tension lap splices do not.

2. ACI 318-19 equations for compression lap splice length in §25.5.5 were not a good fit to the database of 89 test results, with a mean T/C of 2.58 and a coefficient of variation (CV) of 0.60 (although it must be emphasized that all specimens with $T/C > 2.0$ violated the ACI 318-19 minimum lap splice length of 12 in. (300 mm)). A reason for these outcomes is that §25.5.5 does not account for relevant variables including confinement and concrete compressive strength.
3. Compression lap splice length requirements in §25.5.5 can be improved and simplified by removing Eqs. (a) and (c) from §25.5.5 and applying Eq. (b) to all design bar stress ranges (Eq. (b) is currently limited to bar stresses greater than 60 ksi (420 MPa) but less than 80 ksi (550 MPa)). Equation (b) alone has a mean T/C of 1.58 and a CV of 0.16 when compared with the database, although it still omits key variables and can produce design lengths that are longer than the tension development length. Equations proposed by Cairns [13] and Chun, Lee, and Oh [9,12] were also shown to produce more accurate and precise fits to the available data.
4. Six tension development length equations were considered, and all provided a more accurate and precise fit to the dataset than ACI 318-19 §25.5.5. Use of tension development length equations for compression lap splice design would produce more consistent conservatism relative to the database, eliminate the need to calculate both tension and compression development lengths, and prevent design cases where calculated lengths are longer in compression than in tension. A drawback of this approach is that calculated compression lengths would also be longer than currently required for many common cases.
5. Three methods were considered for making compression lap splice length a function of tension development length without causing excessive conservatism:

a. Length multiplier, r_1: Compression lap splice length can be defined as r_1 times the tension development length, where $r_1 < 1$. To illustrate the concept, values of r_1 were derived for six tension development length equations to achieve a minimum T/C of 1.0, although other definitions of acceptable reliability might be appropriate.

b. Stress multiplier, r_2: Compression lap splice length can be calculated using tension development length equations, but for a stress of $r_2 f_y$, where $r_2 < 1$. The stress reduction is because some portion of bar force is transferred through end bearing and not bond. To illustrate the concept, values of r_2 were derived for six tension development length equations to achieve a minimum T/C of 1.0, although other definitions of acceptable reliability might be appropriate.

c. Optimized ψ_y: The tension development length equation from Lepage, Yasso, and Darwin [16] contains a ψ_y modification factor that was redefined to better fit the compression lap splice database and achieve a minimum T/C of 1.0, although other definitions of acceptable reliability might be appropriate.

2.7 Notation

A_b	=	cross-sectional area of spliced bar (in.^{2})
A_s	=	cross-sectional area of spliced bar in fib 2010 Model Code [15] (mm^2)
A_{st}	=	cross-sectional area of one leg of a confining bar, according to fib 2010 Model Code [15] (mm^2)
A_{tr}	=	total cross-sectional area of all transverse reinforcement within spacing s that crosses the potential plane of splitting through the reinforcement being developed (in.^{2})
c	=	$c_{min,408} + 0.5d_b$, ACI 408-03 [1] (in.)

$c_{b,318}$	=	lesser of: (a) the distance from center of a bar or wire to nearest concrete surface, and (b) one-half the center-to-center spacing of bars or wires developed, ACI 318-19 [3] (in.)
$c_{b,408}$	=	bottom clear cover, ACI 408-03 [1] (in.)
$c_{b,fib}$	=	$c_{b,408}$ (mm)
$c_{max,408}$	=	maximum($c_{b,408}$; $c_{s,408}$), ACI 408-03 [1] (in.)
$c_{min,408}$	=	minimum($c_{b,408}$; $c_{s,408}$), ACI 408-03 [1] (in.)
$c_{max,fib}$	=	maximum(c_{si} ; c_{so}), fib Model Code [15] (in.)
$c_{min,fib}$	=	minimum(c_{si} ; c_{so} ; $c_{b,fib}$), fib Model Code [15] (in.)
$c_{s,408}$	=	minimum [c_{so} ; c_{si} + 0.25 in. (6.4 mm)], ACI 408-03 [1] (in.)
c_{si}	=	½ of the bar clear spacing (in.)
c_{so}	=	clear side concrete cover for reinforcing bar (in.)
d_b	=	nominal diameter of bar being developed (in.)
$f_{1c,mod}$	=	measured concrete compressive strength per Reineck [11] in reference to a 6 x 12 in. (150 x 300 mm) cylinder (ksi)
f_c'	=	specified concrete compressive strength (psi)
f_b	=	total bond strength according to Frosch, Fleet, and Glucksman [19] (ksi)
f_{bd}	=	design bond strength in fib 2010 Model Code [15] (MPa)
$f_{bd,0}$	=	basic bond strength in fib 2010 Model Code [15] (MPa)
f_{ck}	=	characteristic value of compressive concrete strength in fib 2010 Model Code [15] (MPa)
F_h	=	60 $f_{bd} A_s$ in fib 2010 Model Code [15] (N)
f_y	=	specified yield stress of reinforcing steel, psi
f_{yd}	=	design yield stress of reinforcing steel in fib 2010 Model Code [15]
f_{yk}	=	characteristic value of yield stress of reinforcing steel in fib 2010 Model Code

[15] (MPa)

f_s = stress in steel reinforcement (psi)

$f_{s,calc}$ = stress in steel reinforcement that has been derived from provisions and calculated with measured specimen and material properties (psi)

$f_{s,test}$ = measured stress in steel reinforcement (psi)

k_d = effectiveness factor dependent on the reinforcement detail for the design bond strength in fib 2010 Model Code [15]

$K_{tr,318}$ = $40A_{tr} / sn$ transverse reinforcement index according to ACI 318-19 (in.)

$K_{tr,408}$ = $(0.52\ t_r\ t_d\ A_{tr}/sn)\sqrt{f_c'}$, transverse reinforcement index according to ACI 408R-03 [1] (in.)

K_{tr}' = $(t_d\ A_{tr}\ \sqrt{f_c'}\ )/(2sn)$, transverse reinforcement index according to Darwin et al. [17] (in.)

$K_{tr,fib}$ = $n_t A_{st}/(n_b\ Ø\ s_t)$ density of transverse reinforcement, relative to the anchored or lapped bars, according to fib 2010 Model Code [15].

l_b = lap length in fib 2010 Model Code [15] (mm)

ℓ_d = calculated development length (in.)

$l_{d,408}$ = development length of straight bars in tension, per Eq. 4-11a of ACI 408R-03 [1] (in.)

ℓ_s = provided lap splice length of a specimen (in.)

ℓ_{sc} = compression lap splice length, per ACI 318-19 §25.5.5.1 (in.)

ℓ_{st} = tension lap splice length for deformed bars and deformed wires in tension, per ACI 318-19 §25.5.2.1 (in.)

n = number of bars being developed or lap spliced at a potential splitting plane

n_b = number of bars being developed or lap spliced at a potential splitting plane, according to fib 2010 Model Code [15]

n_t	=	number of legs of confining reinforcement crossing a potential splitting failure surface at a section, according to fib 2010 Model Code [15]
N_b	=	number of longitudinal reinforcing bars according to Frosch, Fleet, and Glucksman [19]
N_l	=	number of legs of transverse reinforcement crossing the splice plane according to Frosch, Fleet, and Glucksman [19]
N_s	=	number of stirrups in the splice region according to Frosch, Fleet, and Glucksman [19]
p_{tr}	=	mean compression stress perpendicular to the potential splitting failure surface at the ultimate limit state, according to fib 2010 Model Code [15] (MPa)
R_r	=	relative area. Ratio of the projected rib area normal to the bar axis to the product of the nominal bar perimeter and the average center-to-center rib spacing.
s_t	=	longitudinal spacing of confining reinforcement, fib 2010 Model Code [15] (mm)
T/C	=	test-to-calculated steel stress ratio, i.e., the ratio between $f_{s,test}$ and $f_{s,calc}$.
t_d	=	term representing the effect of bar size on the contribution of confining reinforcement to total bond force for tension development length (ACI 408R-03 [1])
t_r	=	term representing the effect of relative rib area of the bar being developed on the contribution of confining reinforcement to total bond force for tension development length (ACI 408R-03 [1])
α_t	=	factor representing the effects of bar size on effectiveness of confinement in fib 2010 Model Code [15]
α_2	=	factor representing the influence of passive confinement from cover in the design bond strength in fib 2010 Model Code [15]

α_3 = factor representing the influence of passive confinement from transverse reinforcement in the design bond strength in fib 2010 Model Code [15]

δ = factor accounting for the presence of transverse reinforcement at the end of the lap splice in the equation by Chun et al. [9]. ($\delta = 1$ if transverse reinforcement is placed at ends or $\delta = 0$ if not)

γ_c = partial safety coefficient for concrete contribution to bond in fib 2010 Model Code [15]

γ_s = partial safety coefficient for steel contribution to bond in fib 2010 Model Code [15]

η_1 = coefficient affecting basic bond strength depending on reinforcement surface (1.75 for ribbed bars, 1.4 for fusion bonded epoxy coated ribbed bars) in fib 2010 Model Code [15]

η_2 = coefficient affecting basic bond strength representing reinforcement casting position (1.0 when good bond conditions are present, 0.7 otherwise) in fib 2010 Model Code [15]

η_3 = coefficient affecting basic bond strength representing bar diameter (1.0 for $Ø \leq 25$ mm, $(Ø/25)^{0.3}$ for $Ø > 25$ mm) in fib 2010 Model Code [15]

η_4 = coefficient affecting basic bond strength representing the characteristic strength of steel reinforcement (1.2 for $f_{yk} = 400$ MPa, 1.0 for $f_{yk} = 500$ MPa, 0.85 for $f_{yk} = 600$ MPa, 0.75 for $f_{yk} = 700$ MPa, 0.68 for $f_{yk} = 800$ MPa, with interpolation permitted, or $\eta_4 = \left(500 \text{ MPa}/f_{yk}\right)^{0.82}$) in fib 2010 Model Code [15]

$Ø$ = diameter of bar being lap spliced, fib 2010 Model Code [15] (mm)

ω = $0.1(c_{max}/c_{min}) + 0.9 \leq 1.25$, in the ACI 408R-03 tension development length

equation [1]

ψ_g = reinforcement grade modification factor in the ACI 318-19 [3] tension development length equation, calculated here as $\psi_g = 0.55 + 0.3(f_{s,calc}/40{,}000)$ (definition in source: 1.0 for Grade 40 or Grade 60, 1.15 for Grade 80, 1.3 for Grade 100)

ψ_e = reinforcement coating modification factor in the ACI 318-19 [3] tension development length equation (1.5 for epoxy-coated or zinc and epoxy dual-coated reinforcement with clear cover less than $3d_b$ or clear spacing less than 6 d_b, 1.2 for epoxy-coated or zinc and epoxy dual-coated reinforcement for all other conditions, 1.0 for uncoated or zinc-coated (galvanized) reinforcement)

ψ_t = casting position modification factor in the ACI 318-19 [3] tension development length equation (1.3 if more than 12 in. (300 mm) of fresh concrete placed below horizontal reinforcement, 1.0 otherwise)

ψ_r = confining reinforcement modification factor for the development length of deformed bars and wires in compression in ACI 318-19 [3] §25.4.9 (0.75 for reinforcement enclosed within a spiral, a circular continuously wound tie with $d_b \geq$ ¼ in. (6 mm) and pitch not more than 4 in. (100 mm), No. 4 (12 mm) bar or D20 wire ties in accordance with ACI 318-19 §25.7.2 spaced no more than 4 in. (100 mm) on center, or hoops in accordance with ACI 318-19 §25.7.4 spaced no more than 4 in. (100 mm) on center ; 1.0 otherwise)

ψ_s = size factor modification factor in the ACI 318-19 [3] tension development length equation (1.0 for No. 7 (22 mm) and larger bars, 0.8 for No. 6 (19 mm) and smaller bars and deformed wires)

ψ_{sc} = $1 + 0.084\ (K_{tr,318} / d_b)$ in the ‘simplified’ compression lap splice equation by

		Chun et al.[12]
ψ_y	=	reinforcement yield stress factor in the Lepage et al. [16] recommended provisions for tension development length
λ	=	factor accounting for lightweight concrete (1.00 for normalweight concrete, 0.75 for lightweight concrete) in ACI 318-19 [3] tension development length (§25.4.2) and compression development length (§25.4.9)

Chapter 3: Embedment Length of Headed Bars in Joints of Special Moment Frames

3.1 Introduction

Reinforcing bars terminating in a head transmit forces into concrete through two mechanisms: bond along the surface of the bar and bearing forces at the head. Compared with hooked bars, use of headed bars for development can reduce reinforcement congestion, promoting ease of construction. Headed bars can be useful in exterior joints of moment frames, where the beam longitudinal reinforcement must be anchored into the column and the reinforcement detailing can be challenging.

Use of headed bars in reinforced concrete construction is permitted and regulated by ACI 318-19 [3]. For design of joints in frames not designated as special moment frames (SMF), the development of headed bars in tension is prescribed by Chapter 25 of ACI 318-19. According to §25.4.4, the development length $\ell_{dt,25.4.4}$ for headed deformed bars in tension shall be:

$$\ell_{dt,25.4.4} = \max\left\{\left(\frac{f_y \psi_e \psi_p \psi_{o,head} \psi_c}{75\sqrt{f'_c}}\right) d_b^{1.5};\ 8d_b;\ 6\text{ in.}\right\} \qquad \text{Eq. (23)}\ \text{(lb, in.)}$$

where ψ_e, ψ_p, $\psi_{o,head}$, and ψ_c are modification factors associated with epoxy coating, parallel tie reinforcement, headed bar location, and concrete strength, respectively.

Requirements for development of hooked, headed, and straight reinforcement in joints of SMFs are articulated in §18.8.2.2:

> "*Longitudinal reinforcement terminated in a joint shall extend to the far face of the joint core and shall be developed in tension in accordance with 18.8.5 and in compression in accordance with 25.4.9.*" - ACI 318-19 [3] §18.8.2.2

For developing headed bars in tension, §18.8.5.2 requires using Eq. (23) from §25.4.4 after replacing f_y with 1.25 f_y. This requirement is consistent with the general provision in §18.8.2.1 for SMFs:

"*Forces in longitudinal beam reinforcement at the joint face shall be calculated assuming that the stress in the flexural tensile reinforcement is 1.25f_y*" - ACI 318-19 §18.8.2.1

Equation (23) thus becomes Eq. (24) for developing headed bars in SMF joints:

$$\ell_{dt,18.8.5.2} = \max\left\{\left(\frac{1.25 f_y \Psi_e \Psi_p \Psi_{o,head} \Psi_c}{75\sqrt{f'_c}}\right) d_b^{1.5};\ 8d_b;\ 6\text{ in.}\right\} \qquad \text{Eq. (24)}\ \text{(lb, in.)}$$

The language in §18.8.2.2 that requires consideration of both tension and compression development has been present in successive versions of the ACI Building Code since ACI 318-83 (Appendix A). Even though earthquakes are expected to subject beam reinforcement terminating in a joint to both tension and compression force demands, the language of §18.8.2.2 is not clear about whether §25.4.9 applies only to straight bars in compression, or also to headed bars under compression. It could be interpreted that the reference to §25.4.9 is only for straight bars in compression since §25.4.9 has no guidance for how it should be applied to headed or hooked bars. This was clarified with new commentary in ACI 318-14:

"*For bars in compression, the development length corresponds to the straight portion of a hooked or headed bar measured from the critical section to the onset of the bend for hooked bars and from the critical section to the head for headed bars.*" - ACI 318-14 [20] §R18.8.2.2

Prior to ACI 318-14, an engineer might have assumed that a headed bar satisfying §18.8.5 was adequately developed because tension development is often more critical than compression

development. The new commentary in §R18.8.2.2 of ACI 318-14 makes clear that engineers must design headed bars so they comply with both §18.8.5 (for tension) and §25.4.9 (for compression).

The compression development length required for joints of SMFs by §18.8.2.2, in accordance with §25.4.9, is the longer of the lengths obtained from Eq. (25):

$$\ell_{dc,25.4.9} = \max\left\{\frac{f_y\psi_r}{50\lambda\sqrt{f_c'}}d_b\ ;\ 0.0003f_y\psi_r d_b;\ 8\text{ in.}\right\} \qquad \text{Eq. (25)}\ \text{(lb, in.)}$$

where ψ_r is a confining reinforcement modification factor and $\sqrt{f_c'} \leq 100$ psi (0.69 MPa).

The implications of designing headed bars for compression development (§25.4.9) are illustrated in Figure 19. Figure 19 shows the ratio between the required headed bar compression development length, $\ell_{dc,25.4.9}$ (ACI 318-19 §25.4.9), and the required headed bar tension development length, $\ell_{dt,18.8.5.2}$ (ACI 318-19 §18.8.5.2, which is 1.25 times the length obtained from §25.4.4), versus specified concrete compressive strength. Separate lines in the figure show the trends obtained for different bar sizes. A steel yield stress of 60 ksi (420 MPa) was assumed for all cases. Unitary values were assumed for the epoxy coating, parallel tie reinforcement, and bar location modification factors ($\psi_e = \psi_p = \psi_{o,head} = 1.0$) for calculating tension development length, while a value of 0.75 was assumed for the confining reinforcement modification factor for calculating compression development length ($\psi_r = 0.75$). These assumptions are valid for uncoated headed bars terminating inside a well-confined joint.

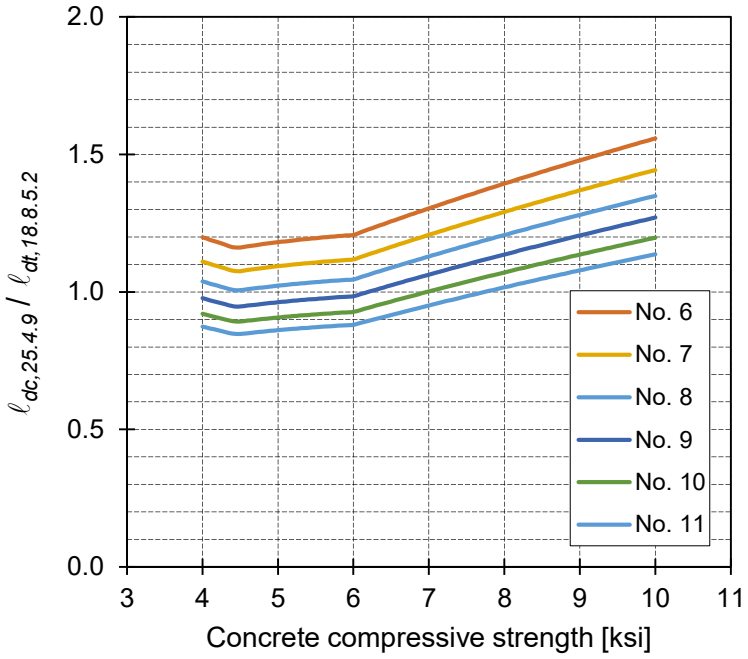

Figure 19 – Ratio of compression to tension development lengths for headed bars (§25.4.9 versus §18.8.5.2) versus specified concrete compressive strength

(1 ksi = 6.895 MPa)

Figure 19 shows that, for $\psi_e = \psi_p = \psi_{o,head} = 1.0$ and $\psi_r = 0.75$, the required compression development length is longer than the required tension development length for No. 8 (25 mm) and smaller headed bars, regardless of the concrete compressive strength. The same is true for No. 9, No. 10, and No. 11 (29, 32, and 36 mm) headed bars when the concrete compressive strength is greater than 6 , 7, and 8 ksi (42, 48, and 55 MPa), respectively. In joints that do not satisfy the conditions necessary to obtain $\psi_p = 1$ (i.e., $A_{th} \geq 0.4A_{hs}$), $\ell_{dt,18.8.5.2}$ will most likely be longer than $\ell_{dc,25.4.9}$ because $\psi_p = 1.6$.

This chapter explores whether the compression development length should indeed frequently govern the embedment length of headed bars in joints of special moment frames. This

is done by examining results from tests of exterior beam-column joints with headed beam reinforcement under reversed cyclic displacements.

3.2 Database Description

A database of test results was used to evaluate headed bar development. The database (Appendix F) includes results from 35 exterior beam-column joint specimens subjected to reversed cyclic loading. Figure 20 shows a schematic of a representative cast-in-place reinforced concrete specimen populating the database.

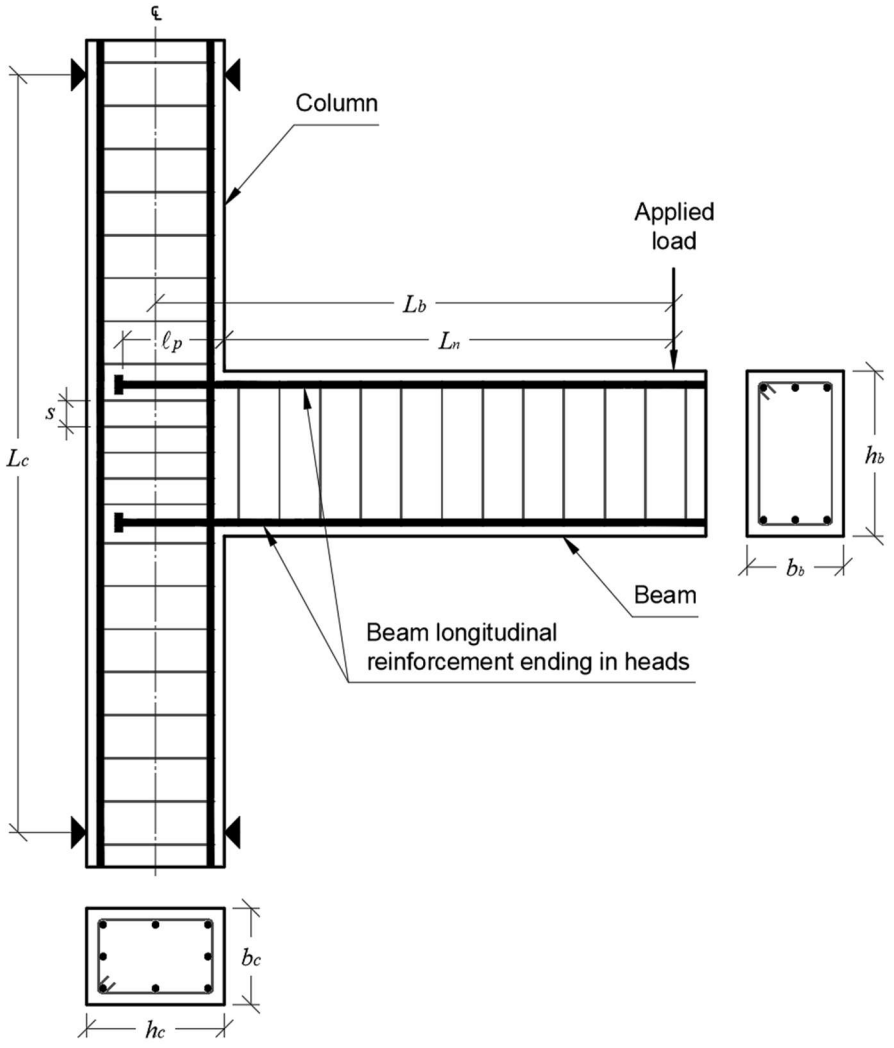

Figure 20 – Schematic of specimens in database (elevation and cross-sections)

Results were obtained from Adachi and Kiyoshi [21]; Bashandy [22]; Chun et al. [23]; Ishida et al. [24]; Kang, Ha, and Choi [25]; Kato [26]; Lee and Yu [27]; Matsushima et al. [28]; Murakami, Fuji, and Kubota [29]; Takeuchi et al. [30]; Tazaki, Kusuhara, and Shiohara [31]; Wallace et al. [32]; and Yoshida, Ishibashi, and Nakamura [33]. The specimens in the database in Appendix F were selected from databases published by Kang et al. [5] and Ghimire, Darwin, and Lepage [6]. The 35 specimens were selected for meeting the following criteria: specimens were included in both the Kang et al. [5] and Ghimire, Darwin, and Lepage [6] databases, the connection had a continuous column and at least one beam with headed bars terminating in the joint, and beam longitudinal reinforcement yield stress was ≤ 85 ksi (586 MPa). These criteria resulted in 35 specimens.

All specimens contained transverse reinforcement within the joint consisting of either column ties (21 of 35, or 60% of, specimens) or hoops (14 of 35, or 40% of, specimens) enclosing the column longitudinal reinforcement. The use of ties (with 90-degree hooks instead of 135-degree hooks) makes clear that not all joints in the database met the requirements for joint confinement in SMFs. The specimens had measured concrete compressive strengths of 3.5 to 10.3 ksi (24.1 to 71.0 MPa), No. 5 to No. 11 (16 to 36 mm) beam longitudinal bars, and measured beam longitudinal reinforcement yield stresses of 53 to 85 ksi (365 to 586 MPa). The distributions of measured concrete compressive strength, headed bar diameter, and measured steel yield stress are shown in Figures 21, 22, and 23, respectively. The provided embedment lengths of the headed bars, ℓ_p, defined as the distance from the face of the column to the bearing face of the head, as shown in Figure 20, ranged between 6.0 and 17.3 times the headed bar diameter and had the distribution shown in Figure 24.

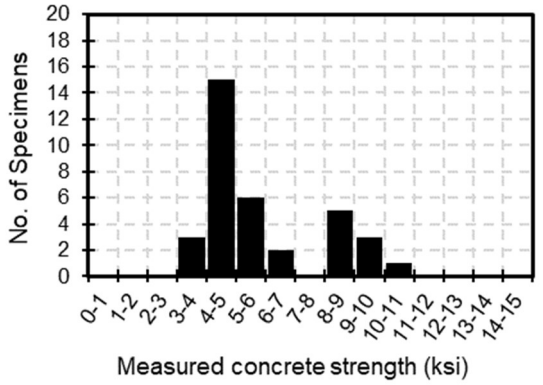

Figure 21 – Histogram of measured concrete compressive strength
(1 ksi = 6.895 MPa)

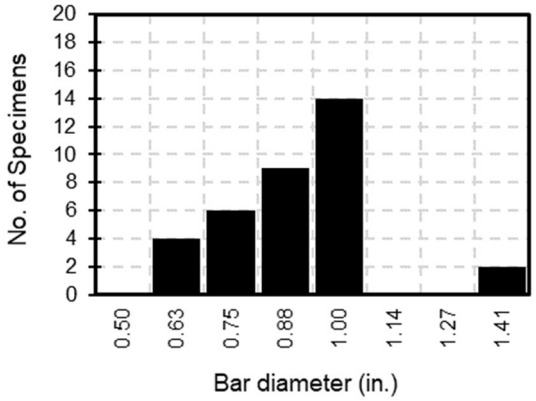

Figure 22 – Histogram of headed bar diameter (each bin includes specimens within ±1/16 in.)
(1 in. = 25.4 mm)

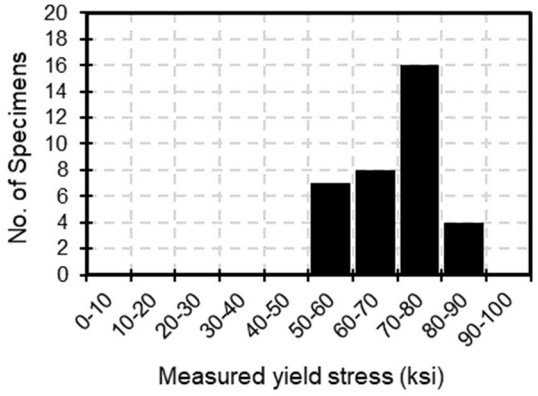

Figure 23 – Histogram of measured headed bar steel yield stress
(1 ksi = 6.895 MPa)

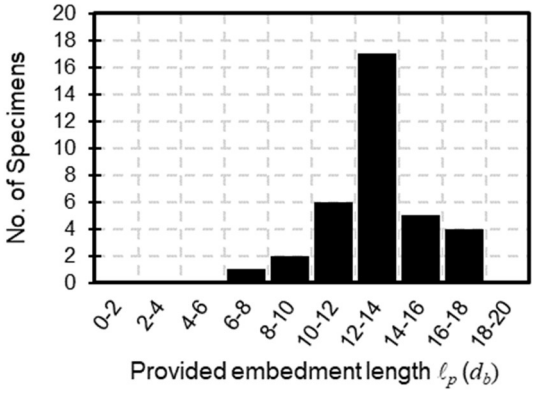

Figure 24 – Histogram of provided headed bar embedment length (column face to bearing face of head)

The specimens were all subjected to a series of fully reversed cyclic displacements of increasing magnitude. The strengths of the specimens were all limited by beam longitudinal bar yielding.

Specimen drift ratio was defined as the vertical displacement of the beam end during testing divided by the beam length measured to the centroid of the column (L_b in Figure 20). The drift ratio capacities in the database were reported by Ghimire, Darwin, and Lepage [6] based on the following definition: $\delta_{0.8peak}$ is "the drift ratio at drop to 80% [of] peak load (post peak)" based on

an envelope of the measured force-drift ratio results that links the peaks of the loading cycles. The reported $\delta_{0.8peak}$ values are the average of values obtained in each loading direction.

The distribution of drift ratio capacities is shown in Figure 25. Drift ratio capacities over 3% are taken to indicate acceptable behavior. All specimens in the database had drift ratio capacities exceeding 3%.

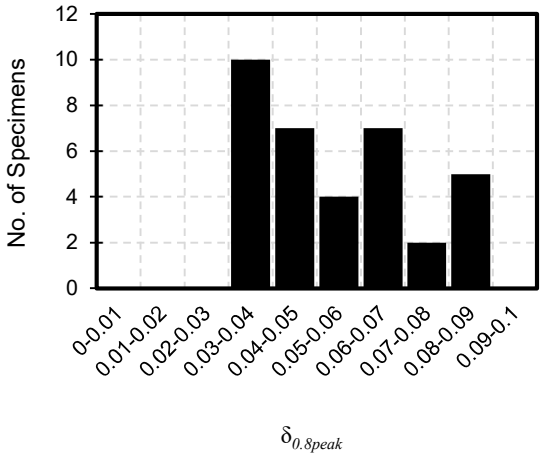

Figure 25 – Histogram of $\delta_{0.8peak}$

The nominal beam flexural strength was calculated at the face of the column using Eq. (26):

$$M_n = f_y A_{hs} (d - a/2) \qquad \text{Eq. (26)}$$

The contribution of compression reinforcement to flexural strength was neglected. In every case the beam section neglecting compression reinforcement was under-reinforced (with calculated tension steel strains at nominal moment greater than or equal to the yield strain, estimated as f_y / E_s).

The maximum bending moment in the beams, M_{peak}, was calculated as the applied force times the beam clear span (distance from the point load to the column face). Peak-to-nominal moment strength ratios, M_{peak}/M_n, were from 0.92 to 1.27 (Figure 26). Most specimens exhibited

beam strengths exceeding their nominal flexural strength based on measured material properties. The relatively high $\delta_{0.8peak}$ and M_{peak}/M_n values are consistent with beam longitudinal bar yielding in every test, likely producing anchorage force demands at the joint face at least equal to the product of bar yield stress and cross-sectional area.

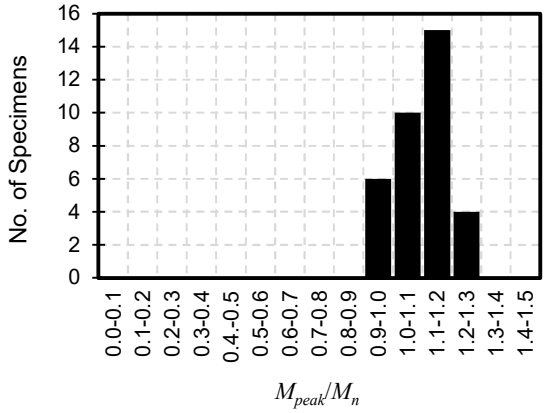

Figure 26 – Histogram of M_{peak}/M_n

The nominal joint shear strength, V_n, was calculated in accordance with ACI 318-19 §18.8.4 using Eq. (27).

$$V_n = R_n \lambda \sqrt{f_c'} A_j \qquad \text{Eq. (27)}$$
(lb, in.)

where R_n is a coefficient representing whether a transverse beam is present and had a value of either 12 or 15 for the specimens in the database. The effective joint area A_j, shown schematically in Figure 27, consists of the product of the joint depth in the plane parallel to the reinforcement generating shear (the height of the column section for these specimens) and the effective joint width, defined as the lesser of b_c , (b_b+h_c), and (b_c+2x).

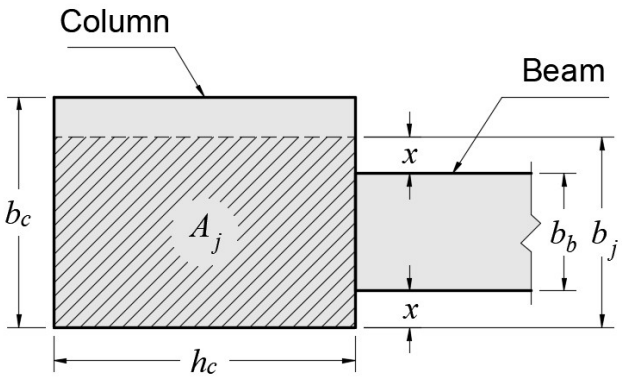

Figure 27 – Definition of effective joint area (plan view), adapted from ACI 318-19 [3] Fig. R15.4.2

Joint shear demand, V_p, was estimated with Eq. (28). Equation 28 is equivalent to the equation used in Ghimire, Darwin, and Lepage [6] except that the second term, which represents the column shear outside of the joint, is multiplied by L_b/L_n. This is necessary because M_{peak} is calculated at the column face.

$$V_p = \left(\frac{M_{peak}}{M_n} \right) n A_b f_y - \frac{M_{peak}}{L_c} \frac{L_b}{L_n} \qquad \text{Eq. (28)}$$

Peak-to-nominal shear strength ratios, V_p/V_n, ranged from 0.39 to 1.36 (Figure 28). For most specimens, the shear demand was less than the nominal shear strength. Even specimens with the highest V_p/V_n did not exhibit shear failures before reaching 3% drift ratio.

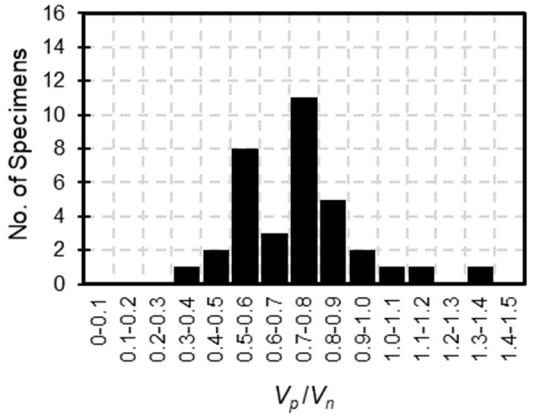

Figure 28– Histogram of V_p/V_n

Two main failure modes were identified by Kang et al. [5] for specimens in the database: beam flexural hinging followed by modest joint deterioration (Type I) and beam flexural hinging followed by joint failure (Type II). Kang et al. [5] also reported tests with joint failures before beam flexural hinging (Type III), but those are not included in Table 2 because all joints with Type III failures had $f_y > 85$ ksi (590 MPa). Kang et al. [5] report that specimens with Type I failures had joint shear distortions (if reported) that did not exceed 1.2% at 3.5% drift ratio and limited bar slip, resulting in sustained strength to at least 3.5% drift ratio and an acceptable level of pinching relative to ACI 374-05 criteria. Specimens with Type II failures exhibited joint damage including joint shear distortions > 1.2% at or before 3.5% drift ratio and evidence of bond distress severe enough to contribute to pinching and strength loss at or above 3% drift ratio. Table 2 shows that all but one specimen with a Type I failure had drift ratio capacities of 0.04 or greater, whereas specimens with Type II failures all had drift ratio capacities of 0.03 to 0.04. Of the nine specimens with Type 2 failures, three had $V_p/V_n > 1$ and six had joint transverse reinforcement ratios that were less than 75% of that recommended in ACI 352 [34].

Figures 29, 30, and 31 show $\delta_{0.8peak}$, M_{peak}/M_n and V_p/V_n versus ℓ_p/d_b, respectively. Closed circles and open triangles correspond to Type I and II failures, respectively. Figure 29 shows that specimens where a Type I failure was reported exhibited larger drift ratio capacities than those with Type II, as expected. All but one of the specimens with a Type I failure had drift ratio capacities of 0.04 or greater, whereas specimens with Type II failures all had drift ratio capacities of 0.03 to 0.04. No correlation is observed between $\delta_{0.8peak}$ and ℓ_p/d_b.

Figure 30 shows that the specimens with the greater peak moments, with respect to their nominal flexural strength, tended to be those with a relatively longer headed bar embedment length, although the trend is weak. It also appears that specimens with Type II failures tended to

have, on average, somewhat lower M_{peak}/M_n. Figure 31 shows that every specimen with $V_p/V_n >$ 1.0 exhibited Type II failures, but no other trends are evident. As expected, there is no correlation between V_p/V_n and ℓ_p/d_b.

Kang et al. [5] observed that specimen behavior was more sensitive to embedment length than head bearing area, so head bearing area is not considered in this analysis. Head bearing areas ranged between 1.7 and 11.4 times the bar area for specimens used in this analysis.

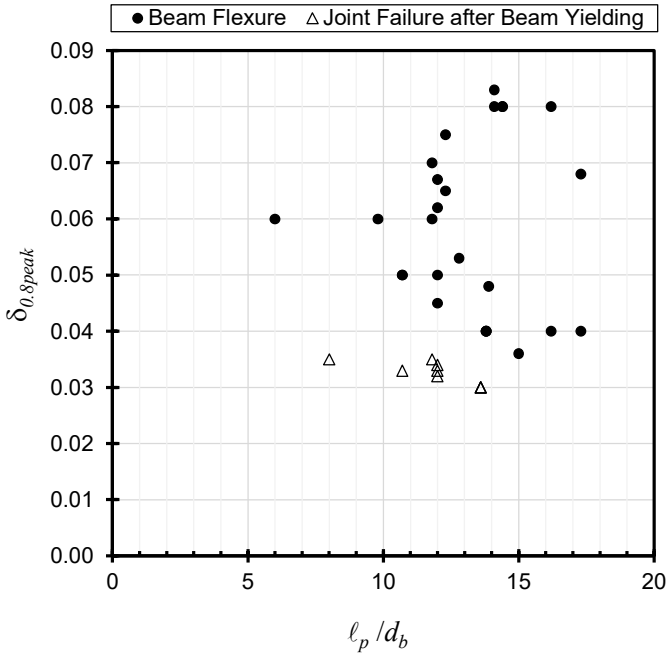

Figure 29 – $\delta_{0.8peak}$ versus ℓ_p(ACI 318-19)/d_b

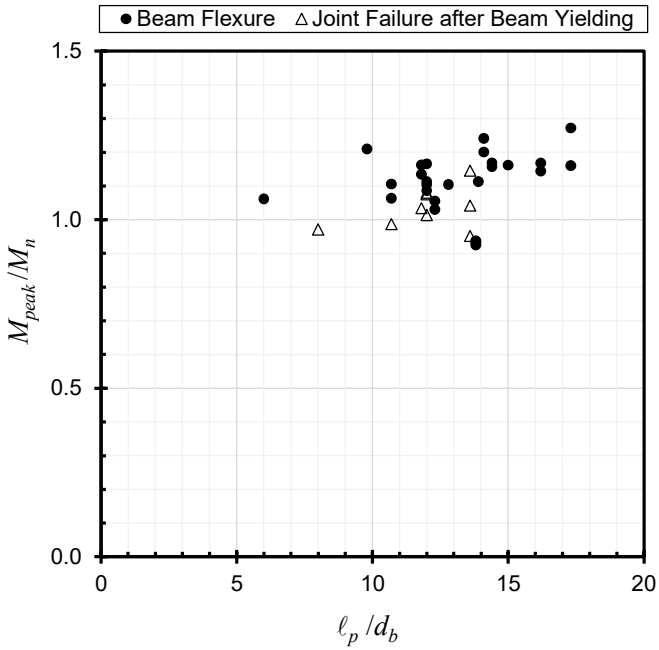

Figure 30 – M_{peak}/M_n versus ℓ_p(ACI 318-19)/d_b

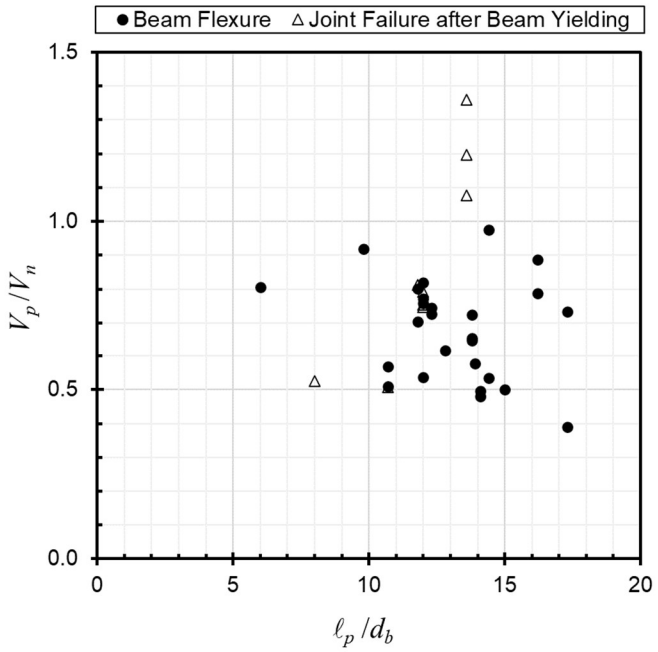

Figure 31 – V_p/V_n versus ℓ_p(ACI 318-19)/d_b

3.3 Evaluation of Database against Current Provisions

The embedment lengths provided for specimens in the database were compared against $\ell_{dt,18.8.5.2}$ and $\ell_{dc,25.4.9}$ to evaluate the appropriateness of the requirement in §18.8.2.2 that headed bars in SMF joints satisfy the compression development length requirements of §25.4.9. Measured material properties were used in all cases.

To calculate the compression development length, $\ell_{dc,25.4.9}$, some interpretation was necessary to define the confining reinforcement modification factor, ψ_r. This factor leads to a reduction of the required compression development length when the transverse reinforcement consists of:

- A spiral,
- A circular continuously wound tie with $d_b \geq$ ¼ in. (6 mm) and pitch not more than 4 in. (100 mm),
- No. 4 (12 mm) bar or D20 wire ties in accordance with ACI 318-19 §25.7.2 spaced no more than 4 in. (100 mm) on center, or
- Hoops in accordance with ACI 318-19 §25.7.4 spaced no more than 4 in. (100 mm) on center.

None of the specimens in the database, which were less than full scale, satisfy any of the conditions necessary for ψ_r = 0.75. However, it is arguably not appropriate to apply these conditions, which are intended for full-scale columns, to the smaller-scale specimens in the database. To identify specimens with transverse reinforcement similar to that required to obtain ψ_r = 0.75 in full-scale columns, a joint transverse reinforcement ratio was calculated for each specimen with Eq. (29):

$$\rho_t = \frac{A_{tr,1} N_{legs}}{s b_c} \qquad \text{Eq. (29)}$$

Specimens were assumed to qualify for $\psi_r = 0.75$ when $\rho_t \geq 0.5\%$, which is the transverse reinforcement ratio in a square column with 20 in. (510 mm) sides and two legs of No. 4 (12 mm) ties spaced at 4 in. (100 mm) (and thus qualifying for $\psi_r = 0.75$). The threshold 0.5% value was selected to represent the transverse reinforcement ratio required in a full-scale column to qualify for $\psi_r = 0.75$.

3.3.1 Results

Figure 32 shows the headed bar embedment lengths versus the required compression development length, $\ell_{dc,25.4.9}$, for all 35 specimens, with both lengths normalized by the headed bar diameter. This plot shows that the provided embedment length was less than the required compression development length, $\ell_{dc,25.4.9}$, in all specimens. In four cases ℓ_p / $\ell_{dc,25.4.9}$ exceeded 2.0, and in one case it exceeded 3.0. Nonetheless, all the specimens performed adequately under reversed cyclic loading without exhibiting anchorage failures. Figure 32 shows that providing an embedment length longer than $\ell_{dc,25.4.9}$ is not necessary to prevent anchorage failures and obtain a drift ratio capacity greater than 3%.

Similarly, Figure 33 shows headed bar embedment lengths versus the required tension development lengths, $\ell_{dt,18.8.5.2}$, normalized by headed bar diameter. Even though all 35 specimens had $\delta_{0.8peak} \geq 3\%$ and beam longitudinal bar yielding, only two of the 35 specimens had $\ell_p \geq \ell_{dt,18.8.5.2}$. It therefore appears that satisfying $\ell_p \geq \ell_{dt,18.8.5.2}$ is also not necessary to prevent anchorage failures and obtain a drift ratio capacity greater than 3%.

These results show that satisfactory connection behavior, characterized by beam longitudinal bar yielding and drift ratio capacities exceeding 3%, can be obtained without satisfying the requirements of either §25.4.9 or §18.8.5.2.

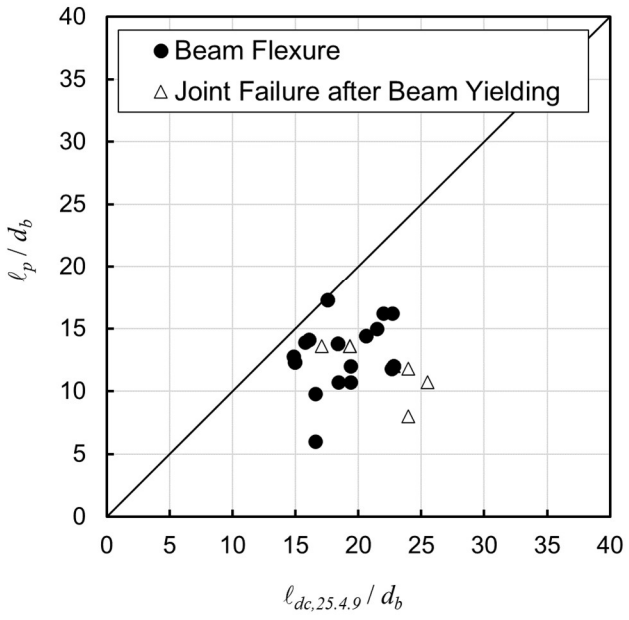

Figure 32 – ℓ_p/d_b versus $\ell_{dc,25.4.9}/d_b$

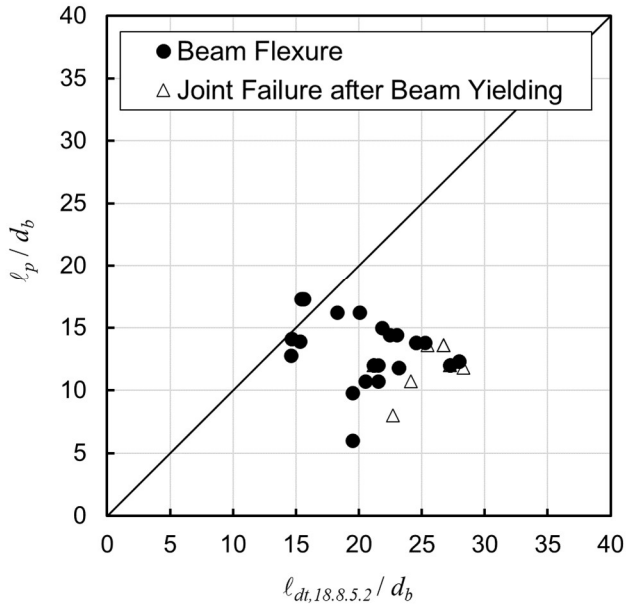

Figure 33 – ℓ_p/d_b versus $\ell_{dt,18.8.5.2}/d_b$

3.4 Evaluation of Database against Other Equations

Both §25.4.9 and §18.8.5.2 are considerably, perhaps excessively, conservative for headed bar development in special moment frame joints. This observation prompts consideration of other equations that might better fit the dataset. Four equations are considered.

3.4.1 Equations Considered

i) Development of headed bars in tension (ACI 318-14 §25.4.4)

ACI 318-14 [20] had different provisions for headed bar development than ACI 318-19. Equation (30) is the development length equation for headed deformed bars in tension from §25.4.4 of ACI 318-14. Equation (30) was replaced with Eq. (23) in ACI 318-19.

$$\ell_{dt,318\text{–}14} = \max\left\{\left(\frac{0.016 f_y \psi_e}{\sqrt{f_c'}}\right) d_b;\ 8d_b;\ 6\text{ in.}\right\} \qquad \text{Eq. (30)}\ (\text{lb, in.})$$

In ACI 318-14, Eq. (30) was applicable to headed bars in SMF joints with the requirement that clear spacing between bars was at least $3d_b$. For comparisons in this report, Eq. (30) was applied to all connections regardless of clear bar spacing. ACI 318-14 capped the values of both the concrete compressive strength and the reinforcing steel yield stress to use in Eq. (30) to 6,000 psi and 60,000 psi (42 and 420 MPa), respectively. In the database, these limits are exceeded in 10 and 28 of the 35 specimens, respectively. These caps, however, were due to a lack of test data at the time of publication, so, for the purpose of this analysis, both limits are disregarded.

ii) Development length of hooked bars in tension in SMF joints (ACI 318-19 §18.8.5.1).

Section 18.8.5.1 of ACI 318-19 has the following development length equation for hooked bars in tension:

$$\ell_{dh} = \max\left\{\frac{f_y d_b}{65\lambda\sqrt{f_c'}};\ 8d_b;\ 6\text{ in.}\right\} \qquad \text{Eq. (31)}\ \text{(lb, in.)}$$

This equation is intended for use with hooked bars and is based on the hooked bar development length provisions in §25.4 of ACI 318-14 and several earlier codes. The coefficient in Eq. (31) incorporates factors to account for bar overstrength, strain hardening, and confinement. It is considered here for headed bars because field and test data do not support requiring substantially different development lengths for hooked and headed bars.

iii) Ghimire, Darwin, and Lepage [6] descriptive equation

Ghimire, Darwin, and Lepage [6] concluded that the anchorage strength of headed bars in beam-column joints under reversed cyclic loading can be estimated using descriptive equations derived from monotonic tests. For the case of headed bars with confining reinforcement, Ghimire, Darwin, and Lepage proposed the following descriptive equation:

$$T_h = \left(781 f_{cm}^{\ 0.24} \ell_{eh}^{\ 1.03} d_b^{\ 0.35} + 48800\frac{A_{tt}}{n} d_b^{\ 0.88}\right)\left(0.0622\frac{c_{ch}}{d_b} + 0.543\right) \qquad \text{Eq. (32)}\ \text{(lb, in.)}$$

$$\text{with } 0.0622 c_{ch}/d_b + 0.543 \le 1.0 \text{ and } A_{tt}/n \le 0.3 A_b$$

The embedment length associated with developing the yield stress of the headed bars, denoted ℓ_{ehy}, can be solved for from Eq. (32) by replacing the anchorage strength T_h by the product of the measured value of the steel yield stress f_y and the cross-sectional area of the (individual) headed bar A_b.

$$\ell_{ehy} = \left[\left(\frac{f_y A_b}{0.0622\frac{c_{ch}}{d_b} + 0.543} - 48800\frac{A_{tt}}{n} d_b^{\ 0.88}\right)\frac{1}{781 f_{cm}^{\ 0.24} d_b^{\ 0.35}}\right]^{1/1.03} \qquad \text{Eq. (33)}\ \text{(lb, in.)}$$

$$\text{with } 0.0622 c_{ch}/d_b + 0.543 \le 1.0 \text{ and } A_{tt}/n \le 0.3 A_b$$

iv) ACI 408R-03 Tension development length with 0.7 reduction factor

The analyses of compression lap splices in Chapter 2 suggest that compression lap splice length can be calculated as a fraction of the tension development length. The fraction differs depending on which tension development equation is used. Here compression development is taken as 0.7 times the length obtained from the ACI 408R-03 tension development length equation (Eq. (34)). If headed bars in special moment frame joints should be designed for compression development, then the embedment lengths provided in the beam-column connection database should generally exceed the length calculated with Eq. (34).

$$l_{dc,408} = 0.7 l_{d,408} = 0.7 \frac{\left(\frac{f_y}{\phi f_c'^{1/4}} - 2400\omega \right) \alpha\beta\lambda}{76.3 \left(\frac{c\omega + K_{tr,408}}{d_b} \right)} d_b \qquad \text{Eq. (34) (lb, in.)}$$

where α, β, and λ are all unity for this database, and with:

$$\omega = 0.1 \frac{c_{max}}{c_{min}} + 0.9 \leq 1.25 \; ; \; t_r = 9.6 R_r + 0.28 \leq 1.72 \; ; \; t_d = 0.03 d_b + 0.22$$

$$K_{tr,408} = \frac{6.26 t_r t_d A_{tr}}{sn} f_c'^{1/2} \quad ; \quad f_c'^{1/4} \leq 11.0 \; ; \; f_y \leq 80 \text{ ksi} \; ; \; \phi = 0.82$$

A relative rib area, R_r, of 0.0727 was assumed for all specimens based on recommendations in ACI 408R-03.

Application of Eq. (34) to headed bars in joints requires some interpretation because identification of potential splitting planes is not as obvious in a beam-column joint as it may be for longitudinal bars in a column or beam; the definition of splitting plane does not readily apply where breakout anchorage failures occur. To bracket the range of possible outcomes, two cases are considered in these analyses: $K_{tr,408} = 0$, which represents a lack of confining reinforcement, and $(c\omega + K_{tr,408})/d_b = 4$, the upper bound recommended in ACI 408R-03. These two cases bracket the

possible required tension development length and, lacking a precise quantification of confinement, both are evaluated for each specimen.

3.4.2 Results

Figures 34 through 39 are analogous to Figures 32 and 33. Each figure shows the development length obtained from the selected equations (Eqs. 23, 30, 31, 33, and 34) plotted versus the provided embedment length, with lengths normalized by headed bar diameter. These equations include the tension development length for headed bars in non-earthquake-resistant design, $\ell_{dt,25.4.4}$ (Eq. (23)); the ACI 318-14 tension development length for headed bars, $\ell_{dt,318\text{-}14}$, with no caps on concrete or steel strengths (Eq. 30); the ACI 318-19 tension development length for hooked bars in special moment frames, $\ell_{dh,18.8.5.1}$, (Eq. 31); the embedment length derived from the anchorage strength descriptive equation from Ghimire, Darwin, and Lepage [6], ℓ_{eyh}, (Eq. 33); and 0.7 times the ACI 408R-03 tension development length, l_d, (Eq. 34) with either $K_{tr,408} = 0$ (Case I) or $(c\omega+K_{tr,408})/d_b = 4.0$ (Case II). For these comparisons, the measured yield stress was used to obtain the calculated lengths.

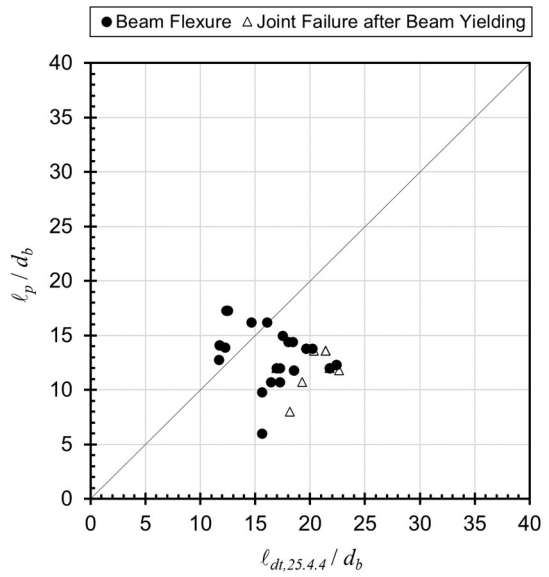

Figure 34 – ℓ_p/d_b versus $\ell_{dt,25.4.4}/d_b$

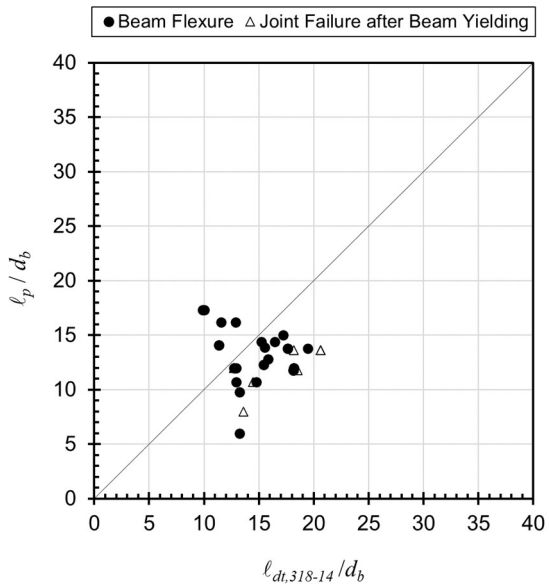

Figure 35 – ℓ_p/d_b versus ℓ_{dt} (ACI 318-14 §25.4.4 with no caps)/d_b

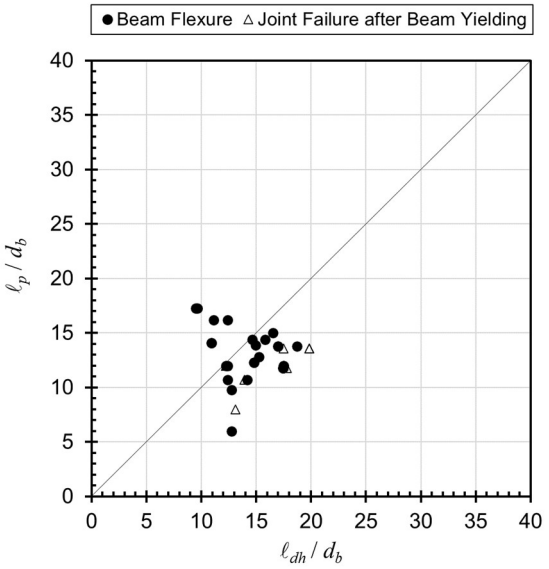

Figure 36 – ℓ_p/d_b versus ℓ_{dh} (ACI 318-19 §18.8.5.1)/d_b

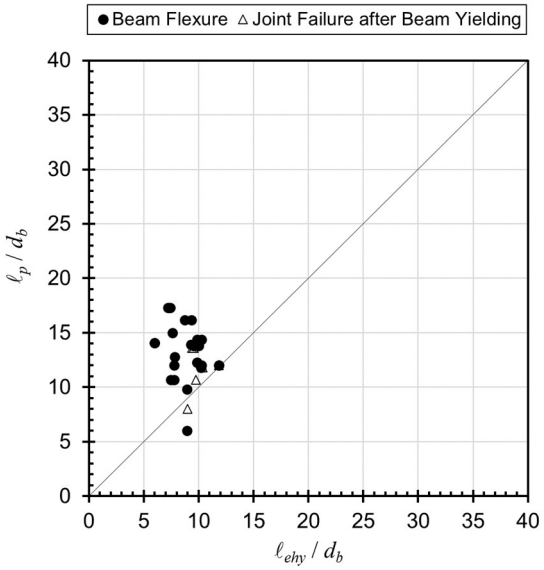

Figure 37 – ℓ_p/d_b versus ℓ_{eyh} (Ghimire, Darwin, and Lepage)/d_b

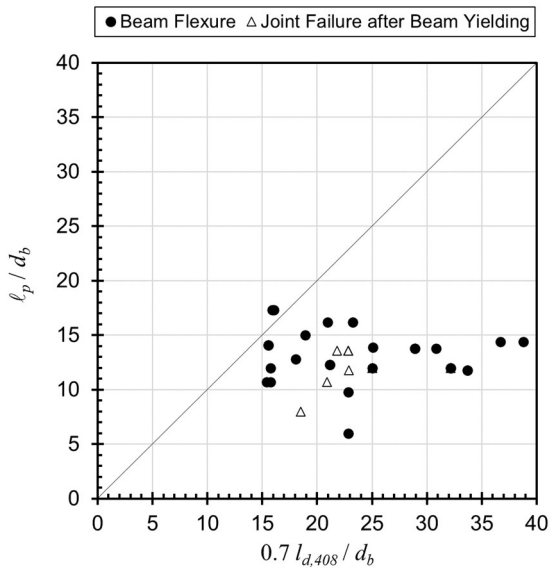

Figure 38 – ℓ_p/d_b versus $0.7l_d$ (ACI 408R-03 Case I: $K_{tr,408} = 0$)/d_b

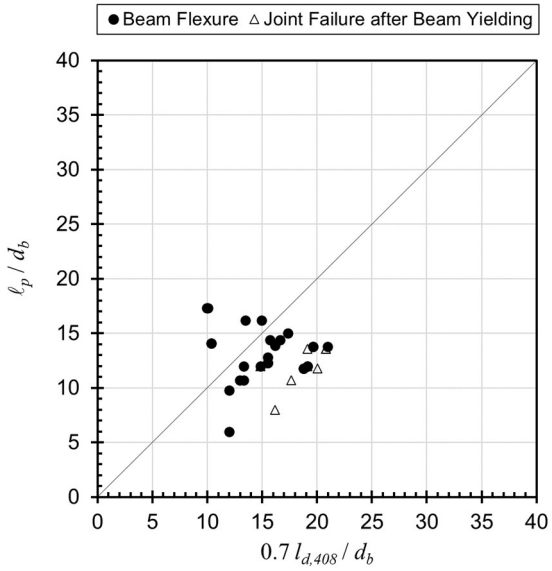

Figure 39 – ℓ_p/d_b versus $0.7l_d$ (ACI 408R-03 Case II: ($c\omega$+$K_{tr,408}$)/d_b = 4.0)/d_b

Since all 35 specimens reached their nominal strength and had a drift ratio capacity of at least 3%, it is reasonable to expect that the provided embedment length typically exceeded or was close to the required development lengths. That was not the case in Figures 32 and 33, which show that ACI 318-19 §25.4.9 and §18.8.5.2 are both conservative. Figures 34 through 39 show that all

the equations considered in this section, except for $0.7\ell_d$ Case I in Figure 38, perform better than $\ell_{dt,18.8.5.2}$ from ACI 318-19. In some specimens, the provided embedment length exceeded the required lengths calculated as $\ell_{dt,25.4.4}$, $\ell_{dh,18.8.5.1}$, ℓ_{eyh} and $0.7l_d$ Case II, which is to be expected in specimens that do not exhibit anchorage failures during reversed cycle loading testing.

The behaviors of $\ell_{dt,25.4.4}$, $\ell_{dt,318\text{-}14}$, $\ell_{dh,18.8.5.1}$, and $0.7\ell_d$ Case II (Figures 35, 36, and 39) are all very similar: some specimens had embedment lengths longer than required while most had embedment lengths that were only somewhat shorter than required. These trends are reasonable for specimens that did not exhibit bond/anchorage failures when compared against design equations with some inherent conservatism. In all cases, specimens with Type II failures, some of which exhibited bond distress, had provided embedment lengths that were less than the calculated lengths, suggesting these equations are useful for distinguishing between adequate and inadequate anchorage.

The trends in Figure 37 for ℓ_{eyh} stand out among the equations considered, with almost all specimens having a longer provided length than what is obtained from the equation, and specimens with Type II failures again tending to have shorter provided lengths than other specimens. This equation is derived from a descriptive equation, which, unlike design equations, has no built-in safety factors. It should therefore be expected that specimens with no evidence of anchorage failures have headed bar embedment lengths longer than ℓ_{eyh}, as indicated by the plotted data.

Table 2 provides another way to compare the different length requirements. The value of each cell represents the mean ratio between the length in the row and the length in the column in question for specimens in the database. An expanded version of the table with values for all lengths against each other can be found in Appendix G.

Table 2 – Average length ratios: length in row / length in column

	ℓ_p	ℓ_{ehy}	Notes
ℓ_p	1	1.43	Provided embedment length
$\ell_{dt,318\text{-}14}$, no caps [Eq. (30)]	1.14	1.66	ACI 318-14 tension development, with $1.0f_y$
$\ell_{dt,25.4.4}$ [Eq. (23)]	1.33	1.93	ACI 318-19 tension development, with $1.0f_y$
$\ell_{dt,18.8.5.2}$ [Eq. (24)]	1.66	2.42	ACI 318-19 tension development, with $1.25f_y$
$\ell_{dc,25.4.9}$ [Eq. (25)]	1.52	2.18	ACI 318-19 compression development, with $1.0f_y$
ℓ_{ehy} [Eq. (33)]	0.70	1	"descriptive" equation, with $1.0f_y$
$\ell_{dh,18.8.5.1}$ [Eq. (31)]	1.09	1.55	ACI 318-14 tension development for hooked bars, with integrated $1.25f_y$ and confinement factors
$0.7l_{d,408}$, Case II [Eq. (34)]	1.18	1.69	Compression development (chapter 2), 0% fractal with $1.0f_y$

The column for ℓ_p in Table 2 shows that all the different length requirements, except for ℓ_{ehy}, surpass, on average, the embedment length that was provided in the specimens, with different levels of conservatism. The tension development length required by the current ACI Building Code provisions, $\ell_{dt,18.8.5.2}$ (Eq. (24)), is by far the most conservative of the equations considered. For the database considered, §18.8.5.2 of ACI 318-19 requires, on average, 66% more embedment length than was provided, even though most specimens did not exhibit bond distress. The next most conservative equation is the compression development length requirement, $\ell_{dc,25.4.9}$ from §25.4.9 of ACI 318-19 (Eq. (25)), which would require, on average, 52% more embedment length than provided in specimens that did not exhibit anchorage failures. In contrast, ℓ_{ehy} (Eq. 33)) was, on average, only 70% of the provided lengths, which is to be expected for a descriptive equation compared against specimens that mostly did not exhibit anchorage failures.

The column for ℓ_{ehy} in Table 2 provides ratios of calculated lengths versus ℓ_{ehy} obtained from the descriptive equation in Eq. (33). If ℓ_{ehy} is taken as the length necessary to develop headed bars in SMF joints without a safety factor, ℓ_p / ℓ_{ehy} should generally exceed 1.0 in specimens that

did not exhibit bond/anchorage failures. Table 2 shows $\ell_p / \ell_{ehy} = 1.43$ for this dataset. Furthermore, if ℓ_{ehy} is taken as the length necessary to develop headed bars in SMF joints without a safety factor, the column for ℓ_{ehy} in Table 2 shows the extent of the conservatism embedded in various equations considered. Both $\ell_{dt,318\text{-}14}$ and $\ell_{dh,18.8.5.1}$ (Eqs. (30) and (31)) are approximately 60% longer than ℓ_{ehy}, whereas both $\ell_{dt,18.8.5.2}$ and $\ell_{dc,25.4.9}$ (Eqs. (24) and (25)) are, on average, more than twice as long as ℓ_{ehy}.

3.5 Conclusions

1. Satisfying the compression development length requirements of §25.4.9 is not a necessary condition to obtain adequate joint behavior under cyclic loads. None of the 35 beam-column connection specimens considered satisfied §25.4.9, even though all had drift ratio capacities not less than 3%. Furthermore, §25.4.9 produced lengths that were, on average, 2.2 times the lengths obtained from the Ghimire, Darwin, and Lepage [16] descriptive equation for headed bar anchorage strength. ACI 318-19 §18.8.2.2 should not require that headed bars satisfy §25.4.9.
2. Satisfying the tension development length requirements of §18.8.5.2, which refer to §25.4.4, is not a necessary condition to obtain adequate joint behavior under cyclic loads. Stated differently, §25.4.4 and thus §18.8.5.2 appear to be substantially conservative for joint design. Only two of the 35 beam-column connection specimens considered satisfied §18.8.5.2, even though all had drift ratio capacities not less than 3%. Section 18.8.5.2 also produced lengths that were, on average, 2.4 times the lengths obtained from the Ghimire, Darwin, and Lepage [6] descriptive equation for headed bar anchorage strength.

3. The equation for hooked bar development length in §18.8.5.1 of ACI 318-19 appears more appropriate for design of specimens like those in the database. It was a more reasonable fit to the database and still conservate relative to the Ghimire, Darwin, and Lepage [6] descriptive equation for headed bar anchorage strength.

3.6 Notation

a	=	depth of equivalent rectangular compressive stress block in beam flexure (in.)
A_b	=	cross-sectional area of an individual headed bar (in.^{2})
A_{hs}	=	total cross-sectional area of headed bars (in.^{2})
A_j	=	effective cross-sectional area of a joint in a plane parallel to plane of beam reinforcement generating shear in the joint, per ACI 318-19 [3] §R15.4.2 = $b_j \times h_c$ (in.^{2})
$A_{tr,1}$	=	cross-sectional area of a tie leg (in.^{2})
A_{tt}	=	total cross-sectional area of effective confining reinforcement parallel to the headed bars (in.^{2})
b_b	=	width of beam (in.)
b_c	=	width of column (in.)
b_j	=	effective joint width, see Figure 27 (in.)
c_b	=	bottom clear cover, ACI 408-03 [1] (in.)
c_{max}	=	maximum(c_b ; c_s) (in.)
c_{min}	=	minimum(c_b ; c_s), ACI 408-03 [1] (in.)
c_s	=	minimum(c_{so} ; c_{si} + 0.25 in. (6.4 mm)) (in.)
c_{si}	=	½ of the bar clear spacing (in.)
c_{so}	=	side concrete cover for reinforcing bar (in.)
d	=	distance between centroid of beam longitudinal tension reinforcing bars and

		extreme compression fiber of beam section (in.)
d_b	=	nominal diameter of bar being developed as straight, headed, or hooked bar (in.)
E_s	=	modulus of elasticity of steel, 29,000 ksi (200 GPa)
f_c'	=	measured concrete compressive strength (psi)
f_y	=	measured yield stress of reinforcing steel (ksi)
h_b	=	height of beam (in.)
h_c	=	height of column (in.)
$K_{tr,408}$	=	transverse reinforcement index according to ACI 408R-03 [1]
n	=	number of headed bars in tension
L_b	=	beam span measured to the center of the column (in.)
L_c	=	length of column between inflection points (in.)
L_n	=	clear beam span (in.)
ℓ_c	=	compression development length of straight bars or wires, as required by ACI 318-19 [3] §25.4.9 (in.)
ℓ_p	=	provided embedment length of headed bars in a specimen, measured from the critical section at the face of column to the bearing face of the head (in.)
ℓ_d	=	development length of straight bars in tension as required by ACI 318-19 [3] §25.4.2 (in.)
$l_{d,408}$	=	development length of straight bars in tension, as required by the recommended provisions by ACI 408R-03, Eq. 4-11a (in.).
$\ell_{dh,18.8.5.1}$	=	development length of a hooked bar in tension, as required by ACI 318-19 [3] §18.8.5.1 for SMF joints (in.)
$\ell_{dt,18.8.5.2}$	=	development length of headed bar in tension ACI 318-19 [3] §18.8.5.2 for SMF joints (in.).

$\ell_{dt,25.4.4}$	=	development length of headed bar in tension ACI 318-19 [3] §25.4.4 (in.).
$\ell_{dt,318\text{-}14}$	=	development length of headed bar in tension ACI 318-14 [20] §25.4.4 (in.).
ℓ_{ehy}	=	embedment length of a headed bar necessary to develop its yield strength, derived from the anchorage strength descriptive equation by Ghimire, Darwin, and Lepage [6]
M_n	=	nominal bending moment capacity of the beam cross section at the face of the column (kip-in.)
M_{peak}	=	the maximum beam moment at the face of the column based on measured forces (kip-in.)
N_{legs}	=	number of legs within a layer of column ties or hoops
R_n	=	coefficient representing whether a transverse beam is present in the calculation of the nominal joint shear V_n, according to ACI 318-19 [3] §15.4.2
s	=	spacing of column hoops or ties (in.)
t_d	=	term representing the effect of bar size on the contribution of confining reinforcement to total bond force for tension development length (ACI 408R-03 [1])
t_r	=	term representing the effect of relative rib area of the bar being developed on the contribution of confining reinforcement to total bond force for tension development length (ACI 408R-03 [1])
V_n	=	nominal joint shear strength according to ACI 318-19 [3] §18.8.4 (kip)
V_p	=	horizontal joint shear demand at mid depth of the beam (kip)
T_h	=	anchorage strength of a headed bar, calculated using the descriptive equation by Ghimire, Darwin, and Lepage [6]
$\delta_{0.8peak}$	=	the drift ratio associated with a 20% strength loss
ε_s	=	strain of steel reinforcement

λ	=	lightweight concrete modification factor for the development length of deformed bars and wires in compression (ACI 318-19 [3] §25.4.9) and the development length of hooked bars in tension (ACI 318-19 [3] §25.4.3)
ρ_t	=	ratio of area of distributed transverse reinforcement to gross concrete area perpendicular to that reinforcement, $A_{tr}/(b_c s)$
$\rho_{t,req}$	=	minimum required ratio of area of distributed transverse reinforcement to gross concrete area perpendicular to that reinforcement (ACI 352R-02 [34])
ψ_c	=	concrete strength modification factor for the development length of headed bars in tension (ACI 318-19 [3] §25.4.4)
ψ_e	=	epoxy coating modification factor for the development length of headed bars in tension (ACI 318-19 [3] §25.4.4 and ACI 318-14 §25.4.4)
$\psi_{o,head}$	=	location modification factor for the development length of headed bars in tension (ACI 318-19 [3] §25.4.4).
$\psi_{o,hook}$	=	location modification factor for the development length of hooked bars in tension (ACI 318-19 [3] §25.4.3)
ψ_p	=	parallel tie reinforcement modification factor for the development length of headed bars in tension (ACI 318-19 [3] §25.4.4)
ψ_r	=	confining reinforcement modification factor for the development length of deformed bars and wires in compression (ACI 318-19 [3] §25.4.9)

Chapter 4: Embedment Length of Hooked Bars in Joints of Special Moment Frames

4.1 Introduction

Hooked bars transmit forces into concrete through bond along the straight and curved portions of the bar and through bearing of the curved portion against concrete. Hooked bars are often used in exterior joints of moment frames, where the beam longitudinal reinforcement must be anchored into the column.

Use of hooked bars in reinforced concrete construction is permitted and regulated by ACI 318-19 [3]. For design of joints in frames not designated as special moment frames (SMFs), the development of hooked bars in tension is prescribed by Chapter 25 of ACI 318-19. According to §25.4.3, the development length $\ell_{dh,25.4.3}$ for hooked deformed bars in tension shall be:

$$\ell_{dh,25.4.3} = \max\left\{\frac{f_y \psi_e \psi_r \psi_o \psi_c}{55\lambda\sqrt{f'_c}} d_b^{1.5} \; ; \; 8d_b \; ; \; 6\text{in.}\right\} \qquad \text{Eq. (35)}$$
$$\text{(lb, in.)}$$

where λ, ψ_e, ψ_r, ψ_o, and ψ_c are modification factors associated with lightweight concrete, epoxy coating, confining reinforcement, hooked bar location, and concrete strength, respectively.

Requirements for development of hooked, headed, and straight reinforcement in joints of SMFs are articulated in §18.8.2.2:

> "*Longitudinal reinforcement terminated in a joint shall extend to the far face of the joint core and shall be developed in tension in accordance with 18.8.5 and in compression in accordance with 25.4.9.*" – ACI 318-19 [3] §18.8.2.2

For developing hooked bars in tension in SMFs, ACI 318-19 §18.8.5.1 requires providing the length given by Eq. (36):

$$\ell_{dh,18.8.5.1} = \max\left\{\frac{f_y d_b}{65\lambda\sqrt{f'_c}} \; ; \; \ell_{dh,18.8.5.1,\min}\right\} \qquad \text{Eq. (36)}$$
$$\text{(lb, in.)}$$

Where $\ell_{dh,18.8.5.1,min}$ is the greater of $8d_b$ and 6 in. (150 mm) for normal-weight concrete and the greater of 10 d_b and 7½ in. (190 mm) for lightweight concrete.

The language in §18.8.2.2 that requires consideration of both tension and compression development has been present in successive versions of the ACI Building Code since ACI 318-83 (Appendix A). Even though earthquakes are expected to subject beam reinforcement terminating in a joint to both tension and compression force demands, the language of §18.8.2.2 is not clear about whether it is sufficient for a hooked bar to satisfy only §18.8.5 or must satisfy both §18.8.5 and §25.4.9. It could be interpreted that the reference to §25.4.9 is only for straight bars in compression. This was clarified with new commentary in ACI 318-14:

> "*For bars in compression, the development length corresponds to the straight portion of a hooked or headed bar measured from the critical section to the onset of the bend for hooked bars and from the critical section to the head for headed bars.*" - ACI 318-14 [20] §R18.8.2.2

This definition is illustrated in Figure 40.

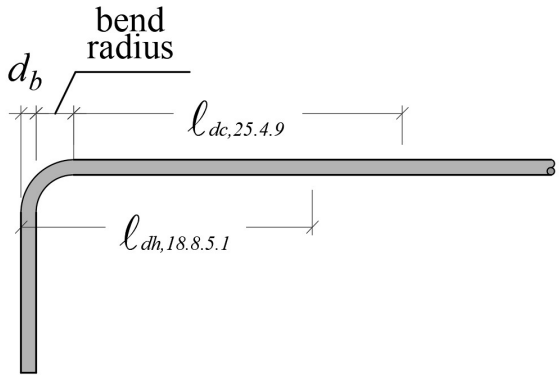

Figure 40 – Illustration of ACI 318-19 §18.8.2.2 applied to a hooked bar

Prior to ACI 318-14, an engineer might have assumed that a hooked bar satisfying §18.8.5 was adequately developed without checking §25.4.9 because tension development is often more critical than compression development, and there is no experimental evidence of hooks adequately anchored in tension failing when subjected to compression. Nevertheless, the new commentary in §R18.8.2.2 of ACI 318-14 makes clear that engineers must design hooked bars so they comply with both §18.8.5 and §25.4.9.

The compression development length required for joints of SMFs by §18.8.2.2, in accordance with §25.4.9, is the longer of the values obtained from the expressions in Eq. (37):

$$\ell_{dc,25.4.9} = \max\left\{\frac{f_y\psi_r}{50\lambda\sqrt{f_c'}}d_b\ ;\ 0.0003 f_y\psi_r d_b; 8\text{ in.}\right\} \qquad \text{Eq. (37)}\ \text{(lb, in.)}$$

where ψ_r is a confining reinforcement modification factor and $\sqrt{f_c'} \leq 100$ psi (0.69 MPa).

The implications of designing hooked bars for compression development (§25.4.9) are shown in Figure 41. Figure 41 shows the ratio between the required hooked bar compression length ($\ell_{dc,25.4.9}$ + bend radius + d_b) and the required hooked bar tension development length, $\ell_{dh,18.8.5.1}$, versus specified concrete compressive strength. For the bar sizes considered, two curves are obtained: one for No. 6 to No. 8 (19 to 25 mm) bars and another for No. 9 to No. 11 (29 to 36 mm) bars.

Normal-weight concrete (λ= 1.0) and a steel yield stress of 60 ksi (420 MPa) were assumed for all cases. A value of 0.75 was assumed for the confining reinforcement modification factor for calculating compression development length (ψ_r = 0.75). These assumptions are valid for uncoated hooked bars terminating inside a well-confined joint. The bend radius was either $3d_b$ (No. 3 through No. 8 (10 through 25 mm) bars) or 4 d_b (No. 9 through No. 11 (29 through 36 mm) bars), as required in ACI 318-19 §25.3.1.

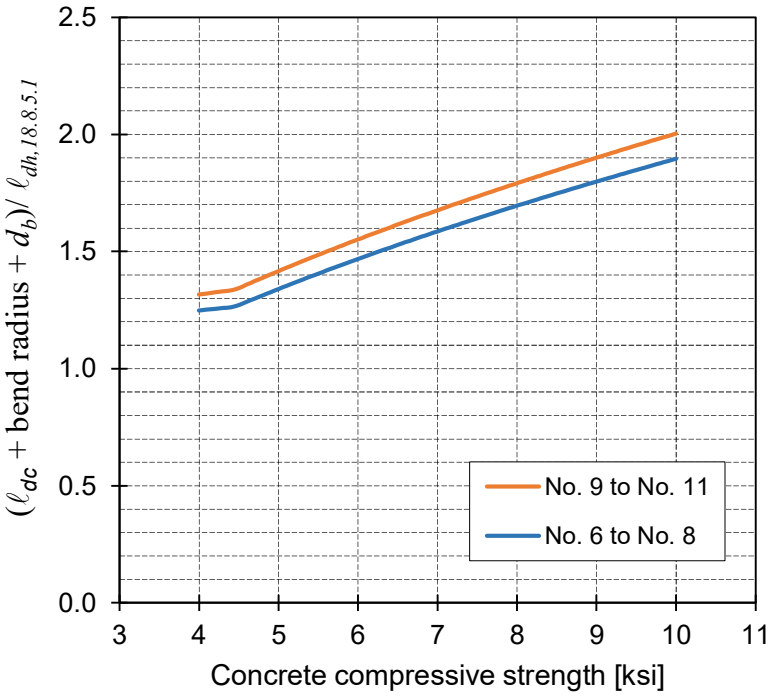

Figure 41 – ACI 318-19 provisions for hooked bars: (ℓ_{dc} + bend radius + d_b)/ℓ_{dh} versus concrete compressive strength

(1 ksi = 6.895 MPa)

Figure 41 shows that, for λ = 1.0 and ψ_r = 0.75, the length required to satisfy the compression development length is longer than the required tension development length for hooked bars of sizes typically used in practice, regardless of the concrete compressive strength.

The effect of ACI 318-19 §18.8.2.2 is considerably more pronounced for hooked bars than for headed bars (Chapter 3, Figure 19). The compression development length requirement is, in all cases, at least 25% longer than the tension development requirement for any of the bar sizes considered (No. 6 through No. 11, or 19 through 36 mm) and the range of concrete compressive strengths considered (4 ksi through 10 ksi, or 28 to 69 MPa).

This chapter explores whether the compression development length should govern the embedment length of hooked bars in SMF joints. This is done by examining results from tests of exterior beam-column joints under reversed cyclic displacements.

4.2 Database Description

A database of test results was used to evaluate hooked bar development. The database (Appendix H) includes results from six studies and consists of 27 exterior cast-in-place reinforced concrete beam-column joint specimens subjected to reversed cyclic loading. Figure 42 shows a schematic of a representative specimen.

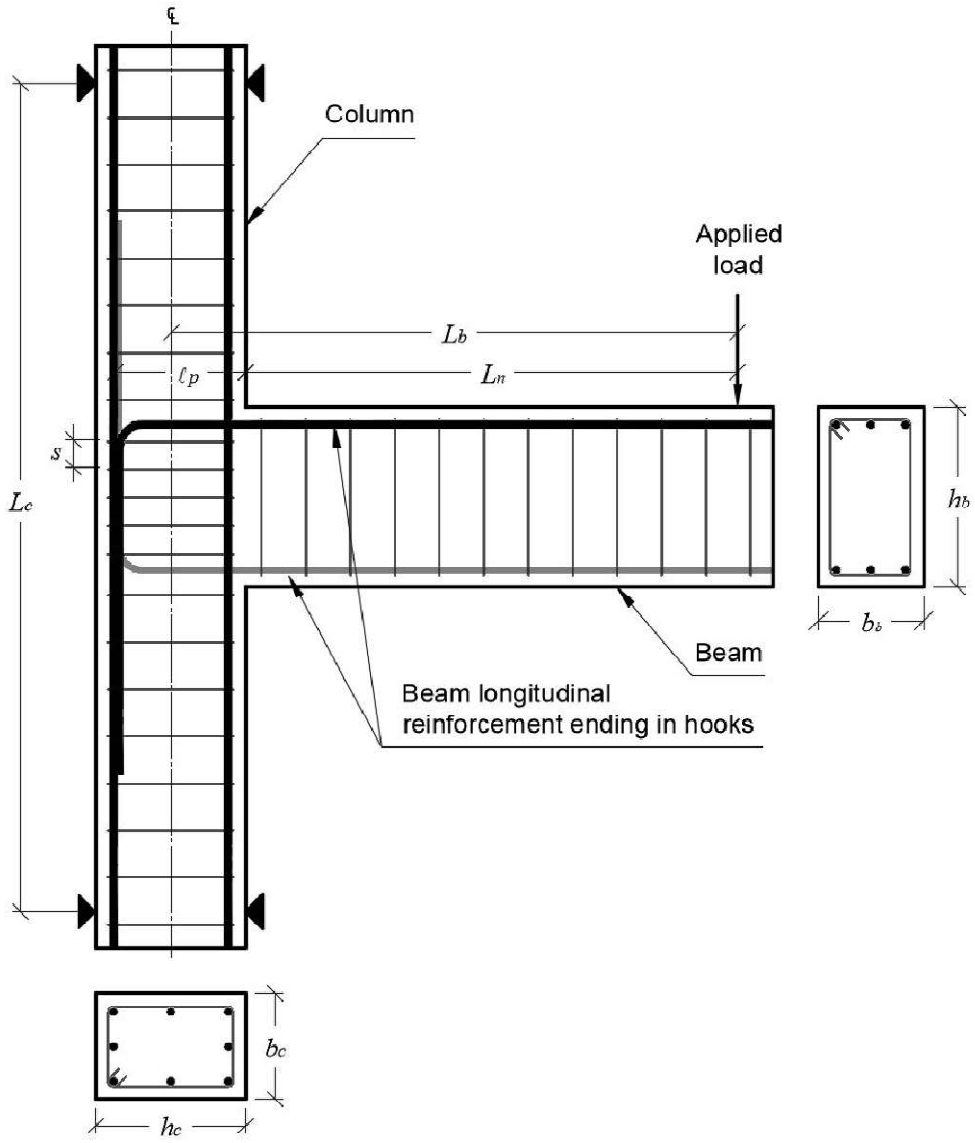

Figure 42 – Schematic of specimens in database (elevation and cross-sections)

Results were obtained from Hanson [35], Uzumeri and Seckin [36,37], Scribner and Wight [38], Ehsani and Alameddine [39,40], Kurose et al. [41], and Hwang et al. [42]. The 27 specimens were selected for meeting the following criteria: (1) specimens were cast-in-place reinforced concrete beam-column connections, (2) columns were continuous through the joint and had a minimum cross-sectional dimension of 12 inches (300 mm), (3) connections were subjected to reversed cyclic displacement demands, (4) beam longitudinal reinforcing bars ended in overlapping 90° hooks placed with the hooks turned towards mid-depth of the joint, (5) hooked beam bar diameter was at least 0.94 in. (24 mm) and no mixed bar sizes were used within the top or bottom layers of beam reinforcement, (6) joints had at least two column hoops, and (7) no intermediate-depth web longitudinal reinforcement was present in the beams (i.e. beams had top and bottom longitudinal bars only).

Specimens with relatively large bars were selected for two reasons. Firstly, large bars (No. 8 and 9 (25 and 29 mm)) are similar to bar sizes used in practice, and secondly, differences between Eq. (35) and Eq. (36) (which represent ACI 318-19 §25.4.3 for non-SMF design and §18.8.5.1 for SMF design) are likely to be most substantial for large bars because the exponent on d_b differs. The exponent on d_b is 1.5 in Eq. (35) and 1.0 in Eq. (36).

Every specimen contained transverse reinforcement within the joint consisting of column hoops, although not all connections satisfy the joint transverse reinforcement requirements of ACI 318-19 [3] for SMF joints.

The specimens had measured concrete compressive strengths of 3.8 to 13.4 ksi (26.2 to 92.4 MPa). Hooked bars had diameters that approximately coincided with No. 8 and No. 9 (25 and 29 mm) bars and measured yield stresses of 50.6 to 71.2 ksi (349 to 491 MPa). The distributions of measured concrete compressive strength, hooked bar diameter, and measured steel yield stress

are shown in Figure 44, 45, and 46, respectively. The provided embedment lengths of the hooked bars, defined as shown in Figure 43, were 10.6 to 16 times the diameter of the hooked bar with the distribution shown in Figure 47.

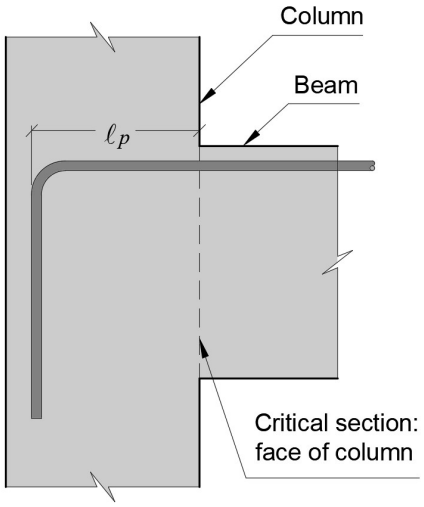

Figure 43 – Definition of the embedment length in specimens, ℓ_p, consistent with ACI 318-19 definition of development length

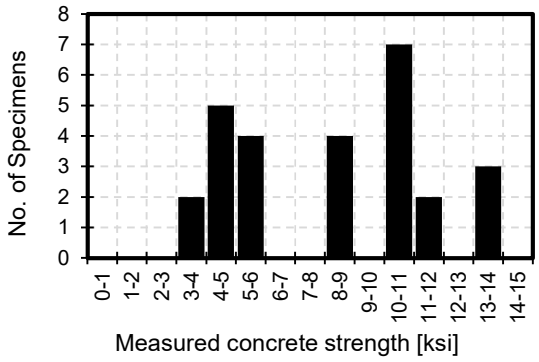

Figure 44 – Histogram of measured concrete compressive strength
(1 ksi = 6.895 MPa)

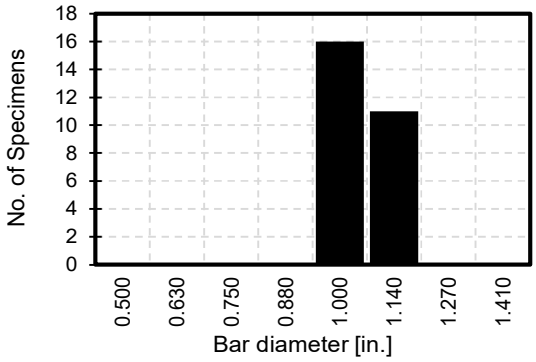

Figure 45 – Histogram of hooked bar diameter (each bin includes specimens within ±1/16 in.)
(1 in. = 25.4 mm)

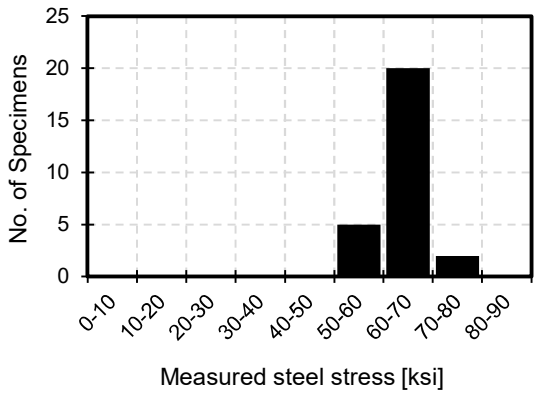

Figure 46 – Histogram of measured hooked bar steel yield stress
(1 ksi = 6.895 MPa)

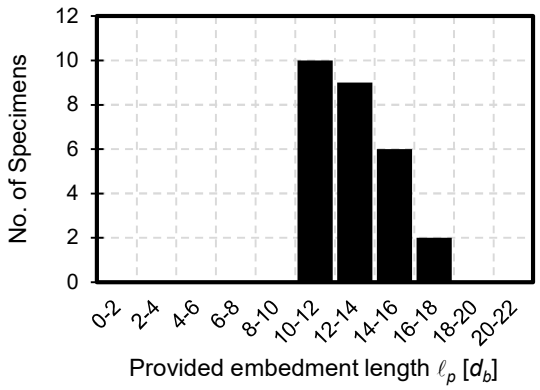

Figure 47 – Histogram of provided hooked bar embedment length (column face to tail of hook)

The specimens were all subjected to a series of fully reversed cyclic displacements of increasing magnitude. The strength of the specimens was limited by beam reinforcement yielding. Specimen drift capacity was limited by deterioration of the joint or the beam near the joint.

Specimen drift ratio was defined as the vertical displacement of the beam end during testing divided by the beam length measured to the centroid of the column (L_b in Figure 42). The drift ratio capacities in the database correspond to the drift ratio at which strength decayed to 0.8 times the peak strength in each loading direction based on an envelope drawn to the peak of each loading cycle. Rather than reporting precise $\delta_{0.8,peak}$ values, which can be difficult to discern accurately from published reports, the database indicates for each specimen either (a) whether $\delta_{0.8,peak}$ was at least 3%, or (b) that insufficient information was available to assess $\delta_{0.8,peak}$. All 24 specimens with published force-displacement results had $\delta_{0.8,peak}$ of at least 3%.

The nominal beam flexural strength was calculated at the column face using Eq. (26):

$$M_n = f_y A_{hs} (d - a/2) \qquad \text{Eq. (26)}$$

The contribution of compression reinforcement to flexural strength was neglected. In every case the beam section neglecting compression reinforcement was under-reinforced (with

calculated tension steel strains at nominal moment greater than or equal to the yield strain, estimated as f_y / E_s).

The maximum bending moment in the beams, M_{peak}, was calculated as the applied force times the beam clear span (distance from the point load to the column face). Peak-to-nominal moment strength ratios, M_{peak}/M_n, were from 0.88 to 1.34 (Figure 48). Most specimens exhibited beam strengths exceeding their nominal flexural strength based on measured material properties. The relatively high $\delta_{0.8peak}$ and M_{peak}/M_n values are consistent with beam longitudinal bar yielding, likely producing anchorage force demands at the joint face at least equal to the product of bar yield stress and cross-sectional area.

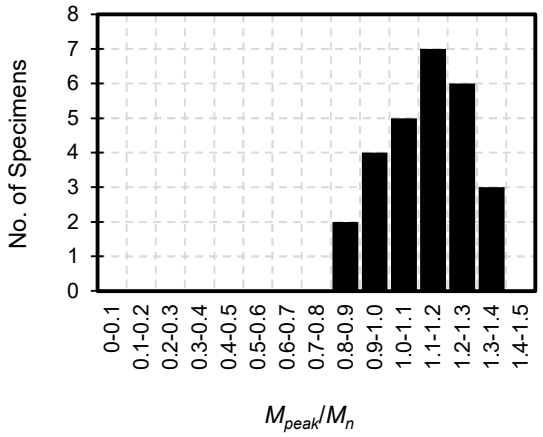

Figure 48 – Histogram of M_{peak} /M_n

The nominal joint shear strength, V_n, was calculated in accordance with ACI 318-19 §18.8.4 using Eq. (27).

$$V_n = R_n \lambda \sqrt{f_c'} A_j \qquad \text{Eq. (27)} \quad \text{(lb, in.)}$$

where R_n is a coefficient representing whether a transverse beam is present. R_n was 12 for 26 of the 27 specimens in the database, and 15 for the specimen from Kurose et al. [41]. The effective

joint area A_j, shown schematically in Figure 49, consists of the product of the joint depth in the plane parallel to the reinforcement generating shear (the height of the column section for these specimens) and the effective joint width, defined as the lesser of b_c, (b_b+h_c), and (b_c+2x).

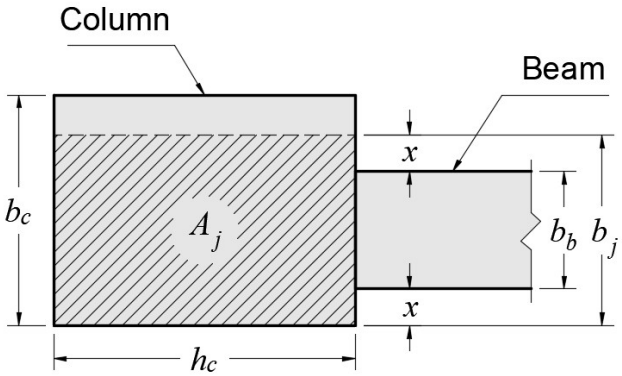

Figure 49 – Definition of effective joint area (plan view), adapted from ACI 318-19 [3] Fig. R15.4.2

Joint shear demand, V_p, was estimated with Eq. (28). Equation (28) is equivalent to the equation used in Ghimire, Darwin, and Lepage [6] for similar tests with headed bars, except that the second term, which represents the column shear outside of the joint, is multiplied by L_b/L_n. This is necessary because M_{peak} is calculated at the column face.

$$V_p = \left(\frac{M_{peak}}{M_n} \right) n A_b f_y - \frac{M_{peak}}{L_c} \frac{L_b}{L_n} \qquad \text{Eq. (28)}$$

Peak-to-nominal shear strength ratios, V_p/V_n, ranged from 0.57 to 1.23 (Figure 50). For 22 of the 27 specimens, the shear demand was less than the nominal joint shear strength.

Figures 51 and 52 show M_{peak}/M_n and V_p/V_n versus ℓ_p/d_b, respectively. Closed circles correspond to specimens with a drift ratio capacity greater than 3%, which is every specimen for which drift data were reported. Open circles indicate specimens for which drift ratio data were not reported.

Figure 51 shows that in specimens with $\delta_{0.8peak} \geq 3\%$, the peak moments were generally greater than the nominal flexural strength. No trend is evident between M_{peak}/M_n and ℓ_p/d_b. As expected, there is no correlation between V_p/V_n and ℓ_p/d_b in Figure 52.

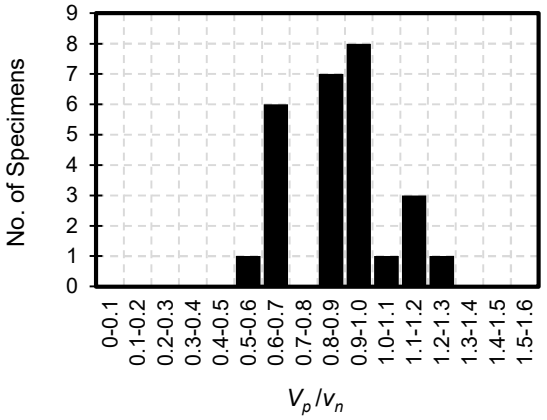

Figure 50– Histogram of V_p/V_n

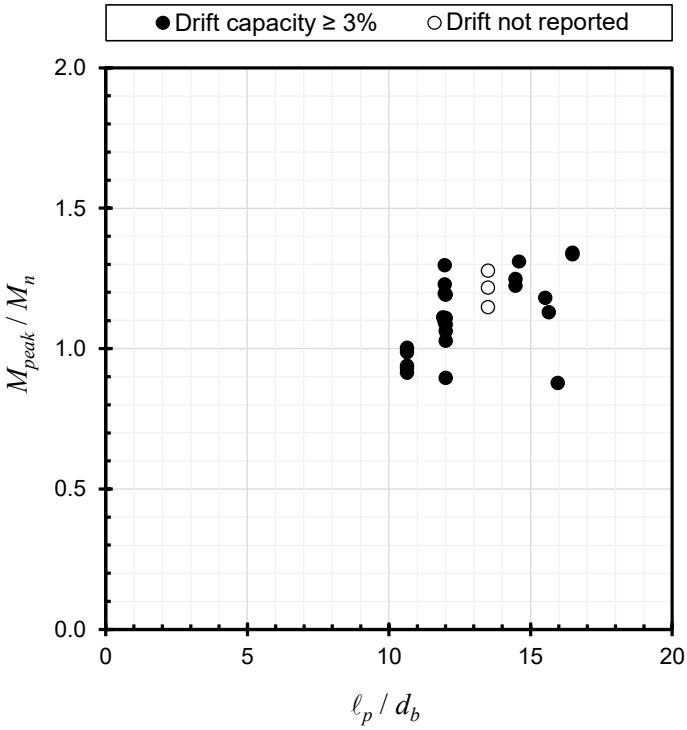

Figure 51 – M_{peak}/M_n versus ℓ_p/d_b

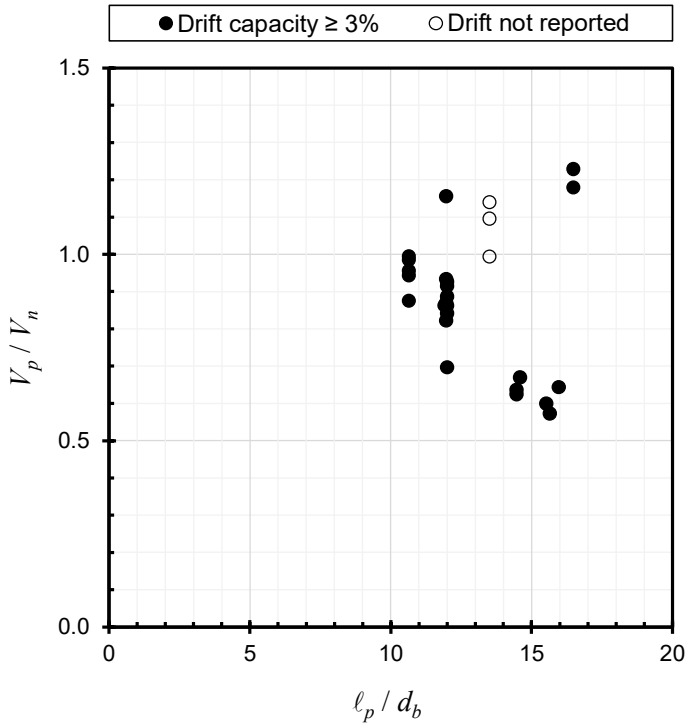

Figure 52 – V_p/V_n versus ℓ_p / d_b

4.3 Evaluation of Database against Current Provisions

The embedment lengths provided for specimens in the database were compared against $\ell_{dh,18.8.5.1}$ and $\ell_{dc,25.4.9}$ to evaluate the appropriateness of the requirement in §18.8.2.2 that hooked bars in SMF joints satisfy the compression development length requirements. Measured material properties were used in all cases.

To calculate the compression development length, $\ell_{dc,25.4.9}$, some interpretation was necessary to define the confining reinforcement modification factor, ψ_r. This factor leads to a reduction of the required compression development length when the transverse reinforcement consists of:

- A spiral,

- A circular continuously wound tie with $d_b \geq$ ¼ in. (6 mm) and pitch not more than 4 in. (100 mm),
- No. 4 (12 mm) bar or D20 wire ties in accordance with ACI 318-19 [3] §25.7.2 spaced no more than 4 in. (100 mm) on center, or
- Hoops in accordance with ACI 318-19 §25.7.4 spaced no more than 4 in. (100 mm) on center.

As with the headed bar database, specimens in the hooked bar database were less than full scale, so it is arguably not appropriate to use the conditions stated in §25.4.9 that are intended for full-scale columns. To identify specimens with transverse reinforcement similar to that required to obtain $\psi_r = 0.75$ in full-scale columns, a joint transverse reinforcement ratio was calculated for each specimen with Eq. (29):

$$\rho_t = \frac{A_{tr,1} N_{legs}}{s b_c} \qquad \text{Eq. (29)}$$

Specimens were assumed to qualify for $\psi_r = 0.75$ when $\rho_t \geq 0.5\%$ in both principal directions, which is the transverse reinforcement ratio in a square column with 20 in. (510 mm) sides and two legs of No. 4 (12 mm) ties spaced at 4 in. (100 mm) (and thus qualifying for $\psi_r = 0.75$). The threshold 0.5% value was selected to represent the transverse reinforcement ratio required in a full-scale column to qualify for $\psi_r = 0.75$.

With this criteria, 26 of the 27 specimens (96%) had hoops that qualified for $\psi_r = 0.75$.

4.3.1 Results

Figure 53 shows the hooked bar embedment lengths versus the required compression length ($\ell_{dc,25.4.9}$ + bend radius + d_b) for all 27 specimens, with both lengths normalized by the hooked bar diameter. This plot shows that the provided embedment length was less than the

required compression embedment length ($\ell_{dc,25.4.9}$ + bend radius + d_b) in all specimens. For specimens with $\delta_{0.8peak} \geq 3\%$, the required length was up to 83% longer than the provided length, and yet the specimens performed adequately under reversed cyclic loading without exhibiting anchorage failures. Providing an embedment length longer than ($\ell_{dc,25.4.9}$ + bend radius + d_b) is therefore not necessary to prevent anchorage failures and obtain a drift ratio capacity greater than 3% for specimens similar to those in the database.

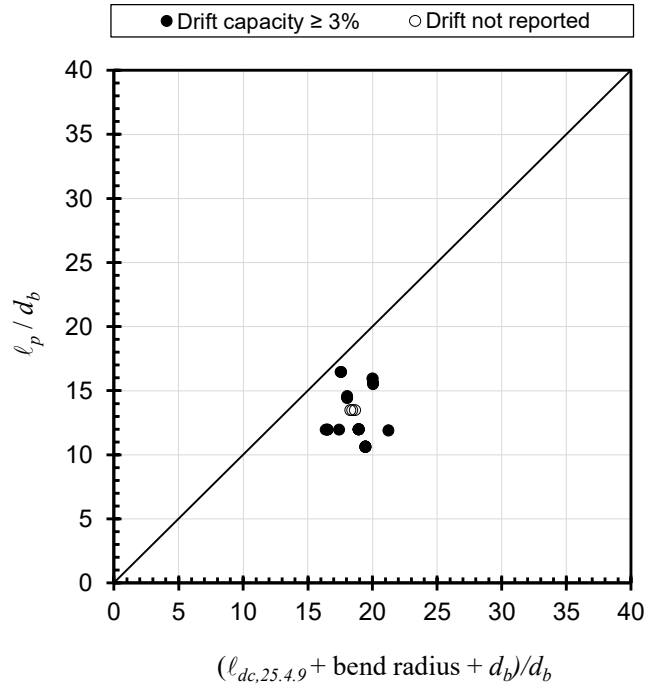

Figure 53 – ℓ_p/d_b versus ($\ell_{dc,25.4.9}$ + bend radius + d_b)

Figure 54 shows hooked bar embedment lengths versus the required tension development length, $\ell_{dh,18.8.5.1}$, normalized by hooked bar diameter. Twenty of the 24 specimens that attained $\delta_{0.8peak} \geq 3\%$ had an embedment length ℓ_p longer than $\ell_{dh,18.8.5.1}$, which should be expected for specimens that did not exhibit anchorage failures. The data therefore suggest that satisfying the tension development length provision for SMF joints, $\ell_{dh,18.8.5.1}$, is an important criterion for design of joints like those in the database. This was not the case for headed bars (Chapter 3), for which it

was shown that both the tension and the compression development requirements from ACI 318-19 §18.8.2.2 are substantially conservative.

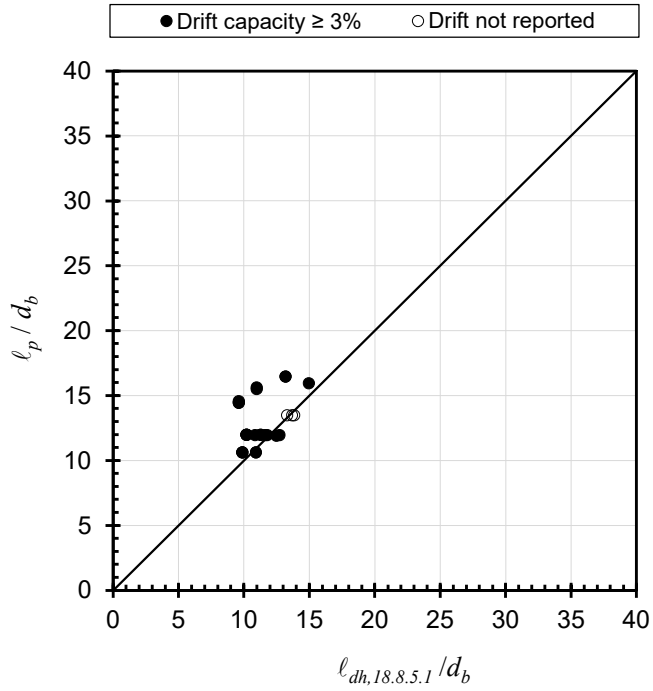

Figure 54 – ℓ_p/d_b versus $\ell_{dh,18.8.5.1}/d_b$

4.4 Evaluation of Database against Other Equations

The compression development length requirements in ACI 318-19 §25.4.9 appear to be considerably, perhaps excessively, conservative for hooked bar development in special moment frame joints. This observation prompts consideration of other equations that might better fit the dataset. Four equations are considered.

4.4.1 Equations Considered

i) Development of hooked bars in tension (ACI 318-14 §25.4.3)

ACI 318-14 [20] had different provisions for hooked bar development than ACI 318-19. Equation (38) is the development length equation for hooked deformed bars in tension from

§25.4.3 of ACI 318-14. This equation was not applicable to hooked bars in SMF joints, but it is used here for comparisons without any increase in bar stress to account for strain hardening.

$$\ell_{dh,318-14} = \max\left\{\frac{f_y \psi_e \psi_c \psi_r}{50\lambda\sqrt{f_c'}} d_b \; ; 8d_b \; ; 6 \text{ in.}\right\} \qquad \text{Eq. (38)} \text{ (lb, in.)}$$

ii) Development of hooked bars in tension (ACI 318-19 §25.4.3)

As stated earlier, Chapter 25 of ACI 318-19 [3] prescribes Eq. (39) for the development length of hooked bars in tension design of frames not designated as special moment frames. For the comparisons reported here, the measured yield stress was used with no increase to account for strain hardening.

$$\ell_{dh,25.4.3} = \max\left\{\frac{f_y \psi_e \psi_r \psi_o \psi_c}{55\lambda\sqrt{f_c'}} {d_b}^{1.5} \; ; 8d_b \; ; 6\text{in.}\right\} \qquad \text{Eq. (39)} \text{ (lb, in.)}$$

iii) Ajaam et al. [43] descriptive equation

Ajaam et al. [43] reported that the hooked bar provisions in ACI 318-14 *"*overestimate the contribution of the concrete compressive strength and the bar size [to] the anchorage strength of hooked bars." They proposed the following descriptive equations for the anchorage strength of a single hooked bar. Equation 40 accounts for the relative distance to other hooked bars and the presence of transverse reinforcement.

- For widely spaced hooked bars ($c_{ch} \geq 6d_b$):

$$T_h = 294 f_{cm}^{0.295} \ell_{eh}^{1.0845} d_b^{0.47} + 55050 \left(\frac{A_{tt}}{n} \right)^{1.0175} d_b^{0.73}$$

- For closely spaced hooked bars ($c_{ch} < 6d_b$) without transverse reinforcement:

$$T_h = \left(294 f_{cm}^{0.295} \ell_{eh}^{1.0845} d_b^{0.47} \right) \left(0.0974 \frac{c_{ch}}{d_b} + 0.3911 \right)$$

$$\text{with } \left(0.0974 c_{ch} / d_b + 0.3911 \right) \leq 1.0$$

Eq. (40)
(lb, in.)

- For closely spaced hooked bars ($c_{ch} < 6d_b$) with transverse reinforcement:

$$T_h = \left(294 f_{cm}^{0.295} \ell_{eh}^{1.0845} d_b^{0.47} + 55050 \left(\frac{A_{tt}}{n} \right)^{1.0175} d_b^{0.73} \right) \left(0.0516 \frac{c_{ch}}{d_b} + 0.6572 \right)$$

$$\text{with} \left(0.0516 c_{ch} / d_b + 0.6572 \right) \leq 1.0$$

The embedment length associated with developing the yield stress of the hooked bars, ℓ_{ehy} (Eq. 41), can be obtained from Eq. (40) by replacing the anchorage strength T_h with the product of the measured value of f_y and the cross-sectional area of the (individual) hooked bar, A_b.

- For widely spaced hooked bars ($c_{ch} \geq 6d_b$):

$$\ell_{ehy} = \left[\frac{f_y A_b - 55050 \left(\frac{A_{tt}}{n} \right)^{1.0175} d_b^{0.73}}{294 f_{cm}^{0.24} d_b^{0.47}} \right]^{\frac{1}{1.0845}}$$

- For closely spaced hooked bars ($c_{ch} < 6d_b$) without confining reinforcement:

$$\ell_{ehy} = \left[\frac{f_y A_b}{\left(0.0974 \frac{c_{ch}}{d_b} + 0.3911 \right) \left(294 f_{cm}^{0.295} d_b^{0.47} \right)} \right]^{\frac{1}{1.0845}} \quad \text{Eq. (41) (lb, in.)}$$

$$\text{with } \left(0.0974 c_{ch} / d_b + 0.3911 \right) \leq 1.0$$

- For closely spaced hooked bars ($c_{ch} < 6d_b$) with confining reinforcement:

$$\ell_{ehy} = \left[\left(\frac{f_y A_b}{0.0516 \frac{c_{ch}}{d_b} + 0.6572} - 55050 \left(\frac{A_{tt}}{n} \right)^{1.0175} d_b^{0.73} \right) \frac{1}{294 f_{cm}^{0.24} d_b^{0.47}} \right]^{\frac{1}{1.0845}}$$

$$\text{with} \left(0.0516 c_{ch} / d_b + 0.6572 \right) \leq 1.0$$

iv) ACI 408R-03 [1] Tension Development length with 0.7 reduction factor

The analyses of compression lap splices in Chapter 2 suggest that compression lap splice length can be calculated as a fraction of the tension development length. The fraction differs depending on which tension development equation is used. Here compression development is taken as 0.7 times the length obtained from the ACI 408R-03 [1] tension development length equation (Eq. (42)). If hooked bars in special moment frame joints should be designed for compression development, then connections in the database that exhibit drift capacities greater than 3% should be expected to often satisfy Eq. (42) plus bend radius and bar diameter.

$$l_{dc,408} = 0.7 l_{d,408} = 0.7 \frac{\left(\frac{f_y}{\phi f_c'^{1/4}} - 2400\omega \right) \alpha\beta\lambda}{76.3 \left(\frac{c\omega + K_{tr,408}}{d_b} \right)} d_b \qquad \text{Eq. (42) (lb, in.)}$$

where α, β, and λ are all unity for this database, and with:

$$\omega = 0.1 \frac{c_{max}}{c_{min}} + 0.9 \le 1.25 \; ; \; t_r = 9.6 R_r + 0.28 \le 1.72 \; ; \; t_d = 0.03 d_b + 0.22$$

$$K_{tr,408} = \frac{6.26 t_r t_d A_{tr}}{sn} f_c'^{1/2} \quad ; \quad f_c'^{1/4} \le 11.0 \; ; \; f_y \le 80 \text{ ksi} \; ; \; \phi = 0.82$$

A relative rib area, R_r, of 0.0727 was assumed for all specimens based on recommendations in ACI 408R-03.

Application of Eq. (42) to hooked bars in joints requires some interpretation. For instance, identification of potential splitting planes is not as obvious in a beam-column joint as it may be for longitudinal bars in a column or beam; the definition of splitting plane does not readily apply where breakout anchorage failures occur. To bracket the range of possible outcomes, two cases are considered in these analyses: $K_{tr,408} = 0$, which represents a lack of confining reinforcement, and $(c\omega + K_{tr,408})/d_b = 4$, the upper bound recommended in ACI 408R-03.

4.4.2 Results

Figures 55 through 59 are analogous to Figures 53 and 54. Each figure shows the provided embedment length plotted versus the development length obtained from the selected equations (Eqs. (38), (39), (41), and (42)) , with lengths normalized by hooked bar diameter. These equations include the ACI 318-14 tension development length for hooked bars, $\ell_{dh,318\text{-}14}$ (Eq. (38)); the ACI 318-19 tension development length for hooked bars, $\ell_{dh,25.4.3}$ (Eq. (35)); the embedment length derived from the anchorage strength descriptive equations from Ajaam et al. [43], ℓ_{eyh}, (Eq. (41));

and 0.7 times the ACI 408R-03 tension development length, l_d, (Eq. (42)) plus bend radius and bar diameter with either $K_{tr,408} = 0$ (Case I) or $(c\omega+K_{tr,408})/d_b = 4.0$ (Case II). For these comparisons, the measured yield stress was used to obtain the calculated lengths.

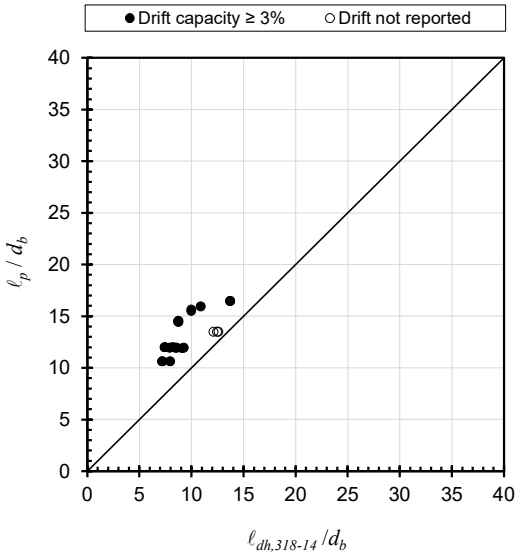

Figure 55 – ℓ_p/d_b versus $\ell_{d,318\text{-}14}/d_b$

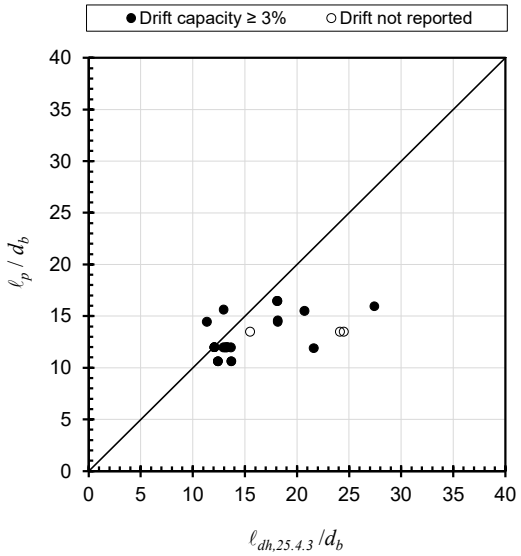

Figure 56 – ℓ_p/d_b versus $\ell_{dh,25.4.3}/d_b$

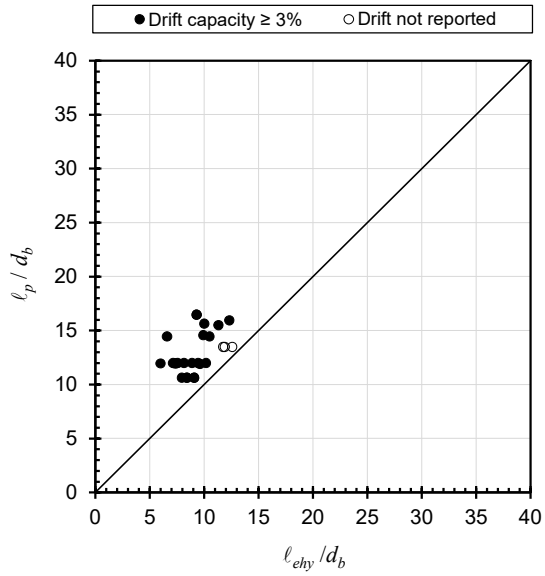

Figure 57 – ℓ_p/d_b versus ℓ_{eyh} (Ajaam et al.)$/d_b$

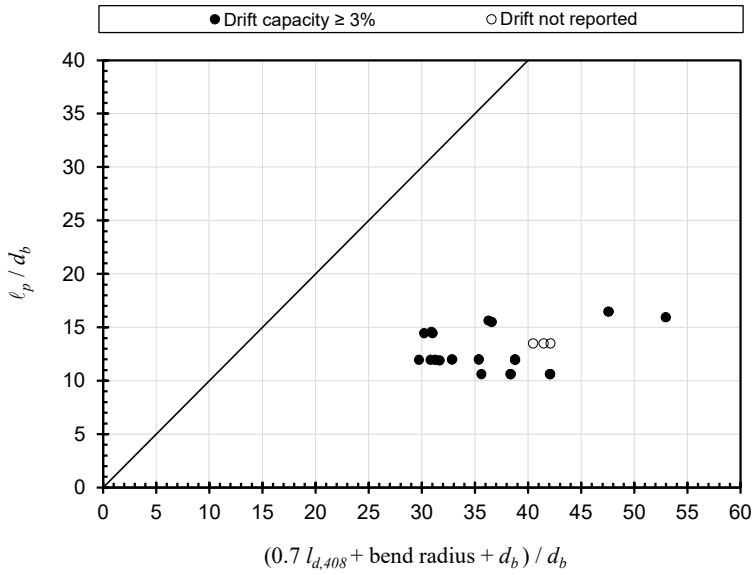

Figure 58 – ℓ_p/d_b versus $(0.7l_d$ [ACI 408R-03 Case I: $K_{tr,408} = 0$] + bend radius + $d_b)/d_b$

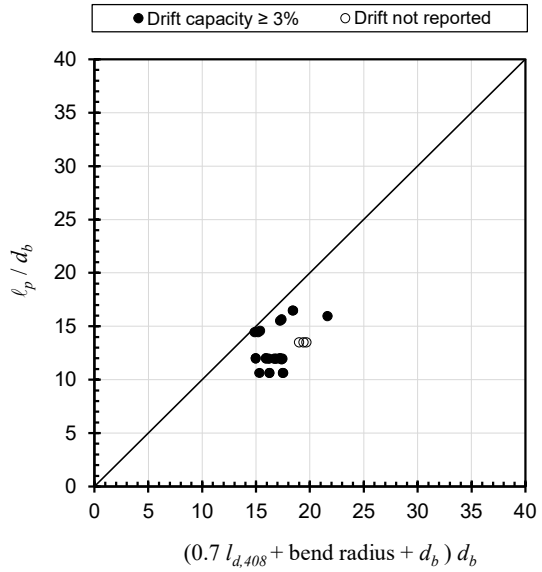

Figure 59 – ℓ_p/d_b versus $(0.7l_d$ [ACI 408R-03 Case II: $(c\omega+K_{tr,408})/d_b = 4.0$] + bend radius + $d_b))/d_b$

Since none of the 24 specimens with $\delta_{0.8peak} \geq 3\%$ were reported to have exhibited anchorage failures, it is reasonable to expect that the provided embedment length in those specimens frequently exceeded or was close to the necessary development lengths. Figures 54, 55, and 57 are consistent with this expectation; each of these figures shows that the provided

embedment lengths were near to or exceeded the calculated lengths based on $\ell_{dh,18.8.5.1}$, $\ell_{d,318\text{-}14}$, and ℓ_{eyh} (Ajaam et al.), respectively.

As discussed previously, that was not the case in Figure 53, which suggested that satisfying ACI 318-19 §25.4.9 is not necessary to obtain adequate joint behavior characterized by $\delta_{0.8peak} \geq$ 3%. Like Figure 53, Figures 56, 58, and 59 also show that the provided embedment lengths were generally less than the calculated lengths based on $\ell_{dh,25.4.3}$ and ($0.7l_d$ + bend radius + d_b) with either $K_{tr,408} = 0$ or 4. The results in Figure 56 suggest that ACI 318-19 §25.4.3 is overly conservative for design of connections similar to those in the database. The results in Figures 58 and 59 show that compression development provisions recommended in chapter 2 do not produce reasonable results when applied to connections similar to those in the database.

Table 3 provides another way to compare the different length requirements. The value of each cell represents the mean ratio between the length in the row and the length in the column. An expanded version of the table with values for all lengths against each other can be found in Appendix I.

Table 3 – Average length ratios: length in row / length in column (all 27 specimens)

	ℓ_p	ℓ_{ehy}	Notes
ℓ_p	1.00	1.45	Provided embedment length
$\ell_{dh,318\text{-}14}$ [Eq. (38)]	0.70	1.02	ACI 318-14 tension development, with $1.0f_y$
$\ell_{dh,25.4.3}$ [Eq. (39)]	1.16	1.70	ACI 318-19 tension development, with $1.0f_y$
$\ell_{dc,25.4.9}$ [Eq. (37)] + bend radius + d_b	1.44	2.10	ACI 318-19 compression development, with $1.0f_y$
ℓ_{ehy} [Eq. (41)]	0.69	1.00	"descriptive" equation, with $1.0f_y$
$\ell_{dh,18.8.5.1}$ [Eq. (36)]	0.87	1.23	ACI 318-14 tension development, with integrated $1.25f_y$ and confinement factors
0.7 $l_{d,408}$ Case I [Eq. (42)] + bend radius + d_b	2.84	4.05	Compression development (chapter 2), 0% fractal with $1.0f_y$ and $K_{tr,408}/d_b = 0$
0.7 $l_{d,408}$ Case II [Eq. (42)] + bend radius + d_b	1.31	1.86	Compression development (chapter 2), 0% fractal with $1.0f_y$ and $(c\omega+K_{tr,408})/d_b = 4.0$

The column for ℓ_p in Table 3 shows that $\ell_{dh,25.4.3}$, ($\ell_{dc,25.4.9}$ + bend radius + d_b), and (0.7 $l_{d,408}$ Cases I and II + bend radius + d_b) (Eqs. (39), (37), and (42)) were on average longer than the embedment length provided in the specimens. For the database considered, providing the required compression development length by means of $\ell_{dc,25.4.9}$ + bend radius + d_b required, on average, 44% more embedment length than was provided. In contrast, Table 3 shows that $\ell_{dh,318\text{-}14}$, ℓ_{ehy}, and $\ell_{dh,18.8.5.1}$ (Eqs. (38), (41), and (36)) were, on average, 70%, 69%, and 87% of the provided embedment lengths in this database.

The column for ℓ_{ehy} in Table 3 provides ratios of calculated lengths versus ℓ_{ehy} obtained from the descriptive equation in Eq. (41). If ℓ_{ehy} is taken as the length necessary to develop hooked bars in SMF joints without a safety factor, ℓ_p / ℓ_{ehy} should generally exceed 1.0 in specimens that did not exhibit bond/anchorage failures. Table 3 shows $\ell_p / \ell_{ehy} = 1.45$ for this dataset. Furthermore, if ℓ_{ehy} is taken as the length necessary to develop hooked bars in SMF joints without a safety factor, the column for ℓ_{ehy} in Table 3 shows the extent of the conservatism embedded in various equations considered. For example, $\ell_{dh,25.4.3}$ (Eq. (39)) is on average 70% longer than ℓ_{ehy} while the previous version of the equation, $\ell_{dh,318\text{-}14}$ (Eq. (38)), is on average only 2% longer than ℓ_{ehy}. Table 3 shows that $\ell_{dh,18.8.5.1}$ (Eq. 36)) requires on average 23% more length than ℓ_{ehy}, and ($\ell_{dc,25.4.9}$ + bend radius + d_b) (Eq. (37)) requires more than twice the length of ℓ_{ehy}.

The same analysis can be done for just the specimens with $\delta_{0.8peak} \geq 3\%$. Table 4 is analogous to Table 3 but includes just the 24 specimens with $\delta_{0.8peak} \geq 3\%$. Again, the compression development length equation is an outlier among ACI 318-19 equations.

Table 4 – Average length ratios: length in row / length in column (specimens with $\delta_{0.8peak} \geq 3\%$: 24 specimens)

	ℓ_p	ℓ_{ehy}	Notes
ℓ_p	1.00	1.49	Provided embedment length
$\ell_{dh,318\text{-}14}$ [Eq. (38)]	0.68	1.02	ACI 318-14 tension development, with $1.0f_y$
$\ell_{dh,25.4.3}$ [Eq. (39)]	1.13	1.70	ACI 318-19 tension development, with $1.0f_y$
$\ell_{dc,25.4.9}$ [Eq. (37)] + bend radius + d_b	1.44	2.17	ACI 318-19 compression development, with $1.0f_y$
ℓ_{ehy} [Eq. (41)]	0.67	1.00	"descriptive" equation, with $1.0f_y$
$\ell_{dh,18.8.5.1}$ [Eq. (36)]	0.86	1.25	ACI 318-14 tension development, with integrated $1.25f_y$ and confinement factors
0.7 $l_{d,408}$ Case I [Eq. (42)] + bend radius + d_b	2.82	4.14	Compression development (chapter 2), 0% fractal with $1.0f_y$ and $K_{tr,408}/d_b = 0$
0.7 $l_{d,408}$ Case II [Eq. (42)] + bend radius + d_b	1.30	1.90	Compression development (chapter 2), 0% fractal with $1.0f_y$ and $(c\omega+K_{tr,408})/d_b = 4.0$

4.5 Conclusions

1. Satisfying the compression development length requirements of §25.4.9 is not a necessary condition to obtain adequate joint behavior under cyclic loads. Of the 24 beam-column connection specimens with drift ratio capacities above 3%, none satisfied §25.4.9. Furthermore, §25.4.9 produced lengths that were, on average, more than twice the lengths obtained from the Ajaam, Darwin, and O'Reilly [43] descriptive equation for hooked bar anchorage strength. ACI 318-19 §18.8.2.2 should not require that hooked bars satisfy §25.4.9.
2. Satisfying the tension development length requirements of §25.4.3 is also not a necessary condition to obtain adequate joint behavior under cyclic loads. Of the 24 beam-column connection specimens with drift ratio capacities above 3%, only two (8%) satisfied §25.4.3. Section 25.4.3 also produced lengths that were, on average, 70% longer than the lengths obtained from the Ajaam, Darwin, and O'Reilly [43] descriptive equation for hooked bar anchorage strength. ACI 318-19 §25.4.3 should not be applied to connections like those in the database.

3. Compression development length requirements recommended in chapter 2 for straight bars do not produce reasonable results when applied to connections similar to those in the database. This suggests that development length equations based on lap spliced bars in compression should not be applied to hooked bars in joints.
4. Results suggest that the tension development length requirements in ACI 318-19 §18.8.5.1 are appropriate for design of hooked bar development in beam-column joints of special moment frames. Section 18.8.5.1 produced lengths that were 23% longer than those obtained from the Ajaam, Darwin, and O'Reilly [43] descriptive equation for hooked bar anchorage strength, suggesting there is some built-in conservatism for connections similar to those in the database. Furthermore, 20 (83%) of the 24 specimens with drift ratio capacities above 3% satisfied §18.8.5.1, suggesting the provisions are useful for identifying specimens with adequately developed reinforcement.

4.6 Notation

a	=	depth of equivalent rectangular compressive stress block in beam flexure (in.)
A_b	=	cross-sectional area of an individual hooked bar (in.^{2})
A_{hs}	=	total cross-sectional area of hooked bars (in.^{2})
A_j	=	effective cross-sectional area of a joint in a plane parallel to plane of beam reinforcement generating shear in the joint, per ACI 318-19 [3] §R15.4.2 = $b_j \times h_c$ (in.^{2})
$A_{tr,1}$	=	cross-sectional area of a tie leg (in.^{2})
A_{tt}	=	total cross-sectional area of effective confining reinforcement parallel to the hooked bars (in.^{2})
b_b	=	beam width (in.)

b_c	=	column width (in.)
b_j	=	effective joint width (Figure 49) (in.)
c_b	=	bottom clear cover, ACI 408-03 [1] (in.)
c_{max}	=	maximum(c_b ; c_s) (in.)
c_{min}	=	minimum(c_b ; c_s), ACI 408-03 [1] (in.)
c_s	=	minimum (c_{so} ; c_{si} + 0.25 in. (6.4 mm)) (in.)
c_{si}	=	½ of the bar clear spacing (in.)
c_{so}	=	side concrete cover for reinforcing bar (in.)
d	=	distance between centroid of beam longitudinal tension reinforcing bars and extreme compression fiber of beam section (in.)
d_b	=	nominal diameter of bar being developed (in.)
E_s	=	modulus of elasticity of steel, 29,000 ksi (200 GPa)
f_c'	=	measured concrete compressive strength (psi)
f_y	=	measured yield stress of reinforcing steel (ksi)
h_b	=	beam height (in.)
h_c	=	column height (in.)
$K_{tr,408}$	=	transverse reinforcement index according to ACI 408R-03 [1]
n	=	number of hooked bars in tension
L_b	=	beam span measured to the center of the column (in.)
L_c	=	length of column between inflection points (in.)
L_n	=	clear span of beam (in.)
ℓ_c	=	compression development length of straight bars or wires, as required by ACI 318-19 [3] §25.4.9 (in.)
ℓ_p	=	provided embedment length of hooked bars in a specimen, measured from the critical section (face of column) to the back of the tail

$l_{d,408}$ = development length of straight bars in tension, as required by the recommended provisions by ACI 408R-03 [1], Eq. 4-11a (in.).

$\ell_{dh,18.8.5.1}$ = development length of hooked bar in tension ACI 318-19 §18.8.5.1 (in.).

$\ell_{dh,18.8.5.1,min}$ = minimum development length of hooked bar in tension according to ACI 318-19 [3] §18.8.5.1 (in.). The greater of $8d_b$ and 6 in. (150 mm) for normal-weight concrete and the greater of $10d_b$ and 7½ in. (190 mm)

$\ell_{dh,25.4.3}$ = development length of hooked bar in tension ACI 318-19 [3] §25.4.3 (in.).

$\ell_{dh,318\text{-}14}$ = development length of hooked bar in tension ACI 318-14 [20] §25.4.3 (in.).

ℓ_{ehy} = embedment length of a hooked bar associated required to develop its yield strength, derived from the anchorage strength descriptive equation by Ajaam et al. [43]

M_n = nominal bending moment capacity of the beam cross section at the face of the column, according to ACI 318-19 [3] (kip-in.)

M_{peak} = the peak recorded bending moment in the beam at the face of the column in the reversed cyclic loading testing history (kip-in.)

N_{legs} = number of legs within a layer of column ties or hoops

R_n = coefficient representing whether a transverse beam is present in the calculation of the nominal joint shear V_n, according to ACI 318-19 [3] §15.4.2

s = spacing of column hoops or ties (in.)

t_d = term representing the effect of bar size on the contribution of confining reinforcement to total bond force for tension development length (ACI 408R-03 [1])

t_r = term representing the effect of relative rib area of the bar being developed on the contribution of confining reinforcement to total bond force for tension development length (ACI 408R-03 [1])

V_n	=	nominal joint shear strength according to ACI 318-19 [3] §18.8.4 (kip)
V_p	=	horizontal joint shear demand at mid depth of the beam (kip)
T_h	=	anchorage strength of a hooked bar, calculated using the descriptive equation by Ajaam et al. [43]
$\delta_{0.8peak}$	=	the drift ratio associated with a 20% strength loss
ε_s	=	strain of steel reinforcement
λ	=	lightweight concrete modification factor for the development length of deformed bars and wires in compression (ACI 318-19 [3] §25.4.9) and the development length of hooked bars in tension (ACI 318-19 [3] §25.4.3)
ρ_t	=	ratio of area of distributed transverse reinforcement to gross concrete area perpendicular to that reinforcement, $A_{tr}/(b_c s)$
ψ_c	=	concrete strength modification factor for the development length of hooked bars in tension (ACI 318-19 [3] §25.4.4)
ψ_e	=	epoxy coating modification factor for the development length of hooked bars in tension (ACI 318-19 [3] §25.4.4 and ACI 318-14 [20] §25.4.4)
$\psi_{o,hook}$	=	location modification factor for the development length of hooked bars in tension (ACI 318-19 [3] §25.4.3)
ψ_p	=	parallel tie reinforcement modification factor for the development length of hooked bars in tension (ACI 318-19 [3] §25.4.4)
ψ_r	=	confining reinforcement modification factor for the development length of deformed bars and wires in compression (ACI 318-19 §25.4.9)

Chapter 5: Summary and Conclusions

Databases of test results were used to examine ACI 318-19 requirements for three cases related to compression development: compression lap splice length, compression development of headed bars in special moment frame (SMF) joints, and compression development of hooked bars in SMF joints. For each case, the distribution of variables within the database was described and ACI 318-19 requirements were compared against test results using ratios of test/calculated (T/C) bar stress. Comparisons were also made against several alternative equations.

These analyses were motivated by two counterintuitive observations. First, ACI 318-19 equations for compression lap splice length in §25.5.5 can produce calculated lengths that are substantially longer than the length of a Class B tension lap splice (§25.5.2). This is counter to expectations since compression lap splices benefit from end bearing and tension lap splices do not. Second, ACI 318-19 §18.8.2.2 requires that headed and hooked bars in SMF joints be developed in tension in accordance with §18.8.5 and in compression in accordance with §25.4.9. Counter to expectations, the compression requirements in §25.4.9 often produce longer development lengths than required in §18.8.5 for common combinations of variables even though tension development is generally thought to be more critical in joints.

On the basis of the analyses, the following were concluded:

Chapter 2: Compression Lap Splice Length

1. ACI 318-19 [3] equations for compression lap splice length in §25.5.5 can produce calculated lengths that are substantially longer than the length of a Class B tension lap

splice (§25.5.2). This is counter to expectations since compression lap splices benefit from end bearing and tension lap splices do not.

2. ACI 318-19 equations for compression lap splice length in §25.5.5 were not a good fit to the database of 89 test results, with a mean T/C of 2.58 and a coefficient of variation (CV) of 0.60 (although it must be emphasized that all specimens with $T/C > 2.0$ violated the ACI 318-19 minimum lap splice length of 12 in. (300 mm)). A reason for these outcomes is that §25.5.5 does not account for relevant variables including confinement and concrete compressive strength.
3. Compression lap splice length requirements in §25.5.5 can be improved and simplified by removing Eq. (a) and (c) from §25.5.5 and applying Eq. (b) to all design bar stress ranges (Eq. (b) is currently limited to bar stresses greater than 60 ksi (420 MPa) but less than 80 ksi (550 MPa)). Equation (b) alone has a mean T/C of 1.58 and a CV of 0.16 when compared with the database, although it still omits key variables and can produce design lengths that are longer than the tension development length. Equations proposed by Cairns [13] and Chun, Lee, and Oh [9,12] were also shown to produce more accurate and precise fits to the available data.
4. Six tension development length equations were considered, and all provided a more accurate and precise fit to the dataset than ACI 318-19 §25.5.5. Use of tension development length equations for compression lap splice design would produce more consistent conservatism relative to the database, eliminate the need to calculate both tension and compression development lengths, and prevent design cases where calculated lengths are longer in compression than in tension. A drawback of this approach is that calculated compression lengths would also be longer than currently required for many common cases.

5. Three methods were considered for making compression lap splice length a function of tension development length without causing excessive conservatism:
    a. Length multiplier, r_1: Compression lap splice length can be defined as r_1 times the tension development length, where $r_1 < 1$. To illustrate the concept, values of r_1 were derived for six tension development length equations to achieve a minimum T/C of 1.0, although other definitions of acceptable reliability might be appropriate.
    b. Stress multiplier, r_2: Compression lap splice length can be calculated using tension development length equations, but for a stress of $r_2 f_y$, where $r_2 < 1$. The stress reduction is because some portion of bar force is transferred through end bearing and not bond. To illustrate the concept, values of r_2 were derived for six tension development length equations to achieve a minimum T/C of 1.0, although other definitions of acceptable reliability might be appropriate.
    c. Optimized ψ_y: The tension development length equation from Lepage, Yasso, and Darwin [16] contains a ψ_y modification factor that was redefined to better fit the compression lap splice database and achieve a minimum T/C of 1.0, although other definitions of acceptable reliability might be appropriate.

Chapter 3: Compression Development of Headed Bars in SMF Joints

1. Satisfying the compression development length requirements of §25.4.9 is not a necessary condition to obtain adequate joint behavior under cyclic loads. None of the 35 beam-column connection specimens considered satisfied §25.4.9, even though all had drift ratio capacities not less than 3%. Furthermore, §25.4.9 produced lengths that were, on average, 2.2 times the lengths obtained from the Ghimire, Darwin, and Lepage [16] descriptive

equation for headed bar anchorage strength. ACI 318-19 §18.8.2.2 should not require that headed bars satisfy §25.4.9.

2. Satisfying the tension development length requirements of §18.8.5.2, which refer to §25.4.4, is not a necessary condition to obtain adequate joint behavior under cyclic loads. Stated differently, §25.4.4 and thus §18.8.5.2 appear to be substantially conservative for joint design. Only two of the 35 beam-column connection specimens considered satisfied §18.8.5.2, even though all had drift ratio capacities not less than 3%. Section 18.8.5.2 also produced lengths that were, on average, 2.4 times the lengths obtained from the Ghimire, Darwin, and Lepage [6] descriptive equation for headed bar anchorage strength.
3. The equation for hooked bar development length in §18.8.5.1 of ACI 318-19 appears more appropriate for design of specimens like those in the database. It was a more reasonable fit to the database and still conservate relative to the Ghimire, Darwin, and Lepage [6] descriptive equation for headed bar anchorage strength.

Chapter 4: Compression Development of Hooked Bars in SMF Joints

1. Satisfying the compression development length requirements of §25.4.9 is not a necessary condition to obtain adequate joint behavior under cyclic loads. Of the 24 beam-column connection specimens with drift ratio capacities above 3%, none satisfied §25.4.9. Furthermore, §25.4.9 produced lengths that were, on average, more than twice the lengths obtained from the Ajaam, Darwin, and O'Reilly [43] descriptive equation for hooked bar anchorage strength. ACI 318-19 §18.8.2.2 should not require that hooked bars satisfy §25.4.9.

2. Satisfying the tension development length requirements of §25.4.3 is also not a necessary condition to obtain adequate joint behavior under cyclic loads. Of the 24 beam-column connection specimens with drift ratio capacities above 3%, only two (8%) satisfied §25.4.3. Section 25.4.3 also produced lengths that were, on average, 70% longer than the lengths obtained from the Ajaam, Darwin, and O'Reilly [43] descriptive equation for hooked bar anchorage strength. ACI 318-19 §25.4.3 should not be applied to connections like those in the database.
3. Compression development length requirements recommended in chapter 2 for straight bars do not produce reasonable results when applied to connections similar to those in the database. This suggests that development length equations based on lap spliced bars in compression should not be applied to hooked bars in joints.
4. Results suggest that the tension development length requirements in ACI 318-19 §18.8.5.1 are appropriate for design of hooked bar development in beam-column joints of special moment frames. Section 18.8.5.1 produced lengths that were 23% longer than those obtained from the Ajaam, Darwin, and O'Reilly [43] descriptive equation for hooked bar anchorage strength, suggesting there is some built-in conservatism for connections similar to those in the database. Furthermore, 20 (83%) of the 24 specimens with drift ratio capacities above 3% satisfied §18.8.5.1, suggesting the provisions are useful for identifying specimens with adequately developed reinforcement.

Chapter 6: References

1. ACI Committee 408 (2003). *Bond and Development of Straight Reinforcing Bars in Tension (ACI 408R-03)*, American Concrete Institute, 49 pp.
2. fib (2014). *Bond and anchorage of embedded reinforcement: Background to the fib Model Code for Concrete Structures 2010*, fib Bulletin No. 72, 170 pp.
3. ACI Committee 318 (2019). *Building Code Requirements for Structural Concrete (ACI 318-19) and Commentary (ACI 318R-19)*, American Concrete Institute, Farmington Hills, MI, 628 pp.
4. ACI Committee 408 (2021). *Compression Lap Splice Database*, American Concrete Institute, Farmington Hills, MI. [Available from ACI Store at concrete.org]
5. Kang, T. H.-K., Shin, M., Mitra, N., and Bonacci, J. F., (2009). "Seismic Design of Reinforced Concrete Beam-Column Joints with Headed Bars." *ACI Structural Journal*, 106(6), 868-877.
6. Ghimire, K. P., Darwin, D., and Lepage, A., (2021). "Headed Bars in Beam-Column Joints Subjected to Reversed Cyclic Loading." *ACI Structural Journal*, 118(3), 27-33.
7. Pfister, J. F., and Mattock, A. H., (1963). “High Strength Bars as Concrete Reinforcement, Part 5. Lapped Splices in Concentrically Loaded Columns,” *Journal of the Portland Cement Association Research and Development Laboratories*, Development Department, 5(2), 27-40.
8. Chun, S. C., Lee, S. H., and Oh, B., (2010). “Compression Lap Splice in Unconfined Concrete of 40 and 60 MPa (5800 and 8700 psi) Compressive Strengths,” *ACI Structural Journal*, 107(2), 170-178.

9. Chun, S. C., Lee, S. H., and Oh, B., (2010). "Compression Lap Splice in Confined Concrete of 40 and 60 MPa (5800 and 8700 psi) Compressive Strengths," *ACI Structural Journal*, 107(4), 476-485.
10. Chun, S. C., Lee, S. H., and Oh, B., (2011). "Compression Splices in High-Strength Concrete of 100 MPa (14,500 psi) and Less," *ACI Structural Journal*, 108(6), 715-724.
11. Reineck, K. H., Kuchma, D. A., Kim, K. S., and Marx, S., (2003). "Shear Database for Reinforced Concrete Members without Shear Reinforcement," *ACI Structural Journal*, 100(2), 240-249.
12. Chun, S. C., Lee, S. H., and Oh, B., (2010). "Simplified Design Equation of Lap Splice Length in Compression," *International Journal of Concrete Structures and Materials*, 4(1), 63-68.
13. Cairns, J. W., (1985). "Strength of Compression Splices: A Reevaluation of Test Data," *ACI Journal Proceedings*, 82(4), 510-516.
14. Cairns, J. W. and Arthur, P. D., (1979). "Strength of Lapped Splices in Reinforced Concrete Columns.", *ACI Journal Proceedings*, 76(2), 277-296
15. fib MC2010, (2013). *fib Model Code for Concrete Structures 2010*, Ernst & Sohn, 434 pp.
16. Lepage, A., Yasso, S., and Darwin, D., (2020). *Recommended Provisions and Commentary on Development Length for High-Strength Reinforcement in Tension*, Structural Engineering and Engineering Materials, SL Report 20-2.
17. Darwin, D., Lutz, L. A., and Zuo, J., (2005). "Recommended Provisions and Commentary on Development and Lap Splice Lengths for Deformed Reinforcing Bars in Tension," *ACI Structural Journal*, 102(6), 892-900.

18. Canbay, E., and Frosch, R. J., (2006). “Design of Lap-Spliced Bars: Is Simplification Possible?”, *ACI Structural Journal*, 103(3), 444-451.

19. Frosch, R., Fleet, E., and Glucksman, R., (2020). *Development and Splice Lengths for High-Strength Reinforcement Volume I: General Bar Development*, Lyles School of Civil Engineering, Purdue University, 358 pp.

20. ACI Committee 318 (2014). *Building Code Requirements for Structural Concrete (ACI 318-14) and Commentary (ACI 318R-14)*, American Concrete Institute, Farmington Hills, MI, 520 pp.

21. Adachi, M., and Kiyoshi, M., (2007). "The Effect of Orthogonal Beams on Ultimate Strength or R/C Exterior Beam-Column Joint using Mechanical Anchorages." *Proceeding of the Architectural Institute of Japan*, Tokyo, Japan, 633-634.

22. Bashandy, T. R., (1996). *Application of Headed Bars in Concrete Members*, PhD dissertation, University of Texas at Austin, Austin, TX, 303 pp.

23. Chun, S. C., Lee, S. H., Kang, T. H.-K., Oh, B., and Wallace, J. W., (2007). "Mechanical Anchorage in Exterior Beam-Column Joints Subjected to Cyclic Loading", *ACI Structural Journal*, 104(1), 102-113.

24. Ishida, Y., Fujiwara, A., Adachi, T., Matsui, T., and Kuramoto, H., (2007). "Structural Performance of Exterior Beam-Column Joint with Wide Width Beam Using Headed Bars - Part 1: Outline of test and failure Modes and Part 2: Test Result and Discussion." *Proceedings of the Architectural Institute of Japan*. Tokyo, Japan, 657-660.

25. Kang, T. H.-K., Ha, S.-S., and Choi, D.-U., (2008). "Seismic Assessment of Beam-to-Column Interaction Utilizing Headed Bars." *Proceedings of the 14th World Conference on Earthquake Engineering*. Beijing, China, 8 pp.

26. Kato, T., (2005). "Mechanical Anchorage Using Anchor Plate for Beam/Column Joints of R/C Frames - Part 2: Pull-Out Behavior and Structural Behavior of T-Shaped Frame Using Frictional Anchor Plate." *Proceedings of the Architectural Institute of Japan*. Tokyo, Japan, 277-278.

27. Lee, H.-J., and Yu, S.-Y., (2009). "Cyclic Response of Exterior Beam-Column Joints with Different Anchorage Methods." *ACI Structural Journal*, 106(3), 329-339.

28. Matsushima, M., Kuramoto, H., Meada, M., Kenta, S., and Ozone, S., (2000). "Test on Corner Beam-Column Joint under Tri-Axial Loadings - Outline for Test: Study on Structural Performance of Mechanical Anchorage (No. 10); Discussion of Test Results: Study on Structural Performance of Mechanical Anchorage (No. 11)." *Proceedings of the Architectural Institute of Japan*. Tokyo, Japan, 861-864.

29. Murakami, M., Fuji, T., and Kubota, T., (1998). "Failure Behavior of External Beam-Column Joints with Mechanical Anchorage in Subassemblage Frames." *Concrete Research and Technology*, 9(1).

30. Takeuchi, H., Hattori, S., Nakamura, K., Hosoya, H., and Ichikawa, M., (2001). "Development of Mechanical Anchorage using Circular Anchor Plate - Part 3: Outline of Exterior Beam-Joint Test and Experimental Results and Part 4: Experimental Results and Discussion of Exterior Beam-Column Joint Test." *Proceedings of the Architectural Institute of Japan*. Tokyo, Japan, 111-114.

31. Tazaki, W., Kusuhara, F., and Shiohara, H., (2007). "Tests of R/C Beam-Column Joints with Irregular Details on Anchorage of Beam Longitudinal Bars (Part 1: Outline of Tests and Part 2: Test Results and Discussions)." *Proceedings of the Architectural Institute of Japan*. Tokyo, Japan, 653-660.

32. Wallace, J. W., McConnell, S. W., Gupta, P., and Cote, P. A., (1998). "Use of Headed Reinforcement in Beam-Column Joints Subjected to Earthquake Loads." *ACI Structural Journal*, 95(5), 590-606.

33. Yoshida, J., Ishibashi, K., and Nakamura, K., (2000). "Experimental Study on Mechanical Anchorage Using Bolt and Nut in Exterior Beam-Column Joint - Part 1: Specimens and Outline of Experiment and Part 2: Analysis of Experiment." *Proceedings of the Architectural Institute of Japan*. Tokyo, Japan, 635-638.

34. ACI Committee 352 (2010). *Recommendations for Design of Beam-Column Connections in Monolithic Reinforced Concrete Structures (ACI 352R-02)*, American Concrete Institute, Farmington Hills, MI, 42 pp.

35. Hanson, N. W., (1971). "Seismic Resistance of Concrete Frames with Grade 60 Reinforcement." *ASCE Journal of the Structural Division*, 97(6), 1685-1700.

36. Uzumeri, S. M., (1977). "Strength and Ductility of Cast-in-Place Beam-Column Joints". *Reinforced Concrete Structures in Seismic Zones*, ACI Symposium Publication, Vol. 52, pp. 293-350.

37. Uzumeri, S. M., and Seckin, M., (1974). *Behavior of Reinforced Concrete Beam-Column Joints Subjected to Slow Load Reversals*, Publication No. 74-05, University of Toronto, 89 pp.

38. Scribner, C. F., and Wight, J. K., (1978). *Delaying Shear Strength Decay in Reinforced Concrete Flexural Members under Large Load Reversals*. Report UMEE 78R2. The University of Michigan. 246 pp.

39. Alameddine, F. F., (1990). Seismic Design Recommendations for High-Strength Concrete Beam-to-Column Connections, Ph.D. Dissertation, University of Arizona, 261 pp.

40. Ehsani, M. R., and Alameddine, F., (1991). “Design Recommendations of Type 2 High-Strength Reinforced Concrete Connections.” *ACI Structural Journal*. 88(3), 277-291.

41. Kurose, Y., Guimaraes, G. N., Zuhua, L. M., Kreger, M. E., Jirsa, J. O., (1991). “Evaluation of Slab-Beam-Column Connections Subjected to Bidirectional Loading”. ACI Symposium Publication, Vol. 123, 39-67.

42. Hwang, S.-J, Lee, H.-J., Liao, T.-F., Wang, K.-C, and Tsai, H.-H., (2005). “Role of Hoops on Shear Strength of Reinforced Concrete Beam-Column Joints” *ACI Structural Journal*, 102(3), 445-453.

43. Ajaam, A., Darwin, D., and O´Reilly, M., (2017). *Anchorage Strength of Reinforcing Bars with Standard Hooks*,. Structural Engineering and Engineering Materials. SM Report No. 125, 372 pp.

Appendix A: History of ACI Compression Development and Lap Splice Provisions

This appendix provides a brief history of ACI Building Code provisions for compression development length, compression lap splice length, and compression development of hooked and headed bars in special moment frame joints.

Section A.1 shows that ACI 318-19 compression development length requirements are directly derived from ACI 318-51 provisions. The ACI 318-51 code limited bond stress using an expression developed based on committee judgement since no test data were available at the time.

Section A.2 shows that ACI 318-19 provisions for compression lap splice length are effectively equivalent to ACI 318-71 provisions. The ACI 318-71 provisions were devised to provide similar minimum lengths as the ACI 318-51 provisions for Grade 50 bars in tied columns. The ACI 318-71 compression lap splice provisions for f_y > 60 ksi (420 MPa) were also informed by test data that demonstrated the important role of end bearing in lap splice behavior.

Section A.3 describes two building code provisions relevant to compression development of hooked bars, and shows they have essentially not changed since their initial adoption in ACI 318-41 for non-earthquake-resistant design and ACI 318-83 for earthquake-resistant design.

A.1 Compression Development Length

This section summarizes the history of ACI building code requirements for development of bars in compression. This history suggests that ACI 318-19 provisions for compression development length are not based on test data. It is also evident that writers of the ACI Building Code have long recognized that more bar force can be developed in compression than in tension

for the same development length. This recognition was implied beginning with ACI 318-51, which specified higher bond stress limits for bars in compression than in tension, and was first explicitly stated in the ACI 318-63 commentary.

A.1.1 ACI 318-47

ACI 318-47 did not specifically address compression development. Instead, Section 305, *Allowable Stresses*, limited bond stresses in tension or compression to:

$$u_{max} \leq \begin{cases} 0.05 f_c' \\ 200 \text{ psi} \end{cases} \qquad \begin{matrix} \text{Eq. A.1} \\ \text{(lb, in.)} \end{matrix}$$

Setting the product of u_{max}, ℓ_{dc}, and bar perimeter equal to the product of bar area and $0.4 f_y$, the allowable stress, suggests minimum compression development lengths, ℓ_{dc}, of:

$$\ell_{dc} \geq \begin{cases} \dfrac{2 f_y}{f_c'} d_b \\ 0.0005 f_y d_b \end{cases} \qquad \begin{matrix} \text{Eq. A.2} \\ \text{(lb, in.)} \end{matrix}$$

A.1.2 ACI 318-51 and ACI 318-56

ACI 318-51 and ACI 318-56 were the first to explicitly address compression development. In these codes, the allowable compression bond stresses in Section 305, *Allowable Stresses*, (Eq. A.3) were 75 to 100% larger than the allowable bond stresses in ACI 318-47 (Eq. A.1). No commentary was provided to explain the change from Eq. A.1.

$$u_{max} \leq \begin{cases} 0.1 f_c' \\ 350 \text{ psi} \end{cases} \qquad \begin{matrix} \text{Eq. A.3} \\ \text{(lb, in.)} \end{matrix}$$

Setting the product of u_{max}, ℓ_{dc}, and bar perimeter equal to the product of bar area and $0.4 f_y$ suggests the minimum ℓ_{dc} given in Eq. A.4. The second expression in Eq. A.4 is similar to that in ACI 318-19.

$$\ell_{dc} \geq \begin{cases} \dfrac{f_y}{f_c'} d_b \\ 0.00029 f_y d_b \end{cases}$$ Eq. A.4 (lb, in.)

A.1.3 ACI 318-63

ACI 318-63 contained provisions for both working stress and ultimate strength design.

Section 1301, *Working Stress Design*, limited the bond stress for compression development of deformed bars to Eq. A.5. The first expression in Eq. A.5 is similar in magnitude to the first expression in Eq. A.3 from ACI 318-51 and ACI 318-56 for f_c' = 4000 psi (411 psi for Eq. A.5 versus 400 psi for Eq. A.3). ACI 318-63 commentary justifies using $\sqrt{f_c'}$ instead of f_c' by reference to tests of tension bar development (Refs [A19] and [A20]).

$$u_{max} \leq \begin{cases} 6.5\sqrt{f_c'} \\ 400 \text{ psi} \end{cases}$$ Eq. A.5 (lb, in.)

Setting the product of u_{max}, ℓ_{dc}, and bar perimeter equal to the product of bar area and $0.4 f_y$ suggests:

$$\ell_{dc} \geq \begin{cases} \dfrac{f_y}{65\sqrt{f_c'}} d_b \\ 0.00025 f_y d_b \end{cases}$$ Eq. A.6 (lb, in.)

Section 1801, *Ultimate Strength Design*, limited the bond stress for compression development of deformed bars to Eq. A.7. The commentary for Chapter 13 of ACI 318-63 states that Eq. A.5 was obtained from Eq. A.7 using a factor of approximately two.

$$u_{max} \leq \begin{cases} 13\sqrt{f_c'} \\ 800 \text{ psi} \end{cases}$$ Eq. A.7 (lb, in.)

Setting the product of u_{max}, ℓ_{dc}, and bar perimeter equal to the product of bar area and f_y suggests the minimum ℓ_{dc} given in Eq. A.8. A stress of f_y is used instead of an allowable stress

of $0.4f_y$ because Eq. A.7 was applicable for ultimate strength design. Equation A.8 is essentially the same as the compression development length equations in ACI 318-19.

$$\ell_{dc} \geq \begin{cases} \dfrac{f_y}{52\sqrt{f_c'}} d_b \\ 0.00031 f_y d_b \end{cases} \qquad \begin{matrix} \text{Eq. A.8} \\ \text{(lb, in.)} \end{matrix}$$

The commentary to Section 1801 stated that "No recent tests of bond strength on compression bars are available, but these bars obviously are not weakened in bond by flexural cracking of concrete. Essentially the splice lengths for column steel in the 1956 Code have been retained for compression bars and the permissible bond stress for compression bars has been set to match." Provisions for compression bond stresses were therefore based on committee judgement and the opinion that (1) bond stress limits should be approximately consistent with lap splice length requirements, and (2) more bar force can be developed in compression than in tension for the same development length.

A.1.4 ACI 318-71

ACI 318-71 was the first ACI code to express bond requirements in terms of development length. Section 12.6, *Development Length of Deformed Bars in Compression*, required:

$$\ell_{dc} \geq \begin{cases} \dfrac{f_y}{50\sqrt{f_c'}} d_b \\ 0.0003 f_y d_b \\ 8 \text{ in.} \end{cases} \qquad \begin{matrix} \text{Eq. A.9} \\ \text{(lb, in.)} \end{matrix}$$

The expressions in Eq. A.9 are essentially equivalent to those in Eq. A.8, making clear that the minimum development length, ℓ_{dc}, was derived from allowable bond stresses from earlier codes. The length calculated with Eq. A.9 was permitted to be reduced by 25% if the development length was enclosed by a spiral not less than 0.25 in. (6 mm) in diameter and not more than 4 in.

(100 mm) in pitch. The commentary to Section 12.6 stated that "The weakening effect of flexural tension cracks is not present for compression bars and usually end bearing of the bars on the concrete is beneficial. Therefore, shorter development lengths have been specified for compression than for tension."

A.1.5 ACI 318-77 through ACI 318-19

The following changes to Eq. A.9 were adopted in ACI 318-77 through ACI 318-19.

1. ACI 318-89 was the first to permit reducing ℓ_{dc} by 25% if the development length was enclosed within No. 4 (12 mm) ties spaced not more than 4 in. (100 mm) on center.
2. ACI 318-08 was the first to include effects of lightweight concrete with the addition of λ in the denominator of the first expression (Eq. A.10). No data were cited supporting this change.

$$\ell_{dc} \geq \begin{cases} \dfrac{f_y}{50\lambda\sqrt{f_c'}} d_b \\ 0.0003 f_y d_b \\ 8 \text{ in.} \end{cases} \qquad \text{Eq. A.10 (lb, in.)}$$

3. ACI 318-14 presented the requirements somewhat differently, by introducing Ψ_r to represent the 25% reduction of ℓ_{dc} permitted with confinement (Eq. A.11 and Table 5).

$$\ell_{dc} \geq \begin{cases} \dfrac{f_y \Psi_r}{50\lambda\sqrt{f_c'}} d_b \\ 0.0003 f_y \Psi_r d_b \\ 8 \text{ in.} \end{cases} \qquad \text{Eq. A.11 (lb, in.)}$$

Table 5 – Modification factors for deformed bars and wires in compression from ACI 318-19 Table 25.4.9.3

Modification factor	Condition	Value of factor
Lightweight λ	Lightweight concrete	0.75
	Lightweight concrete, if f_{ct} is specified	In accordance with ACI 318-19 Section 19.2.4.3
	Normalweight concrete	1.0
Confining reinforcement Ψ_r	Reinforcement enclosed within (1), (2), (3), or (4): (1) a spiral (2) a circular continuously wound tie with $d_b \geq$ ¼ in. (6 mm) and pitch 4 in. (100 mm) (3) No. 4 (12 mm) bar or D20 wire ties in accordance with ACI 318-19 Section 25.7.2 spaced ≤ 4 in. (100 mm) on center (4) hoops in accordance with ACI 318-19 Section 25.7.4 spaced ≤ 4 in. (100 mm) on center	0.75
	Other	1.0

A.1.6 Summary

The ACI 318-19 equation for compression development length is essentially the same as the minimum length obtained using the ACI 318-63 bond stress limits for ultimate strength design. The commentary of ACI 318-63, in turn, makes clear that the development length requirements were selected so that computed compression lap splice lengths would "match" the lengths obtained with earlier code requirements and were not based on test results.

A.2 Compression Lap Splice Length

This section provides a brief history of ACI building code requirements for compression lap splice lengths.

A.2.1 ACI 318-51 and ACI 318-56

ACI 318-51 and ACI 318-56 were the first to explicitly address compression lap splicing, but only in columns and walls. Section 1103(c), *Splices in Vertical Reinforcement,* required the lap splice length of deformed bars in columns and walls to be at least $20d_b$, with an additional d_b of length for each 1 ksi (6.9 MPa) of allowable stress over 20 ksi (140 MPa). The lap length was required to increase by one-third where concrete compressive strengths were less than 3000 psi (21 MPa). There was no commentary for Section 1103 supporting these provisions.

A.2.2 ACI 318-63

Section 805(c), *Splices in Reinforcement in which the Critical Design Stress is Compressive*, required the compression lap splice length of Grade 60 deformed bars to be:

$$\ell_{sc} \geq 24d_b \qquad \text{Eq. A.12}$$

The commentary to Section 805 stated that "The minimum lengths specified for column splices in the 1956 Code have been carried forward and extended to compression bars in beams and to higher strength steels."

Section 805(b), *Splices in Reinforcement in which the Critical Design Stress is Tensile*, required the designer to satisfy the minimum tension lap splice length and check allowable bond stresses. A designer would therefore have had to satisfy both the minimum compression lap length in code section 805(c) and the bond stress limit in code section 305 (see Section A.1).

A.2.3 ACI 318-71

ACI 318-71 Section 7.7, *Splices in Compression*, required compression lap splice lengths to be greater than either the compression development length (Eq. A.9) or the compression lap

splice length (Eq. A.13). The length calculated with Eq. A.13 was permitted to be reduced by 25% if enclosed by a spiral or by 17% if enclosed by ties having an effective area of at least $0.0015hs$.

$$\ell_{sc} \geq \begin{cases} 0.0005 f_y d_b & \text{if} \quad f_y \leq 60 \text{ ksi} \\ (0.0009 f_y - 24) d_b & \text{if} \quad f_y > 60 \text{ ksi} \\ 12 \text{ in.} \end{cases} \qquad \begin{matrix} \text{Eq. A.13} \\ \text{(lb, in.)1} \end{matrix}$$

The commentary to Section 7.7 states that:

> "Bond behavior of compression bars is not complicated by the problem of transverse tension cracking and thus compression splices do not require provisions as strict as those specified for tension splices. The minimum lengths specified for column splices in the 1956 Code have been carried forward and extended to compression bars in beams and to higher strength steels as in the 1963 Code.
>
> "Essentially, lap requirements are repeated from the 1963 Code… The 1963 Code values have been modified to recognize various degrees of confinement and to permit design with steels having up to 80 ksi yield strength. Tests have shown that splice strengths in compression depend considerably on end bearing and hence do not increase proportionally in strength when the splice length is doubled. Accordingly, for yield strengths above 60 ksi, lap lengths have been significantly increased, except where there are spiral enclosures (as in spiral columns) where the increase is only about 10 percent at 75 ksi.
>
> "For steel yield strengths up to 60 ksi, lap lengths for bars enclosed by spirals have been reduced, but those within adequate ties have been slightly modified from the 1963 Code requirements. For splices without surrounding ties or spirals, laps have been increased for steels with yield strengths above 40 ksi. See Table 7-3." (where 1 ksi = 6.895 MPa)

TABLE 7-3—COMPARISON OF COMPRESSION LAP SPLICE REQUIREMENTS—1963 VERSUS 1971 CODE IN BAR DIAMETERS

	Minimum lap splice lengths $f_c' \geqq 3000$				Calculated lap required by bond for full f_y with $f_c' = 2300$	
	1963 Code	1971 Code				
f_y	All bars	Spiral column	Tied Column	Loose	1963 Code	1971 Code*
40	20	15.0	16.6	20	16	16.7
50	20	18.75	20.75	25	20	20.85
60	24	22.5	24.9	30	24	25.0
75	30	32.6	36.2	43.5	30	31.2
80	—	36.0	39.9	48.0	—	33.3

*For $f_c' = 2300$ psi for splices of loose bars or bars in tied columns.

1000 psi = 1 ksi = 6.895 MPa

A.2.4 ACI 318-89

ACI 318-89 requirements for compression lap splices were essentially the same as in ACI 318-71, except that the designer was no longer explicitly required to check both development length and lap splice length requirements when designing a compression lap splice. Section 12.16, *Splices of Deformed Bars in Compression*, required only that lap splices satisfy Eq. A.13. This change had little effect because Eq. A.13 produces longer minimum lengths than Eq. A.9.

A.2.5 ACI 318-95 through ACI 318-19

No changes were adopted to the compression lap splice requirements, which remain essentially unchanged from ACI 318-71.

A.2.6 Summary

The ACI 318-19 equations for compression lap splice length were first adopted in ACI 318-71. The commentary makes clear that these equations were designed to (1) result in similar

splice lengths for lapped Grade 60 bars in tied columns as in ACI 318-56, and (2) be applicable to Grade 80 bars. Test data were not used to establish the minimum lengths in ACI 318-56 that were the basis for the existing requirements. Test results did, however, prompt the use of an expression in Eq. A.13 that is not proportional to f_y for bar stresses greater than 60 ksi (420 MPa). This lack of proportionality was justified due to end bearing.

This section also shows that expressions for compression lap splice length are derived from ACI 318-51 detailing requirements for columns and walls. Until ACI 318-89 it was necessary to satisfy both the minimum lap splice length requirements and, depending on code edition, either the compression bond stress limits or compression development length requirements. Since ACI 318-89 it has been sufficient for compression lap splices to satisfy only the compression lap splice length requirements, since calculated compression development lengths tend to be shorter. The origins of the compression development and lap splice length provisions suggest that differences between the requirements owe more to history than mechanics.

A.3 Compression Development of Hooked Bars

This section provides a history of ACI building code provisions relevant to the development of hooked bars in compression.

A.3.1 Prohibition on Use of Hooks for Developing Bars in Compression

ACI 318-41 Section 906, *Hooks*, stated that: “Hooks shall not be considered effective in adding to the compressive resistance of bars”. This requirement has remained, essentially unchanged, in all subsequent code editions. ACI 318-19 Section 24.4.1.2 states that: “Hooks and heads shall not be used to develop bars in compression.” The accompanying commentary in

R24.4.1.2 states that: “Hooks and heads are ineffective in compression. No data are available to demonstrate that hooks and heads can reduce development length in compression.”

A.3.2 Bar Development in Special Moment Frame Joints

ACI 318-83 was the first to include special provisions for seismic design. ACI 318-83 Section A.6.1.3 states that: “Beam longitudinal reinforcement terminated in a column shall be extended to the far face of the confined column core and anchored in tension according to Section A.6.4 and in compression according to Chapter 12.” Every subsequent edition of ACI 318 has included this code language, with modifications only to update section numbers. In ACI 318-83, Chapter 12 contained the compression development and lap splice length equations given as Eq. A.9 and Eq. A.13.

ACI 318-83 through ACI 318-11 contained no commentary to aid interpretation of the requirement to anchor bars “in compression according to Chapter 12.” It was therefore up to the designer to decide whether that requirement applied only to straight bars terminating in a joint, or all bars terminating in a joint including hooked and headed bars. This ambiguity was addressed with the following commentary that was added in ACI 318-14 and remains in ACI 318-19: “For bars in compression, the development length corresponds to the straight portion of a hooked or headed bar measured from the critical section to the onset of the bend for hooked bars and from the critical section to the head for headed bars.”

Appendix A References

A1. ACI Committee 318 (1947). *Building Code Requirements for Reinforced Concrete (ACI 318-47)*, American Concrete Institute, Detroit, MI, 68 pp.

A2. ACI Committee 318 (1951). *Building Code Requirements for Reinforced Concrete (ACI 318-51)*, American Concrete Institute, Detroit, MI, 68 pp.

A3. ACI Committee 318 (1957). *Building Code Requirements for Reinforced Concrete (ACI 318-57)*, American Concrete Institute, Detroit, MI, 74 pp.

A4. ACI Committee 318 (1963). *Building Code Requirements for Reinforced Concrete (ACI 318-63)*, American Concrete Institute, Detroit, MI, 148 pp.

A5. ACI Committee 318 (1963). *Commentary on Building Code Requirements for Reinforced Concrete (ACI 318-63)*, Special Publication (SP-10), American Concrete Institute, Detroit, MI, 100 pp.

A6. ACI Committee 318 (1971). *Building Code Requirements for Reinforced Concrete (ACI 318-71)*, American Concrete Institute, Detroit, MI, 78 pp.

A7. ACI Committee 318 (1971). *Commentary on Building Code Requirements for Reinforced Concrete (ACI 318-71)*, American Concrete Institute, Detroit, MI, 96 pp.

A8. ACI Committee 318 (1977). *Building Code Requirements for Reinforced Concrete (ACI 318-77)*, American Concrete Institute, Detroit, MI, 104 pp.

A9. ACI Committee 318 (1983). *Building Code Requirements for Reinforced Concrete (ACI 318-83)*, American Concrete Institute, Detroit, MI, 112 pp.

A10. ACI Committee 318 (1989). *Building Code Requirements for Reinforced Concrete (ACI 318-89) and Commentary (ACI 318R-89)*, American Concrete Institute, Detroit, MI, 356 pp.

A11. ACI Committee 318 (1995). *Building Code Requirements for Structural Concrete (ACI 318-95) and Commentary (ACI 318R-95)*, American Concrete Institute, Detroit, MI, 370 pp.

A12. ACI Committee 318 (1999). *Building Code Requirements for Structural Concrete (ACI 318-95) and Commentary (ACI 318R-99)*, American Concrete Institute, Farmington Hills, MI, 392 pp.

A13. ACI Committee 318 (2002). *Building Code Requirements for Structural Concrete (ACI 318-02) and Commentary (ACI 318R-02)*, American Concrete Institute, Farmington Hills, MI, 445 pp.

A14. ACI Committee 318 (2005). *Building Code Requirements for Structural Concrete (ACI 318-05) and Commentary (ACI 318R-05)*, American Concrete Institute, Farmington Hills, MI, 432 pp.

A15. ACI Committee 318 (2008). *Building Code Requirements for Structural Concrete (ACI 318-08) and Commentary (ACI 318R-08)*, American Concrete Institute, Farmington Hills, MI, 468 pp.

A16. ACI Committee 318 (2011). *Building Code Requirements for Structural Concrete (ACI 318-11) and Commentary (ACI 318R-11)*, American Concrete Institute, Farmington Hills, MI, 509 pp.

A17. ACI Committee 318 (2014). *Building Code Requirements for Structural Concrete (ACI 318-14) and Commentary (ACI 318R-14)*, American Concrete Institute, Farmington Hills, MI, 524 pp.

A18. ACI Committee 318 (2019). *Building Code Requirements for Structural Concrete (ACI 318-19) and Commentary (ACI 318R-19)*, American Concrete Institute, Farmington Hills, MI, 628 pp.

A19. Mathey, R. G., and Watstein, D., (1961). “Investigation of Bond in Beam and Pullout Specimens with High-Yield-Strength Deformed Bars,” *ACI Journal Proceedings*, 57(9), 1071-1090.

A20. Ferguson, P. M., and Thompson, J. N., (1962). “Development Length of High Strength Reinforcing Bars in Bond,” *ACI Journal Proceedings*, 59(7), 887-922.

Appendix B: Summary of Lap Splice Database

[1]	[2]	[3]	[4]	[5]	[6]	[7]	[8]
Authors	I.D	Concrete test specimen	f_{cm} (psi)	$f_{1c,mod}$ (ksi)	f_y (ksi)	f_{su} (ksi)	f_{yt} (ksi)
Pfister and Mattock [7]	4B	6x12 in.	3715	3.72	86.0	-	58.5
	5B	6x12 in.	4140	4.14	86.0	-	58.5
	6B	6x12 in.	3950	3.95	86.0	-	58.5
	5B1	6x12 in.	4190	4.19	80.0	-	58.5
	6B1	6x12 in.	3640	3.64	80.0	-	58.5
	$4A^+$	6x12 in.	3530	3.53	88.0	-	62.0
	$5A^+$	6x12 in.	3530	3.53	88.0	-	62.0
	$6A^+$	6x12 in.	3510	3.51	88.0	-	62.0
	$7A^+$	6x12 in.	3510	3.51	88.0	-	62.0
Chun, Lee, and Oh [8]	C40D22-S.75-L10-HO	3.9x7.9 in.	7085	6.86	74.5	89.6	-
	C40D22-S.75-L10-HO-1	3.9x7.9 in.	7085	6.86	74.5	89.6	-
	C40D22-S.75-L15	3.9x7.9 in.	7085	6.86	74.5	89.6	-
	C40D22-S.75-L15-1	3.9x7.9 in.	7085	6.86	74.5	89.6	-
	C40D22-S1.25-L10-H0-1	3.9x7.9 in.	7085	6.86	74.5	89.6	-
	C40D22-S1.25-L15-HO	3.9x7.9 in.	7085	6.86	74.5	89.6	-
	C40D22-S1.25-L15-HO-1	3.9x7.9 in.	7085	6.86	74.5	89.6	-
	C40D22-S1.25-L20-HO-1	3.9x7.9 in.	7085	6.86	74.5	89.6	-
	C40D22-S1.5-L10-H0	3.9x7.9 in.	7085	6.86	74.5	89.6	-
	C40D22-S1.5-L10-H0-1	3.9x7.9 in.	7085	6.86	74.5	89.6	-
	C40D22-S1.5-L15-H0	3.9x7.9 in.	7085	6.86	74.5	89.6	-
	C40D22-S1.5-L15-H0-1	3.9x7.9 in.	7085	6.86	74.5	89.6	-
	C60D22-S.75-L10-HO	3.9x7.9 in.	10181	9.86	74.5	89.6	-
	C60D22-S.75-L10-HO-1	3.9x7.9 in.	10152	9.83	74.5	89.6	-
	C60D22-S1.25-L10-H0	3.9x7.9 in.	10174	9.85	74.5	89.6	-
	C60D22-S1.25-L10-H0-1	3.9x7.9 in.	10142	9.82	74.5	89.6	-
	C60D22-S1.25-L15-HO-1	3.9x7.9 in.	10142	9.82	74.5	89.6	-
	C60D22-S1.5-L10-H0	3.9x7.9 in.	9938	9.62	74.5	89.6	-
	C60D22-S1.5-L10-H0-1	3.9x7.9 in.	10131	9.81	74.5	89.6	-
	C60D22-S1.5-L15-1	3.9x7.9 in.	10360	10.03	74.5	89.6	-
	C40D29-S.75-L10-HO-1	3.9x7.9 in.	9358	9.06	68.4	87.3	-
	C40D29-S.75-L15-1	3.9x7.9 in.	9337	9.04	68.4	87.3	-
	C40D29-S.75-L20	3.9x7.9 in.	8185	7.93	68.4	87.3	-
	C60D29-S.75-L10-HO	3.9x7.9 in.	10425	10.10	68.4	87.3	-
	C60D29-S.75-L10-HO-1	3.9x7.9 in.	10686	10.35	68.4	87.3	-
	C60D29-S1.25-L10-H0	3.9x7.9 in.	10654	10.32	68.4	87.3	-
Chun, Lee, and Oh [9]	C40D22-S.75-L10-HE	3.9x7.9 in.	7085	6.86	74.5	89.6	60
	C40D22-S.75-L10-HE-1	3.9x7.9 in.	7085	6.86	74.5	89.6	60
	C40D22-S.75-L10-HW	3.9x7.9 in.	7085	6.86	74.5	89.6	60
	C40D22-S.75-L10-HW-1	3.9x7.9 in.	7085	6.86	74.5	89.6	60
	C40D22-S1.25-L10-HE	3.9x7.9 in.	7085	6.86	74.5	89.6	60
	C40D22-S1.25-L10-HE-1	3.9x7.9 in.	7085	6.86	74.5	89.6	60
	C40D22-S1.25-L10-HW	3.9x7.9 in.	7085	6.86	74.5	89.6	60
	C40D22-S1.25-L10-HW-1	3.9x7.9 in.	7085	6.86	74.5	89.6	60
	C40D22-S1.5-L10-HE	3.9x7.9 in.	7085	6.86	74.5	89.6	60
	C40D22-S1.5-L10-HE-1	3.9x7.9 in.	7085	6.86	74.5	89.6	60

[1]	[2]	[3]	[4]	[5]	[6]	[7]	[8]
Authors	I.D	Concrete test specimen	f_{cm} (psi)	$f_{1c,mod}$ (ksi)	f_y (ksi)	f_{su} (ksi)	f_{yt} (ksi)
Chun, Lee, and Oh [9] (cont'd)	C40D22-S1.5-L10-HW	3.9x7.9 in.	7085	6.86	74.5	89.6	60
	C40D22-S1.5-L10-HW-1	3.9x7.9 in.	7085	6.86	74.5	89.6	60
	C60D22-S.75-L10-HE	3.9x7.9 in.	10177	9.86	74.5	89.6	60
	C60D22-S.75-L10-HE-1	3.9x7.9 in.	10152	9.83	74.5	89.6	60
	C60D22-S1.25-L10-HE	3.9x7.9 in.	10170	9.85	74.5	89.6	60
	C60D22-S1.25-L10-HE-1	3.9x7.9 in.	10145	9.83	74.5	89.6	60
	C40D29-S.75-L10-HE	3.9x7.9 in.	7892	7.64	68.4	87.3	60
	C40D29-S.75-L10-HW-1	3.9x7.9 in.	9358	9.06	68.4	87.3	60
	C60D29-S.75-L10-HE-1	3.9x7.9 in.	10686	10.35	68.4	87.3	60
Chun, Lee, and Oh [10]	C80D22-L4	3.9x7.9 in.	12096	11.71	67.8	87.5	-
	C80D22-L4-1	3.9x7.9 in.	12259	11.87	67.8	87.5	-
	C80D22-L4-2	3.9x7.9 in.	11592	11.23	67.8	87.5	-
	C80D22-L4-3	3.9x7.9 in.	11709	11.34	67.8	87.5	-
	C80D22-L7	3.9x7.9 in.	12111	11.73	67.8	87.5	-
	C80D22-L7-1	3.9x7.9 in.	12340	11.95	67.8	87.5	-
	C80D22-L7-2	3.9x7.9 in.	11511	11.15	67.8	87.5	-
	C80D22-L7-3	3.9x7.9 in.	11606	11.24	67.8	87.5	-
	C80D22-L10	3.9x7.9 in.	12259	11.87	67.8	87.5	-
	C80D22-L10-1	3.9x7.9 in.	12247	11.86	67.8	87.5	-
	C80D22-L10-3	3.9x7.9 in.	11645	11.28	67.8	87.5	-
	C80D29-L4	3.9x7.9 in.	12542	12.15	71.3	90.2	-
	C80D29-L4-1	3.9x7.9 in.	12876	12.47	71.3	90.2	-
	C80D29-L4-2	3.9x7.9 in.	11888	11.51	71.3	90.2	-
	C80D29-L4-3	3.9x7.9 in.	11865	11.49	71.3	90.2	-
	C80D29-L7	3.9x7.9 in.	12502	12.11	71.3	90.2	-
	C80D29-L7-2	3.9x7.9 in.	11770	11.40	71.3	90.2	-
	C80D29-L7-3	3.9x7.9 in.	11818	11.44	71.3	90.2	-
	C80D29-L10	3.9x7.9 in.	12917	12.51	71.3	90.2	-
	C80D29-L10-2	3.9x7.9 in.	11794	11.42	71.3	90.2	-
	C100D29-L4-1	3.9x7.9 in.	14660	14.20	66.5	87.6	-
	C80D22-L4-HW	3.9x7.9 in.	12352	11.96	67.8	87.5	60
	C80D22-L4-HW-1	3.9x7.9 in.	12318	11.93	67.8	87.5	60
	C80D22-L4-HW-2	3.9x7.9 in.	11454	11.09	67.8	87.5	60
	C80D22-L4-HW-3	3.9x7.9 in.	11696	11.33	67.8	87.5	60
	C80D22-L7-HW-1	3.9x7.9 in.	12329	11.94	67.8	87.5	60
	C80D22-L7-HW-2	3.9x7.9 in.	11592	11.23	67.8	87.5	60
	C80D29-L4-HW	3.9x7.9 in.	12818	12.41	71.3	90.2	60
	C80D29-L4-HW-1	3.9x7.9 in.	12471	12.08	71.3	90.2	60
	C80D29-L4-HW-2	3.9x7.9 in.	12312	11.92	71.3	90.2	60
	C80D29-L4-HW-3	3.9x7.9 in.	12219	11.83	71.3	90.2	60
	C80D29-L7-HW	3.9x7.9 in.	12892	12.49	71.3	90.2	60
	C80D29-L7-HW-3	3.9x7.9 in.	12321	11.93	71.3	90.2	60
	C100D29-L4-HW	3.9x7.9 in.	14394	13.94	66.5	87.6	60
	C100D29-L4-HW-1	3.9x7.9 in.	14550	14.09	66.5	87.6	60

1000 psi = 1 ksi = 6.895 MPa; 1 in. = 25.4 mm; 1 kip = 4.45 kN

[1]	[2]	[9]	[10]	[11]	[12]	[13]	[14]	[15]	[16]
Authors	I.D	Section	b (in.)	h (in.)	b/h	d_b (in.)	A_b (in.^{2})	Symm. Reinf.	L_s (in.)
Pfister and Mattock [7]	4B	R	12.0	10.0	1.20	1.00	0.79	yes	10.0
	5B	R	12.0	10.0	1.20	1.00	0.79	yes	20.0
	6B	R	12.0	10.0	1.20	1.00	0.79	yes	30.0
	5B1	R	12.0	10.0	1.20	1.00	0.79	yes	20.0
	6B1	R	12.0	10.0	1.20	1.00	0.79	yes	30.0
	$4A^+$	C	12.0	-	1.00	1.00	0.79	yes	5.00
	$5A^+$	C	12.0	-	1.00	1.00	0.79	yes	10.0
	$6A^+$	C	12.0	-	1.00	1.00	0.79	yes	20.0
	$7A^+$	C	12.0	-	1.00	1.00	0.79	yes	30.0
Chun, Lee, and Oh [8]	C40D22-S.75-L10-HO	R	7.4	10.5	1.41	0.88	0.60	yes	8.7
	C40D22-S.75-L10-HO-1	R	7.4	10.5	1.41	0.88	0.60	yes	8.7
	C40D22-S.75-L15	R	7.4	10.5	1.41	0.88	0.60	yes	13.0
	C40D22-S.75-L15-1	R	7.4	10.5	1.41	0.88	0.60	yes	13.0
	C40D22-S1.25-L10-H0-1	R	8.3	10.5	1.26	0.88	0.60	yes	8.7
	C40D22-S1.25-L15-HO	R	8.3	10.5	1.26	0.88	0.60	yes	13.0
	C40D22-S1.25-L15-HO-1	R	8.3	10.5	1.26	0.88	0.60	yes	13.0
	C40D22-S1.25-L20-HO-1	R	8.3	10.5	1.26	0.88	0.60	yes	17.3
	C40D22-S1.5-L10-H0	R	8.8	10.5	1.20	0.88	0.60	yes	8.7
	C40D22-S1.5-L10-H0-1	R	8.8	10.5	1.20	0.88	0.60	yes	8.7
	C40D22-S1.5-L15-H0	R	8.8	10.5	1.20	0.88	0.60	yes	13.0
	C40D22-S1.5-L15-H0-1	R	8.8	10.5	1.20	0.88	0.60	yes	13.0
	C60D22-S.75-L10-HO	R	7.4	10.5	1.41	0.88	0.60	yes	8.7
	C60D22-S.75-L10-HO-1	R	7.4	10.5	1.41	0.88	0.60	yes	8.7
	C60D22-S1.25-L10-H0	R	8.3	10.5	1.26	0.88	0.60	yes	8.7
	C60D22-S1.25-L10-H0-1	R	8.3	10.5	1.26	0.88	0.60	yes	8.7
	C60D22-S1.25-L15-HO-1	R	8.3	10.5	1.26	0.88	0.60	yes	13.0
	C60D22-S1.5-L10-H0	R	8.8	10.5	1.20	0.88	0.60	yes	8.7
	C60D22-S1.5-L10-H0-1	R	8.8	10.5	1.20	0.88	0.60	yes	8.7
	C60D22-S1.5-L15-1	R	8.8	10.5	1.20	0.88	0.60	yes	13.0
	C40D29-S.75-L10-HO-1	R	9.6	9.0	1.06	1.13	1.00	no	11.4
	C40D29-S.75-L15-1	R	9.6	9.0	1.06	1.13	1.00	no	17.1
	C40D29-S.75-L20	R	9.6	9.0	1.06	1.13	1.00	no	22.8
	C60D29-S.75-L10-HO	R	9.6	9.0	1.06	1.13	1.00	no	11.4
	C60D29-S.75-L10-HO-1	R	9.6	9.0	1.06	1.13	1.00	no	11.4
	C60D29-S1.25-L10-H0	R	10.7	9.0	1.19	1.13	1.00	no	11.4
Chun, Lee, and Oh [9]	C40D22-S.75-L10-HE	R	7.4	10.5	1.41	0.88	0.60	yes	8.7
	C40D22-S.75-L10-HE-1	R	7.4	10.5	1.41	0.88	0.60	yes	8.7
	C40D22-S.75-L10-HW	R	7.4	10.5	1.41	0.88	0.60	yes	8.7
	C40D22-S.75-L10-HW-1	R	7.4	10.5	1.41	0.88	0.60	yes	8.7
	C40D22-S1.25-L10-HE	R	8.3	10.5	1.26	0.88	0.60	yes	8.7
	C40D22-S1.25-L10-HE-1	R	8.3	10.5	1.26	0.88	0.60	yes	8.7
	C40D22-S1.25-L10-HW	R	8.3	10.5	1.26	0.88	0.60	yes	8.7
	C40D22-S1.25-L10-HW-1	R	8.3	10.5	1.26	0.88	0.60	yes	8.7
	C40D22-S1.5-L10-HE	R	8.8	10.5	1.20	0.88	0.60	yes	8.7
	C40D22-S1.5-L10-HE-1	R	8.8	10.5	1.20	0.88	0.60	yes	8.7

Section: R= rectangular; C =circular. “Symm. Reinf.” = Symmetric Reinforcement.

[1]	[2]	[9]	[10]	[11]	[12]	[13]	[14]	[15]	[16]
Authors	I.D	Section	b (in.)	h (in.)	b/h	d_b (in.)	A_b (in.^{2})	Symm. Reinf.	L_s (in.)
Chun, Lee, and Oh [9] (cont'd)	C40D22-S1.5-L10-HW	R	8.8	10.5	1.20	0.88	0.60	yes	8.7
	C40D22-S1.5-L10-HW-1	R	8.8	10.5	1.20	0.88	0.60	yes	8.7
	C60D22-S.75-L10-HE	R	7.4	10.5	1.41	0.88	0.60	yes	8.7
	C60D22-S.75-L10-HE-1	R	7.4	10.5	1.41	0.88	0.60	yes	8.7
	C60D22-S1.25-L10-HE	R	8.3	10.5	1.26	0.88	0.60	yes	8.7
	C60D22-S1.25-L10-HE-1	R	8.3	10.5	1.26	0.88	0.60	yes	8.7
	C40D29-S.75-L10-HE	R	9.6	9.0	1.06	1.13	1.00	no	11.4
	C40D29-S.75-L10-HW-1	R	9.6	9.0	1.06	1.13	1.00	no	11.4
	C60D29-S.75-L10-HE-1	R	9.6	9.0	1.06	1.13	1.00	no	11.4
Chun, Lee, and Oh [10]	C80D22-L4	R	7.4	10.5	1.41	0.88	0.60	yes	3.5
	C80D22-L4-1	R	7.4	10.5	1.41	0.88	0.60	yes	3.5
	C80D22-L4-2	R	7.4	10.5	1.41	0.88	0.60	yes	3.5
	C80D22-L4-3	R	7.4	10.5	1.41	0.88	0.60	yes	3.5
	C80D22-L7	R	7.4	10.5	1.41	0.88	0.60	yes	6.1
	C80D22-L7-1	R	7.4	10.5	1.41	0.88	0.60	yes	6.1
	C80D22-L7-2	R	7.4	10.5	1.41	0.88	0.60	yes	6.1
	C80D22-L7-3	R	7.4	10.5	1.41	0.88	0.60	yes	6.1
	C80D22-L10	R	7.4	10.5	1.41	0.88	0.60	yes	8.7
	C80D22-L10-1	R	7.4	10.5	1.41	0.88	0.60	yes	8.7
	C80D22-L10-3	R	7.4	10.5	1.41	0.88	0.60	yes	8.7
	C80D29-L4	R	9.6	13.5	1.41	1.13	1.00	yes	4.6
	C80D29-L4-1	R	9.6	13.5	1.41	1.13	1.00	yes	4.6
	C80D29-L4-2	R	9.6	13.5	1.41	1.13	1.00	yes	4.6
	C80D29-L4-3	R	9.6	13.5	1.41	1.13	1.00	yes	4.6
	C80D29-L7	R	9.6	13.5	1.41	1.13	1.00	yes	8.0
	C80D29-L7-2	R	9.6	13.5	1.41	1.13	1.00	yes	8.0
	C80D29-L7-3	R	9.6	13.5	1.41	1.13	1.00	yes	8.0
	C80D29-L10	R	9.6	13.5	1.41	1.13	1.00	yes	11.4
	C80D29-L10-2	R	9.6	13.5	1.41	1.13	1.00	yes	11.4
	C100D29-L4-1	R	9.6	13.5	1.41	1.13	1.00	yes	4.6
	C80D22-L4-HW	R	7.4	10.5	1.41	0.88	0.60	yes	3.5
	C80D22-L4-HW-1	R	7.4	10.5	1.41	0.88	0.60	yes	3.5
	C80D22-L4-HW-2	R	7.4	10.5	1.41	0.88	0.60	yes	3.5
	C80D22-L4-HW-3	R	7.4	10.5	1.41	0.88	0.60	yes	3.5
	C80D22-L7-HW-1	R	7.4	10.5	1.41	0.88	0.60	yes	6.1
	C80D22-L7-HW-2	R	7.4	10.5	1.41	0.88	0.60	yes	6.1
	C80D29-L4-HW	R	9.6	13.5	1.41	1.13	1.00	yes	4.6
	C80D29-L4-HW-1	R	9.6	13.5	1.41	1.13	1.00	yes	4.6
	C80D29-L4-HW-2	R	9.6	13.5	1.41	1.13	1.00	yes	4.6
	C80D29-L4-HW-3	R	9.6	13.5	1.41	1.13	1.00	yes	4.6
	C80D29-L7-HW	R	9.6	13.5	1.41	1.13	1.00	yes	8.0
	C80D29-L7-HW-3	R	9.6	13.5	1.41	1.13	1.00	yes	8.0
	C100D29-L4-HW	R	9.6	13.5	1.41	1.13	1.00	yes	4.6
	C100D29-L4-HW-1	R	9.6	13.5	1.41	1.13	1.00	yes	4.6

Section: R= rectangular; C =circular. "Symm. Reinf." = Symmetric Reinforcement.

[1]	[2]	[17]	[18]	[19]	[20]	[21]	[22]	[23]	[24]	[25]
Authors	I.D	l_s/d_b	N_b	n	R_r	d_{tr} (in.)	A_t (in.^{2})	c_{so} (in.)	c_{si} (in.)	c_b (in.)
Pfister and Mattock [7]	4B	10.0	6	3	0.073	0.25	0.05	1.75	0.63	1.75
	5B	20.0	6	3	0.073	0.25	0.05	1.75	0.63	1.75
	6B	30.0	6	3	0.073	0.25	0.05	1.75	0.63	1.75
	5B1	20.0	6	3	0.073	0.25	0.05	1.75	0.63	1.75
	6B1	30.0	6	3	0.073	0.25	0.05	1.75	0.63	1.75
	4A$^+$	5.00	6	1	0.073	0.25	0.05	1.25	1.18	1.25
	5A$^+$	10.0	6	1	0.073	0.25	0.05	1.25	1.18	1.25
	6A$^+$	20.0	6	1	0.073	0.25	0.05	1.25	1.18	1.25
	7A$^+$	30.0	6	1	0.073	0.25	0.05	1.25	1.18	1.25
Chun, Lee, and Oh [8]	C40D22-S.75-L10-HO	9.9	4	2	0.10	-	-	1.31	0.66	2.19
	C40D22-S.75-L10-HO-1	9.9	4	2	0.10	-	-	1.31	0.66	2.19
	C40D22-S.75-L15	14.8	4	2	0.10	-	-	1.31	0.66	2.19
	C40D22-S.75-L15-1	14.8	4	2	0.10	-	-	1.31	0.66	2.19
	C40D22-S1.25-L10-H0-1	9.9	4	2	0.10	-	-	1.31	1.09	2.19
	C40D22-S1.25-L15-HO	14.8	4	2	0.10	-	-	1.31	1.09	2.19
	C40D22-S1.25-L15-HO-1	14.8	4	2	0.10	-	-	1.31	1.09	2.19
	C40D22-S1.25-L20-HO-1	19.8	4	2	0.10	-	-	1.31	1.09	2.19
	C40D22-S1.5-L10-H0	9.9	4	2	0.10	-	-	1.31	1.31	2.19
	C40D22-S1.5-L10-H0-1	9.9	4	2	0.10	-	-	1.31	1.31	2.19
	C40D22-S1.5-L15-H0	14.8	4	2	0.10	-	-	1.31	1.31	2.19
	C40D22-S1.5-L15-H0-1	14.8	4	2	0.10	-	-	1.31	1.31	2.19
	C60D22-S.75-L10-HO	9.9	4	2	0.10	-	-	1.31	0.66	2.19
	C60D22-S.75-L10-HO-1	9.9	4	2	0.10	-	-	1.31	0.66	2.19
	C60D22-S1.25-L10-H0	9.9	4	2	0.10	-	-	1.31	1.09	2.19
	C60D22-S1.25-L10-H0-1	9.9	4	2	0.10	-	-	1.31	1.09	2.19
	C60D22-S1.25-L15-HO-1	14.8	4	2	0.10	-	-	1.31	1.09	2.19
	C60D22-S1.5-L10-H0	9.9	4	2	0.10	-	-	1.31	1.31	2.19
	C60D22-S1.5-L10-H0-1	9.9	4	2	0.10	-	-	1.31	1.31	2.19
	C60D22-S1.5-L15-1	14.8	4	2	0.10	-	-	1.31	1.31	2.19
	C40D29-S.75-L10-HO-1	10.1	2	2	0.10	-	-	1.69	0.85	2.82
	C40D29-S.75-L15-1	15.2	2	2	0.10	-	-	1.69	0.85	2.82
	C40D29-S.75-L20	20.2	2	2	0.10	-	-	1.69	0.85	2.82
	C60D29-S.75-L10-HO	10.1	2	2	0.10	-	-	1.69	0.85	2.82
	C60D29-S.75-L10-HO-1	10.1	2	2	0.10	-	-	1.69	0.85	2.82
	C60D29-S1.25-L10-H0	10.1	2	2	0.10	-	-	1.69	1.41	2.82
Chun, Lee, and Oh [9]	C40D22-S.75-L10-HE	9.9	4	2	0.10	0.375	0.11	1.31	0.66	2.19
	C40D22-S.75-L10-HE-1	9.9	4	2	0.10	0.375	0.11	1.31	0.66	2.19
	C40D22-S.75-L10-HW	9.9	4	2	0.10	0.375	0.11	1.31	0.66	2.19
	C40D22-S.75-L10-HW-1	9.9	4	2	0.10	0.375	0.11	1.31	0.66	2.19
	C40D22-S1.25-L10-HE	9.9	4	2	0.10	0.375	0.11	1.31	1.09	2.19
	C40D22-S1.25-L10-HE-1	9.9	4	2	0.10	0.375	0.11	1.31	1.09	2.19
	C40D22-S1.25-L10-HW	9.9	4	2	0.10	0.375	0.11	1.31	1.09	2.19
	C40D22-S1.25-L10-HW-1	9.9	4	2	0.10	0.375	0.11	1.31	1.09	2.19
	C40D22-S1.5-L10-HE	9.9	4	2	0.10	0.375	0.11	1.31	1.31	2.19
	C40D22-S1.5-L10-HE-1	9.9	4	2	0.10	0.375	0.11	1.31	1.31	2.19

[1]	[2]	[17]	[18]	[19]	[20]	[21]	[22]	[23]	[24]	[25]
Authors	I.D	l_s/d_b	N_b	n	R_r	d_{tr} (in.)	A_t (in.^{2})	c_{so} (in.)	c_{si} (in.)	c_b (in.)
Chun, Lee, and Oh [9] (cont'd)	C40D22-S1.5-L10-HW	9.9	4	2	0.10	0.375	0.11	1.31	1.31	2.19
	C40D22-S1.5-L10-HW-1	9.9	4	2	0.10	0.375	0.11	1.31	1.31	2.19
	C60D22-S.75-L10-HE	9.9	4	2	0.10	0.375	0.11	1.31	0.66	2.19
	C60D22-S.75-L10-HE-1	9.9	4	2	0.10	0.375	0.11	1.31	0.66	2.19
	C60D22-S1.25-L10-HE	9.9	4	2	0.10	0.375	0.11	1.31	1.09	2.19
	C60D22-S1.25-L10-HE-1	9.9	4	2	0.10	0.375	0.11	1.31	1.09	2.19
	C40D29-S.75-L10-HE	10.1	2	2	0.10	0.375	0.11	1.69	0.85	2.82
	C40D29-S.75-L10-HW-1	10.1	2	2	0.10	0.375	0.11	1.69	0.85	2.82
	C60D29-S.75-L10-HE-1	10.1	2	2	0.10	0.375	0.11	1.69	0.85	2.82
Chun, Lee, and Oh [10]	C80D22-L4	4.0	4	2	0.10	-	-	1.31	0.66	2.19
	C80D22-L4-1	4.0	4	2	0.10	-	-	1.31	0.66	2.19
	C80D22-L4-2	4.0	4	2	0.10	-	-	1.31	0.66	2.19
	C80D22-L4-3	4.0	4	2	0.10	-	-	1.31	0.66	2.19
	C80D22-L7	7.0	4	2	0.10	-	-	1.31	0.66	2.19
	C80D22-L7-1	7.0	4	2	0.10	-	-	1.31	0.66	2.19
	C80D22-L7-2	7.0	4	2	0.10	-	-	1.31	0.66	2.19
	C80D22-L7-3	7.0	4	2	0.10	-	-	1.31	0.66	2.19
	C80D22-L10	9.9	4	2	0.10	-	-	1.31	0.66	2.19
	C80D22-L10-1	9.9	4	2	0.10	-	-	1.31	0.66	2.19
	C80D22-L10-3	9.9	4	2	0.10	-	-	1.31	0.66	2.19
	C80D29-L4	4.1	4	2	0.10	-	-	1.69	0.85	2.82
	C80D29-L4-1	4.1	4	2	0.10	-	-	1.69	0.85	2.82
	C80D29-L4-2	4.1	4	2	0.10	-	-	1.69	0.85	2.82
	C80D29-L4-3	4.1	4	2	0.10	-	-	1.69	0.85	2.82
	C80D29-L7	7.1	4	2	0.10	-	-	1.69	0.85	2.82
	C80D29-L7-2	7.1	4	2	0.10	-	-	1.69	0.85	2.82
	C80D29-L7-3	7.1	4	2	0.10	-	-	1.69	0.85	2.82
	C80D29-L10	10.1	4	2	0.10	-	-	1.69	0.85	2.82
	C80D29-L10-2	10.1	4	2	0.10	-	-	1.69	0.85	2.82
	C100D29-L4-1	4.1	4	2	0.10	-	-	1.69	0.85	2.82
	C80D22-L4-HW	4.0	4	2	0.10	0.375	0.11	1.31	0.66	2.19
	C80D22-L4-HW-1	4.0	4	2	0.10	0.375	0.11	1.31	0.66	2.19
	C80D22-L4-HW-2	4.0	4	2	0.10	0.375	0.11	1.31	0.66	2.19
	C80D22-L4-HW-3	4.0	4	2	0.10	0.375	0.11	1.31	0.66	2.19
	C80D22-L7-HW-1	6.9	4	2	0.10	0.375	0.11	1.31	0.66	2.19
	C80D22-L7-HW-2	6.9	4	2	0.10	0.375	0.11	1.31	0.66	2.19
	C80D29-L4-HW	4.1	4	2	0.10	0.375	0.11	1.69	0.85	2.82
	C80D29-L4-HW-1	4.1	4	2	0.10	0.375	0.11	1.69	0.85	2.82
	C80D29-L4-HW-2	4.1	4	2	0.10	0.375	0.11	1.69	0.85	2.82
	C80D29-L4-HW-3	4.1	4	2	0.10	0.375	0.11	1.69	0.85	2.82
	C80D29-L7-HW	7.1	4	2	0.10	0.375	0.11	1.69	0.85	2.82
	C80D29-L7-HW-3	7.1	4	2	0.10	0.375	0.11	1.69	0.85	2.82
	C100D29-L4-HW	4.1	4	2	0.10	0.375	0.11	1.69	0.85	2.82
	C100D29-L4-HW-1	4.1	4	2	0.10	0.375	0.11	1.69	0.85	2.82

[1]	[2]	[26]	[27]	[28]	[29]	[30]	[31]	[32]
Authors	I.D	N_s (in.)	N_l (in.)	s (in.)	x (in.)	f_{sc} (ksi)	f_{brg} (ksi)	P_e (kip)
Pfister and Mattock [7]	4B	1	4	10.0	5.0	40.0	-	498
	5B	3	4	10.0	0.0	53.0	-	635
	6B	3	4	10.0	5.0	58.0	-	645
	5B1	3	4	10.0	0.0	64.5	-	659
	6B1	3	4	10.0	5.0	68.0	-	688
	$4A^+$	3	1	1.5	0.375	50.0	-	603
	$5A^+$	7	1	1.5	0.375	52.9	-	623
	$6A^+$	13	1	1.5	0.375	67.0	-	725
	$7A^+$	20	1	1.5	0.375	82.6	-	769
Chun, Lee, and Oh [8]	C40D22-S.75-L10-HO	-	-	-	-	57.9	-	540
	C40D22-S.75-L10-HO-1	-	-	-	-	59.0	18.4	637
	C40D22-S.75-L15	-	-	-	-	58.2	16.7	626
	C40D22-S.75-L15-1	-	-	-	-	54.1	14.0	604
	C40D22-S1.25-L10-H0-1	-	-	-	-	46.7	12.4	656
	C40D22-S1.25-L15-HO	-	-	-	-	57.0	18.7	654
	C40D22-S1.25-L15-HO-1	-	-	-	-	64.0	14.6	721
	C40D22-S1.25-L20-HO-1	-	-	-	-	61.4	17.1	677
	C40D22-S1.5-L10-H0	-	-	-	-	47.1	18.4	716
	C40D22-S1.5-L10-H0-1	-	-	-	-	45.6	17.0	703
	C40D22-S1.5-L15-H0	-	-	-	-	60.9	16.3	705
	C40D22-S1.5-L15-H0-1	-	-	-	-	56.8	17.8	743
	C60D22-S.75-L10-HO	-	-	-	-	70.4	18.1	755
	C60D22-S.75-L10-HO-1	-	-	-	-	68.7	21.5	762
	C60D22-S1.25-L10-H0	-	-	-	-	64.5	20.3	824
	C60D22-S1.25-L10-H0-1	-	-	-	-	71.9	21.8	866
	C60D22-S1.25-L15-HO-1	-	-	-	-	67.0	24.1	813
	C60D22-S1.5-L10-H0	-	-	-	-	61.5	16.2	881
	C60D22-S1.5-L10-H0-1	-	-	-	-	73.2	20.4	950
	C60D22-S1.5-L15-1	-	-	-	-	69.2	21.0	889
	C40D29-S.75-L10-HO-1	-	-	-	-	63.1	23.0	804
	C40D29-S.75-L15-1	-	-	-	-	63.8	20.7	806
	C40D29-S.75-L20	-	-	-	-	62.9	11.5	851
	C60D29-S.75-L10-HO	-	-	-	-	66.9	21.8	943
	C60D29-S.75-L10-HO-1	-	-	-	-	63.3	19.7	849
	C60D29-S1.25-L10-H0	-	-	-	-	56.5	18.4	910
Chun, Lee, and Oh [9]	C40D22-S.75-L10-HE	1	2	8.7	0.0	48.9	18.6	582
	C40D22-S.75-L10-HE-1	1	2	8.7	0.0	52.9	19.0	649
	C40D22-S.75-L10-HW	3	2	2.9	0.0	67.5	20.4	627
	C40D22-S.75-L10-HW-1	3	2	2.9	0.0	61.4	19.3	670
	C40D22-S1.25-L10-HE	1	2	8.7	0.0	56.0	18.9	662
	C40D22-S1.25-L10-HE-1	1	2	8.7	0.0	60.2	20.3	700
	C40D22-S1.25-L10-HW	3	2	2.9	0.0	61.3	16.5	641
	C40D22-S1.25-L10-HW-1	3	2	2.9	0.0	66.3	-	695
	C40D22-S1.5-L10-HE	1	2	8.7	0.0	49.4	16.3	723
	C40D22-S1.5-L10-HE-1	1	2	8.7	0.0	55.4	17.5	769

x = estimated distance between tie and splice end

[1]	[2]	[26]	[27]	[28]	[29]	[30]	[31]	[32]
Authors	I.D	N_s (in.)	N_l (in.)	s (in.)	x (in.)	f_{sc} (ksi)	f_{brg} (ksi)	P_e (kip)
Chun, Lee, and Oh [9] (cont'd)	C40D22-S1.5-L10-HW	3	2	2.9	0.0	55.3	17.5	723
	C40D22-S1.5-L10-HW-1	3	2	2.9	0.0	65.8	19.2	783
	C60D22-S.75-L10-HE	1	2	8.7	0.0	70.7	30.3	753
	C60D22-S.75-L10-HE-1	1	2	8.7	0.0	65.6	21.9	804
	C60D22-S1.25-L10-HE	1	2	8.7	0.0	65.9	20.9	820
	C60D22-S1.25-L10-HE-1	1	2	8.7	0.0	72.8	17.9	859
	C40D29-S.75-L10-HE	1	2	11.4	0.0	67.2	22.4	838
	C40D29-S.75-L10-HW-1	3	2	3.8	0.0	66.0	18.2	767
	C60D29-S.75-L10-HE-1	1	2	11.4	0.0	65.4	19.1	747
Chun, Lee, and Oh [10]	C80D22-L4	-	-	-	6.2	60.9	31.1	822
	C80D22-L4-1	-	-	-	6.2	42.9	19.7	797
	C80D22-L4-2	-	-	-	6.2	50.1	19.5	780
	C80D22-L4-3	-	-	-	6.2	49.0	-	767
	C80D22-L7	-	-	-	4.9	64.4	24.2	898
	C80D22-L7-1	-	-	-	4.9	59.6	19.9	847
	C80D22-L7-2	-	-	-	4.9	52.0	22.0	848
	C80D22-L7-3	-	-	-	4.9	63.5	16.9	736
	C80D22-L10	-	-	-	3.6	65.7	25.8	862
	C80D22-L10-1	-	-	-	3.6	63.8	19.6	913
	C80D22-L10-3	-	-	-	3.6	64.1	16.4	830
	C80D29-L4	-	-	-	7.9	52.6	22.4	1297
	C80D29-L4-1	-	-	-	7.9	48.4	24.3	1278
	C80D29-L4-2	-	-	-	7.9	49.3	8.9	1292
	C80D29-L4-3	-	-	-	7.9	51.4	24.9	1290
	C80D29-L7	-	-	-	6.2	61.2	22.1	1432
	C80D29-L7-2	-	-	-	6.2	58.9	26.0	1222
	C80D29-L7-3	-	-	-	6.2	58.4	24.9	1370
	C80D29-L10	-	-	-	4.5	56.7	16.2	1282
	C80D29-L10-2	-	-	-	4.5	62.5	15.7	1212
	C100D29-L4-1	-	-	-	7.9	64.4	25.1	935
	C80D22-L4-HW	1	2	3.9	1.8	56.7	20.9	857
	C80D22-L4-HW-1	1	2	3.9	1.8	57.4	23.1	877
	C80D22-L4-HW-2	1	2	3.9	1.8	59.2	16.6	811
	C80D22-L4-HW-3	1	2	3.9	1.8	59.0	19.0	806
	C80D22-L7-HW-1	2	2	3.9	0.9	54.8	17.2	949
	C80D22-L7-HW-2	2	2	3.9	0.9	66.4	18.8	837
	C80D29-L4-HW	1	2	3.9	0.3	63.3	23.9	1569
	C80D29-L4-HW-1	1	2	3.9	0.3	64.2	26.7	1270
	C80D29-L4-HW-2	1	2	3.9	0.3	59.3	26.2	1541
	C80D29-L4-HW-3	1	2	3.9	0.3	70.9	18.8	1527
	C80D29-L7-HW	2	2	3.9	1.9	60.0	20.3	1747
	C80D29-L7-HW-3	2	2	3.9	1.9	49.7	29.7	1544
	C100D29-L4-HW	1	2	3.9	0.3	66.3	28.1	1608
	C100D29-L4-HW-1	1	2	3.9	0.3	62.0	25.0	1576

x = estimated distance between tie and splice end

Appendix C: Compression Lap Splices: Relationships between Variables within Database

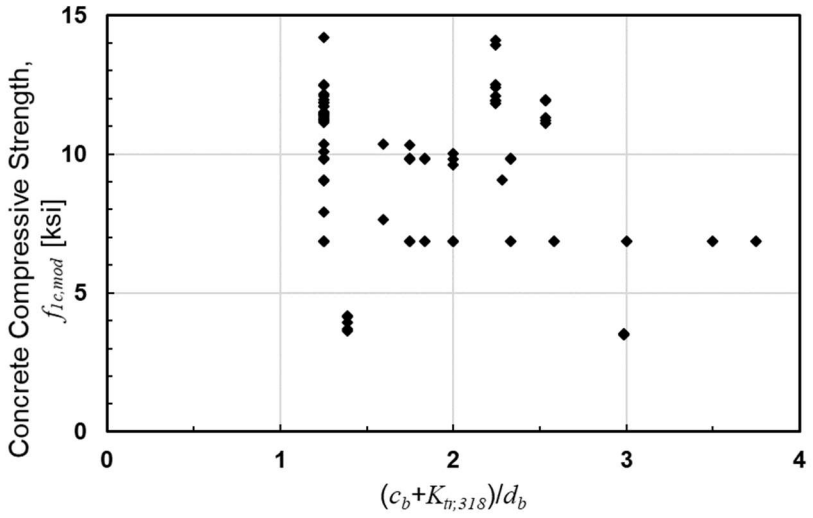

Figure 60 – Correlation between concrete compressive strength and $(c_{b,318}+K_{tr,318})/d_b$

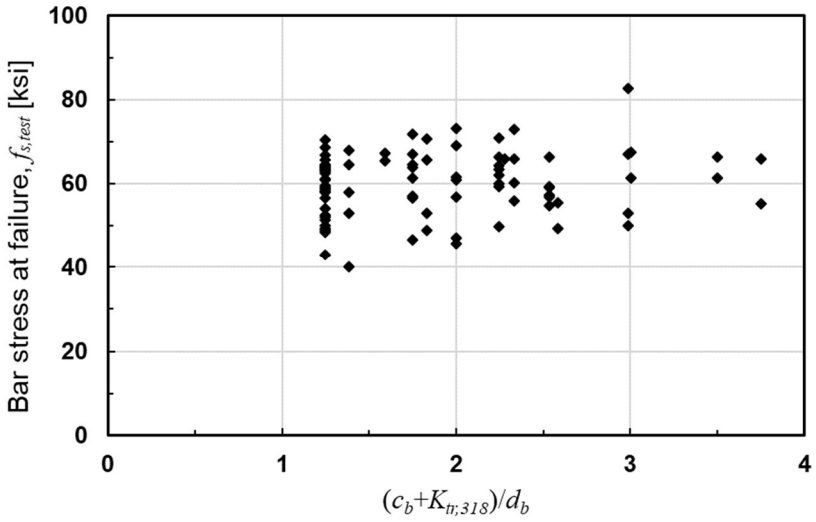

Figure 61 – Correlation between bar stress at failure and $(c_{b,318}+K_{tr,318})/d_b$

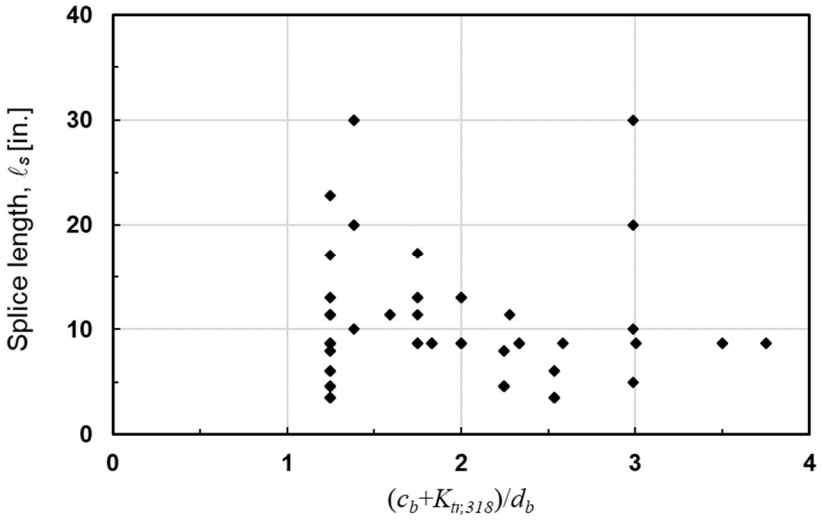

Figure 62 – Correlation between splice length and $(c_{b,318}+K_{tr,318})/d_b$

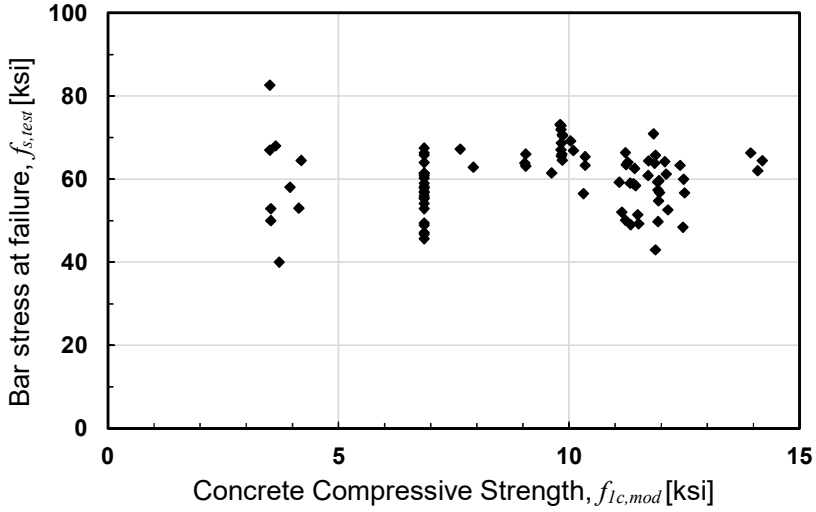

Figure 63 – Correlation between bar stress at failure and concrete compressive strength
(1 ksi = 6.895 MPa)

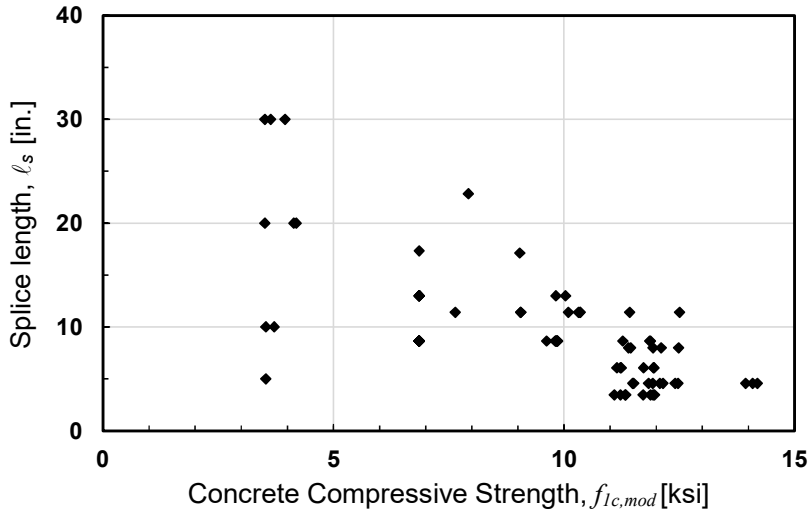

Figure 64 – Correlation between splice length and concrete compressive strength
(1 ksi = 6.895 MPa)

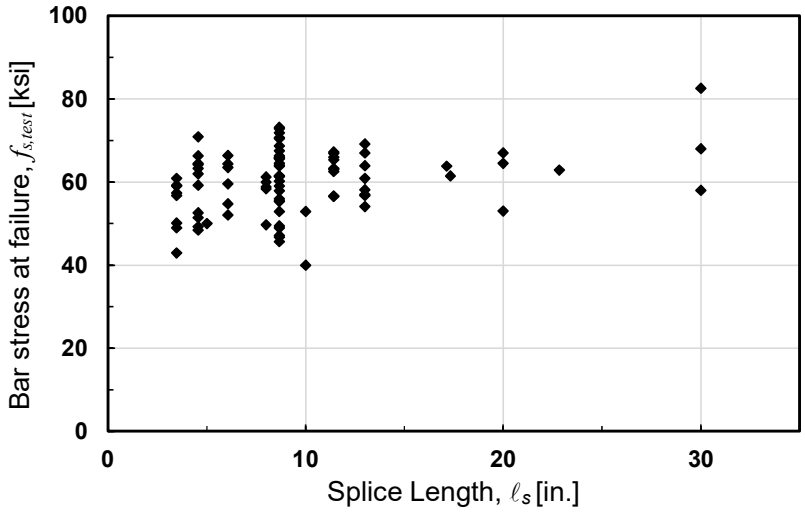

Figure 65 – Correlation between bar stress at failure and splice length
(1 in. = 25.4 mm)

Appendix D: Compression Lap Splices: Behavior of Compression Development or Compression Lap Splice Equations

Plots show the performance of the equations against the database in terms of T/C versus: (a) $(c_{b,318} + K_{tr,318})/d_b$ (b) measured concrete compressive strength, $f_{1c,mod}$ (c) measured steel failure stress, $f_{s,test}$, and (d) provided splice length, ℓ_s.

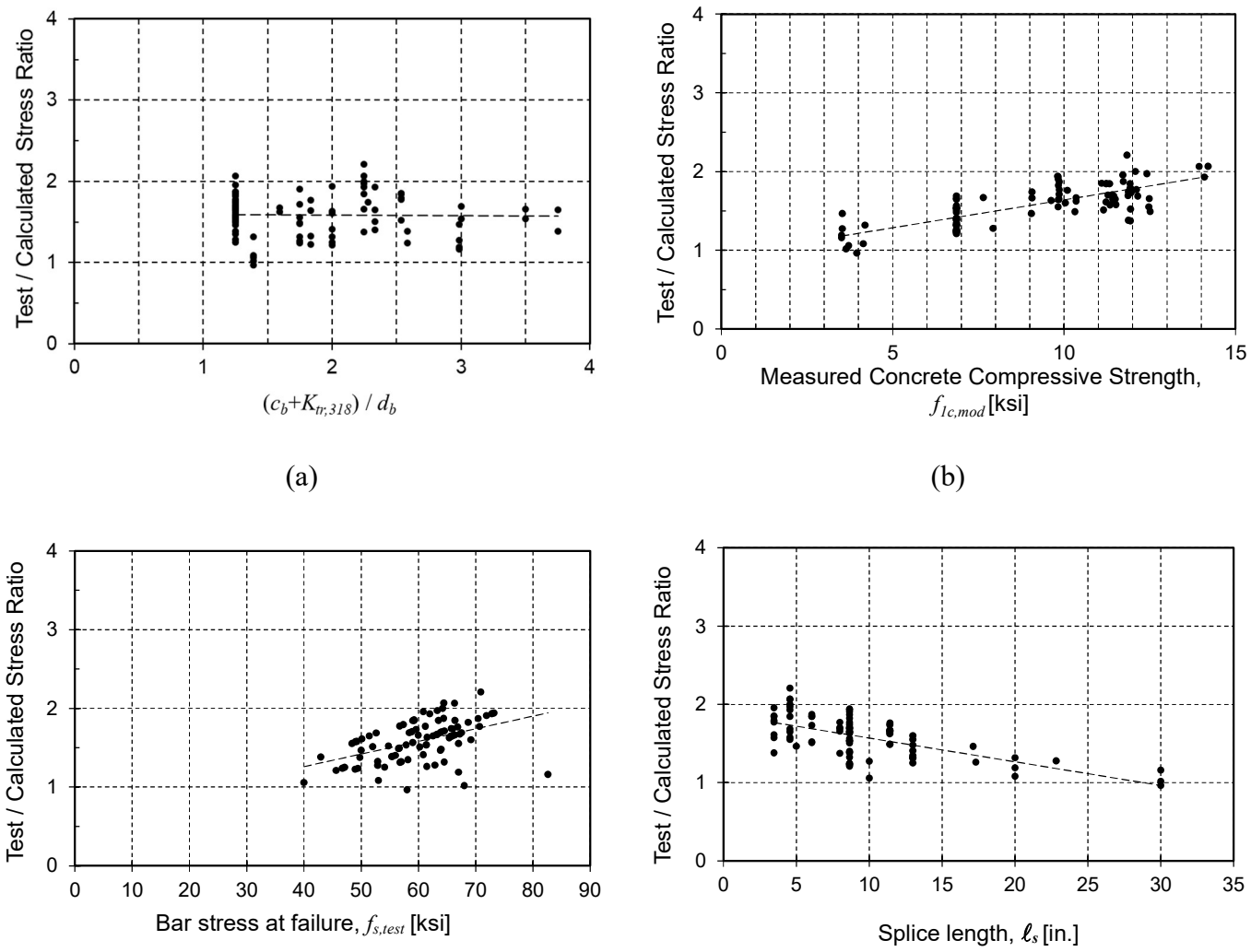

Figure 66 – ACI 318-19 [3] §25.5.5 Compression Lap Splice Eq. (b): T/C vs.: (a) $(c_{b,318}+K_{tr,318})/d_b$ (b) measured concrete compressive strength, $f_{1c,mod}$ (c) measured steel failure stress $f_{s,test}$ (d) provided splice length ℓ_s

(1 in. = 25.4 mm, 1 ksi = 6.895 MPa)

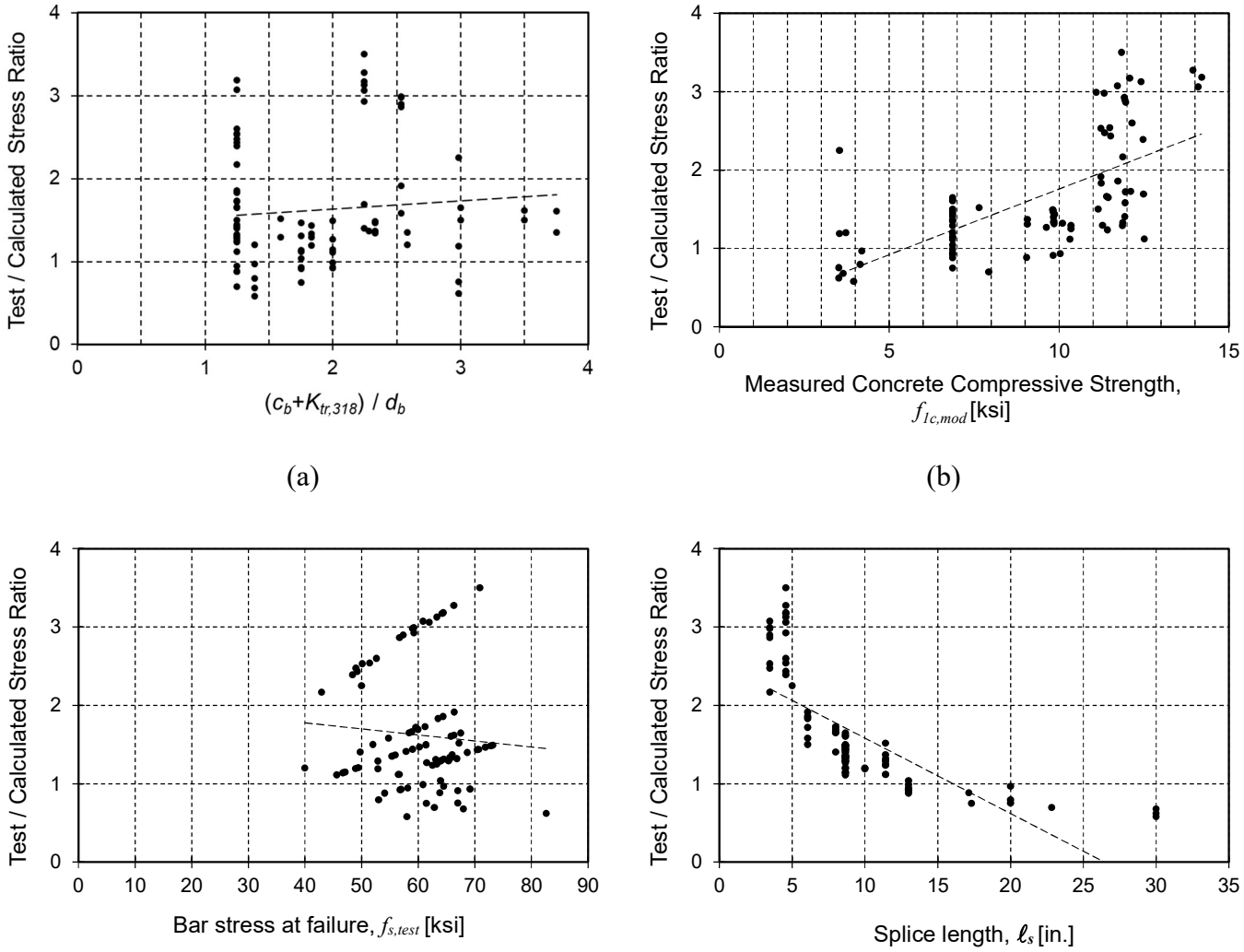

Figure 67 – ACI 318-19 [3] §25.4.9 Compression Development: T/C vs.: (a) $(c_{b,318}+K_{tr,318})/d_b$ (b) measured concrete compressive strength, $f_{1c,mod}$ (c) measured steel failure stress $f_{s,test}$ (d) provided splice length ℓ_s

(1 in. = 25.4 mm, 1 ksi = 6.895 MPa)

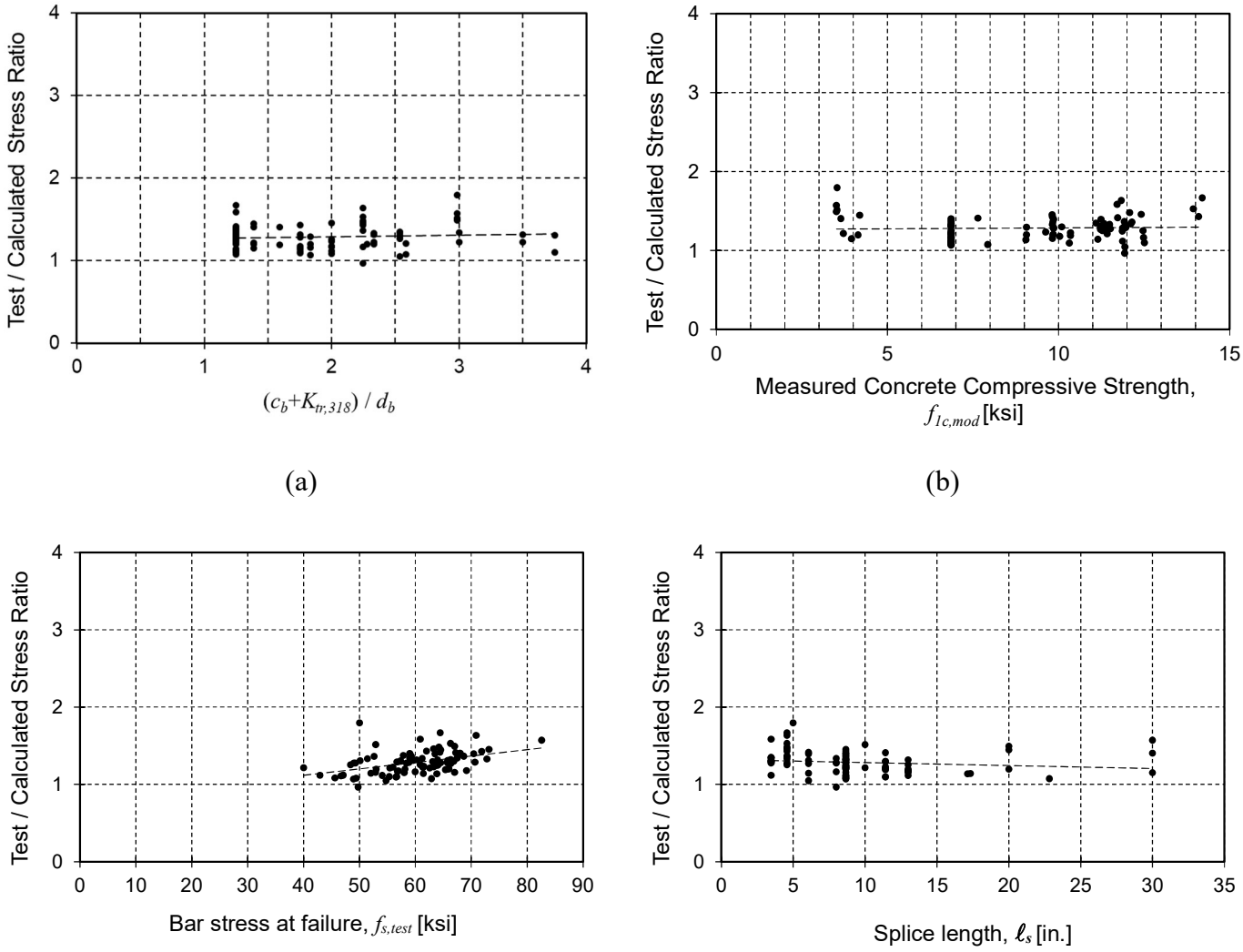

Figure 68 – Chun et al. [9] Compression Splice (Complex): T/C vs.: (a) $(c_{b,318}+K_{tr,318})/d_b$ (b) measured concrete compressive strength, $f_{1c,mod}$ (c) measured steel failure stress $f_{s,test}$ (d) provided splice length ℓ_s

(1 in. = 25.4 mm, 1 ksi = 6.895 MPa)

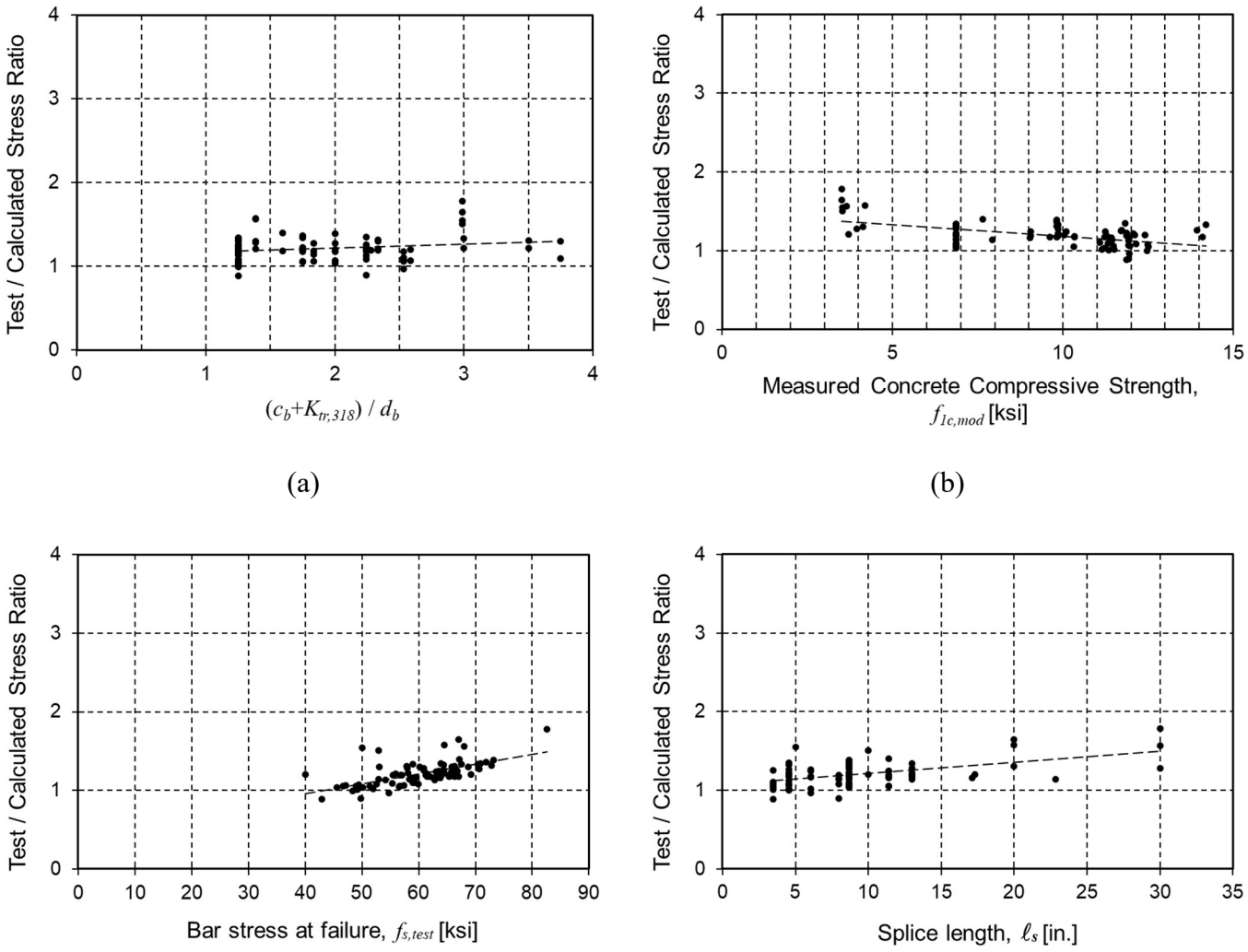

Figure 69 – Chun et al. [8] Compression Splice (Simplified): T/C vs.: (a) $(c_{b,318}+K_{tr,318})/d_b$ (b) measured concrete compressive strength, $f_{1c,mod}$ (c) measured steel failure stress $f_{s,test}$ (d) provided splice length ℓ_s

(1 in. = 25.4 mm, 1 ksi = 6.895 MPa)

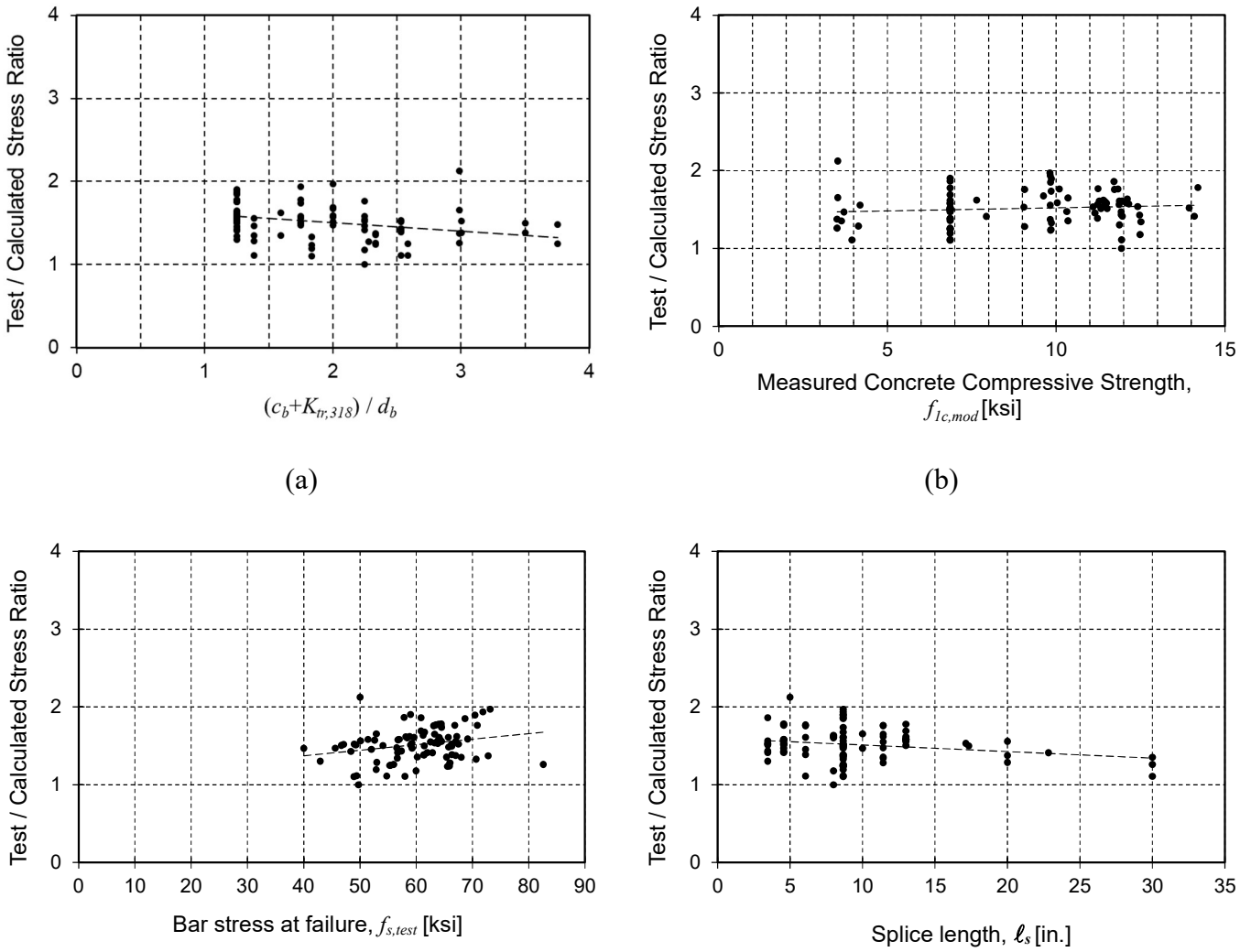

Figure 70 – Cairns Compression Splice: T/C vs.: (a) $(c_{b,318}+K_{tr,318})/d_b$ (b) measured concrete compressive strength, $f_{1c,mod}$ (c) measured steel failure stress $f_{s,test}$ (d) provided splice length ℓ_s

(1 in. = 25.4 mm, 1 ksi = 6.895 MPa)

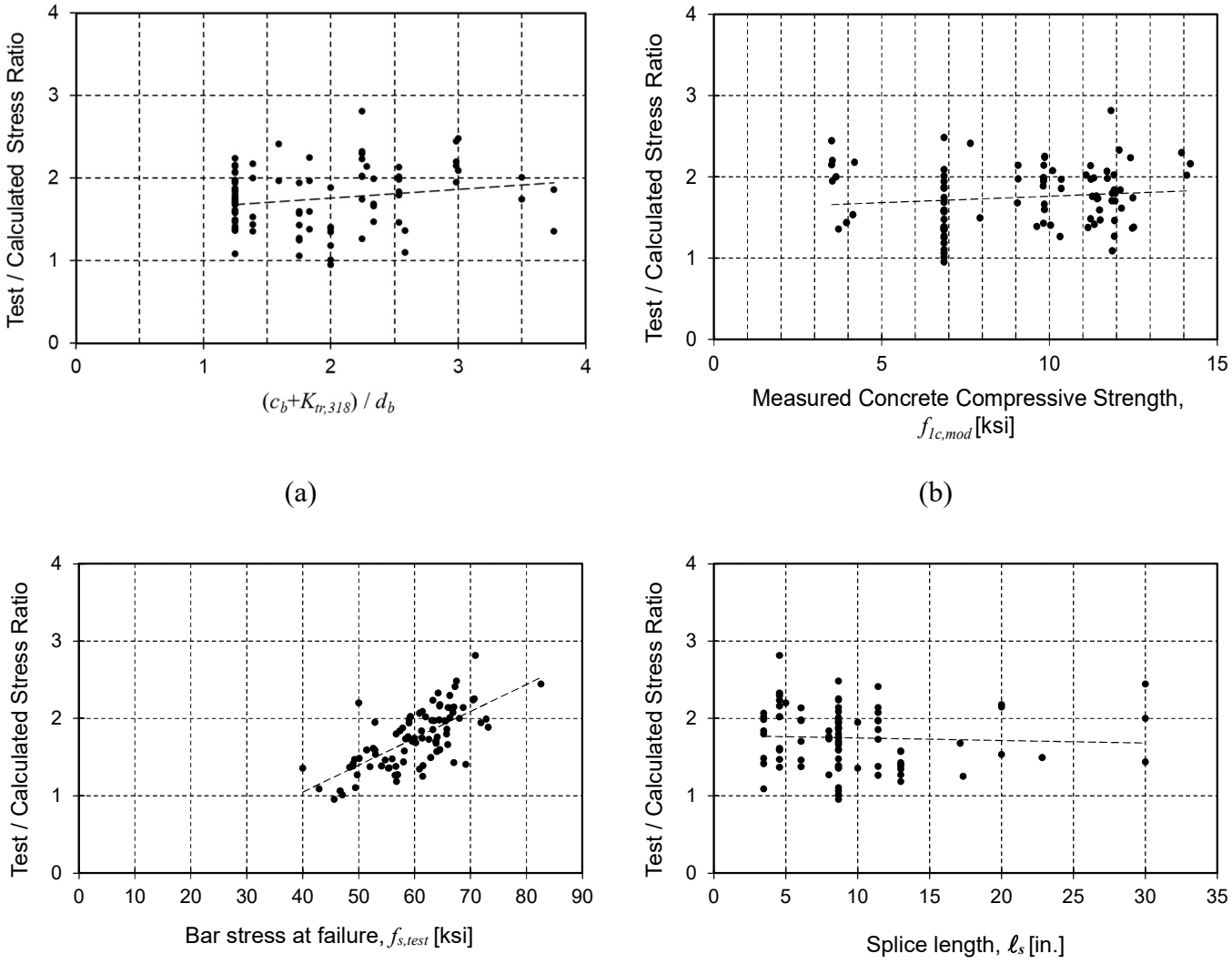

Figure 71 – fib MC 2010: *T*/*C* vs.: (a) $(c_{b,318}+K_{tr,318})/d_b$ (b) measured concrete compressive strength, $f_{1c,mod}$ (c) measured steel failure stress $f_{s,test}$ (d) provided splice length ℓ_s

(1 in. = 25.4 mm, 1 ksi = 6.895 MPa)

Appendix E: Compression Lap Splices: Behavior of Tension Development Length Equations

Plots show the performance of the equations against the database in terms of T/C versus: (i) $(c_{b,318} + K_{tr,318})/d_b$ (ii) measured concrete compressive strength, $f_{1c,mod}$ (iii) measured steel failure stress $f_{s,test}$ (iv) provided splice length ℓ_s. The plots are organized showing the behavior of the original equation, the equation using the derived r_1 factor, and the derived r_2 factor.

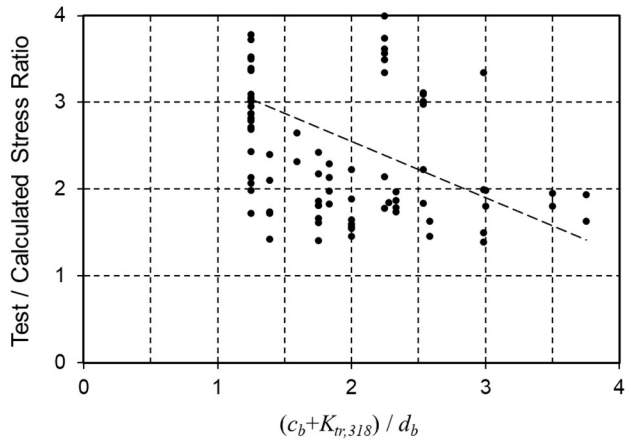

(a) ACI 318-19

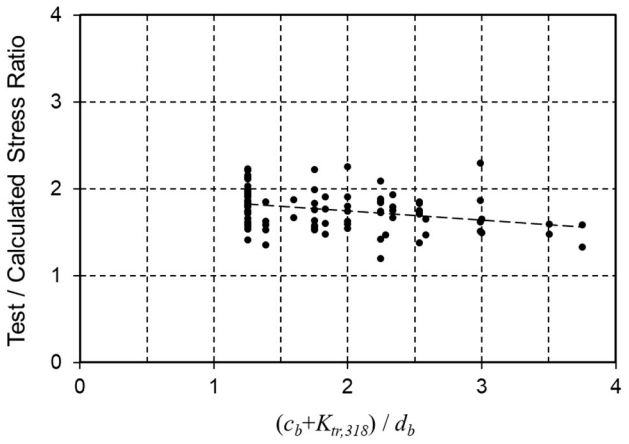

(b) ACI 408R-03

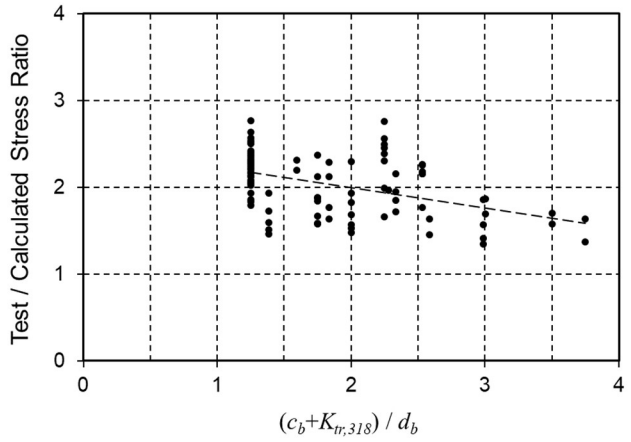

(c) Lepage et al.

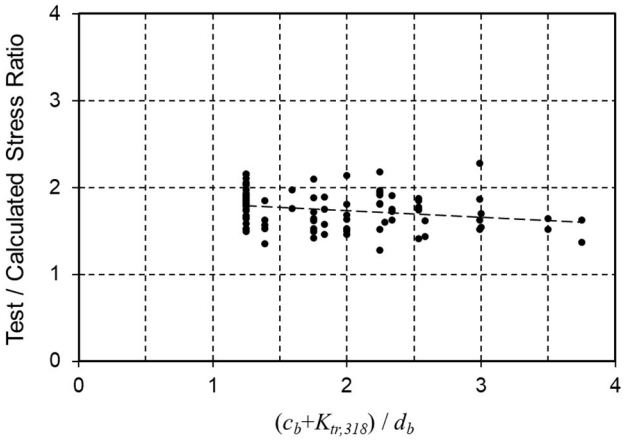

(d) Darwin et al.

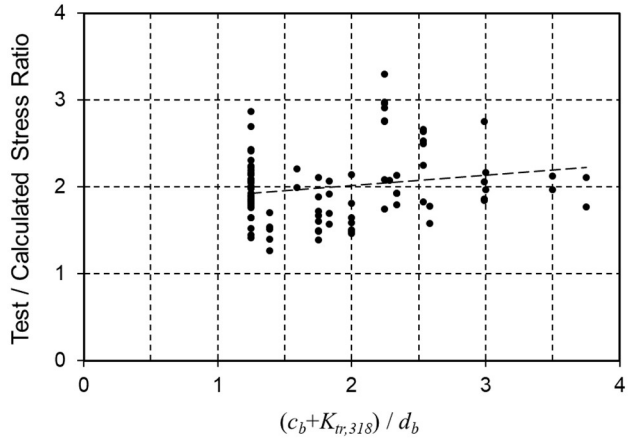

(e) Canbay and Frosch

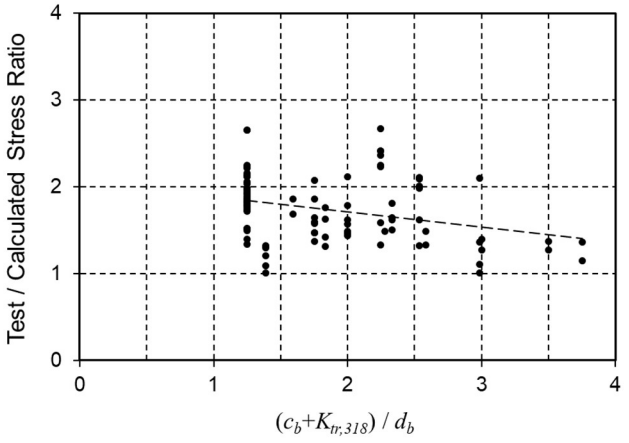

(f) Frosch et al.

Figure 72 - T/C vs. $(c_{b,318}+K_{tr,318})/d_b$ for tension development length equations

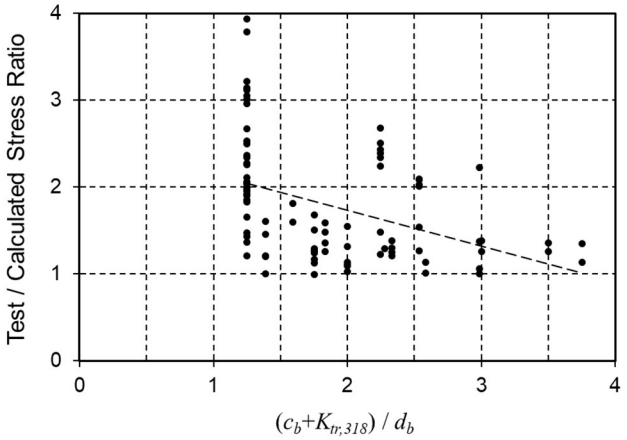

(a) ACI 318-19. $r_1 = 0.61$

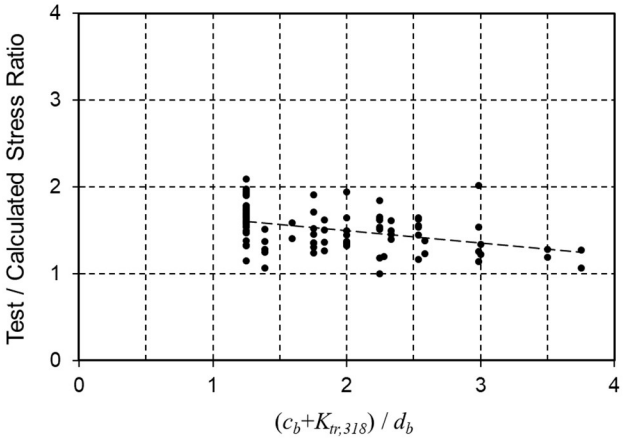

(b) ACI 408R-03. $r_1 = 0.69$

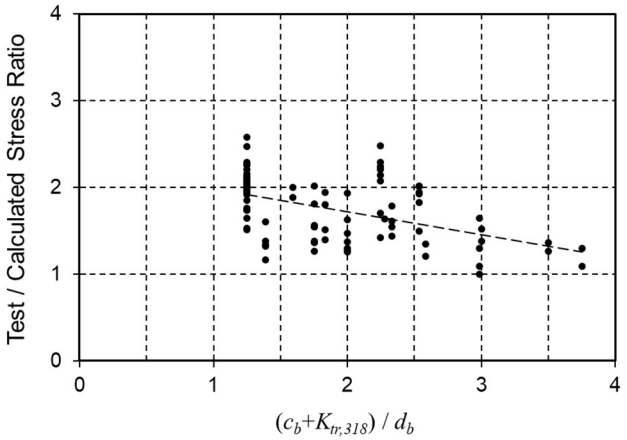

(c) Lepage et al. $r_1 = 0.66$

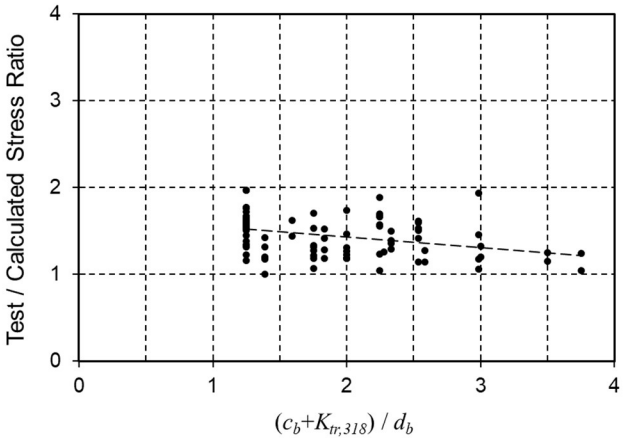

(d) Darwin et al. $r_1 = 0.63$

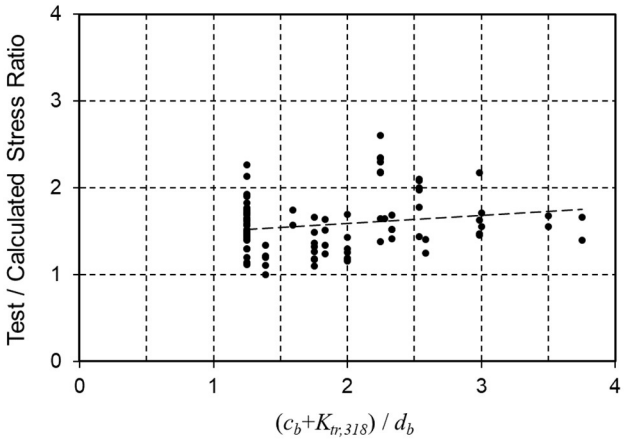

(e) Canbay and Frosch. $r_1 = 0.62$

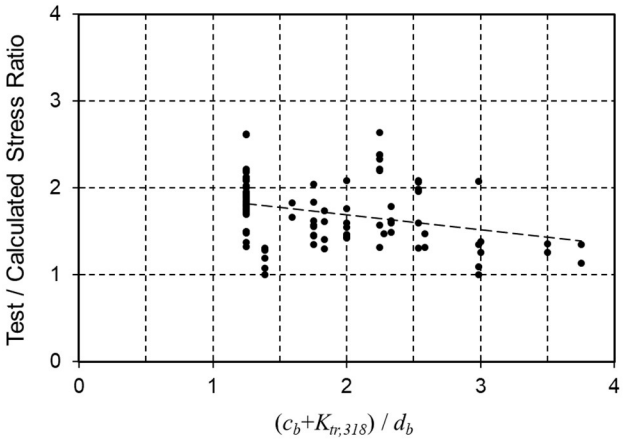

(f) Frosch et al. $r_1 = 0.97$

Figure 73 - T/C vs. $(c_{b,318}+K_{tr,318})/d_b$ for tension development length equations with r_1 factor

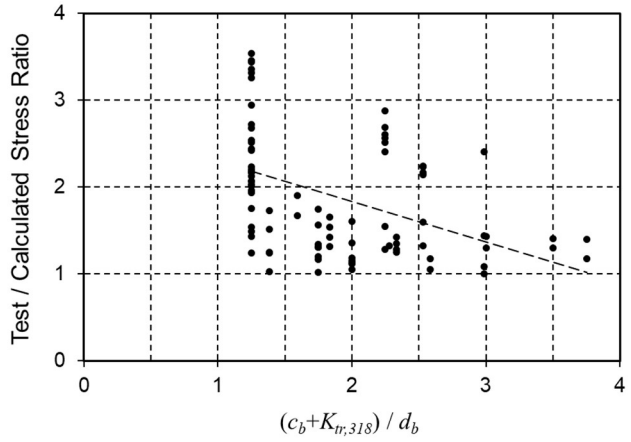

(a) ACI 318-19. $r_2 = 0.72$

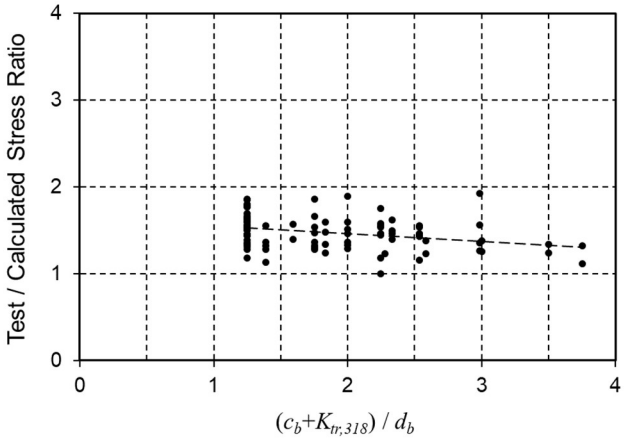

(b) ACI 408R-03. $r_2 = 0.84$

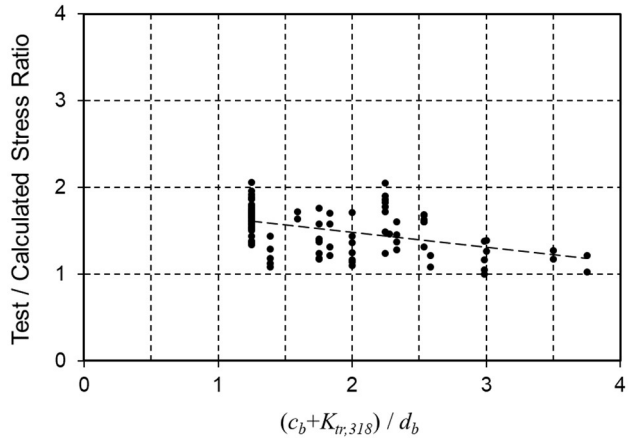

(c) Lepage et al. $r_2 = 0.74$

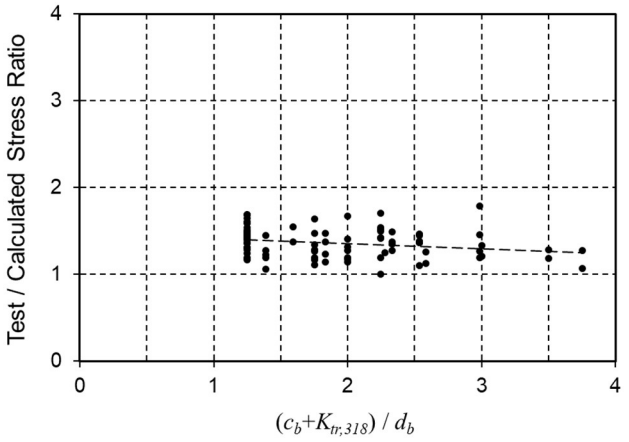

(d) Darwin et al. $r_2 = 0.78$

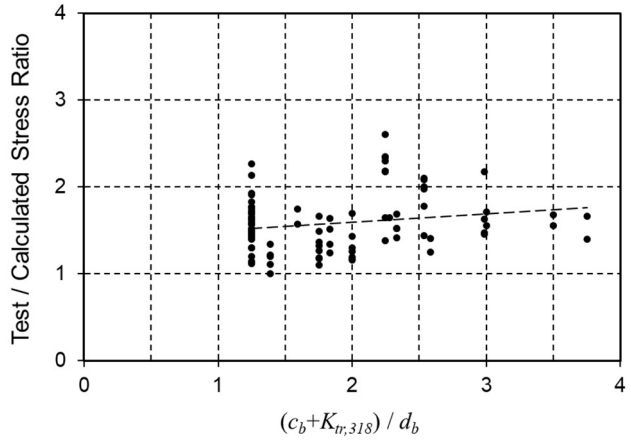

(e) Canbay and Frosch. $r_2 = 0.79$

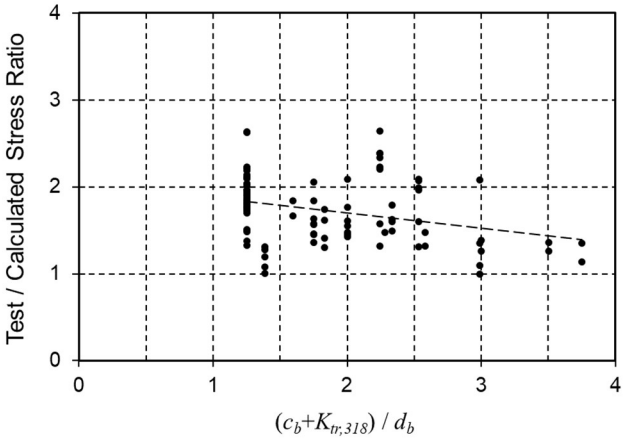

(f) Frosch et al. $r_2 = 0.99$

Figure 74 - T/C vs. $(c_{b,318}+K_{tr,318})/d_b$ for tension development length equations with r_2 factor

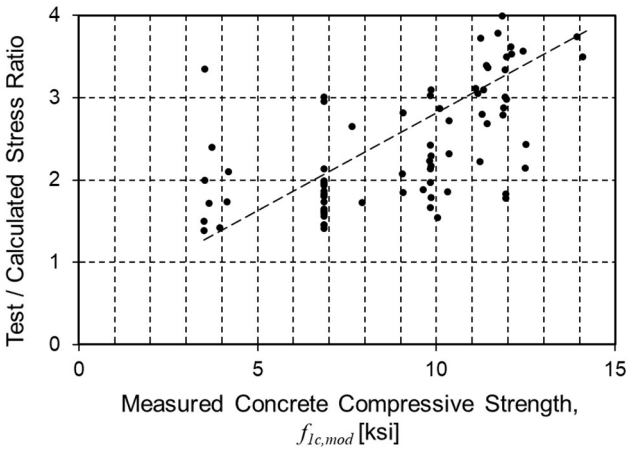

(a) ACI 318-19

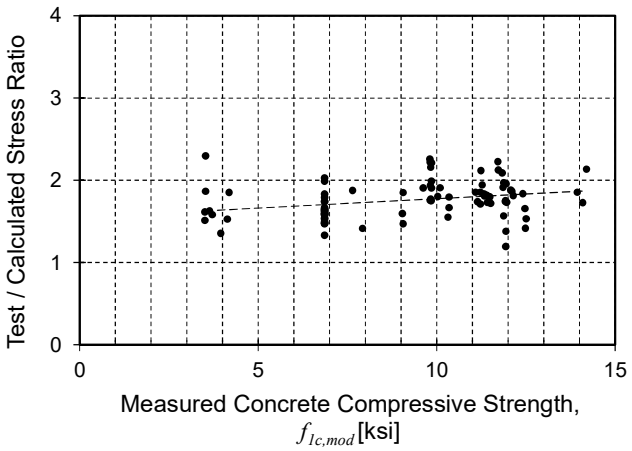

(b) ACI 408R-03

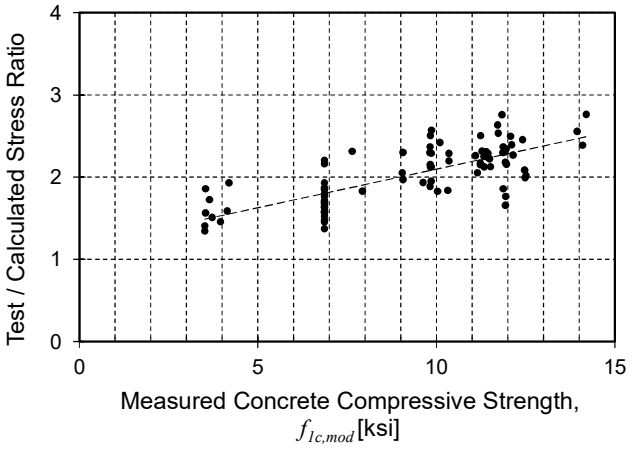

(c) Lepage et al.

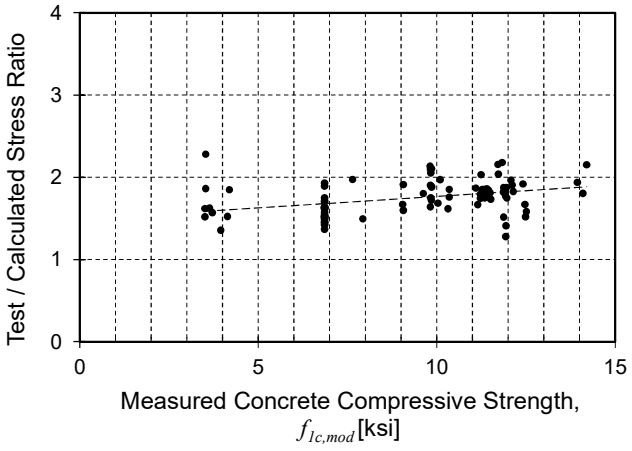

(d) Darwin et al.

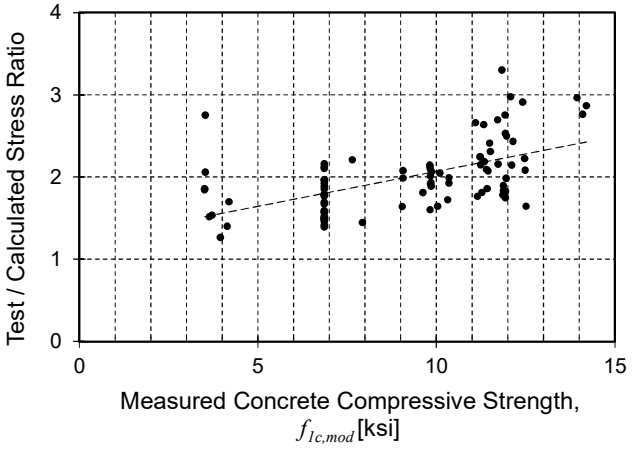

(e) Canbay and Frosch

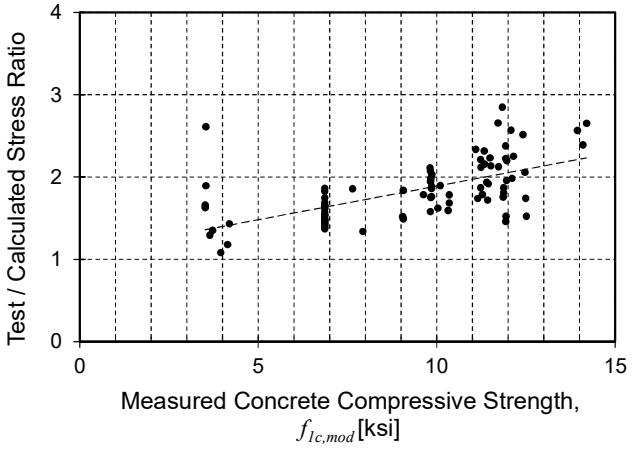

(f) Frosch et al.

Figure 75 - *T*/*C* vs. measured concrete compressive strength, $f_{1c,mod}$, for tension development length equations (1 ksi = 6.895 MPa)

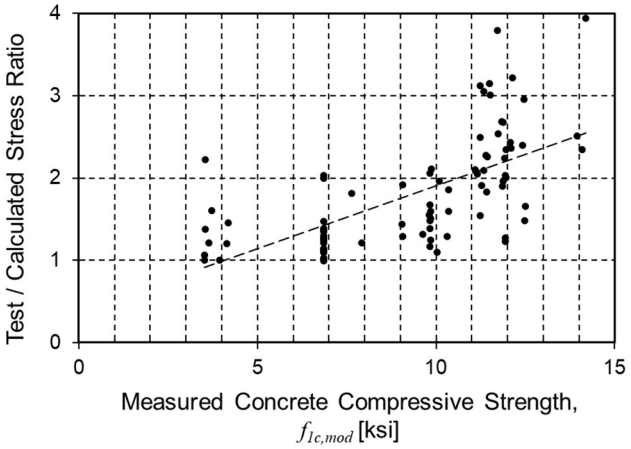

(a) ACI 318-19. $r_1 = 0.61$

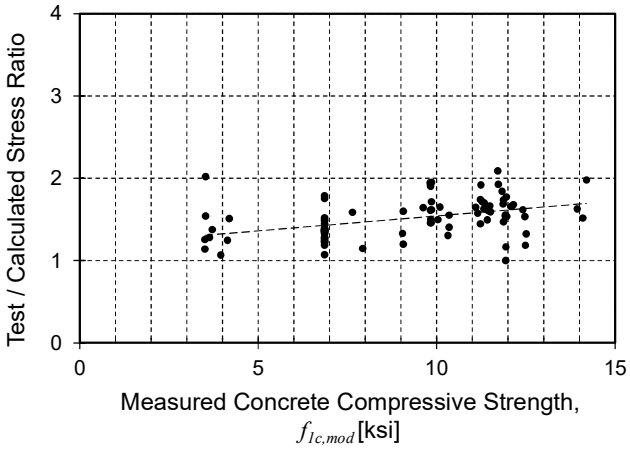

(b) ACI 408R-03. $r_1 = 0.69$

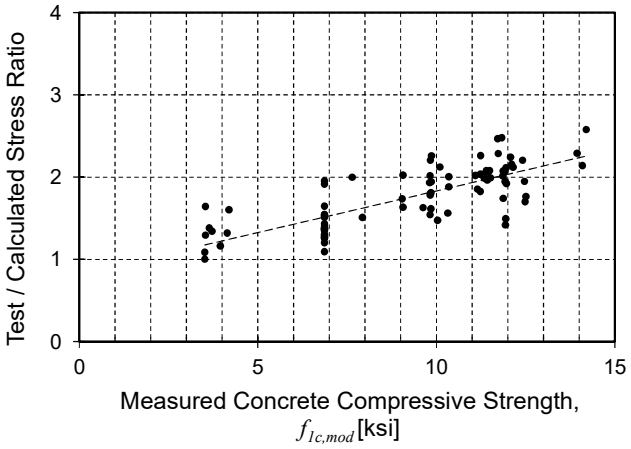

(c) Lepage et al. $r_1 = 0.66$

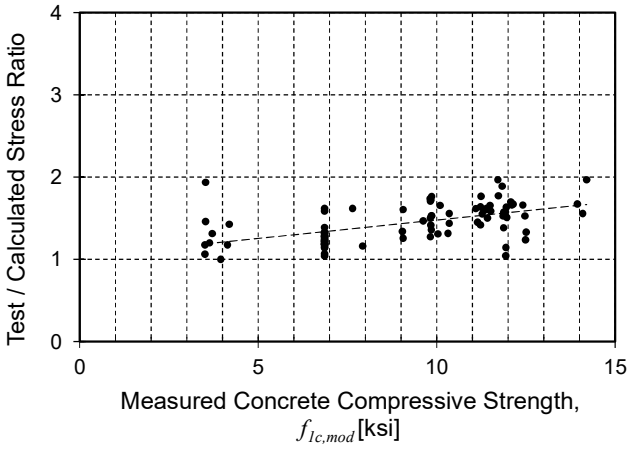

(d) Darwin et al. $r_1 = 0.63$

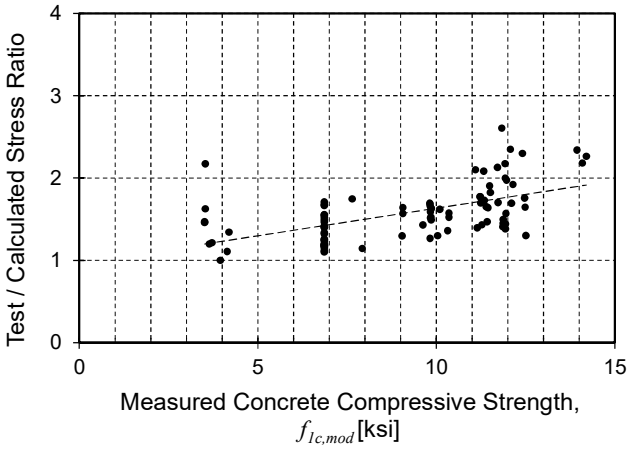

(e) Canbay and Frosch. $r_1 = 0.62$

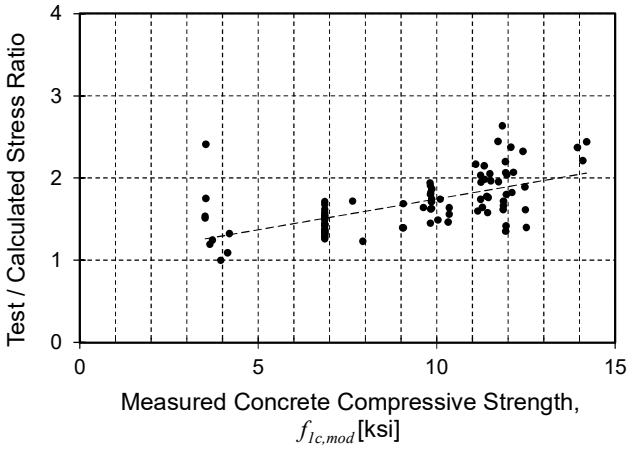

(f) Frosch et al. $r_1 = 0.97$

Figure 76 - T/C vs. measured concrete compressive strength, $f_{1c,mod}$, for tension development equations with r_1 factor (1 ksi = 6.895 MPa)

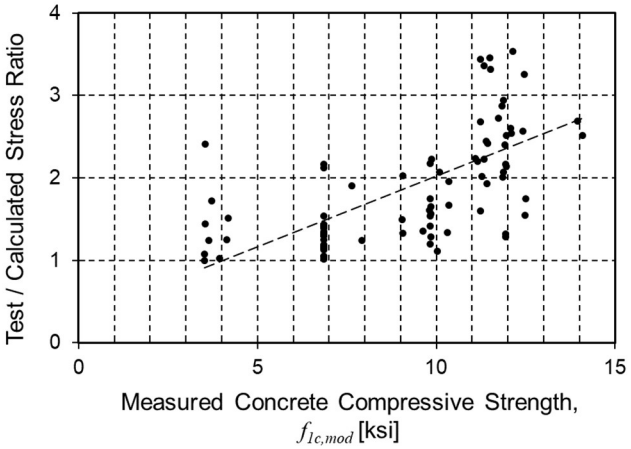

(a) ACI 318-19. $r_2 = 0.72$

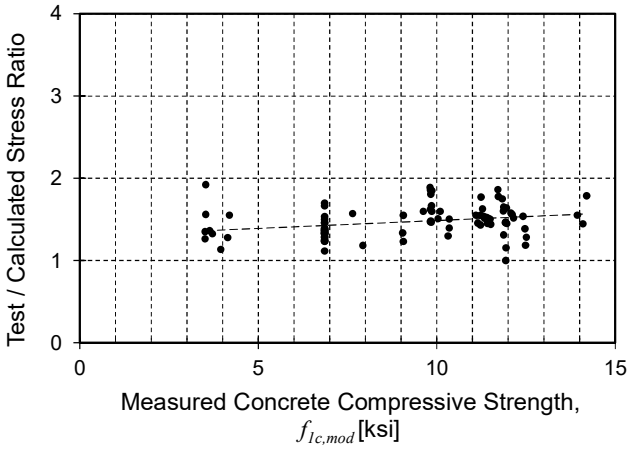

(b) ACI 408R-03. $r_2 = 0.84$

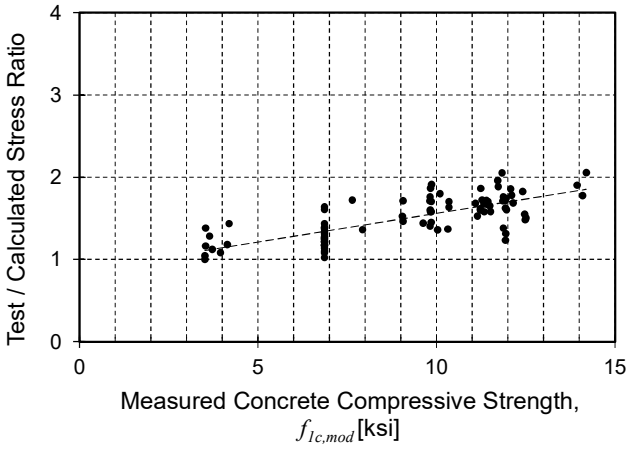

(c) Lepage et al. $r_2 = 0.74$

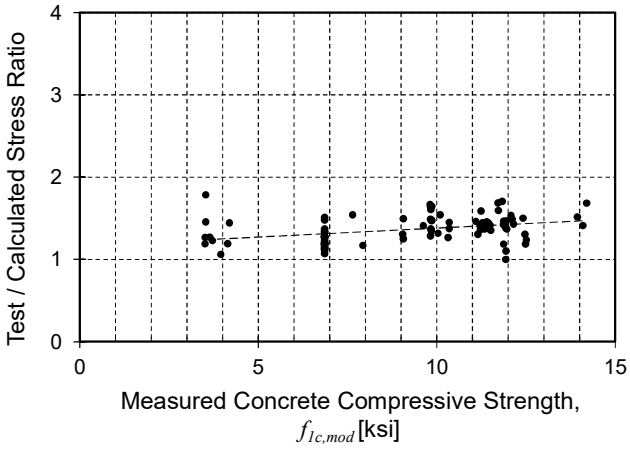

(d) Darwin et al. $r_2 = 0.78$

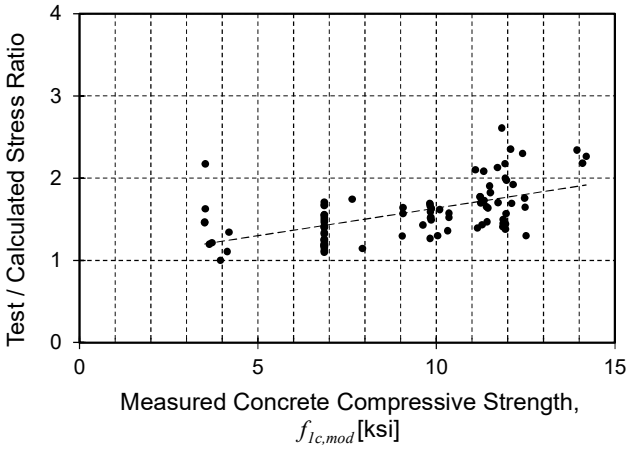

(e) Canbay and Frosch. $r_2 = 0.79$

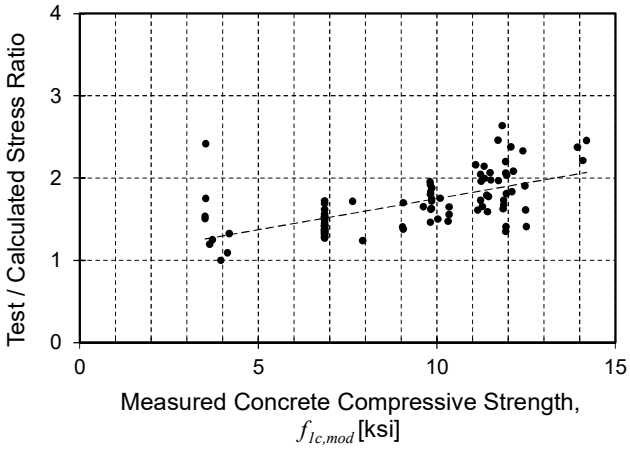

(f) Frosch et al. $r_2 = 0.99$

Figure 77 - T/C vs. measured concrete compressive strength, $f_{1c,mod}$, for tension development equations with r_2 factor (1 ksi = 6.895 MPa)

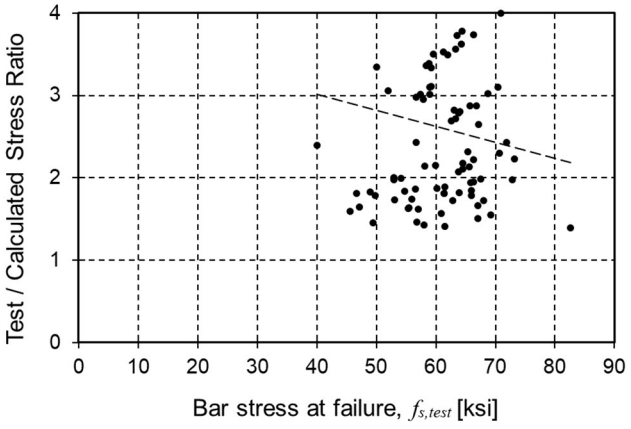

(a) ACI 318-19

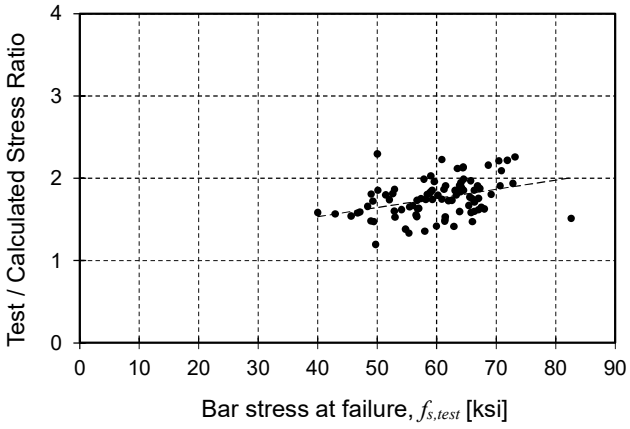

(b) ACI 408R-03

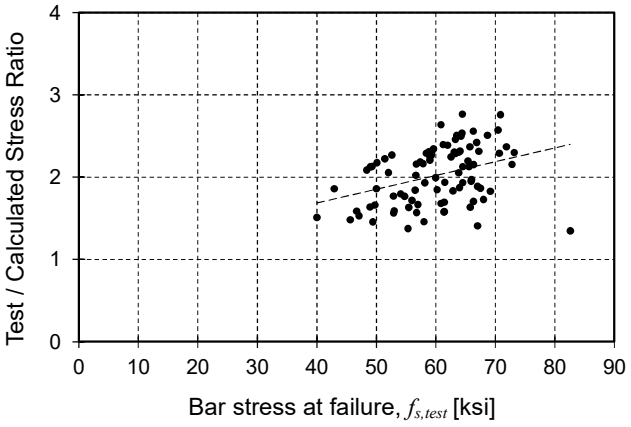

(c) Lepage et al.

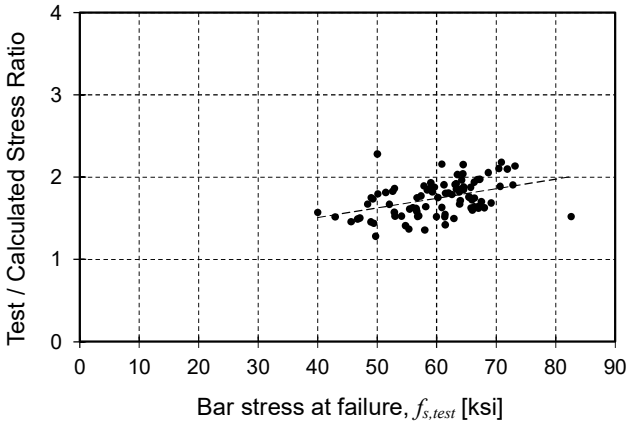

(d) Darwin et al.

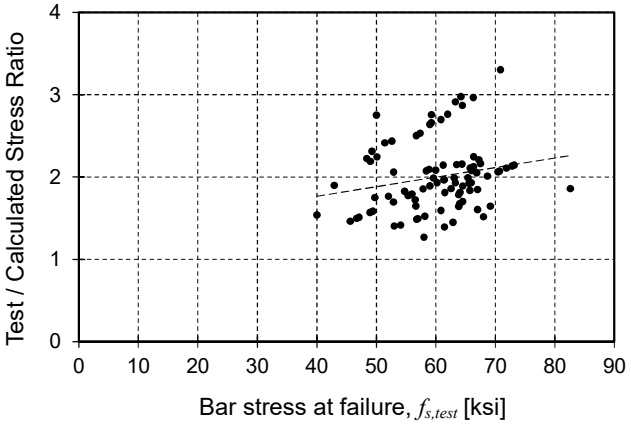

(e) Canbay and Frosch

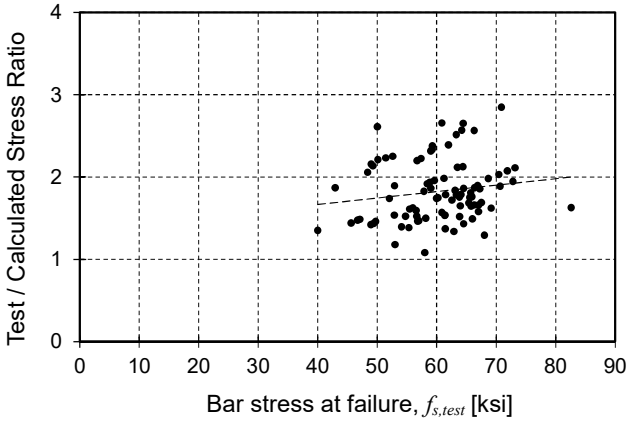

(f) Frosch et al.

Figure 78 - T/C vs. measured steel failure stress $f_{s,test}$ for tension development length equations
(1 ksi = 6.895 MPa)

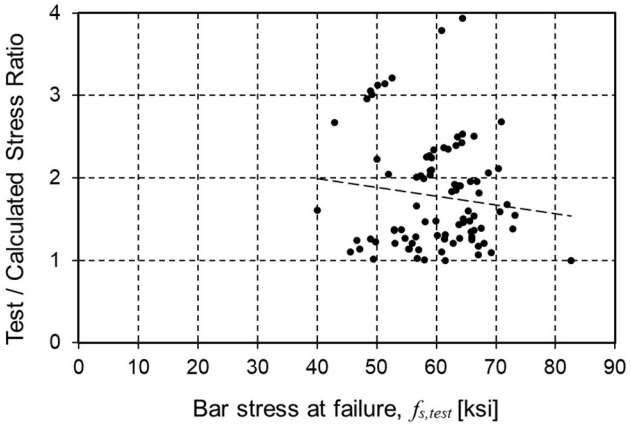

(a) ACI 318-19 $r_1 = 0.61$

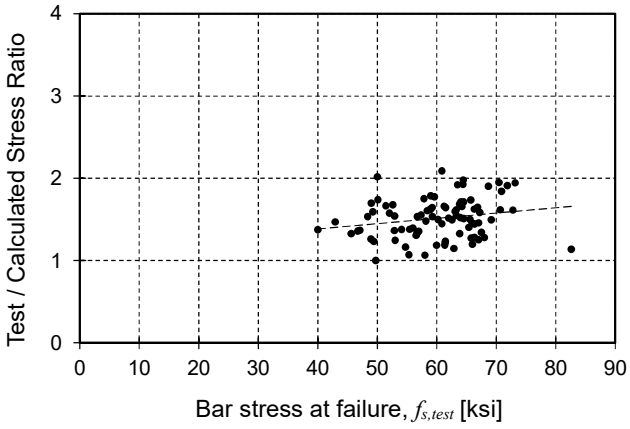

(b) ACI 408R-03 $r_1 = 0.69$

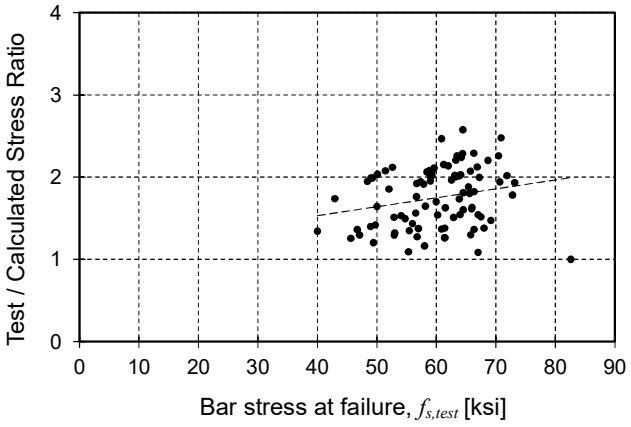

(c) Lepage et al. $r_1 = 0.66$

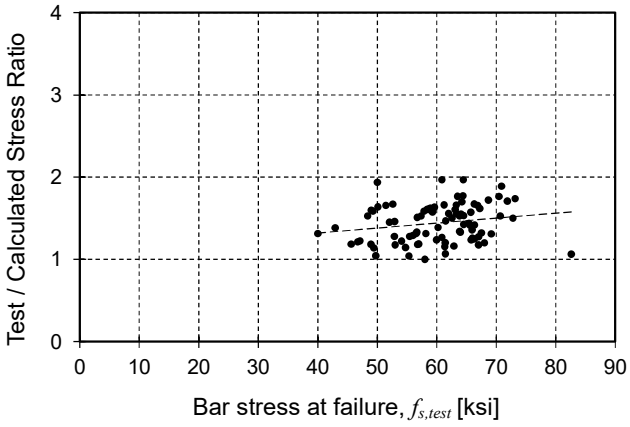

(d) Darwin et al. $r_1 = 0.63$

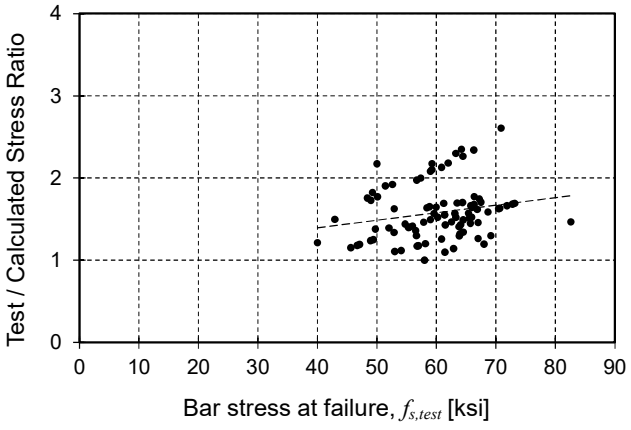

(e) Canbay and Frosch. $r_1 = 0.62$

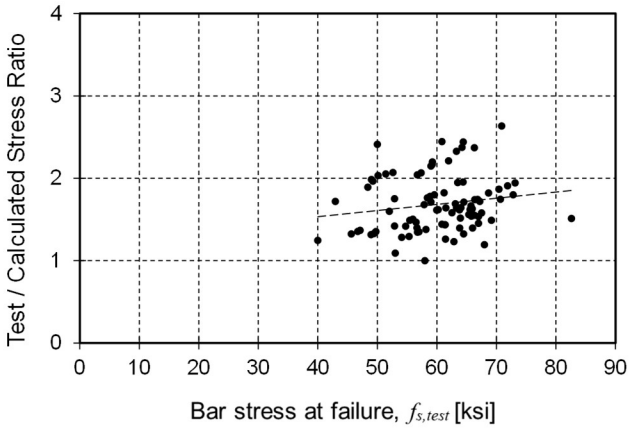

(f) Frosch et al. $r_1 = 0.97$

Figure 79 - *T*/*C* vs. measured steel failure stress $f_{s,test}$ for tension development length equations with r_1 factor (1 ksi = 6.895 MPa)

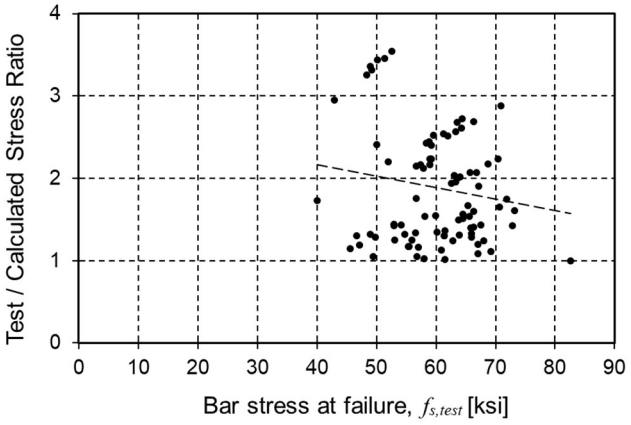

(a) ACI 318-19. $r_2 = 0.72$

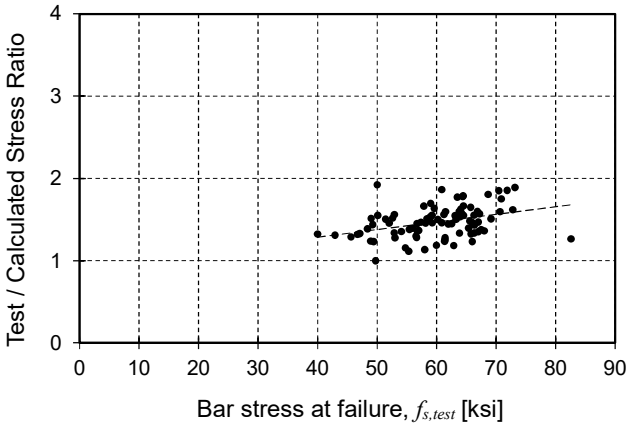

(b) ACI 408R-03. $r_2 = 0.84$

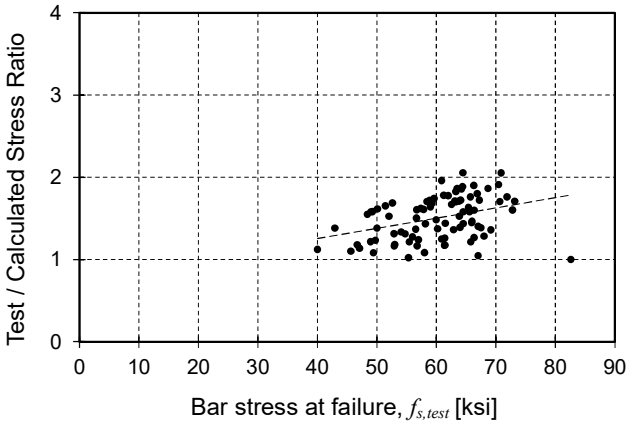

(c) Lepage et al. with $r_2 = 0.74$

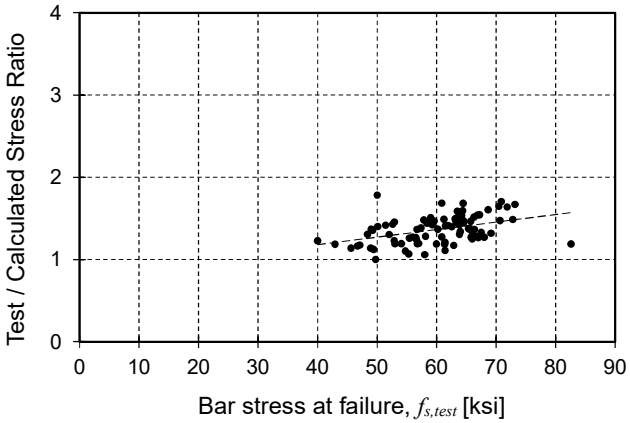

(d) Darwin et al. with $r_2 = 0.78$

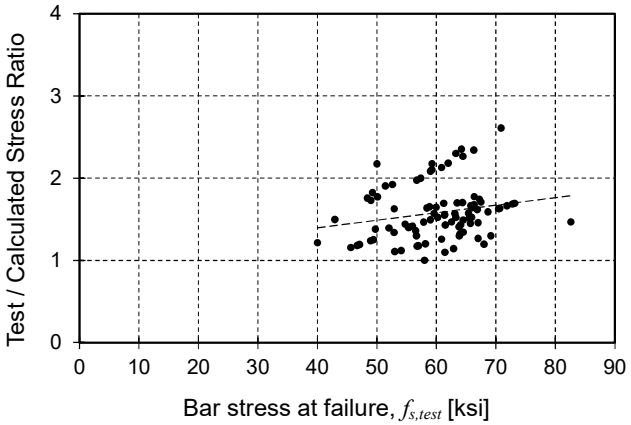

(e) Canbay and Frosch. with $r_2 = 0.79$

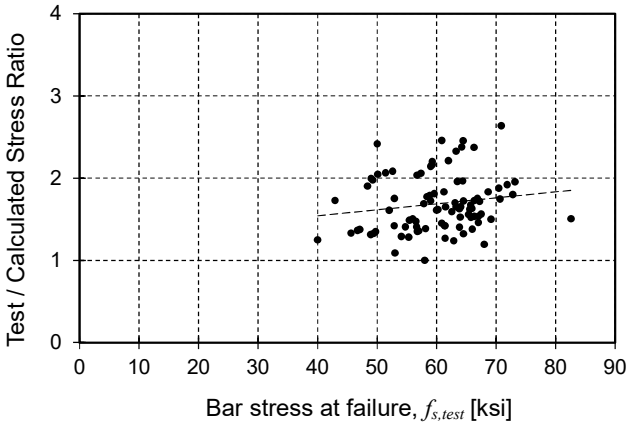

(f) Frosch et al. with $r_2 = 0.99$

Figure 80 - T/C vs. measured steel failure stress $f_{s,test}$ for tension development length equations with r_2 factor (1 ksi = 6.895 MPa)

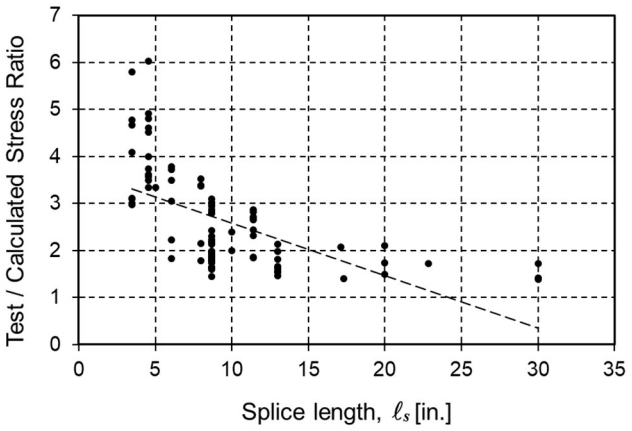

(a) ACI 318-19

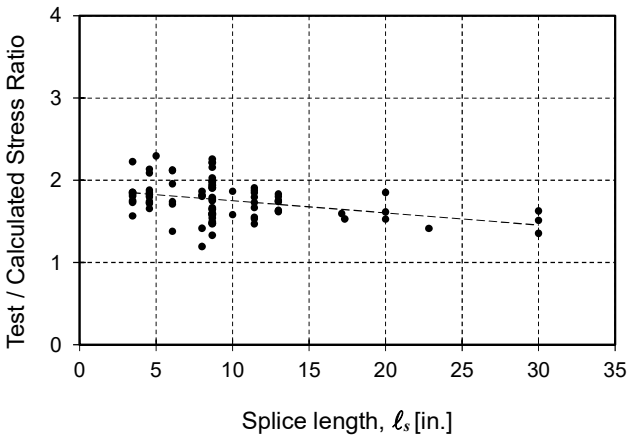

(b) ACI 408R-03

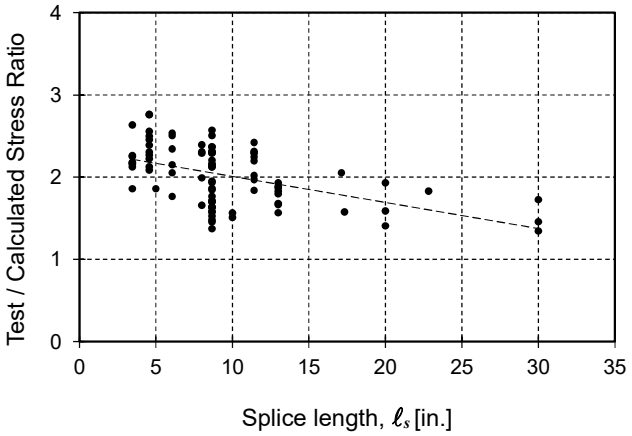

(c) Lepage et al.

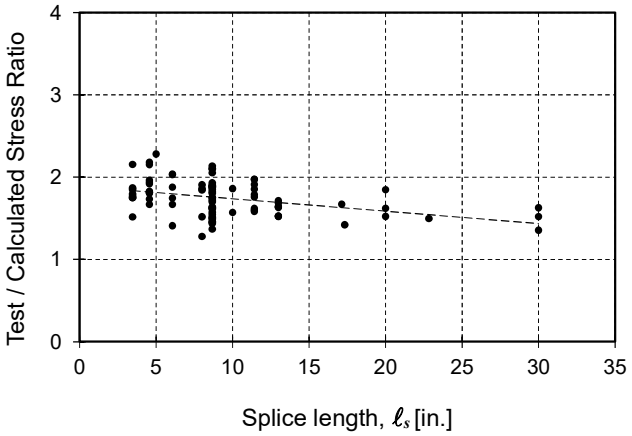

(d) Darwin et al.

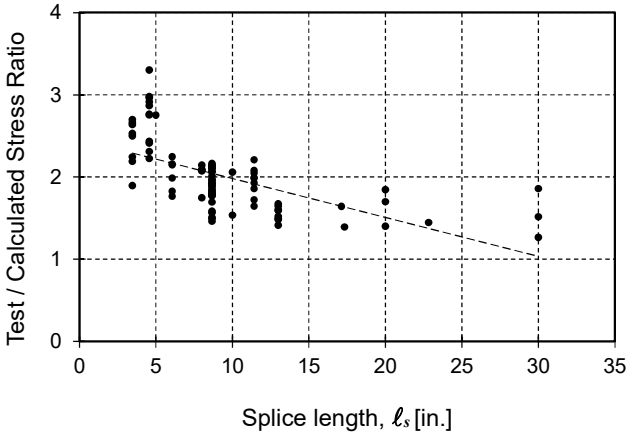

(e) Canbay and Frosch

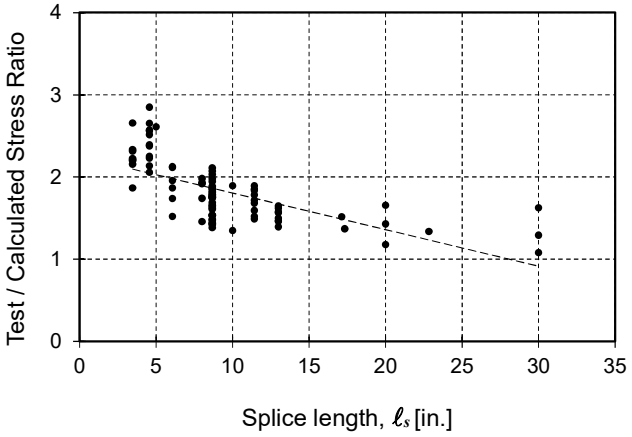

(f) Frosch et al.

Figure 81 - *T*/*C* vs. provided splice length ℓ_s for tension development length equations
(1 in. = 25.4 mm)

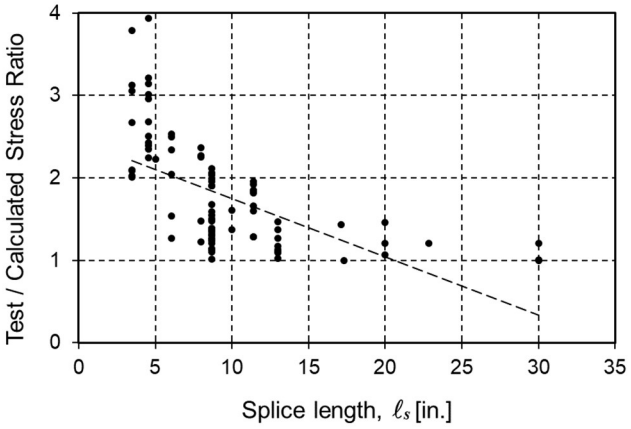

(a) ACI 318-19. $r_1 = 0.61$

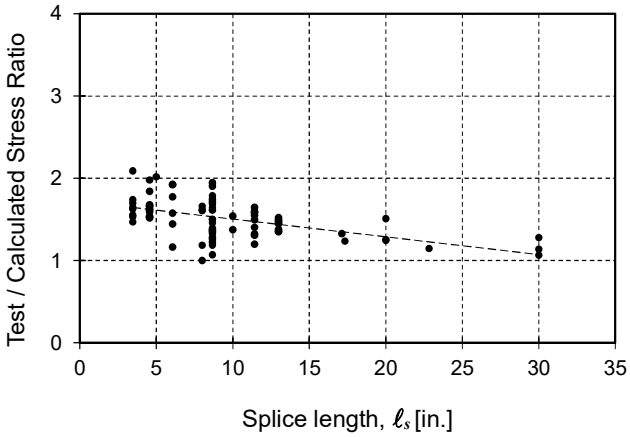

(b) ACI 408R-03. $r_1 = 0.69$

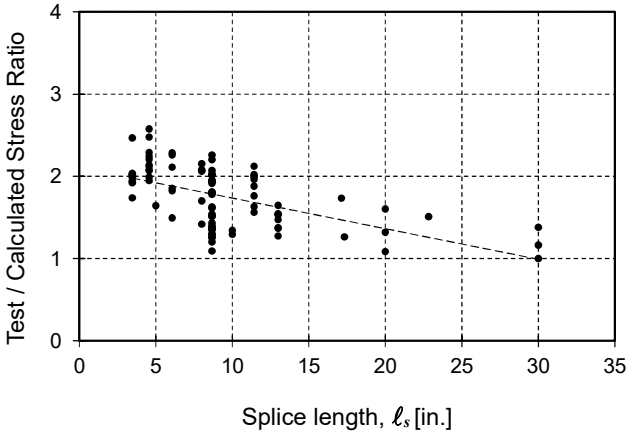

(c) Lepage et al. $r_1 = 0.66$

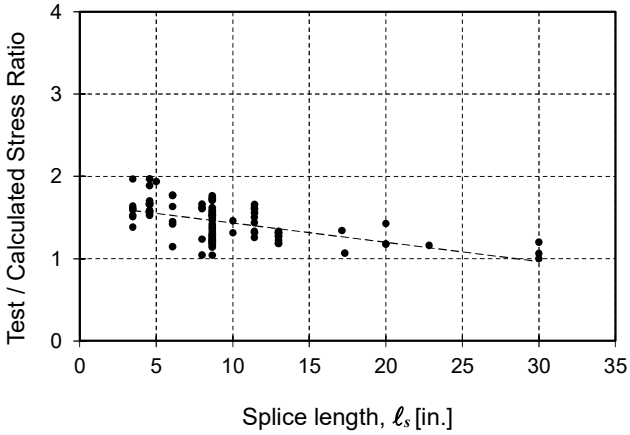

(d) Darwin et al. $r_1 = 0.63$

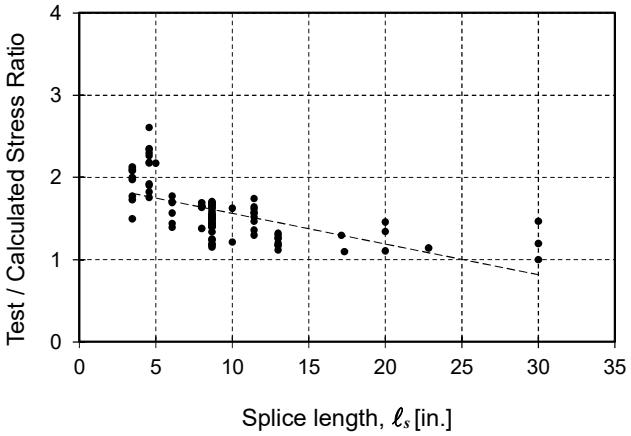

(e) Canbay and Frosch. $r_1 = 0.62$

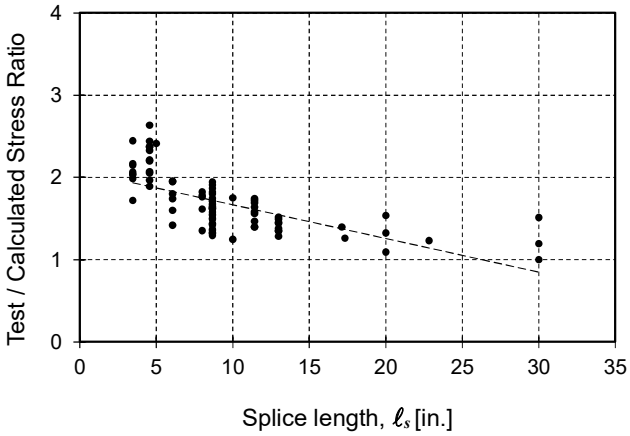

(f) Frosch et al. $r_1 = 0.97$

Figure 82 - *T*/*C* vs vs. provided splice length ℓ_s for tension development length equations with r_1 factor (1 in. = 25.4 mm)

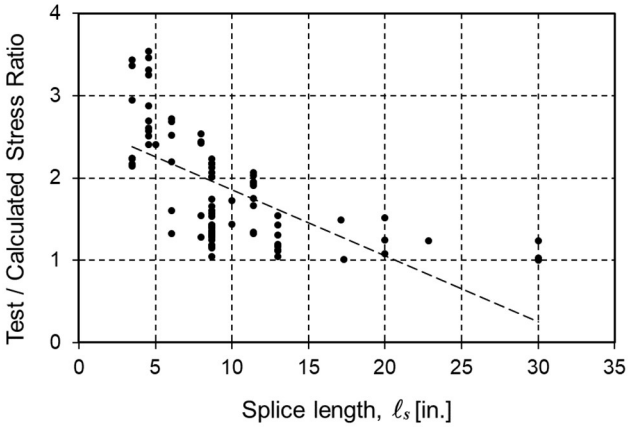

(a) ACI 318-19. r_2 = 0.72

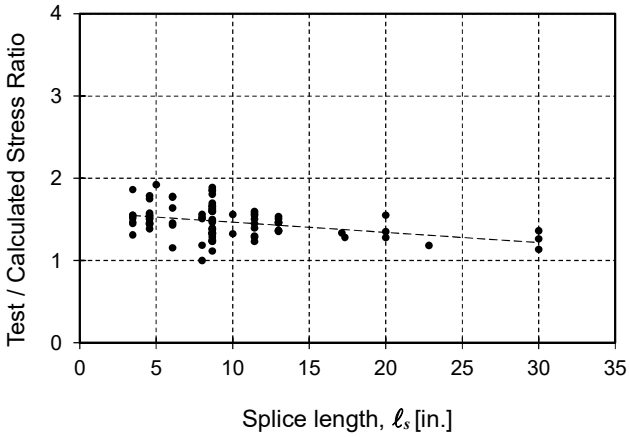

(b) ACI 408R-03. r_2 = 0.84

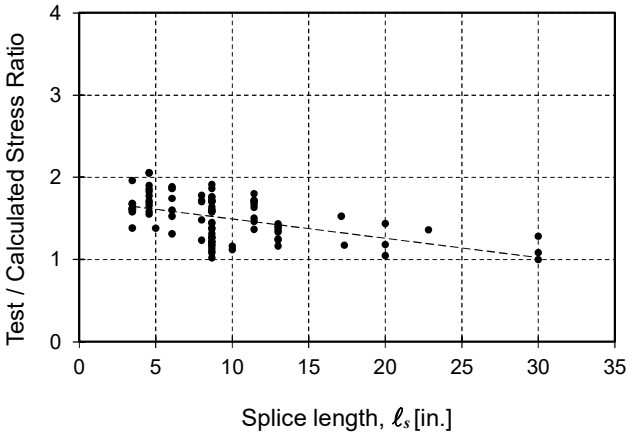

(c) Lepage et al. r_2 = 0.74

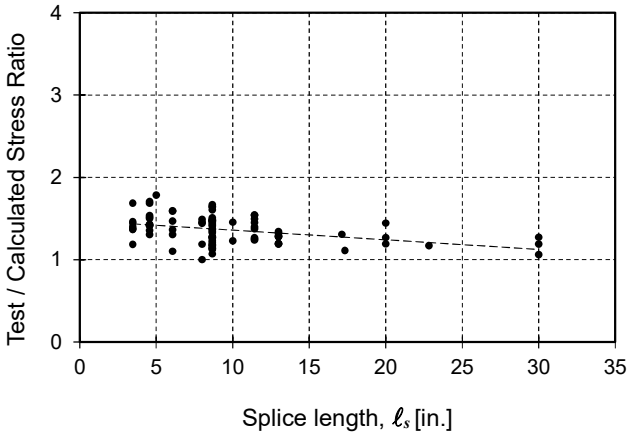

(d) Darwin et al. r_2 = 0.78

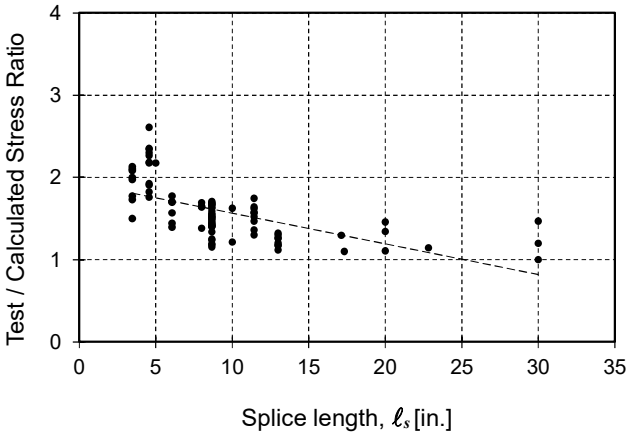

(e) Canbay and Frosch. r_2 = 0.79

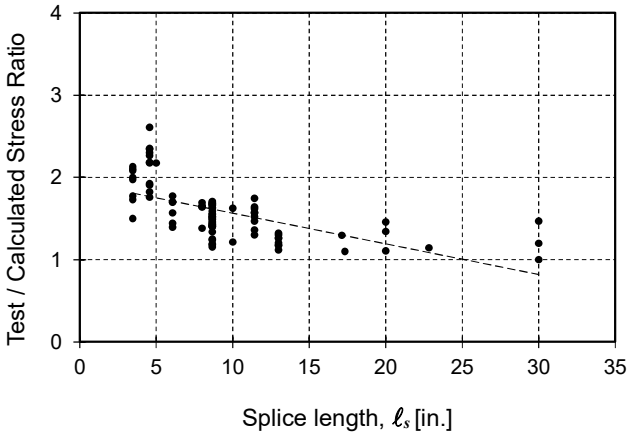

(f) Frosch et al. r_2 = 0.99

Figure 83 - *T*/*C* vs vs. provided splice length ℓ_s for tension development length equations with r_2 factor (1 in. = 25.4 mm)

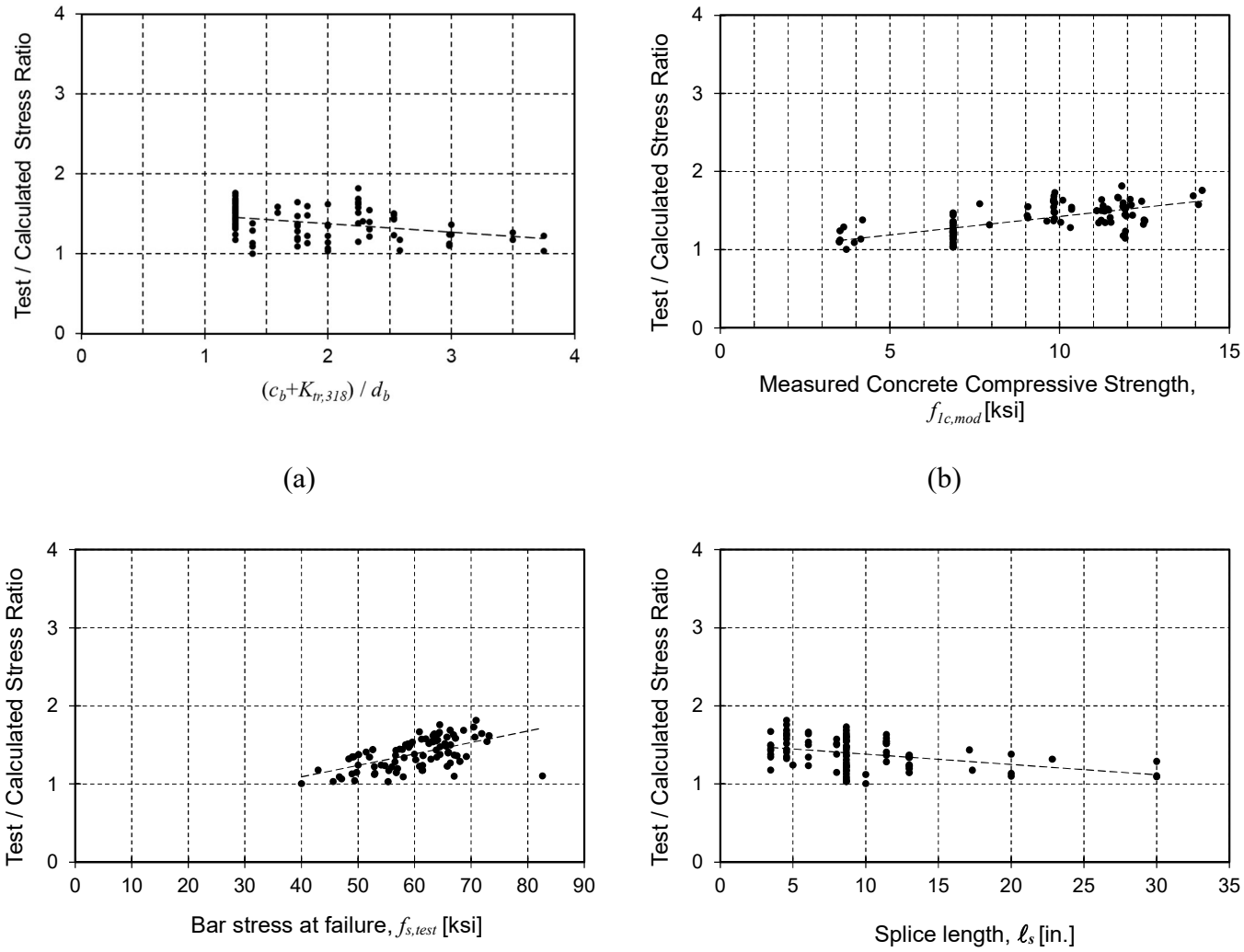

Figure 84 – Lepage et al. [16] with modified ψ_y: T/C vs.: (a) $(c_b + K_{tr,318})/d_b$ (b) measured concrete compressive strength, $f_{1c,mod}$ (c) measured steel failure stress $f_{s,test}$ (d) provided splice length ℓ_s

(1 in. = 25.4 mm; 1 ksi = 6.895 MPa)

Appendix F: Headed Bars: Summary of Database

[1]	[2]	[3]	[4]	[5]	[6]	[7]	[8]
Authors	I.D	F.M.	f_{cm} (psi)	f_y (ksi)	h_c (in.)	h_b (in.)	b_b (in.)
Bashandy [22]	Specimen	I	4290	64.8	15.0	18.0	10.0
Murakami et al. [29]	No. 100	I	5700	53.6	11.8	15.7	10.2
	No. 101	I	5700	53.6	11.8	15.7	10.2
	B8-M	I	4280	74.1	11.8	15.7	10.2
	B7-M	I	4280	74.1	11.8	15.7	10.2
Wallace et al. [32]	BCEJ1	I	5190	70.0	18.0	24.0	18.0
Matsushima et al. [28]	H	II	4770	79.9	15.7	18.9	13.8
	Hs	II	8830	85.0	15.7	18.9	13.8
Yoshida et al. [33]	No.1	I	5470	81.5	13.8	15.7	11.8
	No.2	I	5470	81.5	13.8	15.7	11.8
	No.3	I	4500	81.5	13.8	15.7	11.8
Takeuchi et al. [30]	0-1	I	6400	64.5	15.7	17.7	13.8
	0-2	II	8830	53.6	15.7	17.7	13.8
	0-3	I	3520	54.7	15.7	17.7	13.8
	0-4	I	6400	64.5	15.7	17.7	13.8
Kato [26]	No.1	I	8820	75.6	18.7	17.7	12.8
	No.2	I	10270	73.2	18.7	17.7	12.8
Adachi et al. [21]	J30-12-0	II	4480	76.0	17.7	17.7	13.8
	J60-12-0	II	9150	76.0	17.7	17.7	13.8
	J30-12-P1	I	4480	76.0	17.7	17.7	13.8
	J60-12-P1	II	9150	79.9	17.7	17.7	13.8
	J30-12-P2	I	4480	76.0	17.7	17.7	13.8
	J60-12-P2	I	9150	76.0	17.7	17.7	13.8
Chun et al. [23]	JM-1	I	8950	58.5	19.7	19.7	13.8
	JM-2	I	8720	58.5	19.7	19.7	13.8
	JM-No.11-1a	I	4760	66.4	20.5	19.9	17.7
	JM-No.11-1b	I	4760	66.4	20.5	19.9	17.7
Ishida et al. [24]	P2	II	3480	76.0	15.7	15.7	31.5
	P3	II	3480	76.0	15.7	15.7	31.5
	P4	II	4480	76.0	15.7	15.7	39.5
Tazaki et al. [31]	E1	I	4410	55.0	11.8	11.8	11.8
	E2	I	4410	55.0	11.8	11.8	11.8
Kang et al. [25]	JH	I	4220	69.8	17.7	21.3	17.7
Lee and Yu [27]	W0-M1	I	4450	68.6	16.0	18.0	12.0
	W150-M1	I	5190	68.6	16.0	18.0	12.0

1000 psi = 1 ksi = 6.895 MPa; 1 in. = 25.4 mm; 1 kip = 4.45 kN

F.M. = Failure Mode from [5]. I = Category–I (member flexural hinging followed by modest joint deterioration); II = Category–II (member flexural hinging followed by joint failure)

[1]	[2]	[9]	[10]	[11]	[12]	[13]	[14]
Authors	I.D	Bar Size	d_b (in.)	A_b (in.^{2})	ℓ_p (in.)	n	A_{hs} (in.^{2})
Bashandy [22]	Specimen	D25	1.000	0.79	12.8	2	1.58
Murakami et al. [29]	No. 100	D16	0.625	0.31	8.9	4	1.24
	No. 101	D16	0.625	0.31	8.9	4	1.24
	B8-M	D19	0.750	0.44	8.9	3	1.32
	B7-M	2 D19, 1 D16	0.750,	0.44,0.312	8.9	2,1	1.19
Wallace et al. [32]	BCEJ1	No. 8	1.000	0.79	13.9	4	3.16
Matsushima et al. [28]	H	D25	1.000	0.79	11.8	3	2.37
	Hs	D25	1.000	0.79	8.0	3	2.37
Yoshida et al. [33]	No.1	D19	0.750	0.44	10.4	4	1.76
	No.2	D19	0.750	0.44	10.4	4	1.76
	No.3	D19	0.750	0.44	10.4	4	1.76
Takeuchi et al. [30]	0-1	D25	1.000	0.79	10.5	3	2.37
	0-2	D25	0.980	0.79	10.5	3	2.37
	0-3	D25	1.000	0.79	10.5	3	2.37
	0-4	D25	1.000	0.79	11.8	3	2.37
Kato [26]	No.1	D22	0.875	0.60	14.2	8	4.80
	No.2	D22	0.875	0.60	14.2	8	4.80
Adachi et al. [21]	J30-12-0	D25	1.000	0.79	12.0	4	3.16
	J60-12-0	D25	1.000	0.79	12.0	6	4.74
	J30-12-P1	D25	1.000	0.79	12.0	4	3.16
	J60-12-P1	D25	1.000	0.79	12.0	6	4.74
	J30-12-P2	D25	1.000	0.79	12.0	4	3.16
	J60-12-P2	D25	1.000	0.79	12.0	6	4.74
Chun et al. [23]	JM-1	D22/No.7	0.875	0.60	15.1	4	2.40
	JM-2	D22/No.7	0.875	0.60	15.1	8	4.80
	JM-No.11-1a	D36/No.11	1.410	1.56	17.3	3	4.68
	JM-No.11-1b	D36/No.11	1.410	1.56	17.3	3	4.68
Ishida et al. [24]	P2	D22	0.875	0.60	11.9	7	4.20
	P3	D22	0.875	0.60	11.9	7	4.20
	P4	D22	1.000	0.60	11.9	9	5.40
Tazaki et al. [31]	E1	D16	0.625	0.31	6.1	6	1.85
	E2	D16	0.625	0.31	3.8	6	1.85
Kang et al. [25]	JH	D19	0.750	0.44	11.3	4	1.77
Lee and Yu [27]	W0-M1	D22	0.875	0.60	12.6	4	2.40
	W150-M1	D22	0.875	0.60	12.6	4	2.40

[1]	[2]	[15]	[16]	[17]	[18]	[19]	[20]
Authors	I.D	Conf. by transv. beams*	R_n	b_j (in.)	V_n (kip)	V_p (kip)	V_p/V_n
Bashandy [22]	Specimen	NC	12	13.0	153	94	0.62
Murakami et al. [29]	No. 100	NC	12	11.8	126	61	0.48
	No. 101	NC	12	11.8	126	63	0.50
	B8-M	NC	12	11.8	109	88	0.80
	B7-M	NC	12	11.8	109	77	0.70
Wallace et al. [32]	BCEJ1	C	15	18.0	350	202	0.58
Matsushima et al. [28]	H	NC	12	15.7	204	166	0.81
	Hs	NC	12	15.7	278	146	0.52
Yoshida et al. [33]	No.1	NC	12	13.8	169	109	0.65
	No.2	NC	12	13.8	169	110	0.65
	No.3	NC	12	13.8	153	111	0.72
Takeuchi et al. [30]	0-1	NC	12	15.7	237	120	0.51
	0-2	NC	12	15.7	278	141	0.51
	0-3	NC	12	15.7	175	100	0.57
	0-4	NC	12	15.7	237	127	0.54
Kato [26]	No.1	NC	12	18.7	394	350	0.89
	No.2	NC	12	18.7	420	331	0.79
Adachi et al. [21]	J30-12-0	NC	12	17.7	252	190	0.75
	J60-12-0	NC	12	17.7	360	269	0.75
	J30-12-P1	NC	12	17.7	252	191	0.76
	J60-12-P1	NC	12	17.7	360	285	0.79
	J30-12-P2	NC	12	17.7	252	194	0.77
	J60-12-P2	NC	12	17.7	360	295	0.82
Chun et al. [23]	JM-1	NC	12	16.7	373	146	0.39
	JM-2	NC	12	16.7	369	270	0.73
	JM-No.11-1a	NC	12	21.7	368	274	0.74
	JM-No.11-1b	NC	12	21.7	368	268	0.73
Ishida et al. [24]	P2	NC	12	15.7	174	238	1.36
	P3	C	15	15.7	218	261	1.20
	P4	C	15	15.7	247	267	1.08
Tazaki et al. [31]	E1	NC	12	11.8	111	102	0.92
	E2	NC	12	11.8	111	89	0.81
Kang et al. [25]	JH	NC	12	17.7	244	122	0.50
Lee and Yu [27]	W0-M1	NC	12	24.0	307	164	0.53
	W150-M1	NC	12	12.0	166	162	0.98

*Confinement by transverse beams, per ACI 318-19 §15.2.8, where NC=Not Confined and C=Confined

[1]	[2]	[21]	[22]	[23]	[24]	[25]		[26]	[27]
Authors	I.D	***d*** (in.)	***a*** (in.)	β_1	***c*** (in.)	ε_s		f_y / E_s	***Mn*** (kip-in.)
Bashandy [22]	Specimen	15.5	2.81	0.84	3.36	0.013	≥	0.0022	1440
Murakami et al. [29]	No. 100	13.6	1.34	0.76	1.75	0.022	≥	0.0018	859
	No. 101	13.6	1.34	0.76	1.75	0.022	≥	0.0018	859
	B8-M	13.6	2.63	0.84	3.14	0.012	≥	0.0026	1200
	B7-M	13.6	2.37	0.84	2.84	0.013	≥	0.0026	1090
Wallace et al. [32]	BCEJ1	21.5	2.79	0.79	3.52	0.017	≥	0.0024	4450
Matsushima et al. [28]	H	15.1	3.39	0.81	4.18	0.010	≥	0.0028	2540
	Hs	15.1	3.39	0.81	4.18	0.010	≥	0.0028	2540
Yoshida et al. [33]	No.1	14.0	2.61	0.78	3.37	0.012	≥	0.0028	1820
	No.2	14.0	2.61	0.78	3.37	0.012	≥	0.0028	1820
	No.3	14.0	3.18	0.83	3.85	0.010	≥	0.0028	1780
Takeuchi et al. [30]	0-1	15.6	2.04	0.73	2.80	0.016	≥	0.0022	2220
	0-2	15.6	1.95	0.65	3.00	0.015	≥	0.0029	2940
	0-3	15.6	3.14	0.85	3.69	0.012	≥	0.0019	1810
	0-4	15.6	2.04	0.73	2.80	0.016	≥	0.0022	2220
Kato [26]	No.1	15.5	3.78	0.65	5.82	0.007	≥	0.0026	4920
	No.2	15.5	3.15	0.65	4.84	0.009	≥	0.0025	4880
Adachi et al. [21]	J30-12-0	15.7	4.58	0.83	5.54	0.008	≥	0.0026	3230
	J60-12-0	15.0	3.36	0.65	5.17	0.008	≥	0.0026	4780
	J30-12-P1	15.7	4.58	0.83	5.54	0.008	≥	0.0026	3230
	J60-12-P1	15.0	3.36	0.65	5.17	0.008	≥	0.0026	4780
	J30-12-P2	15.7	4.58	0.83	5.54	0.008	≥	0.0026	3230
	J60-12-P2	15.0	3.36	0.65	5.17	0.008	≥	0.0026	4780
Chun et al. [23]	JM-1	17.3	1.34	0.65	2.06	0.024	≥	0.0020	2330
	JM-2	16.8	2.75	0.65	4.23	0.011	≥	0.0020	4340
	JM-No.11-1a	17.1	4.34	0.81	5.34	0.009	≥	0.0023	4640
	JM-No.11-1b	17.1	4.34	0.81	5.34	0.009	≥	0.0023	4640
Ishida et al. [24]	P2	13.7	3.43	0.85	4.03	0.009	≥	0.0026	3840
	P3	13.7	3.43	0.85	4.03	0.009	≥	0.0026	3840
	P4	13.7	3.51	0.85	4.13	0.009	≥	0.0026	4920
Tazaki et al. [31]	E1	10.0	2.30	0.83	2.77	0.010	≥	0.0019	896
	E2	10.0	2.30	0.83	2.77	0.010	≥	0.0019	896
Kang et al. [25]	JH	19.8	1.94	0.84	2.31	0.024	≥	0.0024	2320
Lee and Yu [27]	W0-M1	16.0	3.63	0.83	4.38	0.010	≥	0.0024	2340
	W150-M1	16.0	3.11	0.79	3.93	0.011	≥	0.0024	2380

[1]	[2]	[28]	[29]	[30]	[31]	[32]	[33]
Authors	I.D	L_b (in.)	L_n (in.)	L_c (in.)	M_{peak} (kip-in.)	M_{peak}/M_n	$\delta_{0.8peak}$
Bashandy [22]	Specimen	64.5	57.0	96.0	1590	1.10	0.053
Murakami et al. [29]	No. 100	59.1	53.2	59.1	1030	1.20	0.080
	No. 101	59.1	53.2	59.1	1070	1.24	0.083
	B8-M	59.1	53.2	59.1	1400	1.16	0.060
	B7-M	59.1	53.2	59.1	1240	1.13	0.070
Wallace et al. [32]	BCEJ1	129.0	120.0	120.0	4950	1.11	0.048
Matsushima et al. [28]	H	78.7	70.9	97.6	2630	1.03	0.035
	Hs	78.7	70.9	97.6	2470	0.97	0.035
Yoshida et al. [33]	No.1	73.8	66.9	78.7	1680	0.92	0.040
	No.2	73.8	66.9	78.7	1700	0.93	0.040
	No.3	73.8	66.9	78.7	1670	0.94	0.040
Takeuchi et al. [30]	0-1	66.9	59.1	57.1	2460	1.11	0.050
	0-2	66.9	59.1	57.1	2900	0.99	0.033
	0-3	66.9	59.1	57.1	1930	1.06	0.050
	0-4	66.9	59.1	57.1	2590	1.17	0.050
Kato [26]	No.1	78.7	69.4	88.6	5740	1.17	0.040
	No.2	78.7	69.4	88.6	5580	1.14	0.080
Adachi et al. [21]	J30-12-0	59.1	50.2	59.1	3490	1.08	0.032
	J60-12-0	59.1	50.2	59.1	4850	1.01	0.033
	J30-12-P1	59.1	50.2	59.1	3510	1.09	0.045
	J60-12-P1	59.1	50.2	59.1	5140	1.07	0.034
	J30-12-P2	59.1	50.2	59.1	3570	1.10	0.062
	J60-12-P2	59.1	50.2	59.1	5320	1.11	0.067
Chun et al. [23]	JM-1	88.6	78.7	102.6	2960	1.27	0.068
	JM-2	88.6	78.7	102.6	5040	1.16	0.040
	JM-No.11-1a	89.0	78.7	102.6	4890	1.06	0.075
	JM-No.11-1b	89.0	78.7	102.6	4780	1.03	0.065
Ishida et al. [24]	P2	44.3	36.4	51.2	4000	1.04	0.030
	P3	44.3	36.4	51.2	4400	1.15	0.030
	P4	44.3	36.4	51.2	4680	0.95	0.030
Tazaki et al. [31]	E1	53.2	47.2	57.9	1080	1.21	0.060
	E2	53.2	47.2	57.9	951	1.06	0.060
Kang et al. [25]	JH	103.4	94.5	141.7	2700	1.16	0.036
Lee and Yu [27]	W0-M1	84.7	76.7	106.3	2730	1.17	0.080
	W150-M1	84.7	76.7	106.3	2750	1.16	0.080

Appendix G: Headed Bars: Average Length Ratios

Table 6 – Headed bars: Average length ratios: length in row / length in column

	ℓ_p	$\ell_{dt,318\text{-}14}$ no caps [Eq. (30)]	$\ell_{dt,25.4.4}$ [Eq. (23)]	$\ell_{dt,18.8.5.2}$ [Eq. (24)]	$\ell_{dc,25.4.9}$ [Eq. (25)]	ℓ_{ehy} [Eq. (33)]	$\ell_{dh,18.8.5.1}$ [Eq. (31)]	$0.7l_d$, Case I [Eq. (34)]	$0.7l_d$, Case II [Eq. (34)]
ℓ_p	1	0.88	0.75	0.60	0.66	1.43	0.91	0.57	0.85
$\ell_{dt,318\text{-}14}$, no caps [Eq. (30)]	1.14	1	0.86	0.69	0.78	1.66	1.04	0.66	0.96
$\ell_{dt,25.4.4}$ [Eq. (23)]	1.33	1.16	1	0.80	0.91	1.93	1.23	0.78	1.13
$\ell_{dt,18.8.5.2}$ [Eq. (24)]	1.66	1.46	1.25	1	1.14	2.42	1.54	0.97	1.42
$\ell_{dc,25.4.9}$ [Eq. (25)]	1.52	1.28	1.10	0.88	1	2.18	1.40	0.88	1.29
ℓ_{ehy} [Eq. (33)]	0.70	0.60	0.52	0.41	0.46	1	0.64	0.40	0.59
$\ell_{dh,18.8.5.1}$ [Eq. (31)]	1.09	0.96	0.81	0.65	0.71	1.55	1	0.63	0.92
$0.7l_d$, Case I [Eq. (34)]	1.74	1.52	1.29	1.03	1.14	2.50	1.58	1	1.52
$0.7l_d$, Case II [Eq. (34)]	1.18	1.04	0.88	0.71	0.78	1.69	1.08	0.66	1

Appendix H: Hooked Bars: Summary of Database

[1]	[2]	[3]	[4]	[5]	[6]	[7]	[8]	[9]
Authors	I.D	f_{cm} (psi)	f_y (ksi)	Beam bar size	d_b (in.)	A_b (in.^{2})	n	A_{hs} (in.^{2})
Hanson [35]	Specimen 3	5200	64.1	No. 8	1.00	0.79	4	3.16
	Specimen 4	5380	63.4	No. 8	1.00	0.79	4	3.16
	Specimen 5	5230	65.0	No. 8	1.00	0.79	4	3.16
Uzumeri [36,37]	Specimen #3	3920	50.8	No. 9	1.128	1.00	3	3.00
	Specimen #4	4490	50.6	No. 9	1.128	1.00	3	3.00
	Specimen #6	5250	51.1	No. 9	1.128	1.00	3	3.00
	Specimen #7	4460	51.1	No. 9	1.128	1.00	3	3.00
	Specimen #8	3820	51.1	No. 9	1.128	1.00	4	4.00
Scribner and Wight [38]	Specimen 9	4940	60.2	No. 8	1.00	0.79	4	3.16
	Specimen 11	4940	60.2	No. 8	1.00	0.79	4	3.16
Ehsani and Alameddine [39,40]	HL8	8200	64.2	No. 9	1.128	1.00	4	4.00
	HH8	8200	64.2	No. 9	1.128	1.00	4	4.00
	HL11	10800	64.2	No. 9	1.128	1.00	4	4.00
	HH11	10800	64.2	No. 9	1.128	1.00	4	4.00
	HH14	13400	64.2	No. 9	1.128	1.00	4	4.00
	LL8	8200	66.3	No. 8	1.00	0.79	4	3.16
	LH8	8200	66.3	No. 8	1.00	0.79	4	3.16
	LL11	10800	66.3	No. 8	1.00	0.79	4	3.16
	LH11	10800	66.3	No. 8	1.00	0.79	4	3.16
	LL14	13400	66.3	No. 8	1.00	0.79	4	3.16
	LH14	13400	66.3	No. 8	1.00	0.79	4	3.16
Kurose et al. [41]	J3	4700	66.6	No. 9	1.128	1.00	5	5.00
Hwang et al. [42]	3T44	11140	62.4	No. 8	1.00	0.79	4	3.16
	3T3	10010	62.4	No. 8	1.00	0.79	4	3.16
	2T4	10300	62.4	No. 8	1.00	0.79	4	3.16
	3T4	10900	71.2	No. 8	1.00	0.79	4	3.16
	2T5	11100	71.2	No. 8	1.00	0.79	4	3.16

1000 psi = 1 ksi = 6.895 MPa; 1 in. = 25.4 mm; 1 kip = 4.45 kN

[1]	[2]	[10]	[11]	[12]	[13]	[14]	[15]	[16]	[17]
Authors	I.D	h_c (in.)	b_c (in.)	h_b (in.)	b_b (in.)	ℓ_p (in.)	side cover (in.)	c_{ch} (in.)	c_b (in.)
Hanson [35]	Specimen 3	15.0	15.0	20.0	12.0	13.5	3.00	2.67	1.500
	Specimen 4	15.0	15.0	20.0	12.0	13.5	3.00	2.67	1.500
	Specimen 5	15.0	15.0	20.0	12.0	13.5	3.00	2.67	1.500
Uzumeri [36,37]	Specimen #3	15.0	15.0	20.0	12.0	13.4	2.88	4.06	1.50
	Specimen #4	15.0	15.0	20.0	12.0	13.5	2.94	4.06	1.44
	Specimen #6	15.0	15.0	20.0	15.0	13.5	2.94	4.06	1.44
	Specimen #7	15.0	15.0	20.0	15.0	13.5	2.94	4.06	1.44
	Specimen #8	15.0	15.0	20.0	15.0	13.5	2.94	2.71	1.44
Scribner and Wight [38]	Specimen 9	18.0	12.0	14.0	10.0	16.5	2.40	2.07	1.03
	Specimen 11	18.0	12.0	14.0	10.0	16.5	2.40	2.07	1.03
Ehsani and Alameddine [39,40]	HL8	14.0	14.0	20.0	12.5	12.0	3.00	2.12	1.94
	HH8	14.0	14.0	20.0	12.5	12.0	3.00	2.12	1.94
	HL11	14.0	14.0	20.0	12.5	12.0	3.00	2.12	1.94
	HH11	14.0	14.0	20.0	12.5	12.0	3.00	2.12	1.94
	HH14	14.0	14.0	20.0	12.5	12.0	3.00	2.12	1.94
	LL8	14.0	14.0	20.0	12.5	12.0	3.00	2.17	2.00
	LH8	14.0	14.0	20.0	12.5	12.0	3.00	2.17	2.00
	LL11	14.0	14.0	20.0	12.5	12.0	3.00	2.17	2.00
	LH11	14.0	14.0	20.0	12.5	12.0	3.00	2.17	2.00
	LL14	14.0	14.0	20.0	12.5	12.0	3.00	2.17	2.00
	LH14	14.0	14.0	20.0	12.5	12.0	3.00	2.17	2.00
Kurose et al. [41]	J3	20.0	20.0	20.0	16.0	18.0	- [1]	2.44	1.50
Hwang et al. [42]	3T44	16.5	16.5	17.7	12.6	14.5	4.04	2.48	2.10
	3T3	16.5	16.5	17.7	12.6	14.6	3.92	2.57	2.10
	2T4	16.5	16.5	17.7	12.6	14.5	4.04	2.48	2.10
	3T4	17.7	17.7	17.7	12.6	15.6	4.63	2.48	2.10
	2T5	17.7	17.7	17.7	12.6	15.5	4.76	2.40	2.10

[1] Side cover within joint not reported where transverse beams are present

[1]	[2]	[18]	[19]	[20]	[21]	[22]	[23]	[24]	[25]
Authors	I.D	Column long. reinforcement		Joint hoops					
		Bar size	d_b (in.)	Bar size	d_{bt} (in.)	*Layers in Joint*	s[1] (in.)	N_{legs}	A_{th} (in.^{2})
Hanson [35]	Specimen 3	No. 11	1.410	No. 4	0.5	3	4.0	2	1.2
	Specimen 4	No. 11	1.410	No. 4	0.5	2	5.3	2	0.8
	Specimen 5	No. 11	1.410	No. 4	0.5	4	3.2	2	1.6
Uzumeri [36,37]	Specimen #3	No. 8	1.00	No. 3	0.375	4	3.0	2	0.9
	Specimen #4	No. 8	1.00	No. 4	0.5	4	3.0	2	1.6
	Specimen #6	No. 8	1.00	No. 4	0.5	8	1.7	2	3.2
	Specimen #7	No. 8	1.00	No. 4	0.5	4	3.0	2	1.6
	Specimen #8	No. 8	1.00	No. 4	0.5	8	1.7	3	3.2
Scribner and Wight [38]	Specimen 9	No. 9	1.13	No. 4	0.5	4	2.0	3	1.6
	Specimen 11	No. 9	1.13	No. 4	0.5	4	2.0	3	1.6
Ehsani and Alameddine [39,40]	HL8	No. 8	1.00	No. 4	0.5	4	2.8	3	2.4
	HH8	No. 8	1.00	No. 4	0.5	6	2.0	3	3.6
	HL11	No. 8	1.00	No. 4	0.5	4	2.8	3	2.4
	HH11	No. 8	1.00	No. 4	0.5	6	2.0	3	3.6
	HH14	No. 8	1.00	No. 4	0.5	6	2.0	3	3.6
	LL8	No. 8 & 7	1 & 0.875	No. 4	0.5	4	2.8	3	2.4
	LH8	No. 8 & 7	1 & 0.875	No. 4	0.5	6	2.0	2	3.6
	LL11	No. 8 & 7	1 & 0.875	No. 4	0.5	4	2.8	3	2.4
	LH11	No. 8 & 7	1 & 0.875	No. 4	0.5	6	2.0	2	3.6
	LL14	No. 8 & 7	1 & 0.875	No. 4	0.5	4	2.8	2	2.4
	LH14	No. 8 & 7	1 & 0.875	No. 4	0.5	6	2.0	2	3.6
Kurose et al. [41]	J3	No. 9	1.128	No. 4	0.5	3	3.2	2	1.8
Hwang et al. [42]	3T44	No. 10	1.27	No. 4	0.5	3	3.1	6	3.6
	3T3	No. 10	1.27	No. 3	0.375	3	3.1	3	1.0
	2T4	No. 10	1.27	No. 4	0.5	2	4.2	3	0.8
	3T4	No. 10	1.27	No. 4	0.5	3	3.1	3	1.8
	2T5	No. 10	1.27	No. 5	0.625	2	4.2	3	1.2

[1] Spacing is estimated based on reported information

[1]	[2]	[26]	[27]	[28]	[29]	[30]	[31]
Authors	I.D	Confinement by transv. beams per ACI 318-19 §15.2.8	R_n	b_j (in.)	V_n (kip)	V_p [at column axis] (kip)	V_p/V_n
Hanson [35]	Specimen 3	Not confined	12	15.0	195	222	1.14
	Specimen 4	Not confined	12	15.0	198	197	0.99
	Specimen 5	Not confined	12	15.0	195	214	1.10
Uzumeri [36,37]	Specimen #3	Not confined	12	15.0	169	146	0.86
	Specimen #4	Not confined	12	15.0	181	169	0.93
	Specimen #6	Not confined	12	15.0	196	161	0.82
	Specimen #7	Not confined	12	15.0	180	157	0.87
	Specimen #8	Not confined	12	15.0	167	193	1.16
Scribner and Wight [38]	Specimen 9	Not confined	12	12.0	182	224	1.23
	Specimen 11	Not confined	12	12.0	182	215	1.18
Ehsani and Alameddine [39,40]	HL8	Not confined	12	14.0	213	210	0.99
	HH8	Not confined	12	14.0	213	212	1.00
	HL11	Not confined	12	14.0	235	206	0.88
	HH11	Not confined	12	14.0	235	225	0.96
	HH14	Not confined	12	14.0	235	222	0.94
	LL8	Not confined	12	14.0	213	195	0.92
	LH8	Not confined	12	14.0	213	189	0.89
	LL11	Not confined	12	14.0	235	164	0.70
	LH11	Not confined	12	14.0	235	218	0.93
	LL14	Not confined	12	14.0	235	198	0.84
	LH14	Not confined	12	14.0	235	203	0.86
Kurose et al. [41]	J3	Confined	15	20.0	411	265	0.64
Hwang et al. [42]	3T44	Not confined	12	16.5	328	205	0.62
	3T3	Not confined	12	16.5	328	220	0.67
	2T4	Not confined	12	16.5	328	209	0.64
	3T4	Not confined	12	17.7	377	216	0.57
	2T5	Not confined	12	17.7	377	226	0.60

[1]	[2]	[32]	[33]	[34]	[35]	[36]		[37]	[38]
Authors	I.D	d (in.)	a (in.)	β_1	c (in.)	ε_s		f_y / E_s	M_n (kip-in.)
Hanson [35]	Specimen 3	18.0	3.82	0.79	4.83	0.011	≥	0.0022	3260
	Specimen 4	18.0	3.65	0.78	4.67	0.011	≥	0.0022	3240
	Specimen 5	18.0	3.85	0.79	4.88	0.010	≥	0.0022	3300
Uzumeri [36,37]	Specimen #3	17.6	3.81	0.85	4.48	0.011	≥	0.0018	2390
	Specimen #4	17.6	3.31	0.83	4.02	0.012	≥	0.0017	2420
	Specimen #6	17.6	2.29	0.79	2.91	0.017	≥	0.0018	2520
	Specimen #7	17.6	2.70	0.83	3.26	0.015	≥	0.0018	2490
	Specimen #8	17.6	4.20	0.85	4.94	0.010	≥	0.0018	3170
Scribner and Wight [38]	Specimen 9	12.1	4.53	0.80	5.64	0.006	≥	0.0021	1870
	Specimen 11	12.1	4.53	0.80	5.64	0.006	≥	0.0021	1870
Ehsani and Alameddine [39,40]	HL8	17.0	2.95	0.65	4.53	0.011	≥	0.0022	3990
	HH8	17.0	2.95	0.65	4.53	0.011	≥	0.0022	3990
	HL11	17.0	2.24	0.65	3.44	0.014	≥	0.0022	4080
	HH11	17.0	2.24	0.65	3.44	0.014	≥	0.0022	4080
	HH14	17.0	1.80	0.65	2.77	0.017	≥	0.0022	4130
	LL8	17.0	2.40	0.65	3.70	0.013	≥	0.0023	3310
	LH8	17.0	2.40	0.65	3.70	0.013	≥	0.0023	3310
	LL11	17.0	1.83	0.65	2.81	0.017	≥	0.0023	3370
	LH11	17.0	1.83	0.65	2.81	0.017	≥	0.0023	3370
	LL14	17.0	1.47	0.65	2.26	0.021	≥	0.0023	3410
	LH14	17.0	1.47	0.65	2.26	0.021	≥	0.0023	3410
Kurose et al. [41]	J3	16.4	5.21	0.82	6.39	0.007	≥	0.0023	4610
Hwang et al. [42]	3T44	15.1	1.65	0.65	2.54	0.017	≥	0.0022	2820
	3T3	15.1	1.84	0.65	2.83	0.015	≥	0.0022	2800
	2T4	15.1	1.79	0.65	2.75	0.015	≥	0.0022	2800
	3T4	15.1	1.93	0.65	2.96	0.014	≥	0.0025	3190
	2T5	15.1	1.89	0.65	2.91	0.015	≥	0.0025	3190

[1]	[2]	[39]	[40]	[41]	[42]	[43]	[44]
Authors	I.D	L_b (in.)	L_n (in.)	L_c (in.)	M_{peak} (kip-in.)	M_{peak}/M_n	$\delta_{0.8peak}$
Hanson [35]	Specimen 3	128	120	120	4160	1.28	N/R
	Specimen 4	128	120	120	3720	1.15	N/R
	Specimen 5	128	120	120	4020	1.22	N/R
Uzumeri [36,37]	Specimen #3	120	113	120	2660	1.11	≥ 3%
	Specimen #4	120	113	120	3140	1.30	≥ 3%
	Specimen #6	120	113	120	3100	1.23	≥ 3%
	Specimen #7	120	113	120	2980	1.20	≥ 3%
	Specimen #8	120	113	120	3470	1.10	≥ 3%
Scribner and Wight [38]	Specimen 9	72	60	96	2510	1.34	≥ 3%
	Specimen 11	72	48	96	2500	1.34	≥ 3%
Ehsani and Alameddine [39,40]	HL8	70	63	141	3710	0.93	≥ 3%
	HH8	70	63	141	3740	0.94	≥ 3%
	HL11	70	63	141	3730	0.91	≥ 3%
	HH11	70	63	141	4090	1.00	≥ 3%
	HH14	70	63	141	4080	0.99	≥ 3%
	LL8	70	63	141	3520	1.06	≥ 3%
	LH8	70	63	141	3400	1.03	≥ 3%
	LL11	70	63	141	3020	0.90	≥ 3%
	LH11	70	63	141	4020	1.19	≥ 3%
	LL14	70	63	141	3700	1.09	≥ 3%
	LH14	70	63	141	3780	1.11	≥ 3%
Kurose et al. [41]	J3	96	86	165	4040	0.88	≥ 3%
Hwang et al. [42]	3T44	83.1	74.8	106	3450	1.22	≥ 3%
	3T3	83.1	74.8	106	3670	1.31	≥ 3%
	2T4	83.1	74.8	106	3500	1.25	≥ 3%
	3T4	83.7	74.8	106	3600	1.13	≥ 3%
	2T5	83.7	74.8	106	3770	1.18	≥ 3%

Appendix I: Hooked Bars: Average Length Ratios

Table 7 – Hooked bars: Average length ratios: length in row / length in column (all 27 specimens)

	ℓ_p	$\ell_{dh,318\text{-}14}$	$\ell_{dh,25.4.3}$	$\ell_{dc,25.4.9}$ + BR + d_b	ℓ_{ehy}	$\ell_{dh,18.8.5.1}$	0.7 $l_{d,408}$ Case I + BR + d_b	0.7 $l_{d,408}$ Case II + BR + d_b
ℓ_p	1	1.43	0.86	0.70	1.45	1.15	0.35	0.76
$\ell_{dh,318\text{-}14}$ [Eq. (38)]	0.70	1	0.60	0.50	1.02	0.81	0.25	0.54
$\ell_{dh,25.4.3}$ [Eq. (39)]	1.16	1.65	1	0.84	1.70	1.37	0.42	0.91
$\ell_{dc,25.4.9}$ [Eq. (37)] + BR + d_b	1.44	2.01	1.19	1	2.10	1.67	0.51	1.10
ℓ_{ehy} [Eq. (41)]	0.69	0.98	0.59	0.48	1	0.81	0.25	0.54
$\ell_{dh,18.8.5.1}$ [Eq. (36)]	0.87	1.24	0.73	0.60	1.23	1	0.31	0.67
0.7 $l_{d,408}$ Case I [Eq. (42)] + BR + d_b	2.84	4.05	2.37	1.97	4.05	3.26	1	2.19
0.7 $l_{d,408}$ Case II [Eq. (42)] + BR + d_b	1.31	1.86	1.10	0.91	1.86	1.50	0.46	1

BR =bend radius

Table 8 – Hooked bars: Average length ratios: length in row / length in column (specimens with $\delta_{0.8peak} \geq 3\%$: 19 specimens)

	ℓ_p	$\ell_{dh,318-14}$	$\ell_{dh,25.4.3}$	$\ell_{dc,25.4.9}$ + BR + d_b	ℓ_{ehy}	$\ell_{dh,18.8.5.1}$	0.7 $l_{d,408}$ Case I + BR + d_b	0.7 $l_{d,408}$ Case II + BR + d_b
ℓ_p	1	1.48	0.89	0.69	1.49	1.17	0.35	0.77
$\ell_{dh,318-14}$ [Eq. (38)]	0.68	1	0.60	0.47	1.02	0.79	0.24	0.52
$\ell_{dh,25.4.3}$ [Eq. (39)]	1.13	1.66	1	0.80	1.70	1.34	0.41	0.89
$\ell_{dc,25.4.9}$ [Eq. (37)] + BR + d_b	1.44	2.11	1.25	1	2.17	1.71	0.52	1.12
ℓ_{ehy} [Eq. (41)]	0.67	0.98	0.59	0.46	1	0.80	0.24	0.53
$\ell_{dh,18.8.5.1}$ [Eq. (36)]	0.86	1.26	0.74	0.59	1.25	1	0.30	0.66
0.7 $l_{d,408}$ Case I [Eq. (42)] + BR + d_b	2.82	4.16	2.44	1.94	4.14	3.28	1	2.20
0.7 $l_{d,408}$ Case II [Eq. (42)] + BR + d_b	1.30	1.91	1.13	0.89	1.90	1.51	0.46	1

BR =bend radius